Simulation and Management of Distributed Generating Units using Intelligent Techniques

Vom Fachbereich Ingenieurwissenschaften der
Universität Duisburg-Essen
zur Erlangung des akademischen Grades eines

Doktoringenieurs (Dr. -Ing.)

genehmigte Dissertation

von

AHMED MOHAMED REFAAT AZMY

aus

Menoufya, Ägypten

Referent: **Prof. Dr.-Ing. habil. István Erlich**

Korreferent: **Prof. Dr.-Ing. Peter Schegner**

Tag der mündlichen Prüfung: 14.01.2005

Acknowledgment

All praises and thanks are to Allah, the Lord of the world, the most Beneficent, the most Merciful for helping me to accomplish this work.

I am beholden to a number of people and organisations, who supported me to carry out this work. First and foremost, my heartily profound thanks, gratitude and appreciation to my advisor ***Univ. Prof. Dr. Eng. habil. István Erlich*** for his encouragement, help and kind support. His invaluable technical and editorial advice, suggestions, discussions and guidance were a real support to complete this dissertation.

I would like also to express my thanks to my co-advisor Prof. Dr.-Ing. Peter Schegner for his critical reading and discussion and also the useful suggestions to my dissertation.

Furthermore, I would like to express my deepest gratitude and thanks to all staff members of "Fachgebiet Elektrische Anlagen und Netze" for contributing to such an inspiring and pleasant atmosphere.

Very special thank to my family, especially my parents and my wife, for their patience, understanding and encouragement during the different phases of my work. They spared no effort until this work comes to existence.

Last but not least, I wish to acknowledge the financial support of the Missions Department-Egypt and the Faculty of Engineering, Tanta University for giving me the opportunity to pursue my doctoral degree in Germany.

Ahmed Mohamed Refaat Azmy
Duisburg, January 2005

To my parents, my brothers, my sister, my wife

and my children Rawan, Maryam and Karim

Abstract

Distributed generation is attracting more attention as a viable alternative to large centralized generation plants, driven by the rapidly evolving liberalization and deregulation environments. This interest is also motivated by the need for eliminating the unnecessary transmission and distribution costs, reducing the greenhouse gas emissions, deferring capital costs and improving the availability and reliability of electrical networks. Therefore, distributed generation is expected to play an increasingly important role in meeting future power generation requirements and to provide consumers with flexible and cost effective solutions for many of their energy needs. However, the integration of these sources into the electrical networks can cause some challenges regarding their expected impacts on the security and the dynamic behaviour of the entire network. It is essential to study these issues and to analyze the performance of the expected future systems to ensure satisfactory operation and to maximize the benefits of utilizing the distributed resources.

The thesis focuses on some topics related to the dynamic simulation and operation of distributed generating units, specifically fuel cells and micro-turbines. The objective of this dissertation is to put emphasis on the following aspects:

- ***Dynamic modelling of fuel cells:*** Analyzing electrical power systems requires suitable dynamic models for all components forming the system. Since fuel cell units represent new promising sources, the research ascribes special consideration to developing models that describe their dynamic behaviour. It is envisaged to develop a simple and flexible model for stability studies and controller-design purposes in addition to an exhaustive nonparametric model for detailed analysis of the fuel cells.

- ***Simulation of a large number of DG units incorporated into a multi-machine network:*** With large numbers of distributed sources, it is expected that decentralized generation impacts the dynamic behaviour of the high voltage network. Therefore, it is intended to investigate the case, where several fuel cells and micro-turbines are integrated into the distribution system of a multi-machine network. This can help in studying the operation of the entire network and highlighting the mutual impact of the high-voltage and low-voltage networks on each other.

- ***Dynamic modelling and simulation of hybrid fuel cell/micro-turbine units:*** The hybrid configuration of fuel cells and micro-turbines exhibits many advantages enabling this technology to represent a considerable percentage of the next advanced power generation systems. The dynamic performance of such units, however, is still not fully understood. Hence, it is desirable for understanding their behaviour to highlight the dynamic interdependencies between the fuel cell and the micro-turbine, the overall system transient performance, and the dynamic control requirements.

- ***Dynamic equivalents of distribution power networks:*** The need for fast and simplified analysis of interconnected power networks obligates developing robust dynamic equivalents for certain electrical power subsystems. Non-parametric dynamic equivalents will avoid the identification of complicated mathematical models, which would adequately reflect the performance of the replaced network under various operating conditions. For distribution systems, the equivalent model has to take into consideration the characteristics of distributed generating units which are mostly connected to the network through inverters and in some cases their operating principles are not based on the electromechanical energy conversion mechanism.

- ***Impact of distributed generation on the stability of power systems:*** The existence of distributed sources with large numbers can impact the stability of the power system considerably. Angle-stability, frequency stability as well as voltage stability can be affected when the power from these units increases. It is essential to study this impact to ensure secure operation of the power system. Therefore, it is envisaged to study the performance of a hypothetical network and to demonstrate different stability classes at different penetration levels of the distributed generating units.

- ***Online management of fuel cells and micro-turbines for residential applications:*** The optimal management of the power in distributed generation for residential applications can significantly reduce the operating cost and contribute towards improving their economic feasibility. The management process, however, has to be accomplished in the online mode and to account for all decision variables that affect the setting values. Therefore, it is aimed to develop an online intelligent strategy to manage the power generated in fuel cells and micro-turbines when used to supply residential loads in order to minimize the daily operating cost and achieve an overall reduction in the electricity price.

Contents

List of Figures

List of Tables

Acronyms and Symbols

Acronyms

AFC	Alkaline Fuel Cells
ANN	Artificial Neural Network
BPFFNN	Back Propagation Feed Forward Neural Network
CFCMT	Combined Fuel Cell/Micro-Turbine
CHP	Combined Heat and Power
DG	Distributed Generation
DT	Decision Tree
FC	Fuel Cell
GA	Genetic Algorithms
IGBT	Insulated Gate Bipolar Transistor
MCFC	Molten Carbonate Fuel Cell
MT	Micro-Turbines
PAFC	Phosphoric Acid Fuel Cell
PEMFC	Proton Exchange Membrane Fuel Cell
PM	Permanent Magnet
PMSG	Permanent Magnet Synchronous Generator
PSD	Power System Dynamics
PST16	Power System Transient test network
PV	Photovoltaic
PWM	Pulse Width Modulation
SOFC	Solid Oxide Fuel Cell

Symbols

Latin Symbols

A_t	Tank surface area of the heat recovery system	cm^2
$a_{1,2}$	Cross section area of heat-exchanger outer and inner tubes respect.	cm^2
$C_{el\text{-}p}$	Tariff of purchased electricity	\$/kWh
$C_{el\text{-}s}$	Tariff of sold electricity	\$/kWh
C_{n1}, C_{n2}	Natural gas tariffs for DG units and residential loads respect.	\$/kWh
C_P^S	Average specific heat of the stack of the fuel cell	cal/gm.K
C_P^W	Average specific heat of the water in the tank	cal/gm.K
C_P^1	Average specific heat of the cooling fluid of the FC stack	cal/gm.K
C_P^2	Average specific heat of the second fluid of the heat exchanger	cal/gm.K
d	Internal diameter of the inner tube of the heat exchanger	cm
DCPE	Daily cost of purchased electricity to supply residential load	\$

DCPF	Daily cost of purchased gas for residential loads	$
DFC	Daily fuel cost for the DG units	$
DOC	Daily total operating cost of the DG units	$
DISE	Daily income for sold electricity	$
F	Faraday's constant= 96485.35	$^{o}C\ mol^{-1}$
f_{max}	Maximum fitness value of individuals	-
f_{ref}	Reference frequency of the micro-turbine unit	p.u.
H	Inertia constant of the PMSG	s
I	Fuel cell stack current	A
$\underline{I}_{a,i}$, $\underline{I}^{0}_{a,i}$	Current of active sources at boundary bus i and its initial value	A
j	No. of boundary buses between replaced and retained systems	-
K_g	Gain of speed governor of the micro-turbine unit	-
K_{gen}	Gain of the generator of the micro-turbine unit	-
$K_{O\&M}$	The operating and maintenance cost per kWh	$/kWh
L	Heat-exchanger tube length	cm
$L_{el,J}$, $L_{th,J}$	Electrical and thermal load demands respectively at interval J	kW
M	Modulation index (ratio) of the PWM inverter	-
$\dot{M}_L$	Water mass flow rate from the storage tank to the load	gm/s
MRT	The minimum running period of the fuel cell	h
MST	The minimum stop period of the fuel cell	h
M_t	Water mass in the tank	gm
$\dot{M}_1$, $\dot{M}_2$	Mass flow rates of the two fluids in the heat exchanger	gm/s
n	Number of cells in series of the fuel cell structure	-
N_{ind}	Number of the individuals within the population of the GA	-
N_{max}	The maximum daily number of starts and stops of DG units	-
$n_{start\text{-}stop}$	The number of starts and stops of DG units per day	-
O&M	Daily operating and maintenance cost of the fuel cell	$
P_a	Power required for auxiliary devices with the fuel cell system	kW
P_{ac}, P_{dc}	AC and DC power respectively of the FC ANN-based model	p.u.
P_{ele}	Input-electrical power to the PMSG of the micro-turbine unit	p.u.
P_{fc}	A signal representing the power contained in the FC exhaust	p.u.
P_i, P_i^0	The active power at bus i and its initial value	kW
P_J	Net electrical power produced in the fuel cell at interval J	kW
$P_{J,t-1}$	The power generated in the fuel cell at interval "t-1"	kW
P_m	Input mechanical power to the PMSG of the MT unit	p.u.
P_{max}	The maximum limit of the generated power in the fuel cell	kW
P_{min}	The minimum limit of the generated power in the fuel cell	kW
P_{ref}	Reference thermal power of the micro-turbine unit	p.u.
P_{th}	Input thermal power of the micro-turbine unit	p.u.

$P_{th,J}$	Thermal power produced in the fuel cell at interval J	kW
Q_{abs1}	Absorbed thermal power by the cooling fluid of the fuel cell	cal/s
Q_{abs2}	Absorbed thermal power by the second fluid in the heat-exchanger	cal/s
Q_{gen}	Generated thermal power in the fuel cell	cal/s
Q_i, Q_i^0	Reactive power at bus i and its initial value	kvar
R	Avogadro gas constant = 8.314	$JK^{-1}mol^{-1}$
R_{H2}	Voltage drop due to anode reaction of the fuel cell unit	Ω
R_L	Load resistance for the fuel cell in the ANN-based model	p.u.
R_{loss}	Nonlinear-loss resistance in the fuel cell equivalent circuit	p.u.
R_{O2}	Voltage drop due to cathode reaction of the fuel cell unit	Ω
R_Ω	Voltage drop due to internal resistance of the fuel cell stack	Ω
STC	Daily start up cost of the fuel cell	$
T	Time duration between two successive settings of the fuel cell	h
T_a	Ambient temperature for the heat recovery system	K
T_{ab}	Absolute cell temperature of the fuel cell	K
T^{off}	The time terminated where the FC unit is in the off mode	h
T_{t-1}^{off}	The fuel cell stop period at time interval “t-1”	h
T_{t-1}^{on}	The fuel cell running period at time interval “t-1”	h
T_S	Stack operating temperature of the fuel cell	K
T_s^{ref}	The reference temperature for the stack of the fuel cell	K
T_t	Temperature of water in the tank of the heat recovery system	K
T_{1c} T_{1h}	Cold and hot temperatures respectively of the fuel-cell cooling fluid	K
T_{2c}, T_{2h}	Cold and hot temperatures respectively of the second fluid in the heat exchanger	K
T_2^{ref}	The reference temperature for the input water to the tank	K
U	Heat transfer coefficient in the heat exchanger	$cal/s.cm^2K$
$\underline{U}_i$, $\underline{U}_i^0$	Voltage at boundary bus i and its initial value	V
U_s	The fuel cell on/off status	-
U_t	Heat transfer coefficient in the water storage tank	$cal/s.cm^2K$
V_c	Maximum value of carrier signal of the PWM inverter	V
$V_{cy,in}$	The rms input voltage to the cycloconverter with the MT	p.u.
$V_{cy,o}$	The rms output voltage of the cycloconverter with the MT	p.u.
V_{dc}	Output DC voltage from the stack of the fuel cell	p.u.
$V_{L,rms}$	rms fundamental component of the modulated Line voltage	V

V_m	Maximum value of modulating signal of the PWM inverter	V
$V_{ph,rms}$	rms fundamental component of the modulated phase voltage	p.u.
V_R	The output signal from the reformer to the stack of the FC	p.u.
V_{ref}	Reference voltage of the micro-turbine unit	p.u.
V_S	Stack volume of the fuel cell	cm^3
V_0	the open circuit reversible potential of the FC	p.u.
V_0^s	The value of V_0 at standard conditions	p.u.
W_f	The turbine input signal of the micro-turbine unit	p.u.
W_{min}	The offset representing the fuel demand at no-load for the MT	p.u.
Y (k)	Output from the ANN-based model of the FC at interval "k"	p.u.
Z_L	Load impedance to the fuel cell for the ANN-based model	p.u.

Greek Symbols

α	Firing angle of the cycloconverter with the MT unit	rad.
α_h	Hot start up cost of the fuel cell	$
$\alpha_h+\beta$	Cold start up cost of the fuel cell	$
α_s	A scaling factor in the crossover process	-
ΔH	Total enthalpy of the reaction in the fuel cell stack	J/mole
$\Delta \underline{I}_{a,i}^n$	Normalized current-deviation of active components at boundary bus i	-
ΔP_D	The lower limit of the ramp rate of the fuel cell	kW/s
ΔP_U	The upper limit of the ramp rate of the fuel cell	kW/s
ΔS	Irreversible entropy change of the reaction in the fuel cell	J/mole.K
$\Delta \underline{U}_i^n$	Normalized voltage-deviation at boundary bus i	-
ΔV_P	Change in reversible potential due to the change in pressure	mV
ΔV_T	Change in reversible potential due to the change of temperature	mV
η_J	Fuel cell efficiency at interval J	-
ω	Angular speed of the PMSG of the MT unit	p.u.
ω_{ref}	Reference angular speed of the PMSG	p.u.
ρ_S	Stack mass density of the fuel cell	gm/cm^3
ρ_1, ρ_2	The mass density of the two fluids in the heat exchanger	gm/cm^3
τ	The fuel cell cooling time constant	h
τ_{cd}	Lag-time constant of compressor discharge of the MT unit	s
τ_f	Lag-time constant of fuel system of the MT unit	s
τ_g	Lag-time constant of the speed governor of the MT unit	s
τ_{gen}	Lag-time constant of generator of the MT unit	s
τ_R , τ_S	Time constants of reformer and stack in the FC system respect.	s
τ_{vp}	Lag-time constant of valve positioner of the MT unit	s

Chapter 1

Introduction

1.1 Motivation

The ever increasing demand for electrical power has created many challenges for the energy industry, which can affect the quality of the generated power in short and long terms [1]. The problem will imminently take a new form when bottlenecks occur in the transmission and distribution infrastructure. At the same time, the wide utilization of conventional fossil fuel-based sources will dramatically impact the quality and sustainability of life on earth. The realization of the problems associated with the conventional sources is defining a new set of power supply requirements that can better be served through Distributed Generation (DG). Therefore, DG is gaining a lot of attention as it provides solutions for both the short and long term problems [2-5]. They are becoming more feasible as a result of falling price of small-scale power plants and intelligent development of data communications and control technologies. Small DG units are expected to spread rapidly within power systems and have the potential to account for 20-30% of the distribution-system demand by 2020 [6, 7]. Among the promising energy sources, Fuel Cells (FCs) [8-11] and Micro-Turbines (MTs) [12-15] are candidate to support the existing centralized power systems.

MTs can produce low-cost low-emission electricity but at low efficiency which is limited by the combustion process. The other advantages of MTs include the compact and simple design, small size, low maintenance requirements, durability, load-following capabilities, the ability to operate on a variety of fuels and the possibility of Combined Heat and Power (CHP) applications [16]. However, the dependency of the efficiency on the inlet fuel parameters and the noisy operation represent the main disadvantages of MTs.

FCs offer the potential for lower emissions and higher efficiencies but are likely to be too expensive for many applications. The first FC unit was discovered and developed in 1839 by Sir William Grove [17]. However, it was not practically used until the 1960's when it was utilized to supply electric power for spacecraft [17]. Nowadays, FCs are being used in many applications because of

their power quality, high efficiency, modularity, and environmental benefits. FC is an emerging small-scale power generation technology that converts hydrogen (from a fuel source) and oxygen (from air) into water and generates electricity from this electrochemical process. Basically, FC consists of two electrodes surrounding an electrolyte, where hydrogen fuel is fed into the anode and oxygen or air enters the cell through the cathode. The electrical energy is produced by controlling the movement of charged hydrogen and oxygen particles towards each other. The material of the electrolyte has to provide a high resistance to the electrons and a very low resistance to the protons. The task of the electrolyte thus is to allow the conduction of protons and insulate electrons to force them to pass to the other electrode through an external electrical circuit. This movement is controlled to generate regulated electrical energy. The conversion of hydrogen to energy takes place without combustion and, as a result, the process is highly efficient, clean and quiet. The modern technology of FCs tends to include a fuel reformer to extract hydrogen from any hydrocarbon fuel like natural gas, ethane, methane and even gasoline. An external fuel reformer is added to low-temperature FCs, while high temperature units contain internal ones for compact structure and high efficiency operation. Fig 1-1 explains the operation principles of FCs.

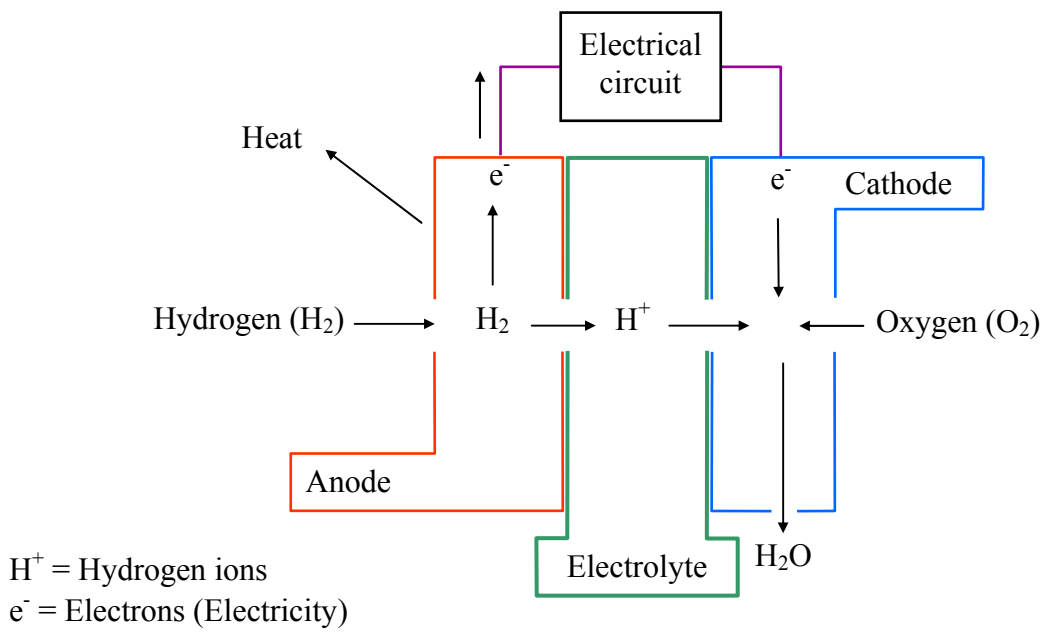

Fig 1-1 Operation principles of fuel cells

A main advantage of MTs and FCs is their ability to supply electrical and thermal power at the same time, which is required for the CHP applications. In addition, the high temperature of the exhaust gases from MTs and some types of

FCs enables the combination of the two units to generate more electricity by utilizing the heat energy [18-19]. This configuration is expected to reduce the fuel consumption and to decrease the cost per unit energy.

In spite of the benefits of utilizing DG units within power systems, such as the increase of the system efficiency and the improvements in the power quality and reliability [20], many technical and operational challenges have to be resolved before DG becomes commonplace. The lack of suitable control strategies for electrical networks with high penetration levels of DG units represents a problem for the futuristic systems. Also, the dynamic interaction between high-voltage parts of the network from one side and DG units from the other side is an essential subject that needs extensive research. To simulate the behaviour of modern electrical networks, suitable static and dynamic models for DG units and the related interface devices are required. In addition, many topics of critical interest regarding the employment of DG have to be investigated. Some of these topics are the overall system stability, the power quality and the interaction between the local regulators with those of the centralized energy plants.

This thesis attempts to highlight some issues related to the use of DG units from different points of view. Intelligent techniques, i.e. Artificial Neural Networks (ANNs), Genetic Algorithms (GAs) and Decision Trees (DTs), are employed in different stages of the research due to their capabilities of dealing with many unconventional problems.

1.2 Objectives of the dissertation

According to the present-day and the expected-future situations regarding DG within power systems, it is extremely important to investigate the following issues, which are the main topics within the scope of this thesis:

- The development of suitable dynamic models for the FC unit for different simulation and investigation purposes. This includes:
  - simplified dynamic model for stability study and control-design purposes
  - more detailed dynamic model for thorough analysis of the unit
- The performance investigation of high-voltage multi-machine networks comprising large numbers of selected DG units. The objective is to address the following topics:
  - the impact of DG on the dynamic behaviour of the high-voltage network and vice-versa

  - the variation on the dynamic behaviour of the low-voltage-network as a result of the influence of integrating DG units on the characteristics of the end-user nodes
- The hybrid configuration based on augmented FC and MT units and the operation of such units within interconnected power systems.
- The development of generic dynamic equivalents for distribution networks containing active DG sources to simplify the analysis of the network.
- The assessment of the potential impacts that DG might have on the stability of electrical power networks.
- The economic operation of DG units when used to supply residential loads by optimizing their daily operating cost and generalizing the optimization process using ANNs or DTs to overcome the disadvantages of the classical optimization techniques.

1.3 Thesis organisation

The work in this dissertation is organized as follows:

In ***CHAPTER 1***, an introduction about the thesis is presented.

As a background, ***CHAPTER 2*** gives an overview of the DG units and their potential impacts on power systems. Also an overview of FC and MT technologies is presented in this chapter.

The main focus in ***CHAPTER 3*** is on the dynamic modelling of FCs as a promising DG unit. A simplified nonlinear dynamic model for stability analysis and control-design purposes is proposed. For detailed analysis, a new approach to get an accurate model from input/output data using a recurrent ANN is presented.

An investigation about the dynamic performance of the expected-futuristic networks that comprise large numbers of DG units is introduced in ***CHAPTER 4***. The mutual dynamic impacts between DG units in the distribution system and high-voltage parts of the network are studied. In addition, this chapter investigates the dynamic modelling and simulation of hybrid units consisting of high-temperature FCs and MTs.

Since the analysis of networks including such large number of DG units is a time consuming process, ***CHAPTER 5*** presents a new dynamic equivalent ap-

proach to replace certain distribution networks by nonparametric equivalents. The idea is to simplify the analysis of the network by replacing these parts of the network by recurrent ANN-based dynamic equivalents.

The objective of ***CHAPTER 6*** is to investigate the impact of integrating selected DG units with different penetration levels on the stability of bulk electrical power systems. In particular, the performance of a hypothetical power system with significant penetration of DG units is described to assess different classes of stability.

CHAPTER 7 deals with the economic issues of DG units when used for residential applications. A new intelligent technique to optimize the daily operation of selected DG units is introduced. The development of the optimization results in a generalized frame using ANNs and DTs is also presented. The online capability of this technique to minimize the daily operating cost by managing the electrical and thermal power in these units is discussed.

Finally, deduced conclusions from the thesis and future directions are summarized in ***CHAPTER 8***.

Chapter 2

Distributed Generation: an Overview

2.1 Introduction

DG can provide many benefits to the power-distribution network [20]. To maximize these benefits, reliable DG units have to be connected at proper locations and with proper sizes [21]. However, such units will not generally be utility owned, which means that the adequate utilization of DG units is not guaranteed [5]. Moreover, some DG units, such as solar and wind, are variable energy sources and depend in their operation on weather conditions. Therefore, it is not ensured whether DG will satisfy and meet all operation criteria in the power system. Some issues arise when these units are connected to power systems including the power quality, proper system operation and network protection [5].

This chapter gives a brief overview of DG units in general and discusses their potential impact on the distribution networks. In addition, a summary of some aspects related to FC and MT units as new promising DG sources is given. The objective is to clarify some critical points about these technologies, whose simulation and economic aspects are extensively studied through the dissertation.

2.2 Definition of distributed generation

DG is defined as the integrated or stand-alone utilization of small, modular electric generation near the end-user terminals [7]. Another generic definition assigns the DG phrase for any generation utilized near consumers regardless of the size or the type of the unit [2, 20]. According to the latter definition, DG may include any generation integrated into distribution system, commercial and residential back-up generation, stand-alone onsite generators and generators installed by the utility for voltage support or other reliability purposes.

2.3 Benefits of utilizing DG units

In many applications, DG technology can provide valuable benefits for both the consumers and the electric-distribution systems [20, 22 and 23]. The small size and the modularity of DG units encourage their utilization in a broad range of

applications. The downstream location of DG units in distribution systems reduces energy losses and allows utilities to postpone upgrades to transmission and distribution facilities. The benefits of utilizing DG can be summarized as follows:

- improving availability and reliability of utility system
- voltage support and improved power quality
- reduction of the transmitted power and, as a result, the transmission and distribution expenditures are postponed or avoided
- power-loss reduction
- possibility of cogeneration applications
- emission reduction

2.4 Applications of DG units

DG can be used for different applications due to their small size, modularity and location in power systems. The main applications of DG units include the following fields [7]:

- generating the base-load power, as in the case of variable-energy DG sources
- providing additional reserve power at peak-load intervals
- providing emergency or back-up power to increase the stability and reliability of important loads
- supplying remote loads separated from the main-grid system
- supporting the voltage and reliability by providing power services to the grid
- cooling and heating purposes

It is also possible to use DG to cover the load demand most of the time. In this case, DG has to be connected to a local grid for back-up power. Another possibility is to use energy storage devices to ensure the continuity of supplying the load.

2.5 System stability requirements

Stability studies on large-scale power systems are concerned with the electromechanical stability of large generators. These studies are performed to evaluate the stability of the system under different disturbances. To some extent, the DG stability studies are similar to traditional ones. However, the size and interface of such units with power systems results in some differences. The small size of DG units compared to the entire power system implies that an individual unit has no significant influence on the stability of the bulk system [24]. However, the stabil-

ity of the DG unit itself has to be investigated to evaluate the ability of these units to remain operating in parallel with the network during and after different disturbances. Effective damping of the oscillatory behaviour is essential for DG unit regarding their stability. In all cases, accurate models of the entire network including DG units are required to perform stability analysis [4].

2.6 Protection requirements

As mentioned earlier, DG units are not generally owned by the utility and hence, their protection is the responsibility of the owner or operator. The distribution utility itself will not take any responsibility for protecting DG units or their infrastructure under any operating conditions. In the following, some requirements of the DG protection system are introduced [3, 5, 25 and 26]:

- it has to be ensured that faults on the utility system will not damage the DG equipments
- DG units have to be completely isolated from faulted areas in the distribution system considering selectivity principals of the network protection system
- DG units have not to energize any de-energized circuits owned by the utility
- DG should be disconnected from the network in the case of an abnormality in voltage or frequency
- the synchronization of DG units with the utility is the responsibility of the operator

The protection system of any DG source has to involve the following devices:

- undervoltage and overvoltage protection
- short circuit current protection
- power directional protection
- frequency protection for over and under frequencies
- synchronizing relay

2.7 Impact of DG on power systems

The utilization of large numbers of DG units within distribution systems impacts the steady state and the dynamics of power networks. Some issues of critical importance are: voltage regulation, power quality and protection coordination in the distribution network. In the following, the potential impact of DG units on the power utility will be discussed regarding these three main points.

2.7.1 Voltage regulation

Generally, DG units provide voltage support due to their proximity to the end user [7, 20]. The voltages in distribution systems, which commonly have radial structure, are regulated using tap changing transformers at substations and/or switched capacitors on feeder. In addition, supplementary line regulators can also be used on feeders [4]. Since the voltage regulation practice depends on radial power flow from substation to loads, the utilization of DG units, which provide electrical power in different directions, may cause confusions to this practice. Feeding power from DG units can cause negative impacts on the voltage regulation in case a DG unit is placed just downstream to a load tap-changer transformer [5]. In this case, the regulators will not correctly measure feeder demands. Rather, they will see lower values since DG units reduce the observed load due to the onsite power generation. This will lead to setting the voltages at lower values than that required to maintain adequate levels at the tail ends of the feeders [5]. However, most favourable locations of DG units near the end user terminals can provide the required voltage support at the feeder nodes.

2.7.2 Power quality

High power quality requires adequate voltage and frequency levels at customer side. This may require voltage and reactive power support to achieve an acceptable level of voltage regulation. In the stand-alone mode, DG units have to involve effective controllers to maintain both voltage and frequency within standard levels. In addition to the level itself, the voltage contents of flickers and harmonics have to be kept as low as possible. The impact of DG units on these two important indices is discussed in the following.

2.7.2.1 Voltage flickers

Voltage flicker is the rapid and repetitive change of voltage that causes visible fluctuations in the light output. Therefore, it is necessary to limit voltage fluctuations to restrict the light flickers. Generally, flicker can be caused by load fluctuations as well as source fluctuations [27]. DG units have the potential to cause unwanted fluctuations and cause noticeable voltage flicker in the local power grid. Step changes in the outputs of the DG units with frequent fluctuations and the interaction between DG and the voltage controlling devices in the feeder can result in noticeable lighting flicker [4]. The standalone operation of DG units gives more potential for voltage flickers due to load disturbances, which cause sudden current changes to the DG inverter. If the output impedance of the inverter is high

enough, the changes in the current will cause significant changes in the voltage drop, and thus, the AC output voltage will fluctuate. Conversely, weak ties in grid integration mode give a chance for fluctuations to take place but with lower degrees than in the standalone mode [5].

At the time where the analysis of voltage flicker itself is a straightforward task, the dynamic behaviour of the machines and their interactions with other sources and regulators can complicate the analysis considerably [4]. The DG fluctuations may not be strong enough to create visible flickers. However, these fluctuations may cause hunting for regulators, which can create visible flickers. To dynamically model DG for its potential flicker impact, a detailed knowledge is required about the characteristics of DG units including prime mover response, generator controls and machine impedance characteristics [4, 5].

2.7.2.2 Harmonic distortion

The DG technology depends usually on inverter interface and, as a result, connecting DG units to power systems will contribute towards harmonics. Since harmonic distortion is an additive effect, the utilization of several DG units can strengthen the total harmonic distortion in some locations in the utility even if the harmonic contribution from one DG unit is negligible [5]. The type and severity of these harmonics depend on the power converter technology, the interface configuration, and the mode of operation [2]. Fortunately, most new inverters are based on the Insulated Gate Bipolar Transistor (IGBT), which uses Pulse Width Modulation (PWM) to generate quasi-sine wave [4]. Recent advances in semiconductor technology enable the use of higher frequencies for the carrier wave, which results in quite pure waveforms [2]. In all cases, the total harmonic distortion must be controlled within standard level as measured at the load terminals.

2.7.3 Protection system of the distribution network

Distribution networks have traditionally been designed for unidirectional power flow from upper voltage levels down to customers located along radial feeders [26]. This has enabled a relatively straightforward protection strategy depending on well-known aspects and experiences. Large scale implementation of DG will convert simple systems into complicated networks, which demands essential modifications in protection systems [3]. Traditional protection schemes may become ineffective and the proper coordination between protection devices of the network and the DG units is extremely important for secure operation of the network [26]. Generally, synchronous generators are capable of feeding large sus-

tained fault currents while currents from inverter-based sources can be limited to lower values [26]. The impact of DG units on the protective system is influenced by the following factors [5, 26]:

- type and size of the DG source
- voltage level at the connection point
- location of the DG unit on the network
- distribution system configuration

In addition to the contribution of DG units on the levels of fault currents, the direction of the currents from these units can adversely impact the operation of protective devices [3]. Some of the typical feeder protection problems, which may be caused by DG, are given in the following [3, 5, 25 and 26]:

- **Change of short-circuit current levels**

Short circuit studies are performed to define the fault currents at different locations in power systems to determine the interrupting ratings of protective devices, which are necessary for coordinated operation of these devices. Generally, the contribution of a small DG unit can not affect the level of the short-circuit current. However, a number of small DG units or a single large unit can cause a significant change in short circuit currents observed by the protective devices [5]. When several DG units are utilized, each protective device may observe different fault current. This can cause miscoordination and, hence, affects the reliability and safety of the distribution system [3].

- **False tripping of feeders**

False tripping is typically caused by synchronous generators, which can feed sustained short-circuit currents [26]. Without proper coordination between protection devices, there is a possibility of unnecessarily disconnection of DG units and/or feeders when faults occur on adjacent feeders fed from the same substation [26]. The basic principle of false tripping is shown in Fig 2-1 [26].

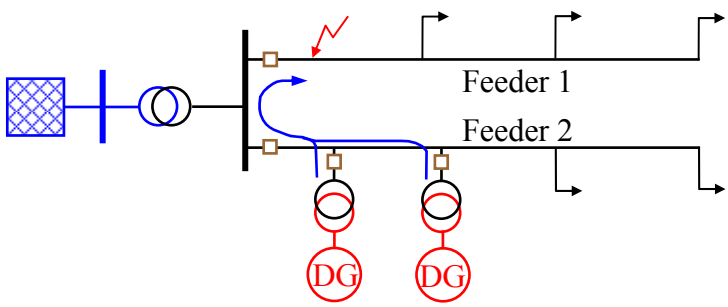

Fig 2-1 Principle of false tripping due to DG

If the total current fed by the DG units as a result of the fault in feeder 1 is high enough, the relay on feeder 2 will trip and the whole feeder will be disconnected. False tripping of healthy feeders can likely be solved by using directional overcurrent relays [26]. Using conventional relays with proper relay settings is also possible conditioned by the adequate coordination between the protection devices of the DG units and the distribution system [3].

- **Preventing the operation of feeder protection**

When a large DG unit or several small ones are connected in the distribution network, the fault current observed by the feeder protection relay may be lower than the actual fault current as seen in Fig 2-2 [26]. This may prevent the operation of the feeder protection relay in the desirable time.

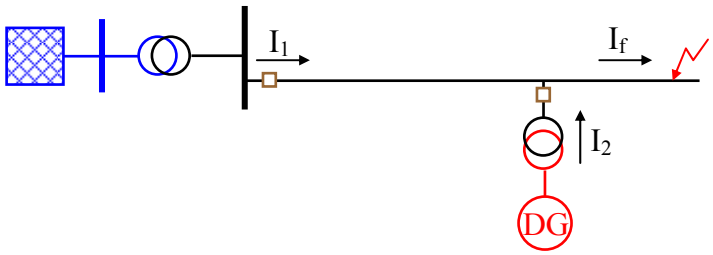

Fig 2-2 Reduction of the observed fault current as a result of utilizing DG units

Reducing the current setting of the feeder protection relay can solve this problem [26]. However, these reduced settings may conflict with the problem of unnecessary disconnection of a healthy feeder [26]. Defining the proper settings to avoid these two problems is essential for reliable operation of the network.

- **Unwanted islanding**

In some cases after a sudden loss of grid connection, parts of the network containing DG units may keep operating as an island [3, 5]. This kind of operation is undesirable since the reconnection of the islanded part to the network becomes complicated [26]. In addition, the power quality in the islanded part is not guaranteed and there is a possibility for abnormal voltage levels or frequency fluctuations [26]. Therefore, anti-islanding protection is necessary in most cases to maintain security and reliability in distribution systems [26].

Generally, the use of DG units in distribution systems will impact the protection system and new coordination strategies have to be applied to avoid the expected problems [5]. Despite the importance of this subject, it is out of the main focus of the research in this thesis.

2.8 Overview of fuel cells

FC systems were previously found to be suitable for on-site cogeneration and transportation applications. Nowadays, projects demonstrate FCs for portable power, transportation, utility power, and on-site power generation for residential applications [17]. In the following, an overview of FCs will be introduced since their modelling, simulation and economic aspects are extensively studied through the dissertation.

2.8.1 Benefits of fuel cells

FC power plants have demonstrated better reliability and durability than other sources. As they rely on chemical instead of combustion process, FCs can run continuously for long time without breakdown due to the absence of combustion and moving parts. The main advantages of utilizing FCs include [17, 28-30]:

- ***Operation at high efficiencies:*** FCs operate at higher efficiencies than combustion-based sources since they eliminate the intermediate steps of combustors and mechanical devices used in turbines and pistons. A typical electrical efficiency of FCs lies in the range of 40% to 60%, while the utilization of both electrical and thermal power increases the overall efficiency to 70% for small units and 75% for large units [30]. Unlike conventional systems, FCs operate at high efficiencies also at partial load and in many cases the part-of-load efficiency is higher than the full load value. In addition, small units provide similar high efficiencies like large units due to their modularity [29].

- ***Reduction of Air Pollution:*** emissions from FCs running on pure hydrogen are just water vapour, which could dramatically reduce greenhouse gas emission. FCs that use reformers to convert hydrocarbon fuels such as natural gas to hydrogen emit small amounts of air pollutants but still much smaller than emissions from the cleanest fuel combustion systems.

- ***Fuel flexibility:*** FC system is capable of generating electricity using hydrogen extracted from a variety of sources like natural gas, ethanol, methanol, coal, and even gasoline. Also, it is possible to utilize hydrogen from renewable sources such as biomass and from wind and solar energy through electrolysis.

- ***Possibility of cogeneration:*** in addition to the electrical energy produced in FCs, a considerable amount of useful exhaust heat is also generated as a result

of the electrochemical process. In some cases, the thermal energy produced is higher than the electrical energy. Thus, FCs are well suited for CHP operation, which contributes in increasing the unit efficiency.

- ***Modularity and simplicity of installation:*** like photovoltaic, FC stack is manufactured by augmenting individual cells in parallel (to reach the required current and capacity) and in series (to obtain the suitable voltage). This advantage enables the operator to form modules with different capacities and voltages to be suitable for different purposes starting from portable units to utility applications.

- ***Silent operation:*** FCs are quiet sources (a 40kW FC power plant has a sound level of 68dB at a point 10 feet from the cabinet) [29]. This gives the chance to place the FC plant in the load centre near the end user, which eliminates the need for long transmission.

- ***Suitable for the integration with renewable energy sources:*** FC power plants can be integrated more efficiently with renewable energy sources [31-32]. They can smooth out the oscillations occurring when using PV arrays or wind turbine and, hence, the power from these sources can be maximized without any modification in the control system. In this case, it will be possible to have significant levels of renewable power penetration. Also, the load requirements will be met more efficiently as the system reliability will be increased.

2.8.2 Disadvantages of fuel cells

The main drawback of FCs is their extremely high cost [29]. Their production cost has to be significantly reduced to become commercially comparable with the conventional power plants. Also, more efforts and researches are required to demonstrate endurance and reliability of high-temperature units [29].

2.8.3 Principle of operation of fuel cells

FCs consist of two electrodes with an electrolyte between them. The principle of operation of FCs is based on the reaction of hydrogen gas (H_2), which is supplied at the anode, and oxygen gas (O_2), which is supplied at the cathode, to form water, heat and electricity [17].

$$2H_2 + O_2 \Rightarrow 2H_2O \qquad (2\text{-}1)$$

The process is attributed to the movement of charged particles towards regions of lower electrochemical energy [17]. The charged particles in hydrogen and oxygen migrate towards each other and connect together since the final products have lower electrochemical energy [17]. It is essential to separate electrons from protons and to regulate the movement of electrons. This can be accomplished by separating the hydrogen and oxygen by an electrolyte, which completely insulates electrons and allow protons from the hydrogen atoms to move through it. An external path is formed for electrons using an electrical load to generate useful electrical energy [17]. Fig 2-3 illustrates the principles of operation of FCs.

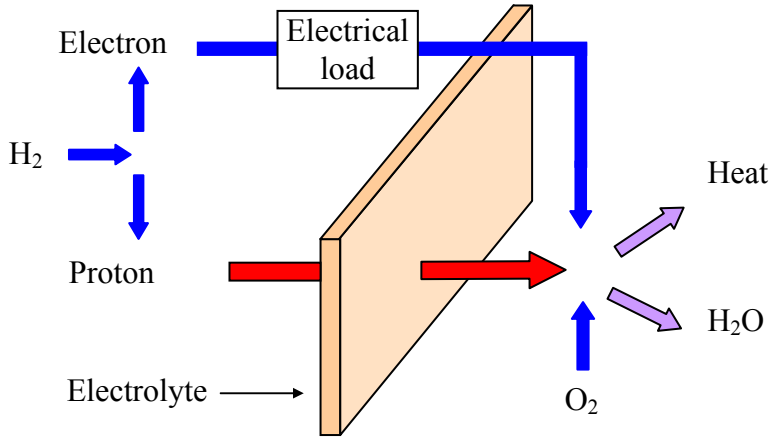

Fig 2-3 Fuel cell: principle of operation

In fact, the actual reaction occurs in two steps: the oxidation reaction at the anode and the reduction reaction at the cathode [30]. The oxidation reaction is the dissociation of hydrogen atoms into protons and electrons. The reduction reaction occurs when the oxygen atoms dissociate and bond with the protons coming through membrane and the electrons from the external circuit forming water. The reactions of Alkaline (AFC), Proton Exchange Membrane (PEMFC), Phosphoric Acid (PAFC), Molten Carbonate (MCFC) and Solid Oxide (SOFC) types are summarized in Table 2-1 [29, 30].

Table 2-1 Summary of chemical reactions in different types of fuel cells

Fuel cell type	Anode reaction	Mobile ion	Cathode reaction
AFC	$H_2 + 2\ OH^- \rightarrow 2\ H_2O + 2\ e^-$	OH^-	$\frac{1}{2}\ O_2 + H_2O + 2e^- \rightarrow 2\ OH^-$
PEMFC	$H_2 \rightarrow 2\ H^+ + 2\ e^-$	H^+	$\frac{1}{2}\ O_2 + 2\ H^+ + 2\ e^- \rightarrow H_2O$
PAFC	$H_2 \rightarrow 2\ H^+ + 2\ e^-$	H^+	$\frac{1}{2}\ O_2 + 2\ H^+ + 2\ e^- \rightarrow H_2O$
MCFC	$H_2O + CO_3^{2-} \rightarrow H_2O + CO_2 + 2\ e^-$	CO_3^{2-}	$\frac{1}{2}\ O_2 + CO_2 + 2\ e^- \rightarrow CO_3^{2-}$
SOFC	$H_2 + O^{2-} \rightarrow H_2O + 2\ e^-$	O^{2-}	$\frac{1}{2}\ O_2 + 2\ e^- \rightarrow O^{2-}$

CO_2: carbon dioxide CO_3^{2-}: carbonate ion e^-: electron H_2: hydrogen H_2O: water
OH^-: hydroxyl ions H^+: hydrogen ion O_2: oxygen O^{2-}: oxygen ion

2.8.4 Fuel cells characteristics

Depending on the Nernst's equation and Ohm's law, the stack output voltage at no load conditions can be calculated as follows [33, 34]:

$$V_0 = \frac{\Delta H - T_{ab}\Delta S}{2F} + \frac{RT_{ab}}{2F} ln \frac{X_{H_2} X_{O_2}^{1/2}}{X_{H_2O}} \tag{2-2}$$

where:

V_0	: the open circuit reversible potential
ΔH	: the total reaction enthalpy
ΔS	: the irreversible entropy change
F	: the Faraday's constant= 96485.35 $^oC\ mol^{-1}$
R	: the Avogadro gas constant = 8.314 $JK^{-1}\ mol^{-1}$
T_{ab}	: the absolute cell temperature
X_i	: the mole fractions of species

The cell resistance and the overpotentials at the anode and the cathode cause a voltage drop, where the terminal voltage (V) can be calculated by:

$$V = \left(V_0 - I \cdot (R_\Omega - R_{H_2} - R_{O_2})\right) \cdot n \tag{2-3}$$

where:

I, n	: the stack current and number of cells in series respectively
$R_\Omega, R_{H_2}, R_{O_2}$	: the voltage drop due to the internal resistance, anode reaction and cathode reaction respectively

The typical voltage-current characteristic of FCs is shown in Fig 2-4. The effect of resistive voltage drop as well as the cathode and anode overpotentials are illustrated separately [35].

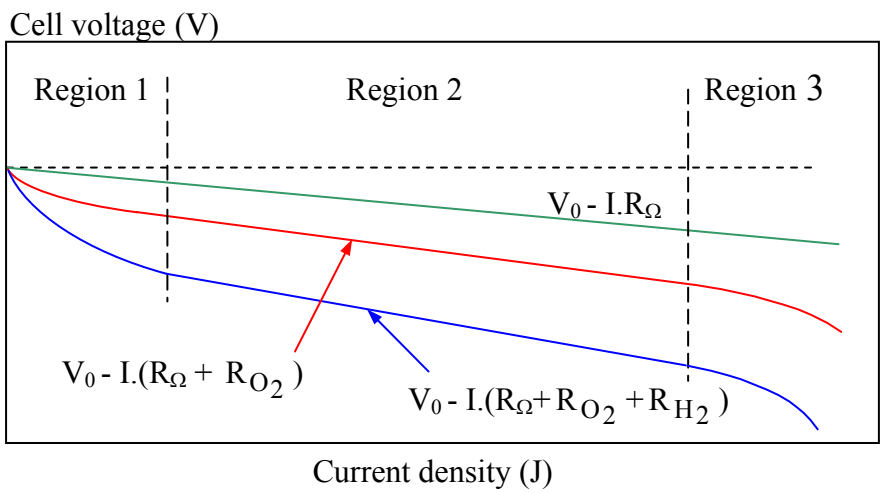

Fig 2-4 Electrical characteristics of the fuel cell

At small currents (region 1), the sharp drop in the voltage is caused by the activation energy associated with the chemical reaction [35]. At relatively higher currents, (region 2), the voltage drop is dominated by the losses in the electrode structure and the electrolyte, which is almost constant [35]. At very high currents (region 3), the voltage drop is defined by the rate of reaction diffusion [35]. Due to the limitation caused by the diffusion process, the current reaches a maximum value called the limiting current. Therefore FCs can not supply currents that exceed their limiting currents. A FC is said to have good characteristics if it has a flatter curve and a higher limiting current [35].

2.8.5 Types of fuel cells

The operating characteristics, constituent materials and fabrication techniques of FCs are significantly different. FCs are usually classified based on the electrolytic material into five main types: AFC, PEMFC, PAFC, MCFC and SOFC. In spite of the different materials and operating temperatures of each type, FCs have the same basic principles of operation. Due to the differences in materials and operating characteristics, each type is suited for specific applications. In the following a brief overview of the characteristics, advantages and disadvantages of the main types of FCs is introduced.

2.8.5.1 Alkaline Fuel Cell (AFC)

AFC was one of the first modern FCs to be developed, beginning in 1960 when it is used by NASA on space missions [17]. A liquid solution of potassium hydroxide is used in AFC as an electrolyte. Generally, the slowness of FCs is defined by the cathode reaction because it takes more time to react than the anode reaction. AFC is characterized by a faster cathode reaction than other types of FCs, which enhances its overall performance and speeds up its electrical response. The lower operating temperature (80-100°C) gives a fast-start advantage for this type of FCs, which can achieve efficiencies up to 60% [29].

However, AFCs are intolerant of carbon dioxide and, hence, it cannot use normal outside air directly as a source of oxygen [17]. A system that removes the carbon dioxide from intake air streams has to be employed. Also, the life time of this type of FCs is relatively short due to the use of a corrosive electrolyte, which gradually wears out the other parts. Since the use of expensive catalysts such as platinum results in a high manufacture cost, the use of other less expensive catalysts, such as low cost carbon and metal oxide based electrodes, is also being investigated [17].

2.8.5.2 Proton Exchange Membrane Fuel Cells (PEMFC)

PEMFCs have gained a lot of attention in the last few years as one of the most promising FC types [28, 36]. It uses a solid organic polymer poly-perflourosulfonic acid as an electrolyte [30]. The solid electrolyte in PEMFCs has a very high resistance to gas crossover, and its membrane, which is made of a Teflon-like material, represents an excellent conductor of protons and an insulator of electrons [30]. The other benefits of utilizing a solid electrolyte include the lower corrosion and the absence of the liquid management.

The efficiency of PEMFCs at rated current reaches 50% when operated on hydrogen and pressurized air. A major advantage of PEMFCs is their high power density, which is higher than any other FC except for AFC [30]. Like AFC, the low operating temperature (80-100°C) results in a quick start-up and, hence, PEMFCs are favourable in many fields like residential applications and vehicles. Another advantage of PEMFCs is their long operating life as proven in laboratory experiments. The high efficiency and power density and the fast start-up make PEMFCs an attractive alternative to conventional automobile engines [28].

The low operating temperature, however, results in slow chemical kinetics, where precious metal catalyst, typically platinum, is needed to facilitate the reactions [36]. In spite of the attempts that succeeded to reduce the required amount of platinum, further reduction of platinum is needed in order to bring the cost of PEMFCs in competition with combustion engines. Another disadvantage of PEMFCs is their sensitivity to carbon monoxide [17].

2.8.5.3 Phosphoric Acid Fuel Cell (PAFC)

PAFC has been under development for more than 20 years and was the first commercial FC [30]. This caused a significant reduction in the cost and remarkable increase in the efficiency. It utilizes a liquid phosphoric acid as an electrolyte with an operating temperature of 200°C. This temperature is high enough to facilitate the recovery of heat for water and space heating. It prevents also the water, which is produced as a sub-product, from dissolving in the liquid electrolyte [30]. Higher operating temperatures are not possible since the phosphoric acid begins to decompose at 210 °C [17]. PAFC generates electricity at more than 40% efficiency, which can be significantly increased with the use of the produced steam in cogeneration [37]. It can efficiently process impure fuels and therefore, PAFC systems are relatively cheaper than other types due to the reduction in the reformer cost [17].

The expensive catalysts of the PAFCs, typically platinum, increase the overall price of the stack [17]. Also, the high operating temperature necessitates a warm-up period, which increases the start up time. Due to their low power densities, the large size represents another disadvantage for PAFCs. PAFCs are sometimes used in vehicle applications because of their tolerance to fuel impurities. However, this is restricted by their large size, which represents a barrier for employing PAFCs in this field of applications.

2.8.5.4 Molten Carbonate Fuel Cell (MCFC)

Many of the disadvantages related to low-temperature FCs can be alleviated by increasing the operating temperature. MCFC is a promising high-temperature FC (operates at 650 °C), which uses molten alkali carbonate mixture as an electrolyte (usually consists of lithium carbonate and potassium carbonate) [30]. At these high temperatures, precious metal catalysts are not required for the FC reactions, rather, the cell reactions occur with nickel catalysts [30]. In addition, the heat available from the stack is high enough for cogeneration applications [29]. The rejected cell heat can also be used to drive a gas turbine and/or produce a high-pressure steam for use in a steam turbine. Furthermore, internal reforming can be utilized, which reduces the size and the cost of the unit. Another advantage of the MCFC is the possibility of operating efficiently with CO, hydrogen, natural gas, propane marine diesel and simulated coal gasification products [30].

However, MCFC needs a source of CO_2 at the cathode (usually recycled from anode exhaust) to form the carbonate ions [30]. The high operating temperature results in some material problems, particularly mechanical stability that reduces the unit life. Therefore, the use of stainless steel as the cell hardware material is required [30]. To achieve economically viable operation of MCFC, it is designed for median-size and large stationary power applications. However, the target markets for MCFC technology include small DG systems for utilities as well as building cogeneration systems at sizes of 0.1 to 2.0MW [30].

2.8.5.5 Solid Oxide Fuel Cells (SOFC)

The SOFC has the longest continuous development period, starting in the late 1950s [9, 10, 38]. It usually uses a solid ceramic material (yttria-stabilised zirconia) instead of a liquid electrolyte, allowing the operating temperature to reach 1000 ^{o}C, which is the highest temperature of all FC systems [29, 30]. The solid ceramic material represents an excellent insulator for negatively charged ions at high temperatures. Like MCFC, SOFC can use carbon dioxide as well as hydro-

gen as its direct fuel but without any requirements for CO_2 at the cathode. The high temperature helps to increase the unit efficiency and gives the SOFC the ability to use a wide variety of less expensive catalysts than the low temperature FCs. The configuration of SOFC is also simpler due to possibility of internal reforming [29]. The high operating temperature gives also the facility for developing cogeneration systems or using hybrid configurations, where SOFC is augmented with gas turbines and/or steam units [38]. Furthermore, the solid electrolyte eliminates the corrosion and management problems, which regularly happen with liquid electrolytes.

On the other hand, the high operating temperature has some disadvantages since it speeds up the breakdown of the cell components, which shortens the life of many parts of the unit [30]. SOFCs are being considered mainly for medium and large-scale power generation. However, efforts succeeded to develop SOFC for small applications. Since the electrolyte is solid, the cell can be formed in a variety of configurations such as tubular and planar types.

Table 2-2 summarizes the different properties of the five mentioned types of FCs including the operating temperature, utilized gas and oxidant, system efficiency and electrolyte materials [17, 29, 30, 36].

Table 2-2 Properties of the main types of fuel cells

Type	Operating temperature	Cell gas	Oxidant	Efficiency	Electrolyte
AFC	80~100 ^oC	Pure H_2	Pure O_2	50~60 %	Potassium hydroxide
PEMFC	80~100 ^oC	H_2	O_2, air	35~50 %	Solid organic polymer
PAFC	160~200 ^oC	CH_4 or H_2	O_2, air	40 %	Liquid phosphoric acid
MCFC	650 ^oC	CH_4, H_2 or coal gas	O_2, air	45~65 %	Molten carbonate
SOFC	800~1000 ^oC	CH_4, H_2 or coal gas	O_2, air	50~70 %	Solid ceramic material

2.8.6 Applications of fuel cells

In spite of the similarity in the operating principles, the variety of materials, operating temperatures, power densities and utilized gases expands the applications of FCs to cover most of known fields. Some of these applications are given in the following [30, 36].

2.8.6.1 Portable Power

Portable power refers to systems that generate power of few watts up to few hundred watts. In portable power applications, FCs would be merged to the electronic device with a small container of fuel or compressed hydrogen inserted into

an inlet port [36]. A very small blower can be used to supply air, which can also be supplied by natural convection. A new fuel container can replace the old one when the fuel is completely depleted [30]. Unlike batteries, recharging would not be necessary and also new fuel container would be lighter and less expensive. Examples include power for portable electronic devices such as laptops and power for soldiers deployed in the field.

2.8.6.2 Transportation

FCs are expected to thrive in the field of vehicle application as they represent a clean-energy technology [28]. Many attempts are directed to advance the FC technology to produce a power source at a cost and volume that are competitive with the existing internal combustion engine. PEMFC has attained a special attention due to its fast acceleration rate and high power densities, which reduces the required accommodation place. Most of the technical objectives are directed to decrease the production cost and to solve the fuel supply problems [36].

2.8.6.3 Stationary Power generation

FCs are promising sources for stationary applications including distributed power generation for utilities, backup power generation industry and cogeneration applications [17, 28]. As DG units, FCs are advantageous due to their high efficiency, modularity, and low environmental impacts. Also, they can be beneficial and attractive sources in remote areas to solve many problems in the congested distributed systems. In these cases, it would be more economical to add a new decentralized source near the load than upgrading the utility grid. For large-scale stationary applications, FCs will operate continuously and, hence, the long time required to reach the operating temperature from a cold start, which characterizes high-temperature FCs will not represent an important drawback. Thus, MCFC and SOFC systems can be considered, where the energy content in the exhaust gas can also be utilized to drive a downstream turbine producing more useful electrical energy. For small-scale stationary applications, FCs can be used near the end users to provide power, and in most cases heat, to residential homes and small businesses. During the summer, FCs serving a residence can provide electricity while supplying thermal energy for heating water. In the winter they can meet electrical demand and supply thermal energy for space and water heating. In this case, the produced thermal energy can offset some of the electricity-production cost reducing the overall energy costs [29, 36].

2.9 Overview of micro-turbines

MTs are small high-speed gas turbines that produce power in the range of 25 to 500kW [13, 52]. They operate on the same principles of conventional gas turbines depending on Brayton (constant pressure) cycle [13, 15]. Small gas turbines are firstly developed by Allison in the 1960s, where the first application was to supply a radar set and engagement control station of U.S. Army Patriot Missile system [15]. The technical and manufacturing developments during the last decade have encouraged the utilization of MTs in many applications including their utilization as DG units.

2.9.1 Construction of micro-turbines

The construction of the MT unit is shown in Fig 2-5. The main components include an air compressor, a combustor, a recuperator, a turbine and a generator.

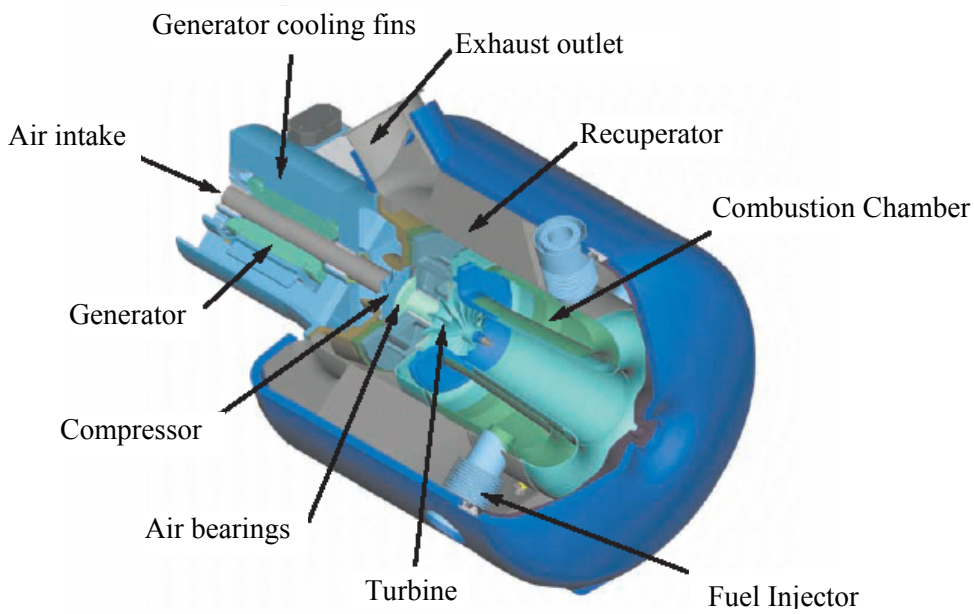

Fig 2-5 Construction of the micro-turbine unit

Filtered air at atmospheric pressure and temperature is pressurized in the compressor before entering the combustor. A controlled amount of injected fuel is mixed with the compressed air in the combustor and the mixture is ignited. The combustion products at high temperature and pressure flow and expand over the turbine blades to produce mechanical energy. Most constructions of MTs depend on a single shaft designed to rotate at high speeds in the range of 50000 to 120000rpm [15]. Hence, a high-speed Permanent Magnet Synchronous Generator "PMSG" is used to produce variable-voltage AC power at high angular frequen-

cies up to 10000rad/s. A part of the extracted horsepower in the turbine is used for driving the air compressor. The recuperator is used to improve the overall efficiency of the system by transferring the waste heat from the exhaust gas to the combustion air stream. The high frequency of the generated power can be reduced using cycloconverters or rectifier-inverter systems.

2.9.2 Advantages of micro-turbines

The newly developed MTs have the following advantages [15]:

- low installation and infrastructure requirements, about 700 $/kW
- low maintenance costs, about 0.005$/kWh
- smaller and lighter than other engines with the same capacity
- reliable and durable due to the simplicity of the structure
- fuel flexibility since they can run on a variety of fuels including natural gas, diesel, ethanol, propane and gasoline
- high efficiency, with fuel energy-to-electricity conversion reaching 25%-30%
- possibility of cogeneration by using the waste heat recovery, which could achieve overall energy efficiency levels reaching 75%
- environmental superiority of MTs operating on natural gas

2.9.3 Applications of micro-turbines

The availability of small, low cost, high efficient MTs is well suited for the following applications [15]:

- firm power for isolated communities, small commercial buildings and light industry
- peak shaving for utility-system in order to decrease the required incremental cost to serve additional loads
- standby and emergency power for more reliable operation of the utility and with important loads
- uninterruptible power supply (UPS) since they provide low initial cost, low maintenance requirements and high reliability

Chapter 3

Dynamic Modelling of Fuel Cells

3.1 Introduction

Besides the studies that concentrate on the use of FCs in small-size applications, the recent technology advancs have extended their energy products to include large-scale electricity generation [39]. The development of FCs has been extensively discussed in the technical literature [35-41]. However, most studies concern with the static performance depending on the Nernest and Butler-Volmer equations [31, 40]. Recently, there have been some studies about the dynamic performance of the FCs with respect to thermo-dynamical behaviour [10, 29]. The investigation of any generating unit, however, requires dynamical models, which can describe the physical system. The modelling process depending on a detailed theoretical analysis is very complicated and a time consuming task especially when the parameters are not easy to be defined. This is the case when considering FCs where the electrical, chemical and thermo-dynamical processes interact strongly with each other in a nonlinear form.

In this chapter, a simplified third-order mathematical model is proposed to represent the dynamical behaviour of the FC including temperature and pressure variations. Furthermore, a heat recovery system is simulated for CHP applications. For more detailed analysis, a recurrent ANN-based model, which can be obtained directly from measured input/output data, is developed to capture the dynamics of the FC. The objective is to avoid the complicated mathematical analysis and to develop flexible models with proper orders for FCs.

3.2 Proposed dynamic equivalent circuit for fuel cells

The FC generating unit consists of three main parts: the reformer, the stack and the power conditioner. The task of the reformer is to process the raw fuel to get a hydrogen-rich gas. The reformed fuel and the oxidant are directed with an electrochemical process through the stack (power section) to combine. As a result of this combination, DC power is generated and heat and water are produced. A power conditioner is required for DC/AC power conversion, where the AC power can then be used for either utility or stand-alone applications. These processes are

accomplished at high efficiency since the FC has no moving parts. In addition to the three main components, there are also three auxiliary components, namely the air management, water management and thermal management subsystems [30]. The construction of the FC system is shown in Fig 3-1.

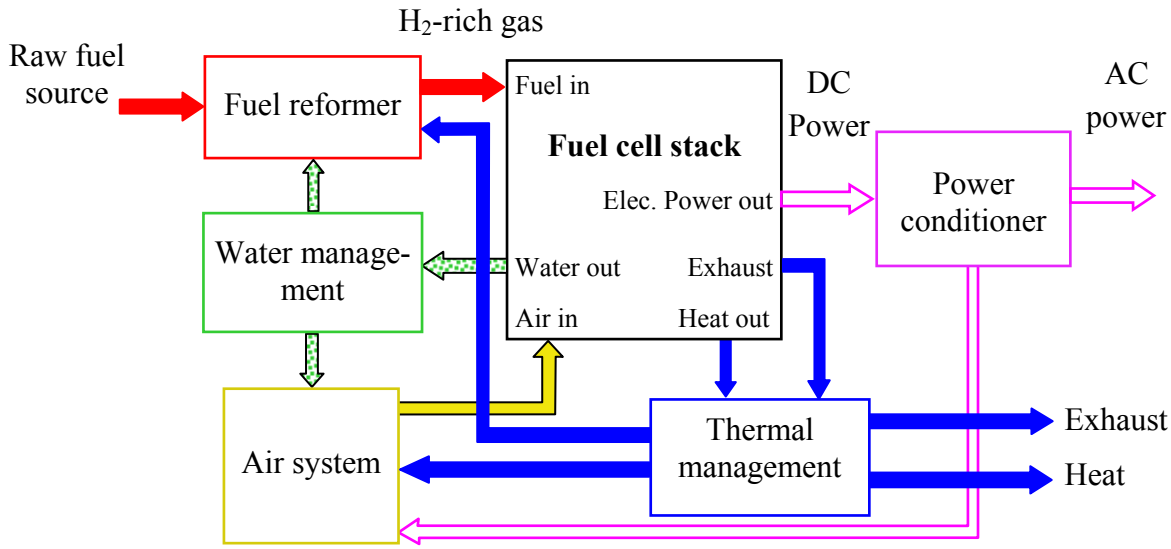

Fig 3-1 Block diagram of the fuel cell

Due to the interaction between FC components with each other in a complex nonlinear form and due to the difficulty of defining its parameters accurately, the task of getting a complete precise model for the FC system is extremely complicated [41]. It is suggested to use a simplified equivalent circuit to model the dynamic performance of the FC taking into account the main electrical processes within the unit. Physical interactions and relations can be approximated by electrical models with adequate accuracy.

The model of the reformer can be simulated by a first-order time delay element as it slows down the variations of the hydrogen-rich gas to follow the variations in the input raw fuel. This causes similar delays to the electrical quantities. Since both anode and cathode reactions need time to be accomplished, similar delay takes place in the stack. Normally, the time constant of the reformer delay is much longer than that of the stack [41]. Depending on the type of the cell, steady-state characteristics of FCs are defined by the voltage-current relation as described in section 2.8.4 (see Fig 2-4). A non-linear resistance is introduced to account for all kinds of voltage drops within the cell. Firstly, the voltage drop is calculated by subtracting the operating voltage from the open-circuit value. Then, the voltage drops are divided by the corresponding values of supplied currents to get the resistance at all operating conditions. Nonlinear functions are developed

using the curve fitting technique to derive the resistance as a function of the supplied current. This can be done for all FC types, which have different voltage-current characteristics. Typical voltage-drop and the nonlinear loss resistance curves are shown in Fig 3-2. Furthermore, a series inductor is inserted to take into account the time constant associated with the current.

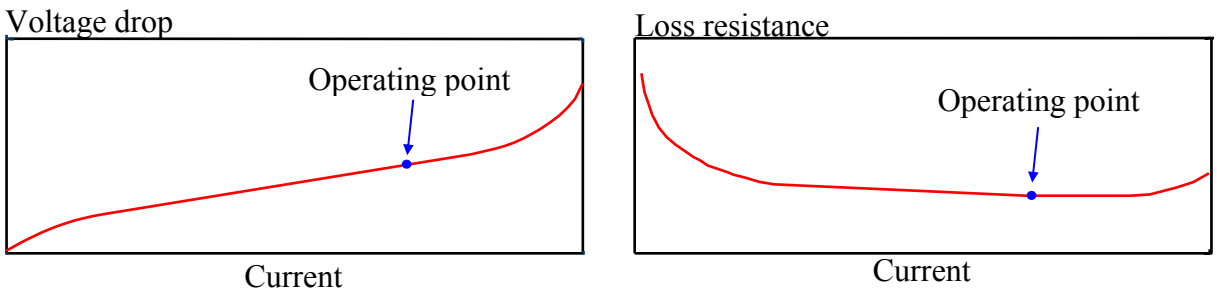

Fig 3-2 V-I characteristic and loss resistance

A DC/AC Pulse-Width Modulation (PWM) inverter is used to convert the stack DC power to AC power as shown in Fig 3-3 using the general terminology S for the inverter switches [42]. The carrier and modulating waves used to control the turn-on and turn-off of the inverter switches are also illustrated in the figure. During the conversion to AC power through the inverter, both the frequency and the voltage (or reactive power) from the FC are regulated. The AC voltage is calculated for a balanced three-phase system based on the DC value and assuming that the ratio of the carrier-wave frequency to the modulating wave frequency is greater than 9 [42]. The rms value of the fundamental component of the modulated line-line voltage is describes by the following equation [42]:

$$V_{L,rms} = \frac{\sqrt{3}}{2\sqrt{2}} M.V_{dc} \qquad 0 \le M \le 1 \qquad (3\text{-}1)$$

where:

V_{dc} : output DC voltage from the stack
$V_{L,rms}$: rms fundamental component of the line modulated voltage
M : modulation index (ratio) $=V_m/V_c$
V_m, V_c : peak modulating and carrier voltages respectively

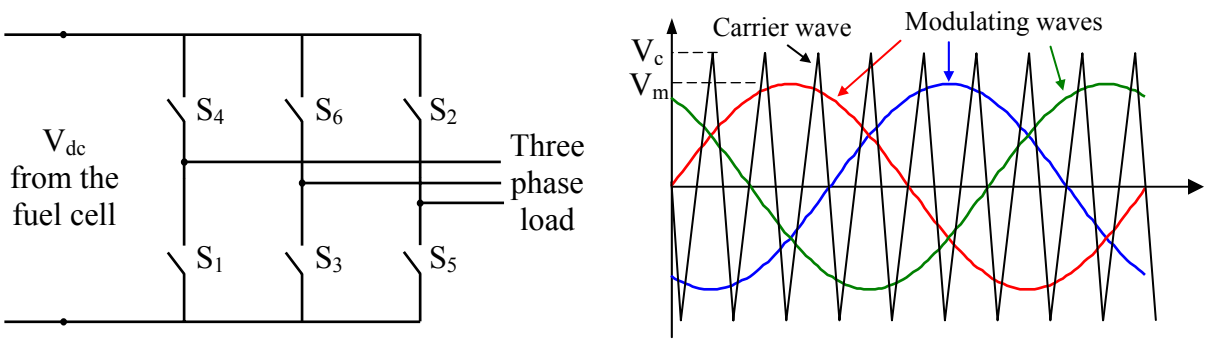

Fig 3-3 Three-phase PWM inverter

Fig 3-4 illustrates the proposed equivalent circuit of the FC unit.

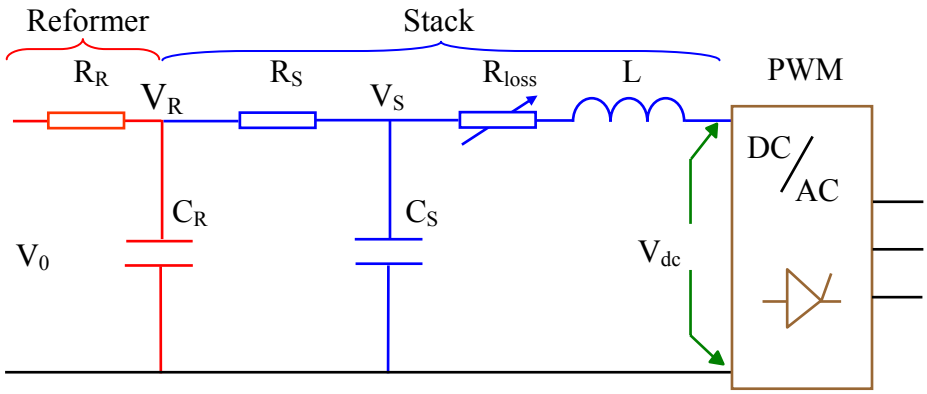

Fig 3-4 Dynamic equivalent circuit of the fuel cell

where:

V_0 : the open circuit reversible cell potential (representing the input fuel rate)

V_R : a signal representing the output from the reformer (input to the stack)

R_{loss} : nonlinear-loss resistance

The time constants of the reformer (τ_R) and the stack (τ_S) are given in terms of the equivalent-circuit parameters by the following equations [41]:

$$\tau_R = R_R \,.\, C_R \tag{3-2}$$

$$\tau_S = R_S \,.\, C_S \tag{3-3}$$

This simple third-order non-linear equivalent circuit is suitable to approximate the FC behaviour as seen from the network side. The model is flexible and the values of the time constants and inductance can be modified according to the type and capacity of the unit. On the other hand, the loss resistance is derived depending on the type of the FC based on its V-I characteristic. Thus, different types and capacities can be considered by selecting the suitable parameters in the equivalent circuit.

The variations of the operating temperature and pressure affect the open circuit reversible cell potential of the FC (V_0). This effect can be introduced by considering the value of the open circuit reversible potential as a function of the pressure and temperature. The general form of this dependency is given as follows [29]:

$$V_0 = V_0^S + \Delta V_T + \Delta V_P \tag{3-4}$$

where

V_0^S : the value of V_0 at standard temperature and pressure conditions

ΔV_T : change in the reversible potential due to change of the temperature

ΔV_P : change in the reversible potential due to change in the pressure

Empirical formulas can be used to describe ΔV_T and ΔV_P for each FC type. For instance, a change in the operating pressure from (P_b) to (P) and a change in the operating temperature from (T_b) to (T) result in a change in the reversible potential of MCFC as follows [29]:

$$\Delta V_P\,(\text{mV}) = 76.5 \log (P/P_b) \tag{3-5}$$

$$\Delta V_T\,(\text{mV}) = \begin{cases} 2.16 \cdot (T - T_b) & 575\ ^oC \le T < 600^oC \\ 1.40 \cdot (T - T_b) & 600\ ^oC \le T < 650^oC \\ 0.25 \cdot (T - T_b) & 650\ ^oC \le T < 700^oC \end{cases} \tag{3-6}$$

Similar relations can be used for the other types of FCs to modify the input signal in the equivalent circuit so as to take into account the effect of varying the operating pressure and temperature [29].

A FC unit is simulated in the stand-alone mode to supply an isolated constant-resistance load. The parameters used in this model are given in appendix A. However, these values can be changed depending on the capacity and the type of the unit. Fig 3-5 illustrates the voltage response of the FC to a 20% step decrease in the load resistance. The input fuel rate is held constant and, hence, the open circuit reversible potential is also unchanged. However, the increase of the supplied current results in more voltage drop and, as a result, the steady-state terminal voltage decreases.

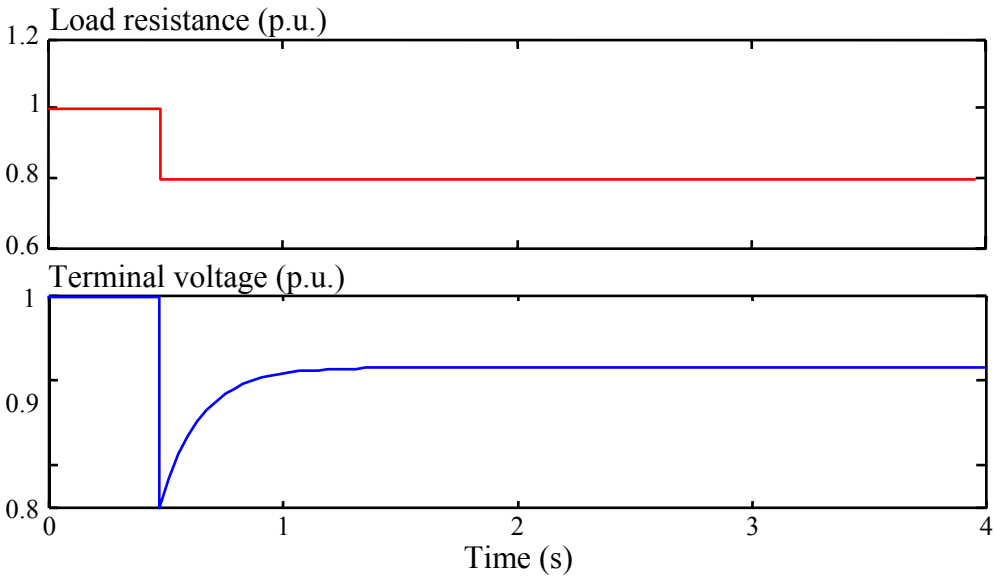

Fig 3-5 Response of the FC to a 20% step decrease in the load resistance

Another disturbance is a 20% step decrease in the input fuel rate, while the load resistance is maintained constant. The voltage response is shown in Fig 3-6, where the terminal voltage is decreased as a direct result of the reduction in the input signal but with certain time delay defined by equations (3-2) and (3-3).

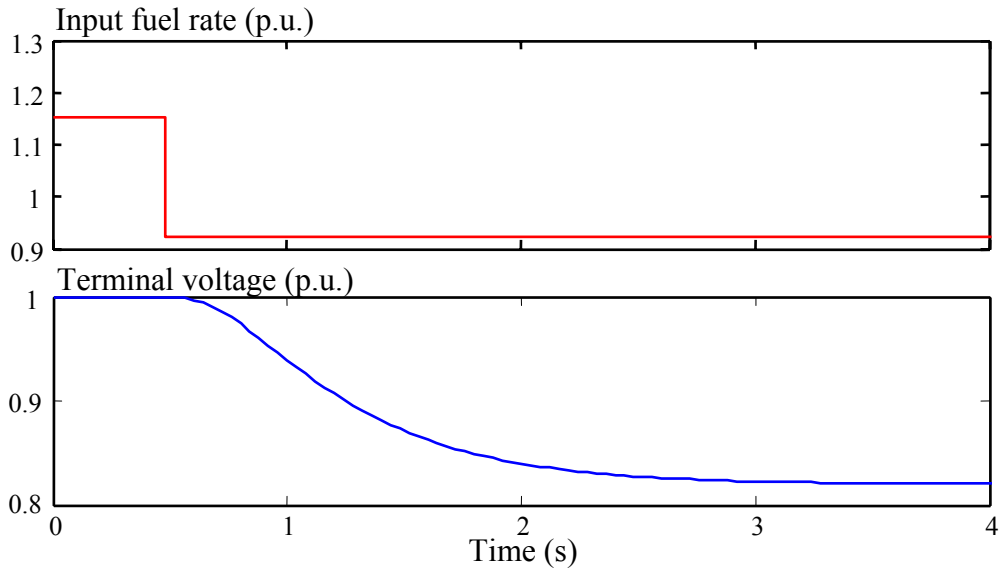

Fig 3-6 Response of the FC to 20% step decrease in the input fuel rate

Fig 3-7 and Fig 3-8 illustrate the response of the FC to simultaneous disturbances in the load and the input fuel rate. In the first case, the load resistance is decrease by 20% and the input fuel rate is increased to 120 %, while a 20% step increase in the load resistance and a 30% step decrease in the input fuel rate are simulated in the second case. In both cases, the variations of the load resistance cause sudden changes in the terminal voltage, while the response to the variations in the input fuel rate requires certain delay time.

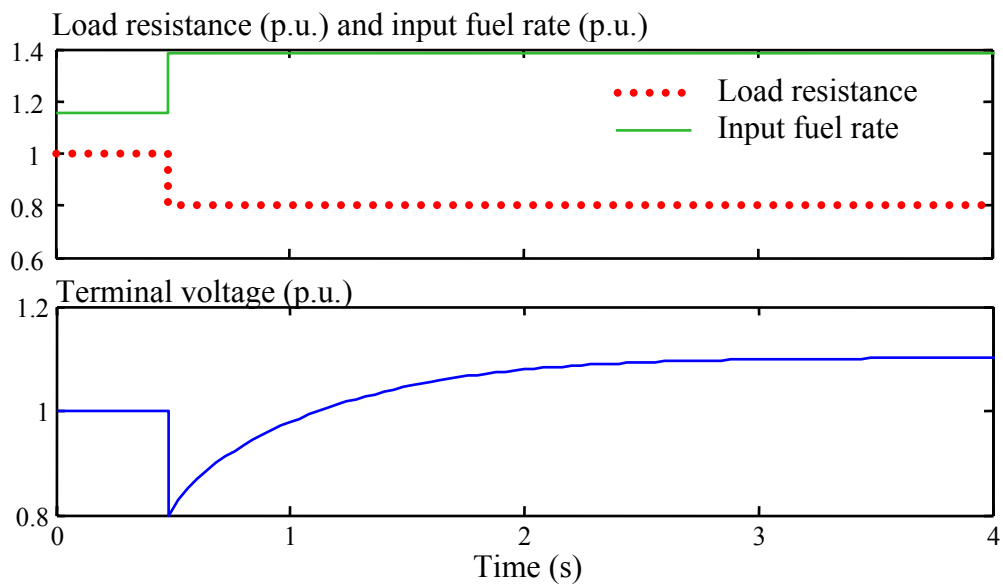

Fig 3-7 Response to 20% step decrease in the load resistance and 20% step increase in the input fuel rate

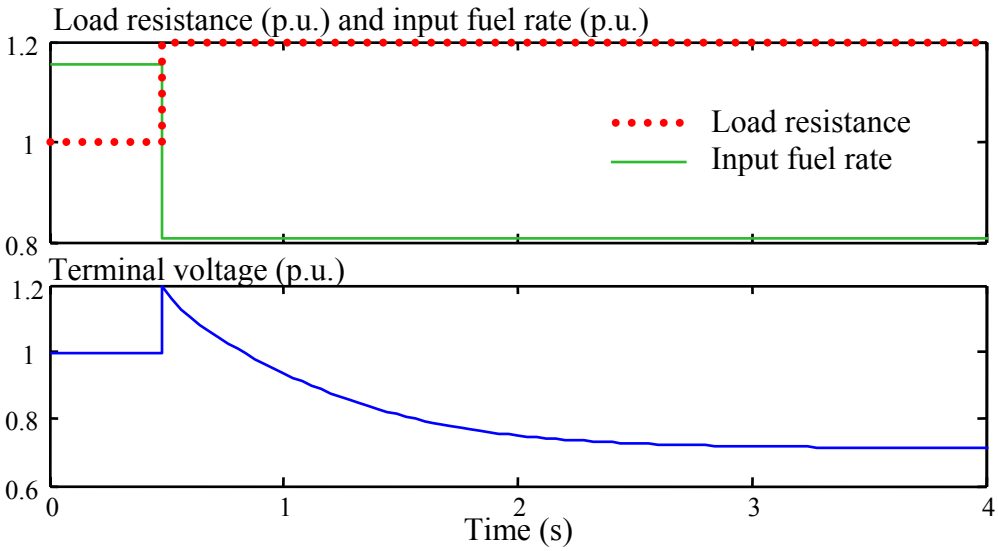

Fig 3-8 Response to 20% step increase in the load resistance and 30% step decrease in the input fuel rate

It is important to notice that no controllers are considered, at this stage, to regulate the performance of FC units. Suitable controllers, however, are then designed depending on the application in which the FC unit will be used.

3.3 Heat recovery system

A heat recovery system is required with each FC unit to maintain the operating temperature of the stack constant at its rated value at all conditions. The excess thermal energy can be absorbed using a working fluid and then can be used for water and space heating or other applications depending on the operating temperature. A simple heat recovery system, which consists of a heat exchanger and a water storage tank, is shown in Fig 3-9.

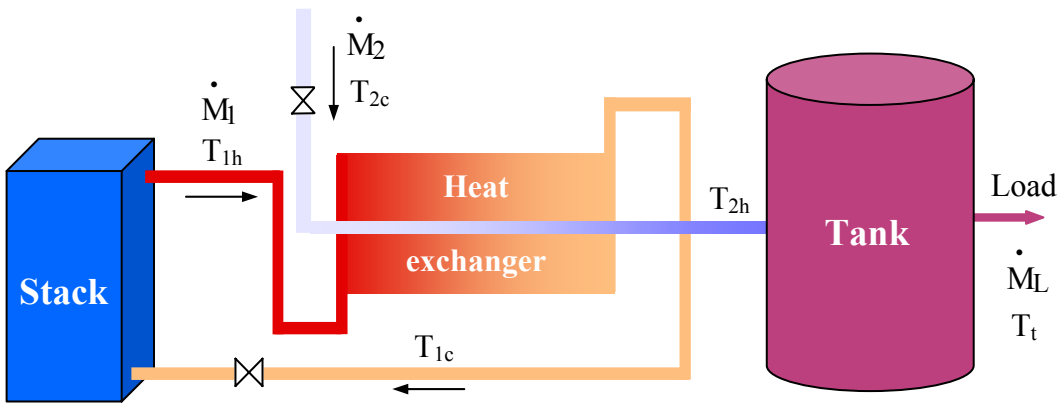

Fig 3-9 A simple heat recovery system

The fluid used to absorb the thermal power from the stack is used at the same time for water heating in the heat exchanger. The cold water flows through the inner tube of the heat exchanger, where it is heated by the surrounding hot fluid,

which flows concurrently around the inner tube. The heated water is stored in a special tank and is then used to meet the thermal load demand. To develop a suitable thermal model of the heat recovery system, the following assumptions are made to simplify the modelling process [43]:

- the heat exchanger and the storage tank are sufficiently isolated and, as a result, no heat transfer to the surroundings is assumed
- the liquid volumes in the shell and the inner tubes are assumed to be constant
- the fluids under consideration have constant chemical and physical properties
- the overall heat transfer coefficients are constant

The generated thermal power in the stack depends on the generated electrical power as in equation 3-7. The relation is almost linear with more curvature at higher power values.

$$Q_{gen} = f(P_{ele}) \tag{3-7}$$

The stack temperature depends on both the generated and the absorbed thermal power and the differential equation describing this temperature is given as [44]:

$$\rho_S \cdot C_P^S \cdot V_S \cdot \frac{dT_S}{dt} = Q_{gen} - Q_{abs1} \tag{3-8}$$

where

V_S, ρ_S, C_P^S : the stack volume, mass density and average specific heat respect.

T_S : Stack operating temperature

Q_{gen} : Generated thermal power in the stack of the FC

Q_{abs1} : Absorbed thermal power by the fluid between the stack and the heat exchanger

The absorbed thermal power from the stack is calculated according to the mass flow rate of the fluid between the stack and the heat exchanger and its average specific heat in addition to the difference between temperatures at entrance and exit of the heat exchanger [44]:

$$Q_{abs1} = \dot{M}_1 \cdot C_P^1 \cdot (T_{1h} - T_{1c}) \tag{3-9}$$

where:

$\dot{M}_1$: mass flow rate of the cooling fluid

C_P^1 : average specific heat of the cooling fluid

T_{1c}, T_{1h} : cold and hot temperatures of the cooling fluid respectively

Considering energy balance relations in the heat exchanger, the following equations can be used to describe the temperatures of the two fluids at the exit of the heat exchanger [43, 45]:

$$\frac{dT_{1c}}{dt} = \frac{1}{L \cdot \rho_1 \cdot a_1}\left(\dot{M}_1 \cdot (T_{1h} - T_{1c}) + \frac{L \cdot U \cdot \pi \cdot d}{C_P^1}(T_{2h} - T_{1c})\right) \tag{3-10}$$

$$\frac{dT_{2h}}{dt} = \frac{1}{L \cdot \rho_2 \cdot a_2}\left(\dot{M}_2 \cdot (T_{2c} - T_{2h}) + \frac{L \cdot U \cdot \pi \cdot d}{C_P^2}(T_{1c} - T_{2h})\right) \tag{3-11}$$

where

T_{2c}, T_{2h} : cold and hot temperatures respect. of the water in the heat exchanger

L : length of the heat exchanger tube

ρ_1, ρ_2 : the mass densities of the two fluids in the heat exchanger

a_1, a_2 : cross section areas of the outer and inner tubes of the heat exchanger respectively

$\dot{M}_2$: mass flow rate of the water in the heat exchanger

C_P^2 : average specific heat of the water in the heat exchanger

U : heat transfer coefficient in the heat exchanger

d : internal diameter of the inner tube

The absorbed thermal power from the fluid in the shell tube to be transferred to the water in the inner tube is given by [43, 44]:

$$Q_{abs2} = \dot{M}_2 \cdot C_P^2 \cdot (T_{2h} - T_{2c}) \tag{3-12}$$

To calculate the mass of the stored water in the tank, the difference between the mass flow rates of the input and the output water into and out of the tank can be used as follows [44]:

$$\frac{dM_t}{dt} = \dot{M}_2 - \dot{M}_L \tag{3-13}$$

Finally the temperature of the stored water depends on the energy balance of the tank. Assuming that the absorbed thermal power by the water in the inner tube of the heat exchanger will completely be transferred to the water in the tank, the following differential equation can be used to calculate the temperature of the stored water in the tank [44]:

$$Q_{abs2} = M_t \cdot C_P^W \cdot \frac{dT_t}{dt} + U_t \cdot A_t \cdot (T_t - T_a) \tag{3-14}$$

where

$\dot{M}_L$: water mass flow rate to the thermal load

M_t : water mass in the tank

Q_{abs2} : absorbed thermal power by the water in the inner tube

C_P^W : average specific heat of the water in the tank

T_t, T_a : temperature of water in the tank and the ambient temperature respect.

A_t, U_t : tank surface area and its heat transfer coefficient respectively

The parameters of a heat recovery system with MCFC are given in appendix B. However, these parameters as well as the value of the stack-reference temperature depend on the type of the FC itself.

For stable operation of the FC with the heat recovery system, the temperatures of the stack and the stored water in the tank have to be held constant for all conditions. To achieve this objective, two PI controllers are designed to regulate the mass flow rates of the fluids as shown in Fig 3-10. Feedback signals from the stack and water temperatures are compared with reference values (T_s^{ref} for the stack and T_2^{ref} for the water in the tank) to produce the proper correction signals from the controllers.

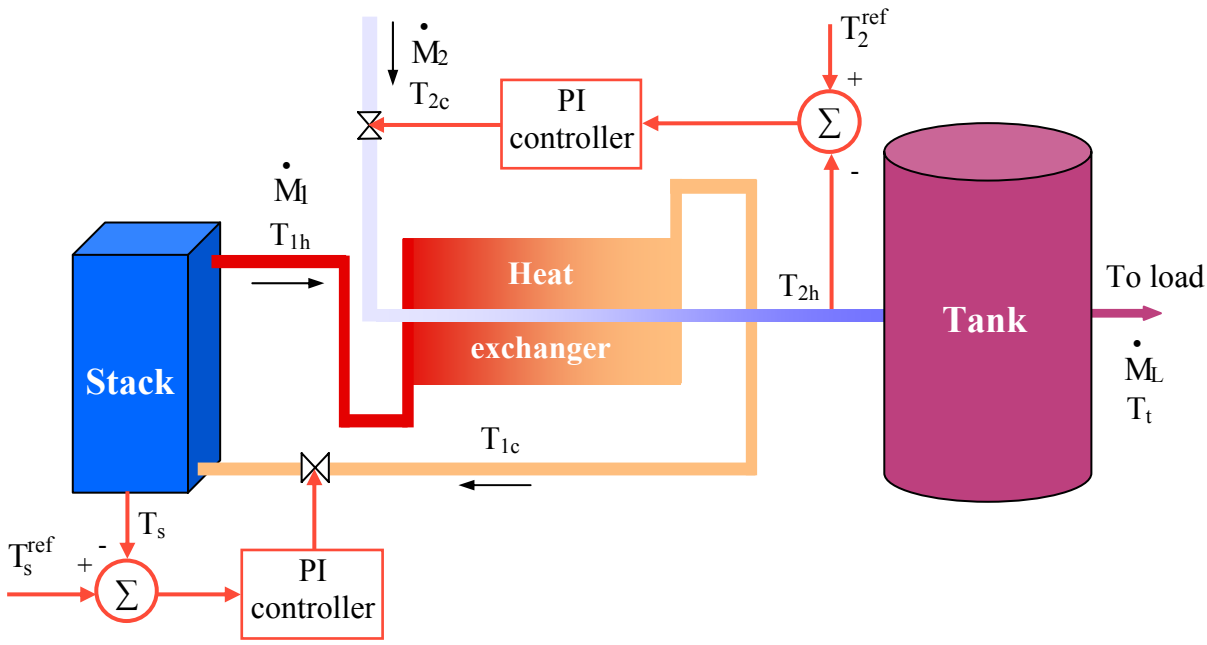

Fig 3-10 Controllers associated with the heat recovery system

The model of the heat recovery system is augmented with the dynamic model presented in section 3.2 to simulate the dynamic performance of the FC system.

At each time interval, the electrical power generated in the FC is used to calculate the thermal power according to equation (3-7). Then, the thermal model is activated to calculate all thermal variables including the stack temperature using equation (3-8). The stack temperature is used according to empirical formulas such as equation (3-6) to define the change in the reversible potential as given by equation (3-4). A PI controller is used to regulate the terminal AC voltage of the unit and the input fuel rate is also controlled to supply the required load demand. Results related to two disturbances are illustrated in Fig 3-11 and Fig 3-12. The first disturbance is a 15% step increase in the load impedance, while the second one is a 10% step decrease in the load impedance.

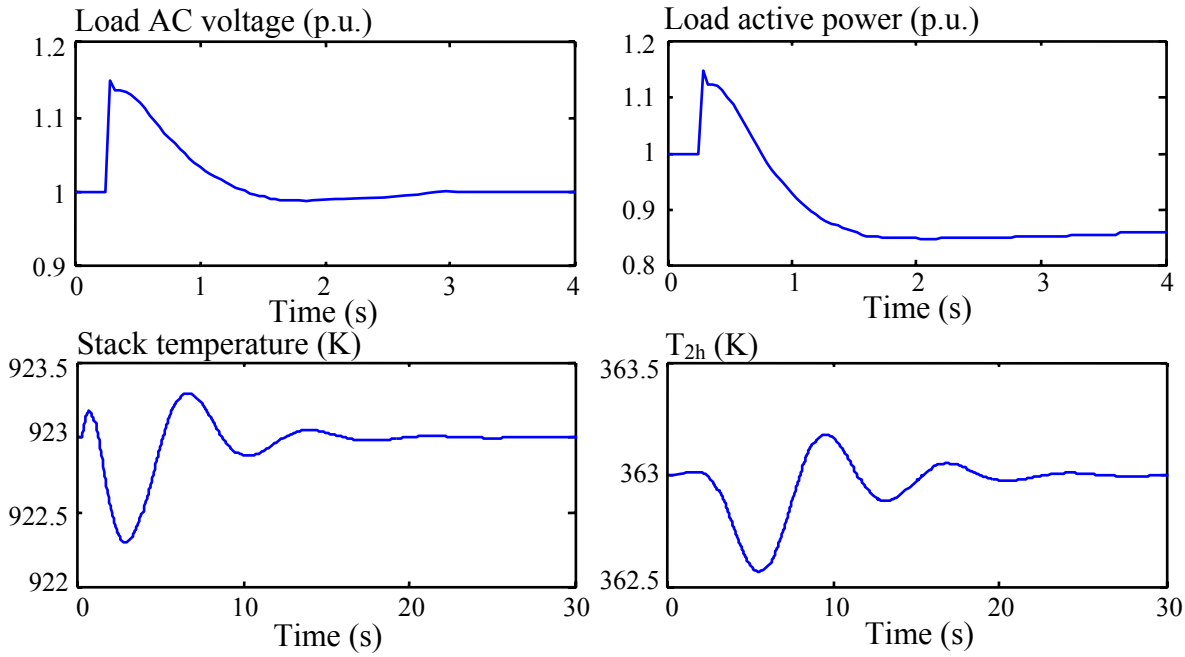

Fig 3-11 Response of the FC to a 15% step increase in the load impedance

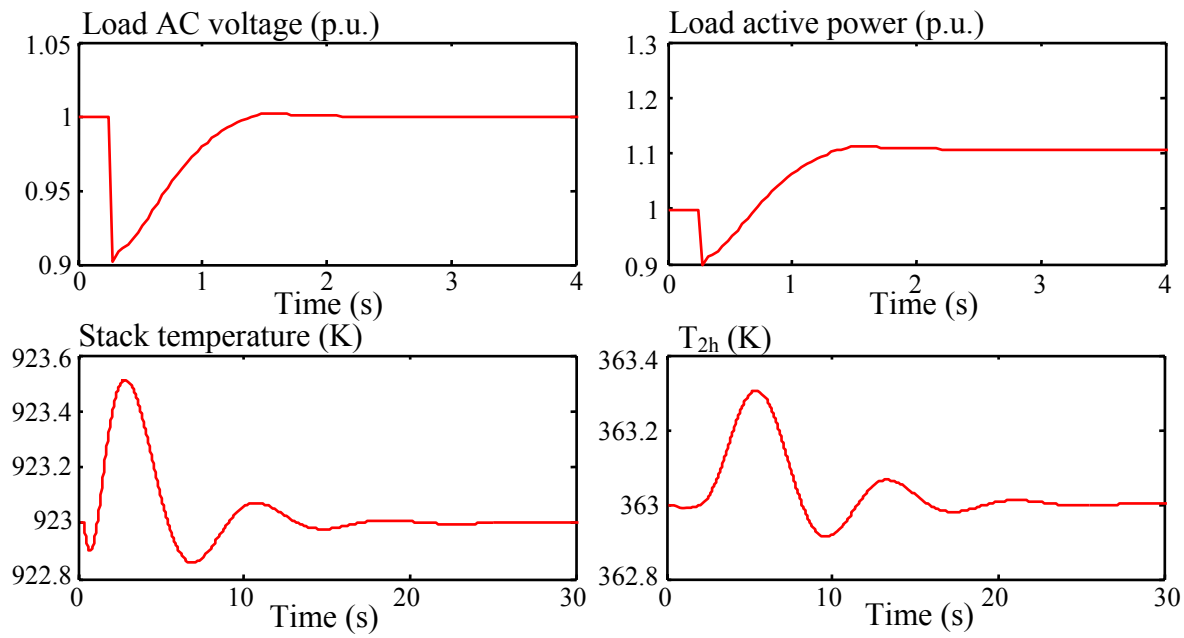

Fig 3-12 Response of the FC to a 10% step decrease in the load impedance

The electrical variables have lower time constants compared to that of the thermal variables. Therefore the voltage takes only 4 seconds to reach its new steady-state value, while the temperatures require about 30 seconds to finally restore their final values.

3.4 ANN-based dynamic modelling of fuel cells

The abovementioned model of the FC takes into account the main dynamic processes in the unit. However, it is required in some cases to extend the study by introducing other factors affecting the dynamic behaviour like fuel and air utilization factors and the air humidity. In this case it will be difficult to develop a suitable dynamic model using mathematical theories. During the past years, ANNs have gained a wide success in many applications and, therefore, they are being applied now to an increasing number of real-world problems of considerable complexity [46-49]. One of the applications in which the ANN is successfully used is the dynamic modelling, when the physical processes are not understood or highly complex. The use of feedforward ANN for dynamic modelling has proven successful in many steady-state and some dynamic applications. Recurrent networks are a new generation of ANNs, which implement feedback loops. Consequently, they are suitable for use with dynamic systems [46].

A proposed approach is to use a recurrent ANN to simulate the performance of the FC with all details depending on input/output data. Thus, all factors affecting the dynamic behaviour of the FC can be taken into account. It will be required to measure the inputs and outputs of the FC at different operating conditions to develop a database for training and testing the ANN. For comparison reasons, the proposed technique is highlighted depending on data obtained from the proposed equivalent circuit under various disturbances. The objective is to verify the applicability of the proposed approach and the capability of the recurrent ANN to resemble the dynamics of the FC. Similar procedures can be followed to develop the ANN-based model for any FC type using suitable measured data.

3.4.1 ANN configuration

There are many ways to employ the conventional ANNs for dynamic modelling. The recurrent networks are one possible solution, where recursive loops are used to feed the output signals back to the input layer with time delays. However, training such networks is relatively difficult in many situations and the convergence in the training process is not guaranteed [46]. An alternative is to modify

the processing in the neurons and the connections between them to introduce the dynamic action. This structure, however, still requires more investigations to be suitably applicable [46]. The most straightforward way is to use time histories to incorporate dynamics. Past inputs and/or outputs are used to predict the present outputs, where the training process is accomplished offline. A drawback of this method is the accumulation of error when the developed model is used in the online mode. The error at each step affects the following steps and also the overall performance of the model. This problem does not arise in the training phase since predefined values are used at the input layer without real recurrent loops. To avoid this accumulation of error, high accuracy is an essential requirement in the training phase to ensure adequate performance in the online mode. The latter technique is employed to develop the ANN-based model for FCs taking into account the necessity of reducing the training error to the minimum available level.

A Back Propagation Feed Forward Neural Network (BPFFNN) is developed with one hidden layer comprising eight neurons. A third order dynamic model is assumed to give enough accuracy with respect to the actual data and, therefore, three past values of the output voltage are used at the input layer. Tanh-sigmoid transfer functions are chosen for all neurons in the hidden layer, while a linear transfer function is selected for the neuron in the output layer. The structure of the ANN is illustrated in Fig 3-13 with the DC voltage is chosen as an output.

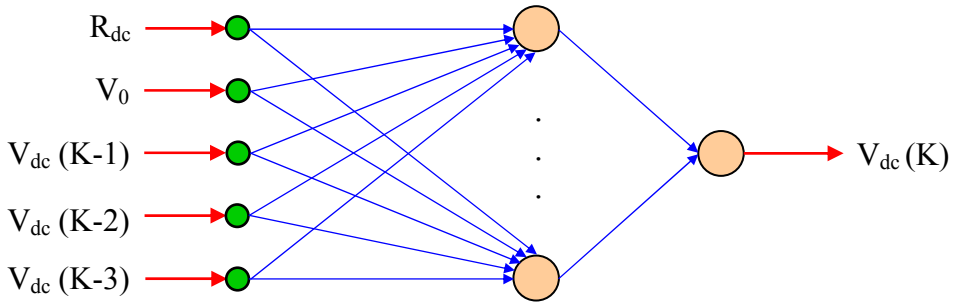

Fig 3-13 The structure of the Artificial Neural Network

The DC voltage depends on the input fuel rate and the equivalent resistance of the load as seen from the FC side. The equivalent resistance of the load impedance can be deduced by equalling the active power in both the DC and the AC sides of the PWM inverter assuming a lossless inverter.

$$P_{dc} = P_{ac} \rightarrow \frac{V_{dc}^2}{R_{dc}} = 3.\left|\frac{V_{ph,rms}}{Z_L}\right|^2 \cdot R_L \qquad (3\text{-}16)$$

Substituting from equation (3-1) yields:

$$R_{dc} = 2.67 \frac{|Z_L|^2}{R_L M^2} \tag{3-17}$$

where

P_{dc}, P_{ac} : DC power and AC active power respectively

$V_{ph,rms}$: rms fundamental component of the modulated phase voltage

R_L, Z_L : load resistance and impedance respectively

R_{dc} : the equivalent resistance of the load impedance as seen in the FC side

At each time interval, the load impedance and the equivalent DC resistance can be calculated to prepare the ANN inputs to get the new DC output voltage.

3.4.2 Training the artificial neural network

To get a suitable database, step changes in the input fuel rate and the load resistance are simulated and the corresponding voltage curves are observed. Some of these results are used in the training process, while the remainder are left for testing the trained ANN. The MATLAB toolbox is used for training the ANN, where the mean square error, which represents the average squared error between the network output and the target, is in the order of 10^{-7}. Depending on the results obtained from the training process, a third order non-linear mathematical model is developed to describe the dynamics of the FC in the following form:

$$V_{dc}(k) = f\,(R_{dc}, V_0, V_{dc}(k-1), V_{dc}(k-2), V_{dc}(k-3)) \tag{3-15}$$

The function (*f*) given in equation (3-15) is derived from the construction and parameters of the ANN. The order of this model is defined depending on the number of recurrent loops and can be changed to get a suitable accuracy with respect to the measured data. The required decision variables can be introduced as inputs to the ANN to take into account their impact. The model is initially subjected to some disturbances that are used in the training process. Fig 3-14 and Fig 3-15 show comparisons between the target response and the response of the ANN-based model for two disturbances. The first disturbance “case (1)” is a 30% step decrease in the equivalent load resistance and a 20% step increase in the input fuel rate, while the second one “case (2)” is a 20% step decrease in the equivalent load resistance and 40% step decrease in the input fuel rate.

The comparisons indicate that the ANN succeeded to capture the nonlinear performance of the original system and to behave in the same manner, which reflects the success of the training process.

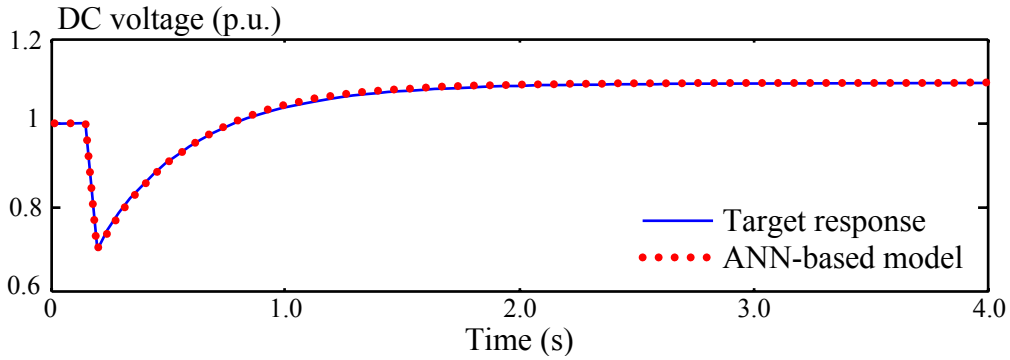

Fig 3-14 Evaluating the performance of the ANN-based model in the training phase: case (1)

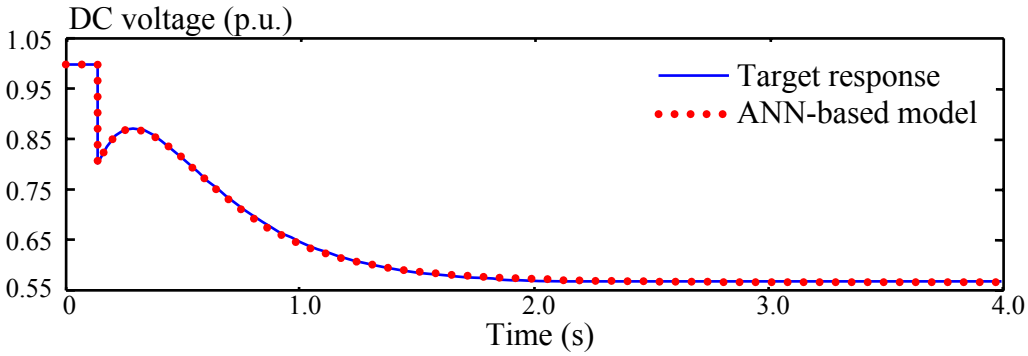

Fig 3-15 Evaluating the performance of the ANN-based model in the training phase: case (2)

3.4.3 Testing the trained ANN

To examine the generalization capability of the ANN-based model when subjected to new disturbances that are not used in the training process, two new disturbances are applied to the model. The first disturbance "test (1)" is a 40% step decrease in the equivalent load resistance and a 50% step decrease in the input fuel rate, while the second one "test (2)" is a 20% step decrease in the equivalent load resistance and 25% step increase in the input fuel rate. Fig 3-16 and Fig 3-17 compare the responses of the ANN-based model with the target responses in the two test cases.

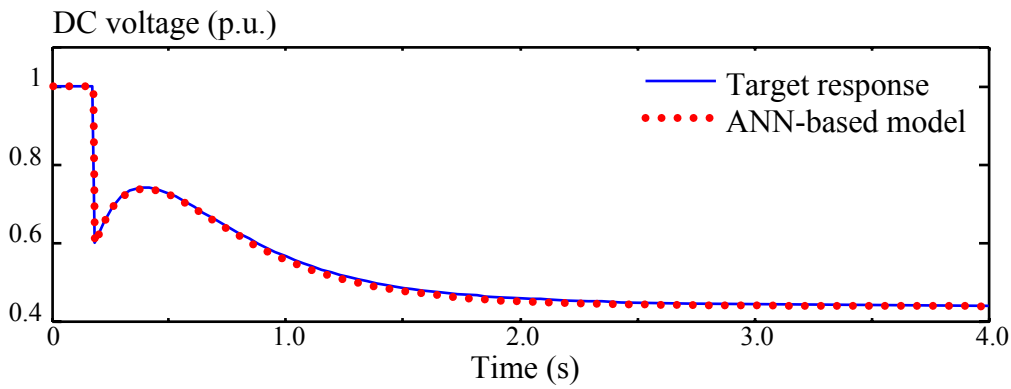

Fig 3-16 Testing the response of the ANN-based model under new disturbances: test (1)

The results confirm the high accuracy of the ANN-based dynamic model with respect to the original dynamic behaviour of the FC unit. This similarity not only

reflects the success of the ANN to capture the non-linear dynamics of the actual system, but also ensures the possibility of using the proposed technique to develop models to simulate other types of FCs with high accuracy. Thus, the performance of the FC units can be investigated in detail taking into consideration the effect of all important variables that affect this performance.

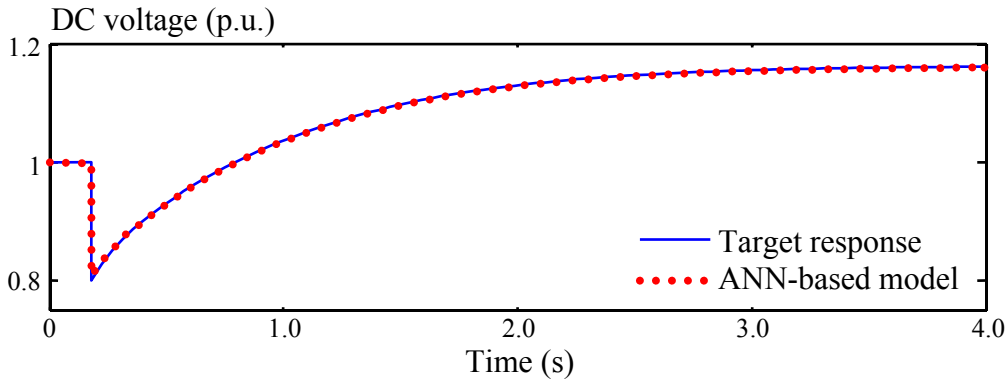

Fig 3-17 Testing the response of the ANN-based model under new disturbances: test (2)

3.5 Conclusion

To analyze the dynamic performance of FCs, proper dynamic models are required for different investigation purposes. Therefore, a third-order equivalent circuit, which reflects the physical processes within FCs, is proposed to simulate the dynamics of FCs for stability studies and control-system design purposes. The effect of varying the operating temperature and pressure is considered using empirical formulas. A simple model is also developed to simulate the heat recovery system with suitable controllers to maintain constant temperatures for the stack and the stored water in the tank.

The use of a recurrent ANN to develop a detailed model directly from measured input/output data to avoid the use of complex mathematical analyses is also discussed. The structure of the ANN can be modified to consider the required decisions, as inputs to the ANN, and to change the order of the model to achieve acceptable agreement with the actual data. The comparisons between the responses of the ANN-based model and the target responses prove the capability of the ANN to capture the nonlinearity associated with the FC dynamics. Depending on these results, the ANN is candidate to be used to give suitable models for different types of FC generating units directly from the input/output measurements.

Chapter 4

Simulation of a Large Number of DG Units Incorporated into a Multi-Machine Network

4.1 Introduction

The centralized power plants, which are the main sources for electric grid systems, can not continue in meeting the increasing demand of electricity at a high degree of quality. DG units can solve many difficulties associated with the conventional power systems and provide an important support to the main centralized power plants [12]. New trends aim to increase the penetration levels of the DG units in distribution systems. The expected large power from DG units necessitates the investigation of two main topics. The first one is related to the issues concerning with the dynamic interaction between DG units and the overlaying high-voltage networks. This includes the impact of the dynamics from such units on the performance of the high-voltage networks and vice versa. This issue will take new dimensions in the near future, when the contributions of DG units further increase due to the technological progress according to the political and social expectations. The second topic is the modelling of this large number of DG units within the power system. It is not acceptable to model the distribution networks with many active sources using lumped load representation. Also, modelling the distribution systems in detail will be an overcomplicated task [50].

This chapter concerns with the first topic, while the second topic is discussed in the next chapter. The investigation presented in this chapter is accomplished in two stages. In the first stage, a study for the case where many individual FCs and MTs are connected to different nodes in the distribution system of a multi-machine network is presented. MT and FC units are chosen since they are candidate to be used in large scales especially when technical solutions for hybrid units consisting of FCs and MTs are well developed [18]. It is assumed that up to 30% of the total demand in the low-voltage area is covered by the DG units. The performance of the network is deeply investigated and the dynamic interaction between low-voltage and high-voltage areas is studied. In the second stage, dynamic models and the corresponding simulation results of hybrid FC/MT units are presented. The dynamic interdependencies between the FC and the MT units,

the system transient performance, and the dynamic control requirements are discussed through the investigation.

4.2 Modelling the investigated network

The investigated network comprises several FCs and MTs with different capacities integrated into a multi-machine power system. The ratings of these units vary from 150 to 400kW for MTs and from 250 to 500kW for FCs. It is expected that the generated power from the DG units impacts the dynamic behaviour of the high-voltage network. Therefore, the high-voltage grid and the corresponding conventional power plants are modelled in detail. Furthermore, the low voltage network, where the DG units are integrated, has to be modelled. Therefore, one 110kV network and the underlying voltage levels are modelled with representative equivalents. Typical configurations and parameters are used to model and simulate the network, which is called Power System Transient network "PST16" denoting the 16 conventional generating units in the network [51].

4.2.1 Network description

The PST16 network is a test network developed for stability analysis and dynamic performance studies. The system consists of three main areas with relatively weak connectors between them to enable the simulation of natural phenomena like the interarea oscillations occurring in real power systems. Area A is considered as the largest generating part and, hence, it is a power exporting area. On the other hand, area C is a load demanding area and, therefore, it imports power from area A directly and indirectly through area B. The load demand in area B exceeds the generation by about 450MW and, as a result, it imports also power from area A. Table 4-1 lists the main data of the PST16 network including the number of components in addition to load and generation status of each area, while Fig 4-1 shows the one line diagram of the PST16 network.

Table 4-1 Information about the different areas in the PST16 network

	Buses	Lines	Transformers			Generators				Generation (MW)	Load (MW)
			Two winding	Three winding	Total	Hydro	Thermal	Nuclear	Total		
Area A	17	12	6	3	9	5	1	0	6	4.840	2.000
Area B	21	15	5	5	10	0	1	4	5	5.641	6.100
Area C	28	24	5	4	9	0	5	0	5	5.450	7.470
Total	66	51	16	12	28	5	7	4	16	15.931	15.570

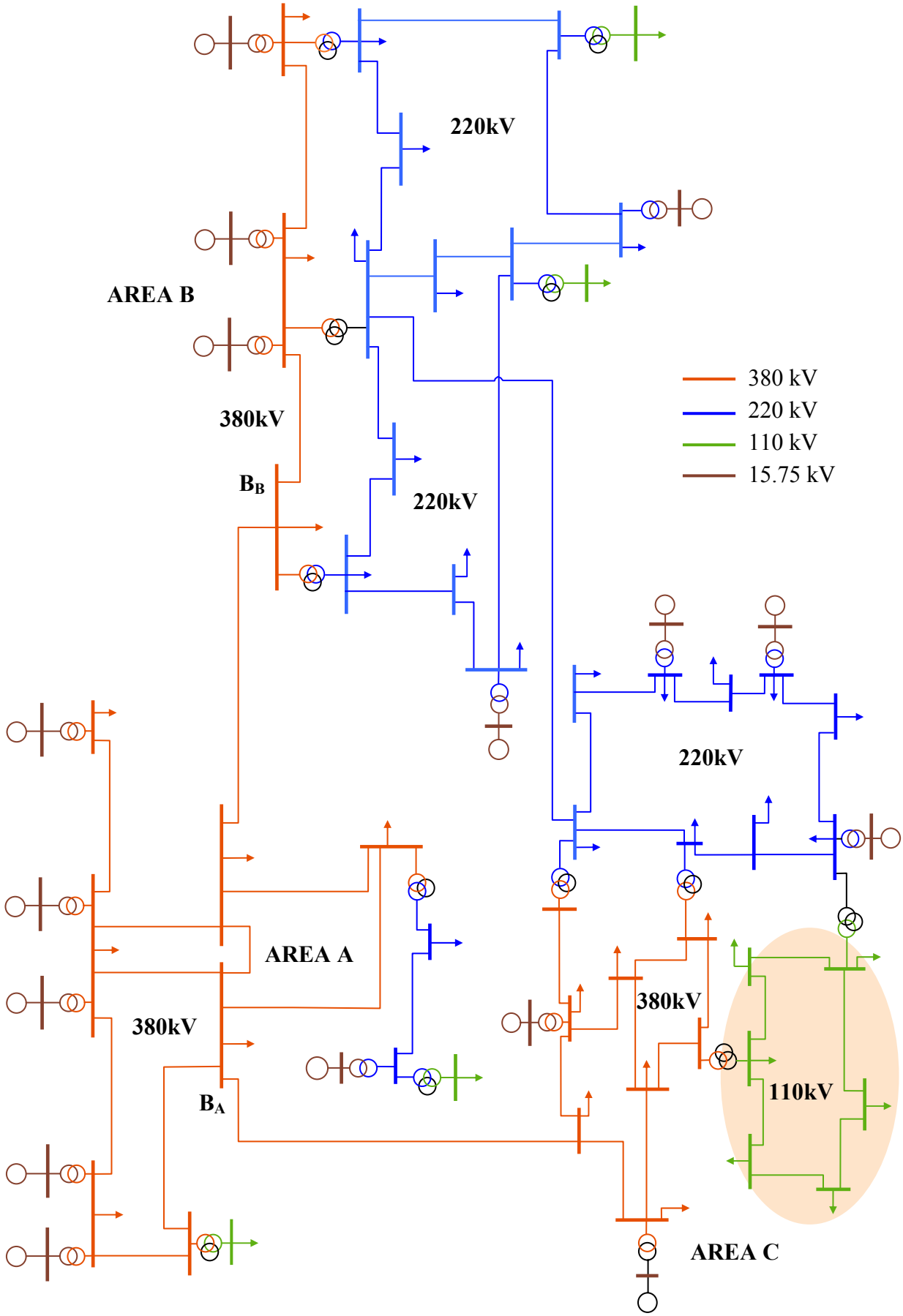

Fig 4-1 The one line diagram of the PST16 network

The 16 synchronous generating units are all represented by fifth-order models, where typical parameters are used considering thermal, hydro and nuclear types with ratings of 220MW, 247MW and 259MW for the three types respectively. IEEE standard regulators are used for modelling the speed governors and the excitation systems. The nominal voltages in the network are 380, 220 and 110kV. One 110kV network, the marked area in Fig 4-1, with the underlying 10 and 0.4kV parts is modelled in detail. Fig 4-2 illustrates the modelling of the medium-and the low-voltage sections showing the integration of the DG units near the end user terminals.

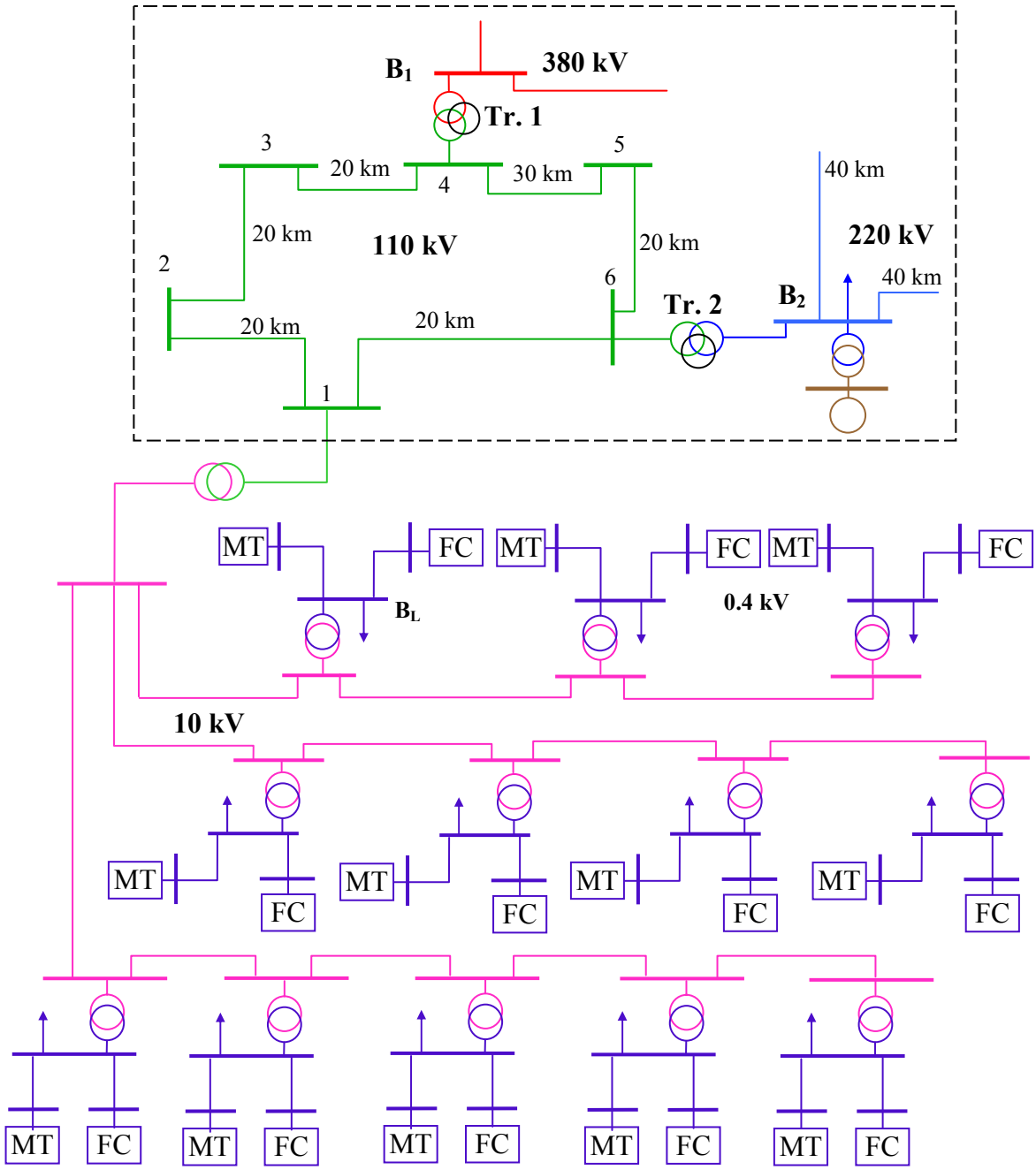

Fig 4-2 Modelling the medium and the low-voltage sections showing the integration of the DG units near the end user terminals

As shown in the figure, two standard steps of transformation are used to reach the 0.4kV level starting from the 110kV system. The first step is from 110kV to 10kV and the second one is from 10kV to 0.4kV. A MT and a FC are located near each of the 56 load nodes in the low-voltage area. The configuration of the distribution system is illustrated starting from one 110kV bus, i.e. bus 1. The other five busses, i.e. bus 2 through bus 6, have similar configurations, where the DG units are connected to the load centres with 100-300m cables.

With the abovementioned configuration, consumers in the low-voltage area are supplied through two sources: the centralized power plants through the 10/0.4kV transformers and the DG units. The power transfer to the 110kV area from the other high-voltage parts is carried out via "Tr. 1" and "Tr. 2" as shown in Fig 4-2. Utilizing DG units with this configuration reduces the power required in the low-voltage area and increases the reliability at the consumer terminals

4.2.2 Modelling of micro-turbines

As mentioned earlier, MT system comprises three main components: the compressor, the combustor and the turbine in addition to the electrical generator. The dynamic modelling of the MTs is based on the dynamics of these components. Fig 4-3 shows the block diagram of the MT dynamic model used in this investigation [13, 52].

The PMSG is represented in this study by a simple first order model as shown in Fig 4-3, while the following function is used to simulate the performance of the turbine [13, 52]:

$$f = 1.3\,(W_f - W_{min}) + 0.5\,(1 - \omega) \qquad (4\text{-}1)$$

where

W_{min} : the offset representing the fuel demand at no-load condition

W_f : the turbine input signal

ω : the angular speed

To reduce the frequency of the generated power to standard values, a cycloconverter is used to interface the PMSG with the utility. The cycloconverter is used not only to reduce and control the unit frequency but can also be used to regulate the unit voltage. For this purpose two PI controllers are implemented with each cycloconverter.

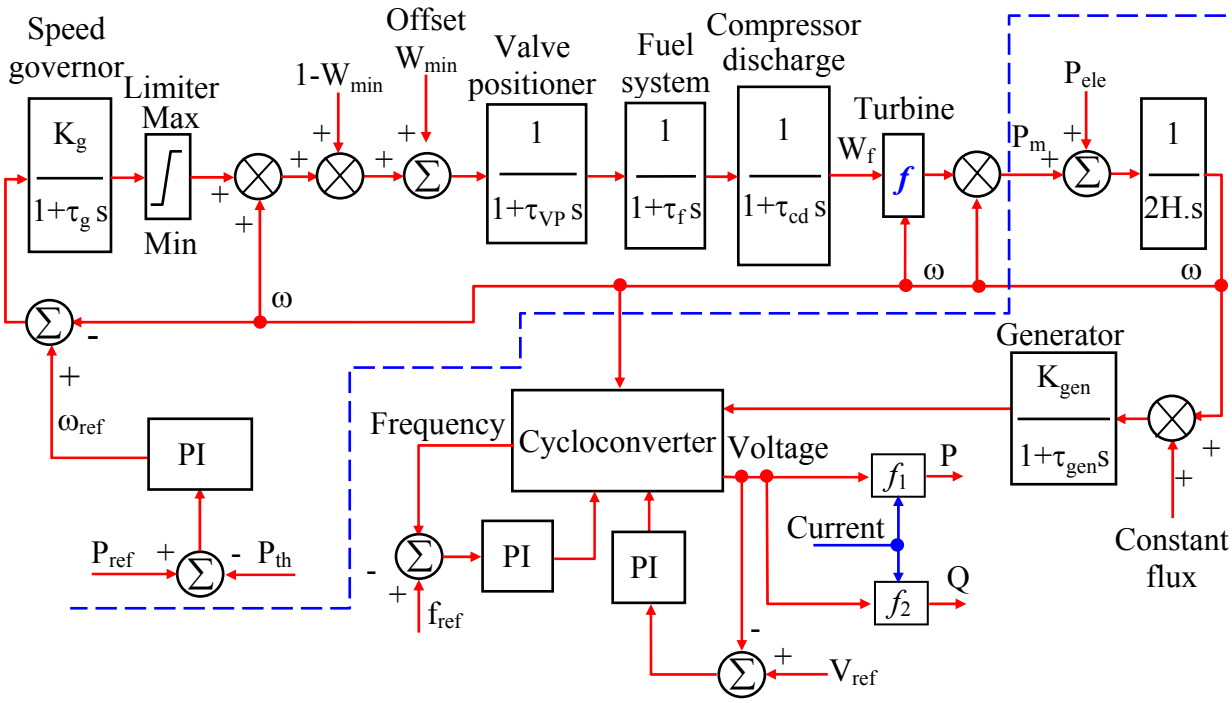

The main symbols in the figure are as follows:

H	: inertia constant
K_g, K_{gen}	: gains of the speed governor and the generator respectively
τ_g, τ_{vp}, τ_f, τ_{cd}, τ_{gen}	: lag-time constants of the speed governor, the valve positioner, the fuel system, the compressor discharge and the generator respectively
ω	: angular speed of the PMSG
P_{ele}, P_m, P_{th}	: input-electrical, mechanical, and thermal power respectively
V_{ref}, f_{ref}, ω_{ref}, P_{ref}	: reference voltage, frequency, angular speed, and thermal power respect.

Fig 4-3 Block diagram model of the micro-turbine generating unit

The first controller is used to maintain the frequency of the unit constant by regulating the operating time of both the positive and the negative converters [53]. The second PI controller regulates the output voltage through the firing angle (α) in the basis of the three-phase controlled rectifiers [53]. The rms output voltage in the utility side of the cycloconverter is calculated as follows [53]:

$$V_{cy,o} = V_{cy,in}\sqrt{\frac{1}{\pi}\left(\pi - \alpha + \frac{\sin(2\alpha)}{2}\right)} \tag{4-2}$$

where

$V_{cy,in}$, $V_{cy,o}$: the rms input and output voltages of the cycloconverter respect.

α : firing angle

The utilization of the turbine exhaust gas in CHP applications is also considered in this study. A PI controller is used to modify the reference speed to enable the thermal power to meet the thermal load demand. It is common to consider the thermal demand as a constant value during the simulation of the electrical behaviour of power systems since the electrical time constants are very small compared to the thermal ones. Therefore, the setting value of the thermal power is maintained constant during the simulation.

The part of the model over the dotted line in Fig 4-3 describes the dynamics of the three main parts of the MT. The blocks under the dotted line represent the machine inertia, the generator model, and the cycloconverter with its controllers. The parameters used in the MT model are listed in appendix C [13, 52].

4.2.3 Modelling of fuel cells

The proposed equivalent circuit of FCs introduced in chapter 3 (section 3.2) is used to simulate the dynamics of the FC units. Typical V-I-characteristics are used to develop the loss-resistances as functions of the supplied currents for different types of FCs [10, 54, 55]. This includes the PEMFC with 250 and 350kW ratings, the AFC with 400kW rating and the SOFC with 450 and 500kW ratings. The parameters of these models are given in appendix D.

Similar to the MT, the heat produced in the stack of the FC is high enough to be used for CHP applications. It is assumed that meeting thermal load demand has priority in the FC control. For simplicity, the thermal power is assumed to be in proportional with the generated electrical power. A PI controller, which regulates the input fuel rate, is used to control the thermal power. The thermal output power from the FC is calculated as a function of the output electrical power and compared with the thermal load demand. The error signal is used to activate the PI controller, which regulates the input fuel rate in order to readjust the thermal output power from the unit.

4.3 Implementation in the *PSD* simulation package

The simulation program PSD is a package for modelling and simulating power systems including online transient simulation and steady state analysis [56]. It is based on the principles of electromechanical-transient computations in electrical networks. The package has a strong library providing accurate dynamic models for most known elements in power systems. Synchronous machine, two and three

winding transformers and transmission lines are some examples of these components. For instance, the user can chose a suitable model for the synchronous machine among the second-, fifth- and sixth-order models and define the parameters himself. It is also possible to build special units like FC, MT and FACTS devices in a so-called "regulator files" depending on their block diagram models. These models are integrated into the described network through connecting nodes, which helps the operator to build his own models for the regularly variant components like the voltage and speed-governor regulators. The interaction between the built units and the network is accomplished through selected variables, which are exchangeable during the simulation process. The PST16 network is built using the standard models found in the library of the PSD. On the other hand, the models of FCs and MTs are built in regulator files depending on their block diagram models using special code in the PSD. Fig 4-4 and Fig 4-5 show respectively the implementation of the FC and the MT models in the PSD package.

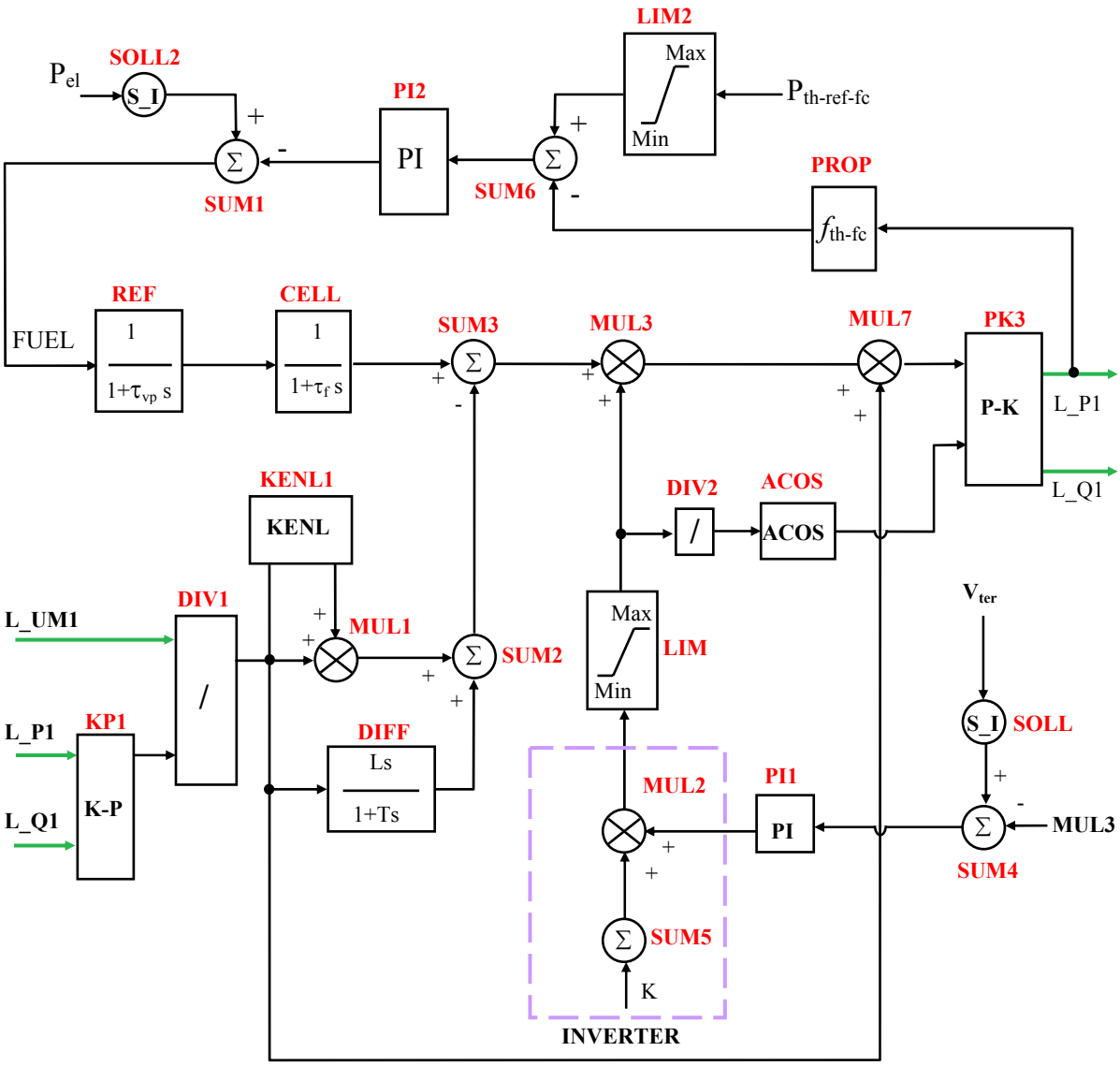

Fig 4-4 Implementation of the fuel cell model in the PSD package

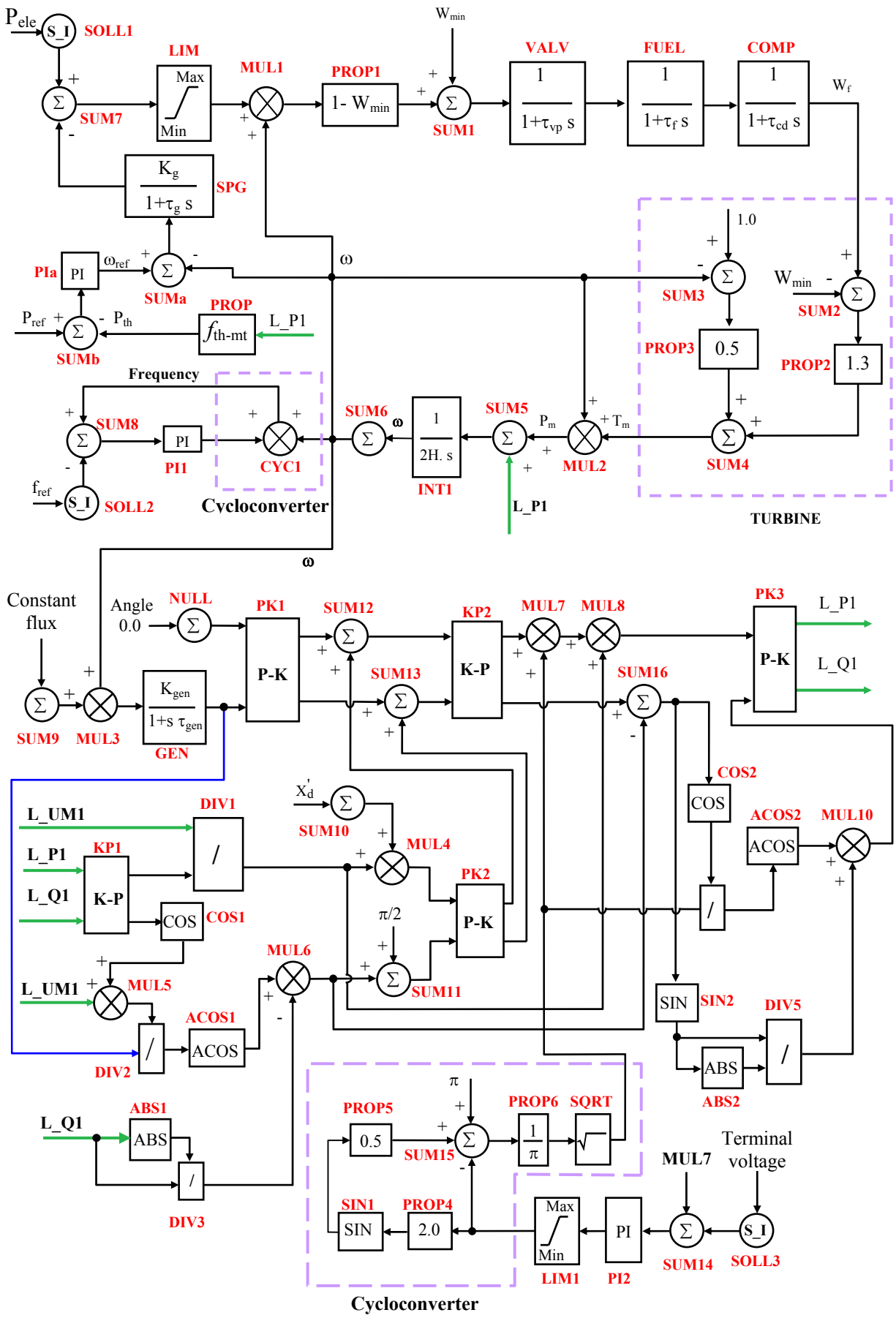

Fig 4-5 Implementation of the micro-turbine model in the PSD package

The model structures are implemented using a special standard code in the PSD simulation package. The blocks shown in the previous figures represent the models of the FC and the MT given by the equivalent dynamic models shown in Fig 3-4 and Fig 4-3 respectively. Each unit has at least one set-value element "S_I" to adjust its initial condition. The interface of the units with the external network is accomplished through the output active and reactive power from the unit (L_P1 and L_Q1) at each time interval. Per unit system is used inside the unit models, while actual values are used in the electric network side.

4.4 Simulation results and discussion

After simulating the whole network and implementing the DG units with the abovementioned configuration in the PSD simulation package, the dynamic performance of the network is studied. Firstly, a power flow calculation is carried out to define the initial operating condition of the network. Different disturbances are then simulated in both the high-voltage and the low-voltage areas of the network including load switching and three-phase short circuits. Fig 4-6 and Fig 4-7 show the behaviours of a selected FC and a selected MT when switching on a load of 500+j100kVA at a 0.4kV load bus "bus B_L in Fig 4-2". The switching point is 100m away from both the FC and the MT units in the low voltage system. The reactions of the other units vary depending on their locations with respect to the switching point and also depending on their parameters.

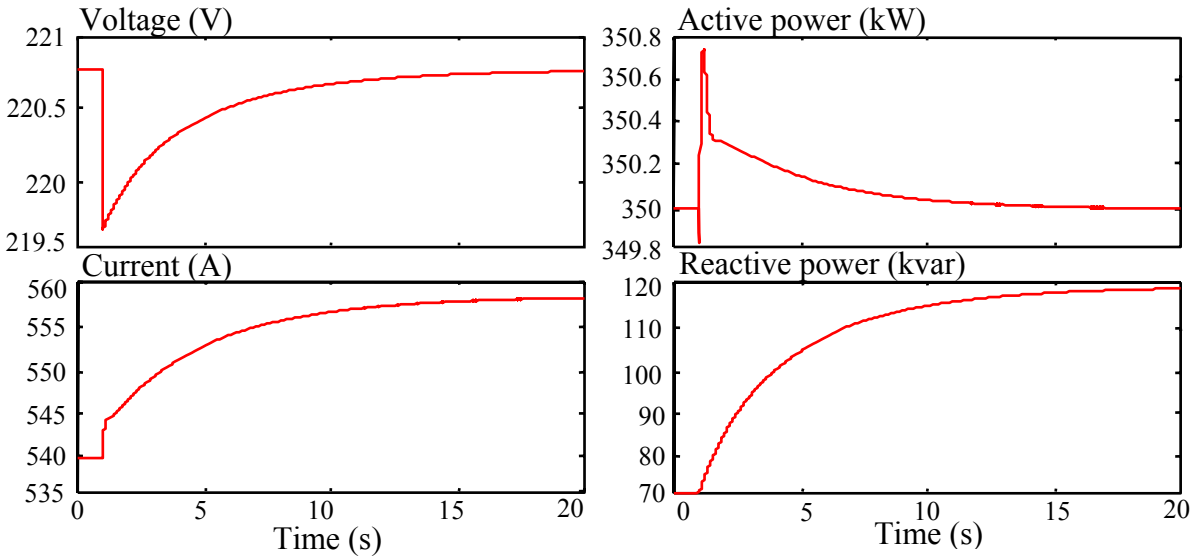

Fig 4-6 Response of a selected fuel cell to a load switching in the low-voltage area

The PI voltage controllers with the PWM inverter of the FC unit and the cycloconverter of the MT unit succeeded to restore the original values within 20 seconds. Since the thermal load demand for both the FC and the MT units is assumed to be always constant, the set points of the active power controllers are

maintained also constant. As a result, the active electrical power from the units returned back to the initial values at the new steady state conditions. The change in the active power demand, however, is covered from the high-voltage network itself through the 110/10kV transformers. The variations in the reactive power are to compensate the voltage reduction occurred as a result of the disturbance. Thus, the terminal voltage moves back to its initial value. Since the set point of the thermal power is kept constant, the thermal output power from the MT unit has also to be maintained constant after the load switching. This requires keeping the turbine active power constant due to the proportional between electrical and thermal power. Thus, the reference angular speed is adjusted using the controller action (see Fig 4-3) forcing the turbine, and hence the PMSG, to operate at a lower angular speed. However, the frequency will not incorporate such reduction due to the action of the frequency controller with the cycloconverter.

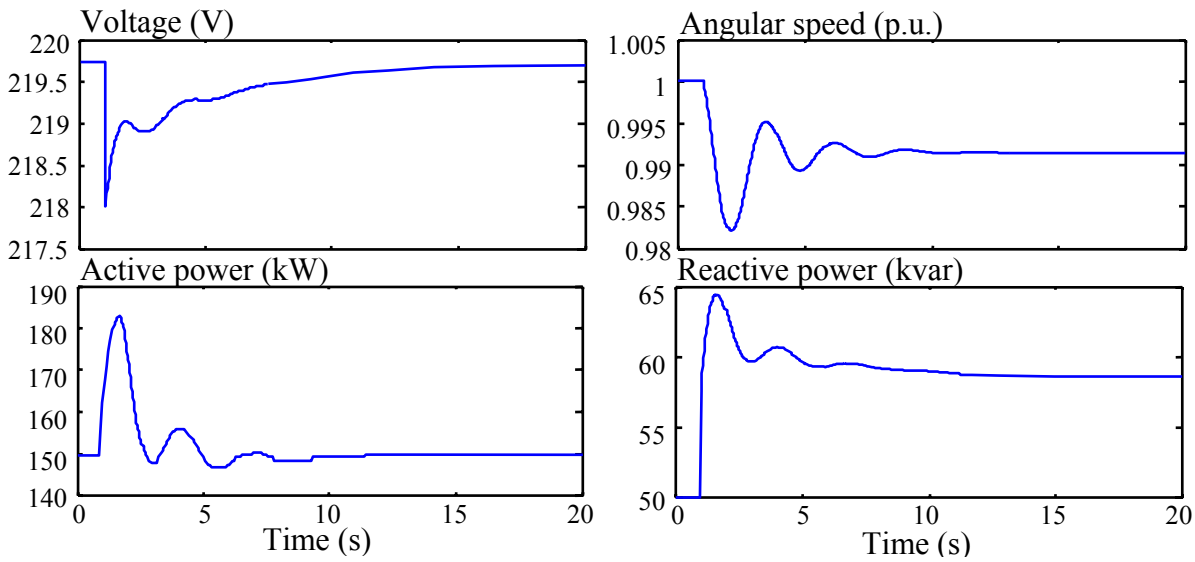

Fig 4-7 Response of a selected micro-turbine to a load switching in the low-voltage area

The previous load switching represents a local disturbance and hence the high-voltage parts did not effectively contribute in defining the response of DG units. To highlight the effect of load switching in the high-voltage areas on the dynamic performance of DG units, Fig 4-8 and Fig 4-9 show respectively the response of the same FC and MT to a 100+j20MVA load switching in area A at bus "B_A", which is a boundary bus between area A and area C (see Fig 4-1). Since the switching point is in the high-voltage area away from the DG units, they are affected to the same degree regardless of their locations within the distribution network. However, the response of the units depends on their own parameters and hence on their capacities. The oscillatory behaviour of the DG units reflects the impact of the dynamics from the high-voltage parts on their response.

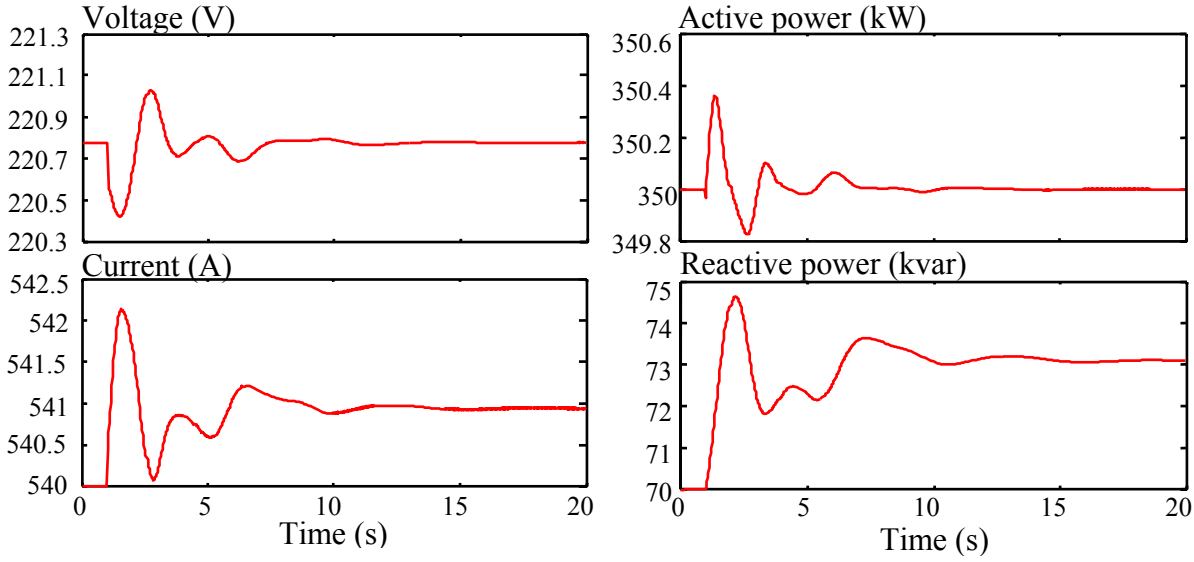

Fig 4-8 Response of a selected fuel cell to a load switching in the high-voltage area

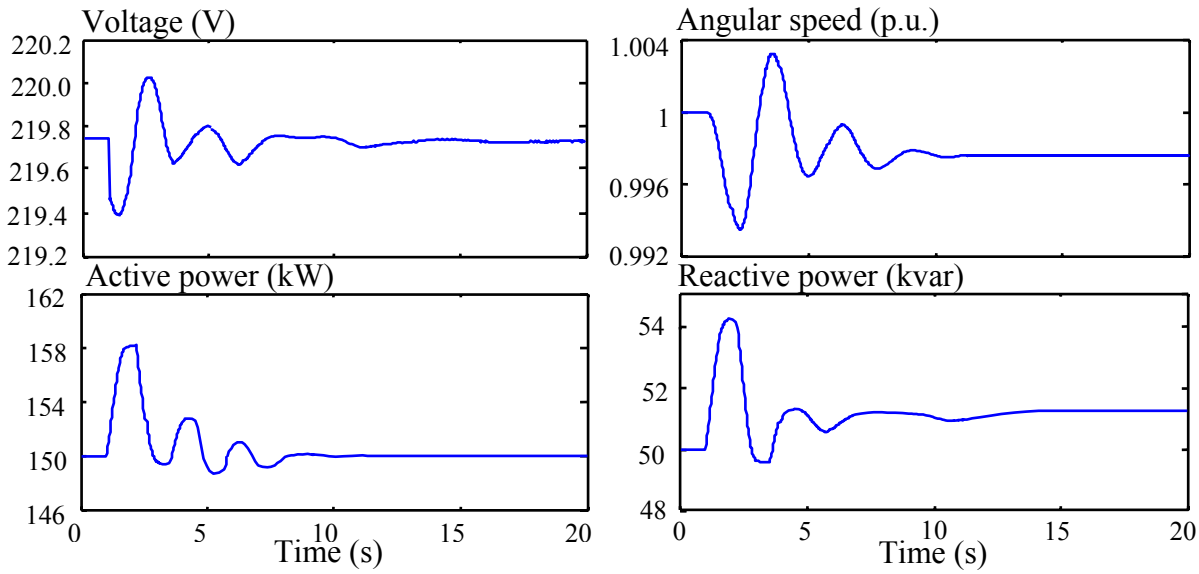

Fig 4-9 Response of a selected micro-turbine to a load switching in the high-voltage area

To evaluate the performance under relatively large disturbances, Fig 4-10 and Fig 4-11 illustrate respectively the responses of a FC and a MT to an 80 ms short circuit in the 380kV area. The fault occurred in area "B" at node "B_B" (see Fig 4-1). All units succeeded to absorb this short circuit and to restore their initial conditions in a short time. The units succeeded to withstand to other three-phase faults in different location within the high-voltage area. Generally, active power oscillations of both FCs and MTs are not as strong as those of the reactive power. More damping is achieved due to the direct action of the controllers operating to regulate the active power. On the other hand, the compensation of the voltage variations causes stronger oscillations in the reactive power. Furthermore, it is clear that the oscillations associated with the MTs are stronger than those of the FC. The mechanical nature and the stored energy in the mass of the MTs enable large-instantaneous power variations as shown in Fig 4-11. The FCs, as static

converters, cannot provide such large instantaneous variations in the current and power. With the tendency for large current increase, the internal resistance of the cell increases and accordingly the voltage drops sharply as shown in Fig 2-4 and Fig 3-2. The increase of the internal resistance prevents the large increase of the current supplied from the unit. This protects the unit against sudden changes and explains the small variations of the power from the FCs compared to the MTs.

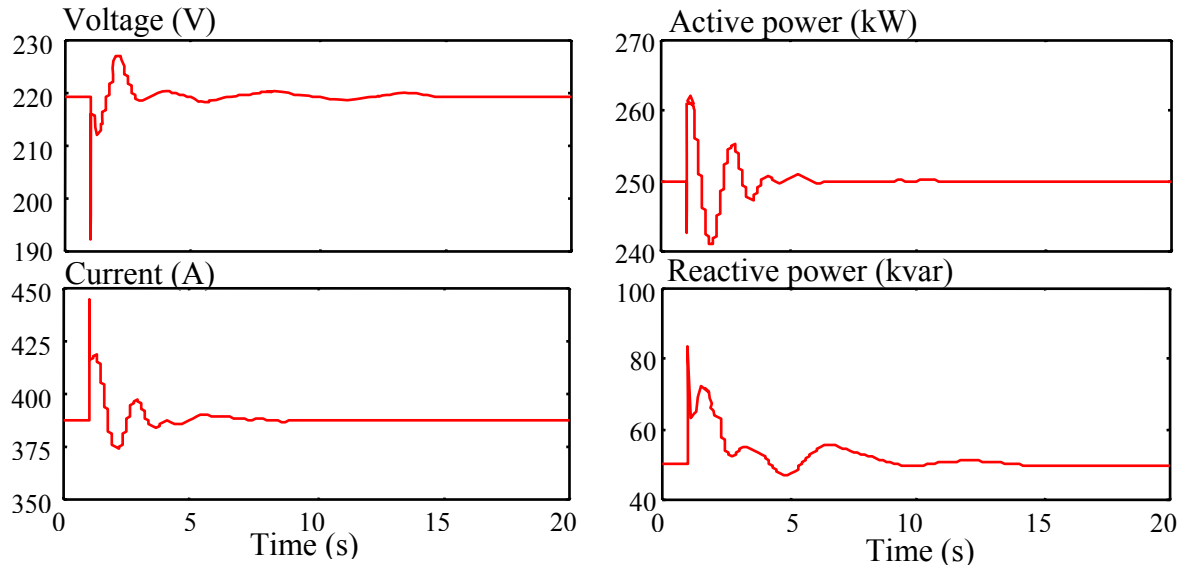

Fig 4-10 Response of a selected fuel cell to a short circuit in the 380kV area

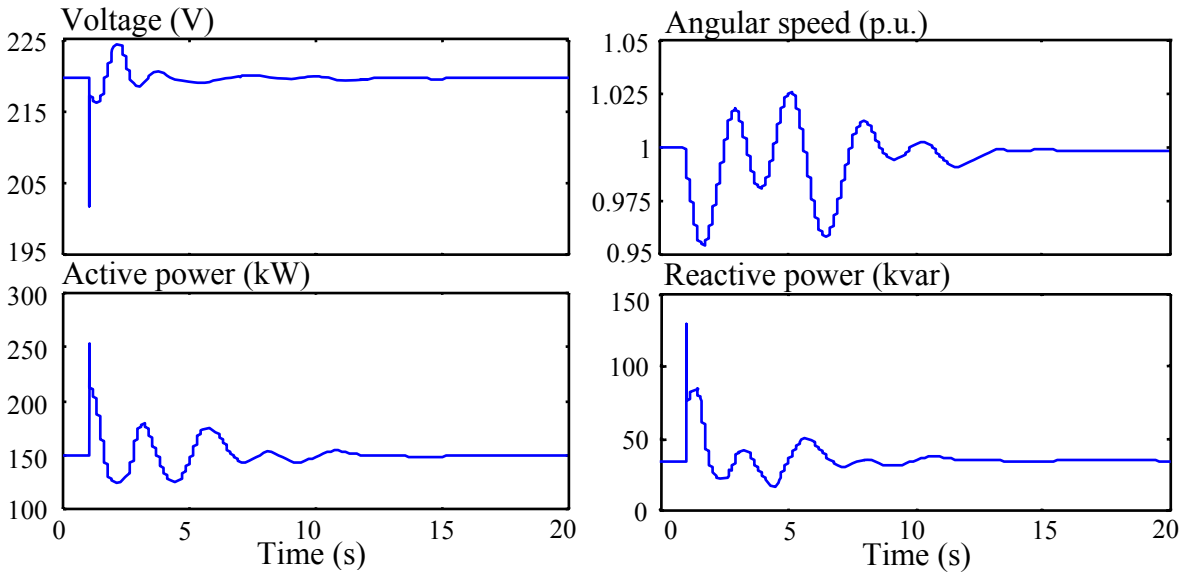

Fig 4-11 Response of a selected micro-turbine to a short circuit in the 380kV area

After illustrating and discussing the performance of the DG units as a part of the network, it is adequate to highlight the interaction between the high-voltage parts of the network and the low-voltage distribution system. Also, it is important to study the effect of introducing the DG units on the dynamic behaviour of the low-voltage system. Fig 4-12 shows the response of the active power transferred to the 110kV area from the other parts in the high-voltage network to the above-mentioned three-phase short circuit. This power transfer occurs through the trans-

formers 380/110kV "Tr. 1" and 220/110kV "Tr. 2" shown in Fig 4-2. From Fig 4-12 raises the question regarding the strong oscillations in the power transfer to the 110kV network. Even with the fact that 30% of the total power demand is produced in the DG units, it is obvious that the observed phenomenon can not be explained by the reaction of the DG units. Considering that the changes of the active power through the first transformer are similar and in opposition to those through the second one, it will be clear that the swings are caused by the high voltage system in the form of interarea oscillations. The network parts surrounding the 110kV area oscillate against each other through the 110kV network. The effect of the interarea oscillations does not extend to the low voltage area and, hence, they are not noticeable in the dynamics of the DG units (see Fig 4-10 and Fig 4-11). To compensate the interarea oscillations appearing in the figure, it is required to regulate the performance of the network as a whole. It is not possible to achieve this objective from the 110kV area alone.

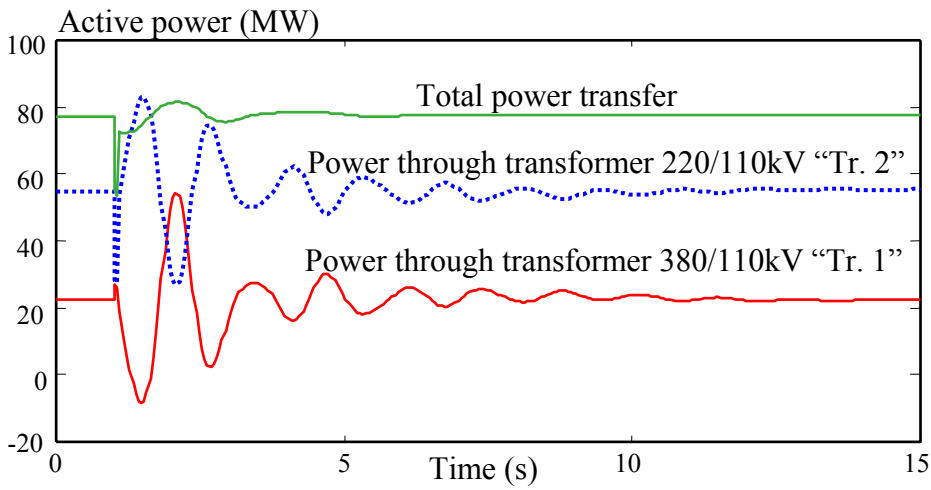

Fig 4-12 Active power transferred to the 110kV network

For comparison purposes, the network is modelled after removing all DG units from the distribution system and the dynamic behaviour is investigated under the same disturbances. The loads, which are always kept constant, are supplied exclusively from the medium voltage side. Furthermore, the voltages at the low voltage nodes are lower because of the higher voltage drops on the lines and transformers. Fig 4-13 gives a comparison between the change in the total power transfer to the 110kV system with and without DG units after the abovementioned fault. It is obvious from the figure that the existence of DG units achieves more damping to the power transferred, which generally enhances the performance of the low-voltage part. In addition, the power is not strongly decreased in the faulty system when the DG units are utilized, which reduces the impact of the fault on the consumers.

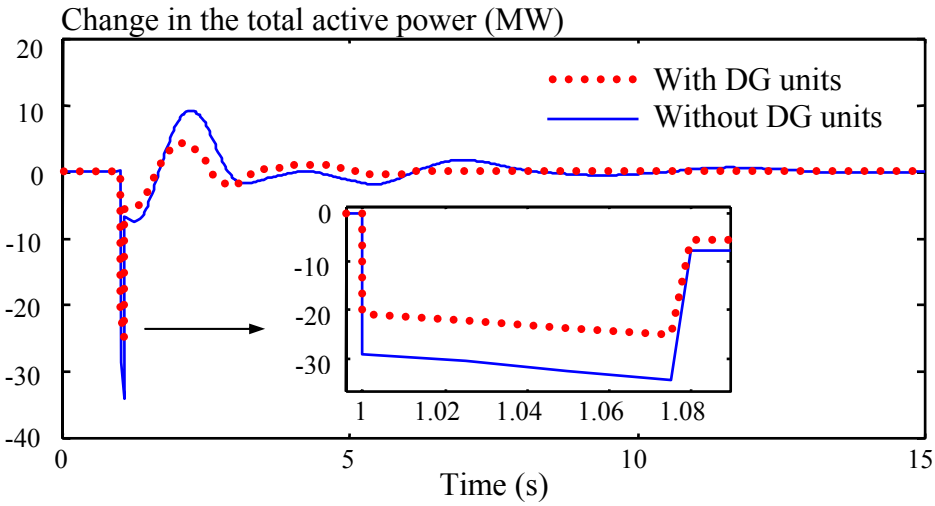

Fig 4-13 Change in the total active power transfer with and without DG units as a result of a 3-phase short circuit in the 380kV network

Fig 4-14 illustrates the voltage variations of a selected 0.4kV load bus "B_L" (see Fig 4-2) as a result of the three-phase short circuit with and without DG units. The figure shows some improvements in the voltage profile in addition to the increase of the voltage level when the DG units are used due to the reduction of the voltage drop over the lines and the transformers.

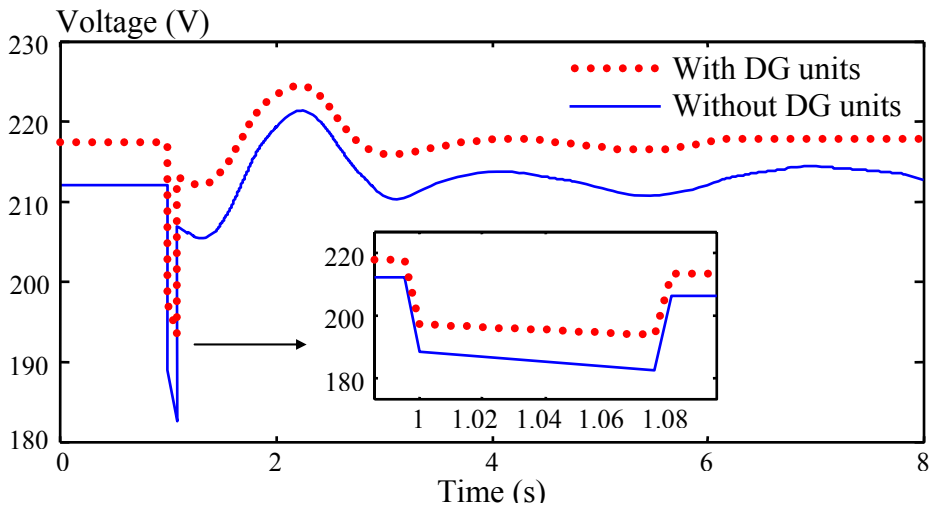

Fig 4-14 Voltage variation at a low voltage bus with and without DG units as a result of a three-phase short circuit in the 380kV network

4.5 Hybrid fuel-cell/micro-turbine unit

Recently, many attempts are directed to develop small advanced Combined Fuel-Cell/Micro-Turbine "CFCMT" units [18, 19]. Future versions of SOFCs are likely to be augmented with MTs in hybrid systems that could achieve efficiencies as high as 70%, which can increase to 85% when the waste heat is utilized. The advantages of this hybrid configuration include also: fuel flexibility, superior environmental performance, high power quality, simplicity of sitting near con-

sumers, possibility of independent operation of the FC and MT units and lower capital cost compared to that of the FC alone [18, 19]. One project is now under development in California depending on SOFC technology to manufacture a 190kW unit with emission that is 50 times less than natural gas turbines [57]. The unit has an overall efficiency of 70% and it is planned to develop a 20 MW unit by the year 2015 with an overall efficiency exceeding 80%. Another project in Italy aims at developing and demonstrating a 100kW system combining a MCFC with a MT unit [58].

The construction of the CFCMT unit and some related technical aspects are discussed in few literatures [18, 19, 57, 58]. The dynamic behaviour of the augmented unit and the integration of such units into large networks are other approaches, which need to be investigated. The dynamic interdependencies between the FC and the MT, the dynamic performance of the entire system, and the dynamic control requirements are some points, which are still ambiguous. The main objective of following sections is to emphasis on a new framework that deals with the dynamic performance of the CFCMT unit with multi-machine networks.

4.5.1 Unit structure

The CFCMT unit consists of a high-temperature FC with an internal reformer, an air compressor, a high-speed low-capacity gas turbine, and a PMSG. The exhaust air from the FC, which still contains energy, can be used to drive a downstream turbine replacing the classical combustor. Another approach is to utilize the residual energy in the power cycle more efficiently by using the hot exhaust from the turbine as an air supply to the FC. The former configuration is known as the “topping mode” while the latter is called the “bottoming mode” regarding the location of the FC with respect to the turbine. SOFCs can operate effectively in the “topping” mode due to their high temperature which reaches 1000°C, while MCFCs, which operates at 650°C, are more suitable for the “bottoming” mode [19]. In both configurations, electric power is generated by the FC (DC power) and the MT generator (AC power) using the same fuel/air flow.

4.5.1.1 Topping mode

In the topping mode, the FC replaces the classical combustor of the MT [57]. During normal operation, the compressor is used to pressurize air before entering a heat exchanger. The pressurized air is then preheated in the heat exchanger before entering the FC. An internal reformer is used to produce hydrogen rich reformed gas, which is also pressurized using a fuel pump and is then introduced to

the FC. The gas is electrochemically processed along the cells to produce water, heat and DC power. The hot pressurized exhaust from the FC is used as a working fluid in the expander section of the downstream turbine to extract mechanical energy. The generated mechanical energy in the turbine is used to drive both the compressor and the PMSG. The gases from the expander pass through the heat exchanger to preheat the air before entering the FC and then they are exhausted. As with the individual units, a power conditioner is used to convert the FC power to the AC form, while a cycloconverter is employed with the MT to reduce its frequency to standard values. A start up combustor is used to drive the turbine and in some cases it is also used in the running mode to increase the power from the turbine. Analysis indicates that this configuration gives the possibility to achieve an electrical efficiency up to 70% with some sophisticated MTs. Fig 4-15 illustrates the main components of the hybrid unit in the topping-mode [57].

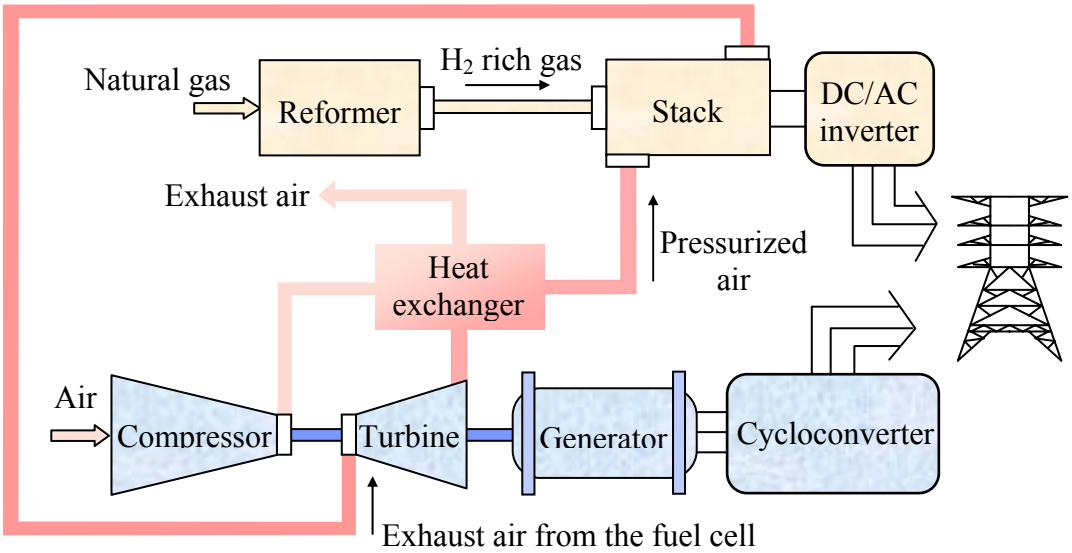

Fig 4-15 The augmented unit (Topping mode)

4.5.1.2 Bottoming mode

The relative locations of the FC and the turbine are exchanged with respect to each other in the bottoming mode configuration. In some arrangements, a heat exchanger is utilized alone to capture the heat of the exhaust gas from the FC replacing the turbine combustor. In this case, the exhaust air from the turbine is used directly as an air supply to the FC. This configuration is suitable for turbines, which are designed to operate at relatively lower temperatures. In another configuration, an oxidizer is also added as shown in Fig 4-16 to obtain more energy [19]. The oxidization process increases the temperature of the exhaust air from the stack and the turbine before entering the heat exchanger. The high-temperature clean gas from the oxidizer is used in the heat exchanger, which re-

places the conventional combustor of the turbine. The turbine power is used to drive the motor of the air compressor through a shaft between them and to produce AC electrical power at high frequency within a PMSG. The DC power, which is produced in the stack of the FC, is converted to AC power using a DC/AC power conditioner.

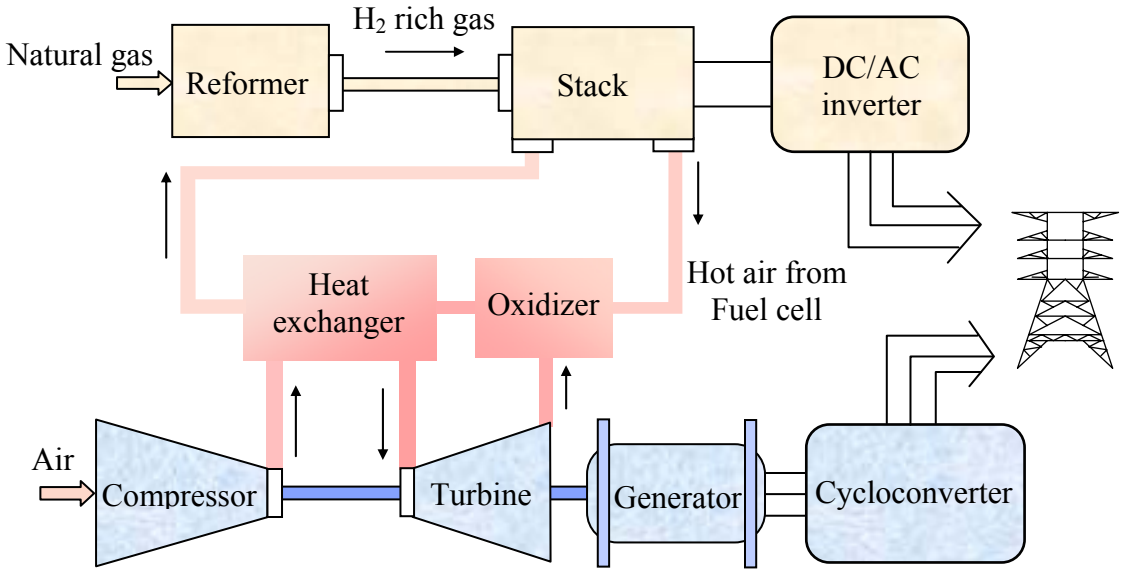

Fig 4-16 The augmented unit (Bottoming mode)

The developed projects concentrate only on the topping mode configuration as it represents a more established technology, while the bottoming construction is still under consideration [18]. Therefore, this research will consider only the topping-mode configuration.

4.5.2 Dynamic modelling

As shown in Fig 4-15, the FC works independently on the MT with separate fuel source and controllers. The inputs and outputs of the unit are not directly affected by the MT dynamics. Hence, the equivalent circuit dynamic model of the FC is used separately from the MT model. Regarding the control strategy, the input fuel rate to the FC is assumed to be constant instead of tracing back the thermal load demand, which is not considered in this case. On the other hand, the turbine mechanical power depends on the energy contained in the exhaust air from the FC, which is assumed to be in proportional with the output electric power from the FC. To model the dynamic interdependency with the topping-mode construction, the mechanical power of the turbine is calculated depending on both the output power from the FC and the control action of the speed governor as shown in Fig 4-17. The speed governor regulates the angular speed by con-

trolling the amount of the exhaust gas utilized in the turbine, which defines the mechanical power, and rejecting the remainder.

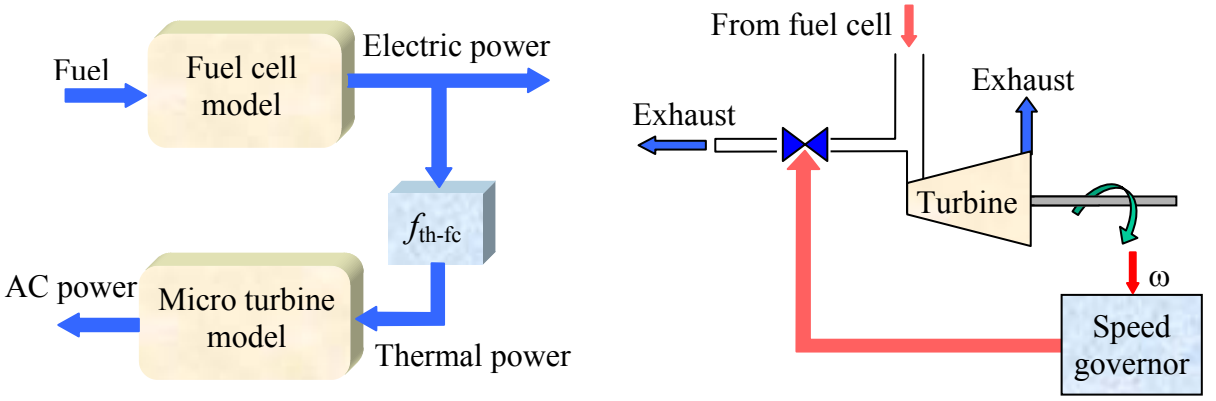

a) Dependency of MT on the power from FC b) Regulating exhaust by the speed governor

Fig 4-17 Dynamic interdependency of the fuel cell and the micro-turbine

Fig 4-18 shows a part of the MT block diagram with some modifications introduced to the standard model used in the previous sections. A signal representing the power contained in the FC exhaust "P_{fc}" is added to the output signal from the speed governor, which represents the rejected exhaust to control the angular speed. The power contained in the FC exhaust is calculated depending on the electrical power from the unit using the function ($f_{th\text{-}fc}$). The sum, which represents the net working fluid in the MT, is used as an input signal to the turbine. Another modification is related to the reference speed, which is maintained always constant in this case since the thermal load demand has not to be followed. The other components of the MT are the same as the original block-diagram model given in Fig 4-3. A similar structure can also be used if an additional combustor is assumed. In this case, the exhaust from the FC provides the basic energy to the turbine while the fuel source with the MT, which is regulated by the speed governor, is used to produce more power in the turbine.

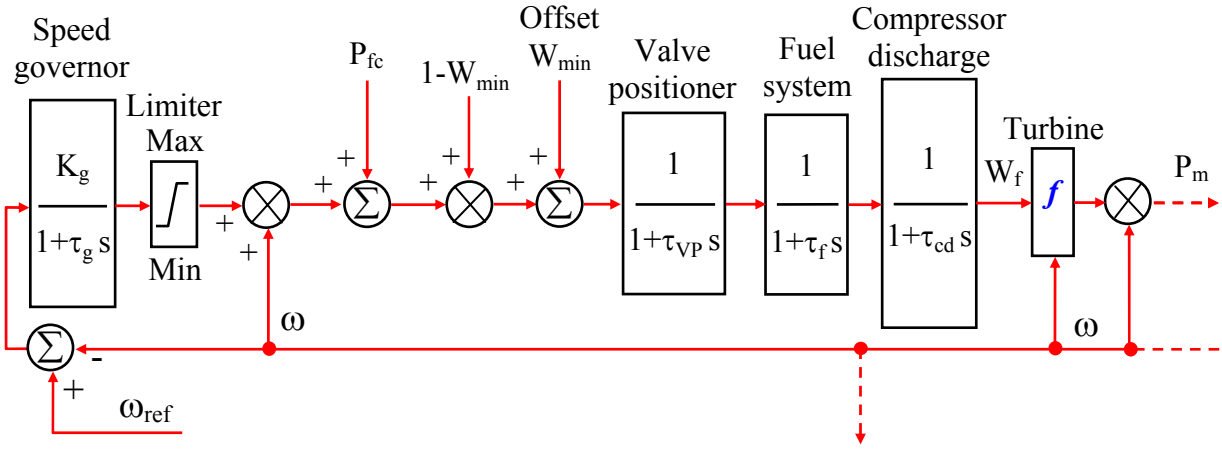

Fig 4-18 Introducing the effect of FC output power on MT mechanical power

4.5.3 Network modifications

Some modifications are introduced to the distribution system to study the performance of the hybrid units. Instead of 112 DG units, the low-voltage area comprises 56 CFCMT units, where the FCs are augmented with the MTs to form the hybrid units. This is accomplished by connecting a SOFC and a MT unit to the same bus and introducing a signal from the FC output power to the MT model as explained earlier. Technical developments show that the FC can produce from 55% up to 90% of the unit electricity, while the turbine produces the reminder [19]. The 56 hybrid units are modelled with different capacities from 400kW to 900kW. Based on the capacities of the individual units, the percentage power from the FCs varies in the range of 55.6 up to 77% of the total power in the hybrid-units. As the previous case, the power from the CFCMT units reaches up to 30% of the total demand in the 110kV area. The parameters used in the modelling vary depending on their capacities as given with the individual units.

4.5.4 Simulation results and discussion

The control strategy is to regulate the terminal voltages using PI controllers incorporated with both the cycloconverter and the PWM inverter. An attempt to regulate the turbine speed through the fuel source of the FC failed to achieve a satisfactory operation. The fuel source regulates the electrical and thermal power in the FC and, consequently, the mechanical power of the turbine. However, at the time where the turbine performance is improved the reaction of the FC seems to be poor and vice versa. It is found that regulating the performance of the FC and the turbine at the same time using the fuel source of the FC is very difficult. It will be adequate to use separate controllers with each part to give better results.

Different disturbances are applied to test the performance of the network including the new CFCMT units. For comparison reasons, the response of the system to the same disturbances simulated in the network with individual units is introduced. Fig 4-19 illustrates the response of a selected hybrid unit to a 500+j100kVA load switching at a 0.4kV load bus “bus B_L in Fig 4-2”. More than 7kW additional active power from the CFCMT unit is supplied, while different contributions from the other units are achieved depending on their locations relative to the switching point. Despite the fact that the input fuel rate to the FC is constant, more exhaust from the FC is utilized in the turbine to compensate for the angular-speed reduction as a result of increasing the load demand. On the other hand, the increase of the output power from the FC is caused only due to the change of the operating point and, as a result, the internal power loss.

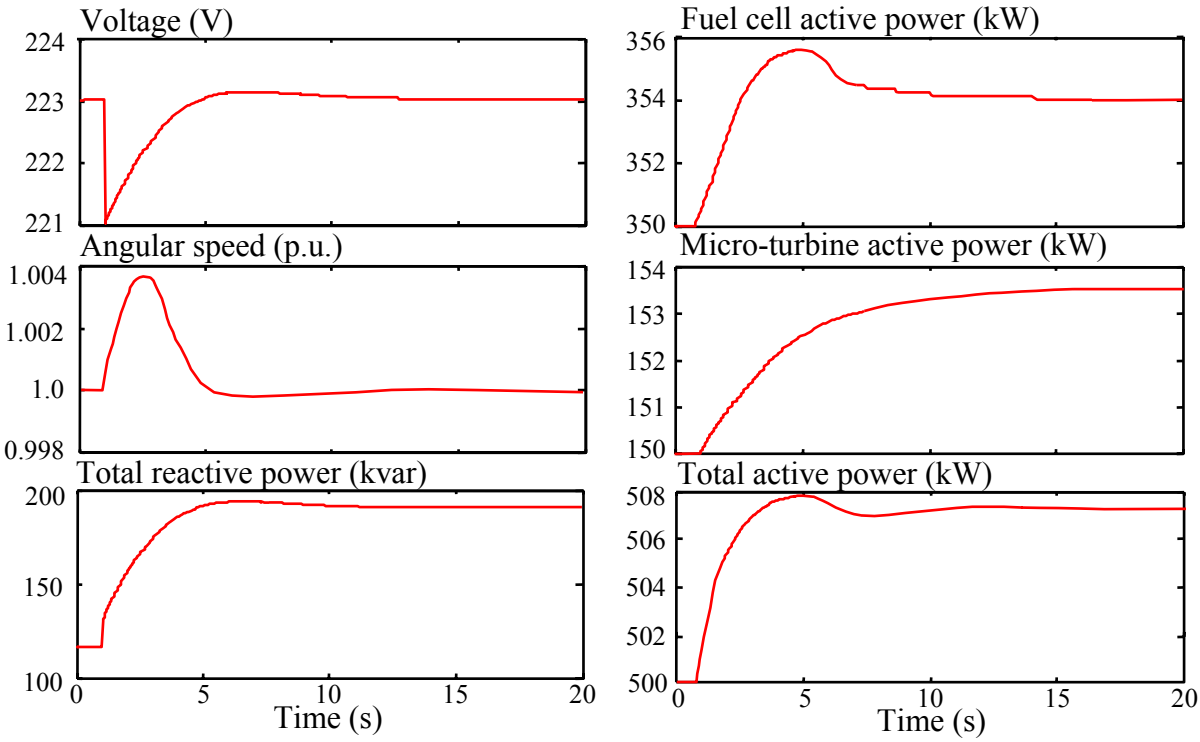

Fig 4-19 CFCMT response to a 500+j100kVA load switching in the low-voltage area

Also, Fig 4-20 illustrates the response of another hybrid unit to a 100+j20MVA load switching in area A at bus "B_A". The CFCMT units share in covering the additional power but with small contributions due to the distance of the disturbance. It is important to notice the instantaneous acceleration occurred to the PMSG after the load switching in both cases even with the increase of the output electrical power from the generator.

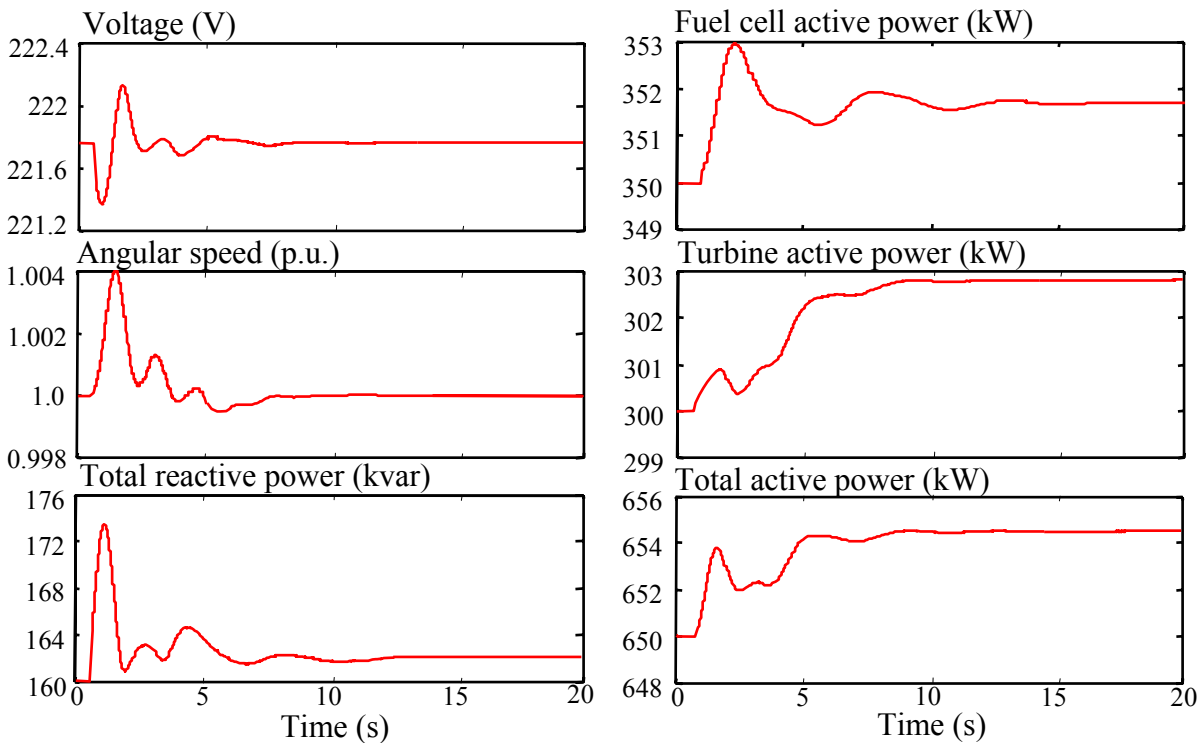

Fig 4-20 CFCMT response to a 100+j20MVA load switching in the high-voltage area

Any increase in the electrical output power of a conventional MT causes a deceleration to the generator as shown in Fig 4-7 and Fig 4-9. In the hybrid configuration, on the other hand, the angular speed will be defined according to both the turbine input mechanical power and the output electrical power. The fast increase of the electrical power in the FC causes an increase to the mechanical power of the turbine. Since the instantaneous value of the mechanical power exceeds that of the electrical output power, the PMSG is accelerated.

The response of a CFCMT to a 80ms three-phase short circuit in area "B" at node "B_B" (see Fig 4-1) is shown in Fig 4-21. Similar to the previous cases, the PMSG is accelerated unlike the performance of the separate MT unit shown in Fig 4-11. The Turbine receives more mechanical power, due to the rise in the electrical power in the FC, while the generator output power is decreased.

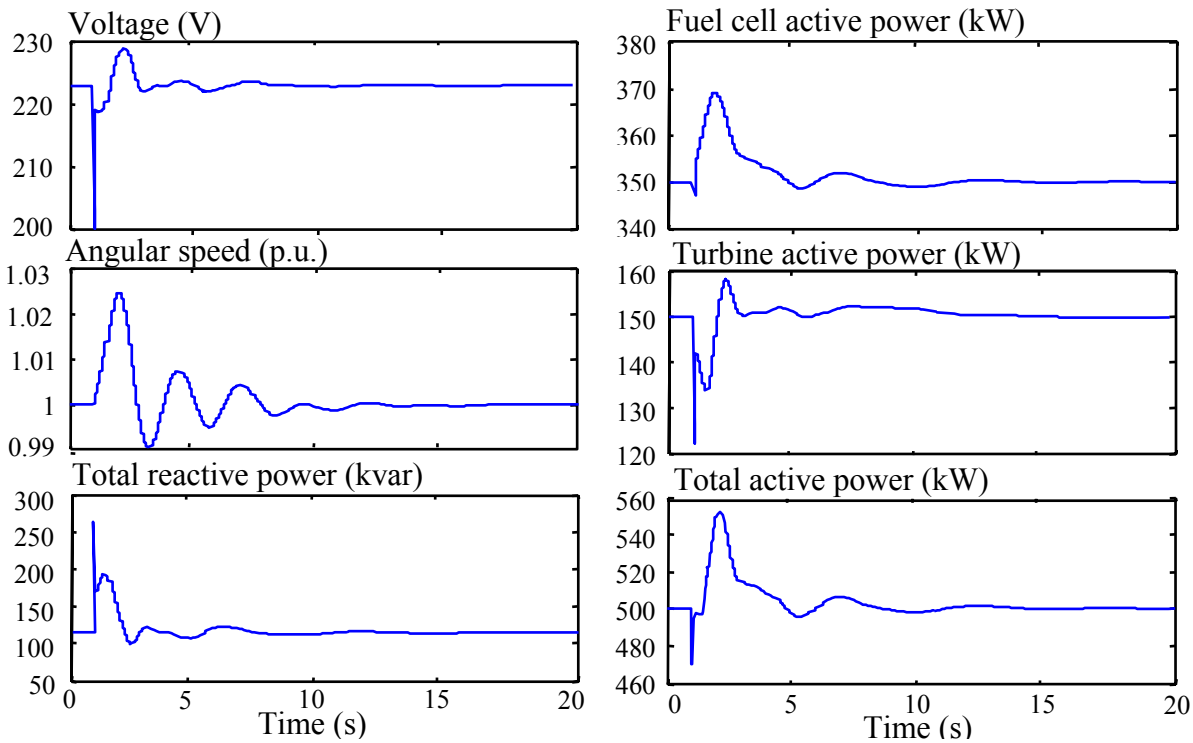

Fig 4-21 Response of a hybrid unit to a 80ms short circuit in the high-voltage area

To highlight the difference between the performance of the hybrid unit and individual units operating in parallel, the FCs and the MTs are modelled and connected without any constructional connections between them. The response of the parallel units to the same 80ms short circuit is shown in Fig 4-22. From Fig 4-21 and Fig 4-22, the similarity of the voltage, which is defined by the network rather than the DG units, is obvious. As a result, the reactive power varies also in the same manner despite its relatively stronger oscillations with the hybrid units. On the other hand, the turbine active power and the angular speed react differently. This means that the main effect of the hybrid structure is on the active power and

the related variables. Generally, the hybrid units show stronger oscillations regarding the reactive power, while lower overshoots and power variations during the fault are achieved in the active power compared to the parallel operation.

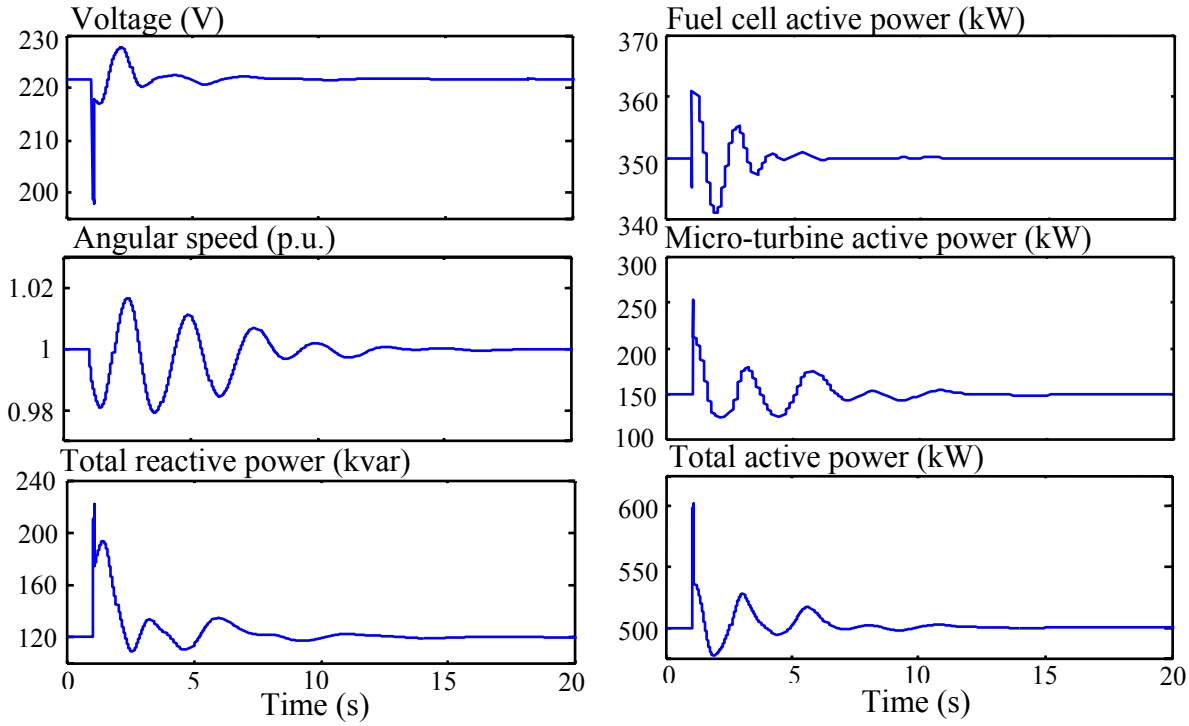

Fig 4-22 Response of two individual FC and MT units operating in parallel to a 80ms short circuit in the high-voltage area

Fig 4-23 gives a comparison between the change in the total active power transferred to the 110kV system as a result of the thee-phase fault without DG units, with separate FCs and MTs units and with CFCMT units. The comparison shows that both parallel operation and hybrid configuration are likely to be similar from the damping point of view. However, a significant reduction in the power variation during the fault occurs with the hybrid units. This emphasizes the previous result of the lower active power variation in the faulty system.

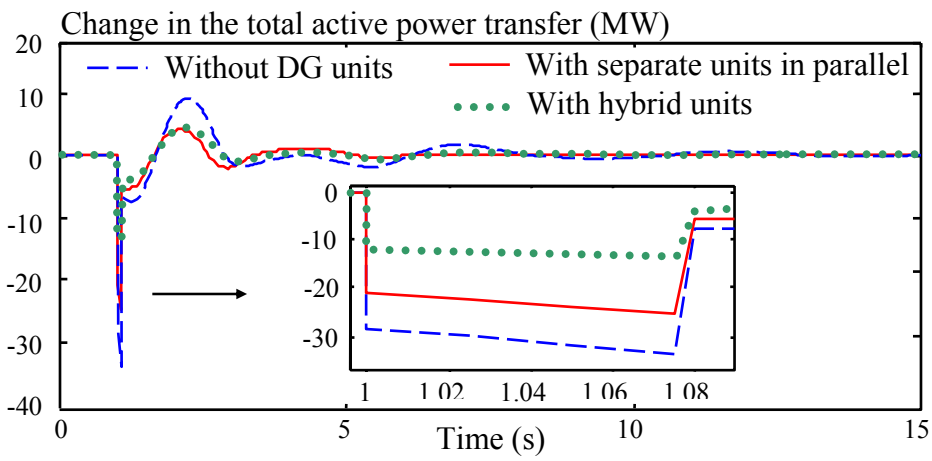

Fig 4-23 Change in the total power transferred to the 110kV area with three different cases as a result of a three-phase short circuit in the 380kV network

Fig 4-24 shows the voltage profile at a load bus in the three cases, where the utilization of CFCMT units causes similar behaviour like that of the separate units.

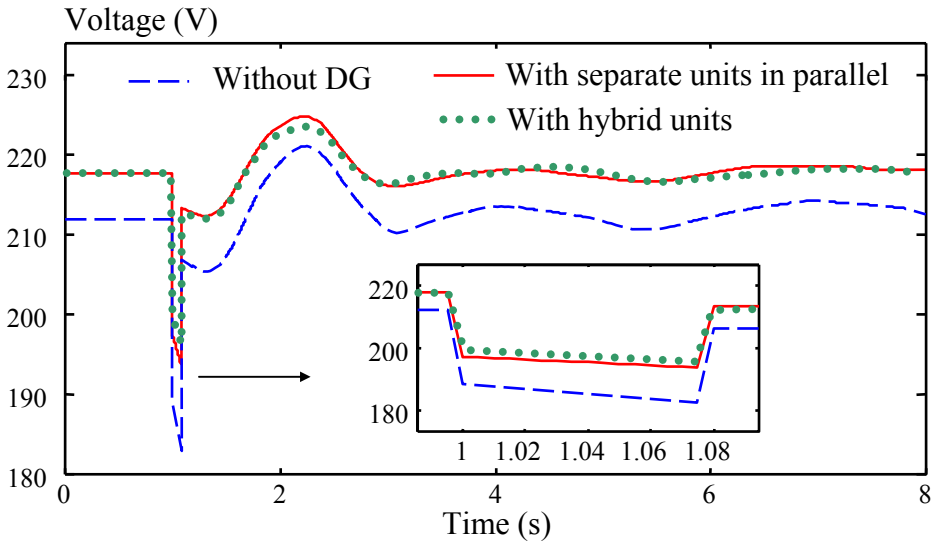

Fig 4-24 Voltage variation at a low-voltage bus with and without DG units as a result of a three-phase short circuit in the 380kV network

4.6 Conclusion

The dynamic behaviour of a hypothetical power system containing a large number of FCs and MTs has been investigated. Also, construction and dynamic performance of hybrid CFCMT units are analysed. In both cases, the power from the DG units covers up to 30% of the total demands at the 0.4kV level. Because of the expected impact from such high power on the overlying parts of the network, the system model includes also a high voltage network.

Generally, the results show that the DG units can absorb, to some extent, large disturbances within the network. However, due to the local task of the controllers, the DG units did not respond to the interarea oscillations. The results show also some improvement in the dynamic performance of the low-voltage area, which is caused on one hand by the smaller voltage drop over the transmission lines and transformers and on the other hand by utilizing the active voltage sources near the load centres.

The active power of the hybrid CFCMT unit is significantly affected by the new structure due to the impact of the FC dynamics on the power of the turbine. As a result, the angular speed of the PMSG is also strongly affected. A similar behaviour from the reactive power is obtained since it depends on the terminal voltage, which is defined by the network rather than the DG units.

Chapter 5

Artificial Neural Network-Based Dynamic Equivalents for Distribution Systems Containing Active Sources

5.1 Introduction

Accurate modelling of electric power systems is essential for stability studies from both planning and operation points of view. The computational difficulty associated with large interconnected power systems increases dramatically with the rapid increase of the size of networks [59]. It is not practical, and also in most cases not necessary, to fully model the large interconnected networks. It will be also formidable computational task to simulate power systems in detail when a large number of active DG sources are considered within distribution systems [59]. On the other hand, approximating the dynamics of the distribution networks using passive lumped loads will lack the sufficient accuracy to simulate the dynamics of DG units. The need for fast simplified analysis of power systems obligate the reduction of certain subsystems that are outside the investigation focus. However, any realistic dynamic model has to give reasonable approximations to the dynamics of active sources and their impacts on the high-voltage networks. Replacing distribution systems that comprise hundreds or thousands of active components with suitable dynamic equivalents will achieve large simplification for the analysis of power systems [60].

In this chapter, a generic nonlinear dynamic equivalent model based on recurrent ANNs is presented and used to replace the 110kV area and the underlying distribution systems in the PST16 network. The development of such dynamic equivalent does not obligate specifying a particular model configuration in advance. Rather, the equivalent model is specified based on the structure and the parameters describing the ANN (activation functions, biases and weights). The main advantage of this equivalent is the need for measurements only at boundary buses between reduced and retained subsystems. Hence, the parameters, topology and complexity of the replaced subsystem will not affect the procedures. Furthermore, the accuracy of the developed model is not significantly affected by changing the operating point, i.e. it is not restricted to certain initial power-flow

conditions. Once trained and tested, the ANN-based equivalent model can be used in simulation, analysis and control-design procedures.

5.2 Survey over existing approaches

The approaches for dynamic equivalencing and model reduction can be classified as linear and nonlinear methods.

5.2.1 Linear-based approaches

Linear techniques substitute the replaced subsystem in the investigated power system by a linear generic model, which can be developed based on modal analysis or model identification [61, 62]. The low-order dynamic equivalent is defined depending on input/output data using the pre-fault operating conditions of the replaced subsystem. Then, the complex nonlinear representation is reduced by identifying a linear equivalent model as shown in Fig 5-1. When coupling this model with the retained subsystem, it will consistently resemble the dynamic behaviour of the original system around the initial operating point.

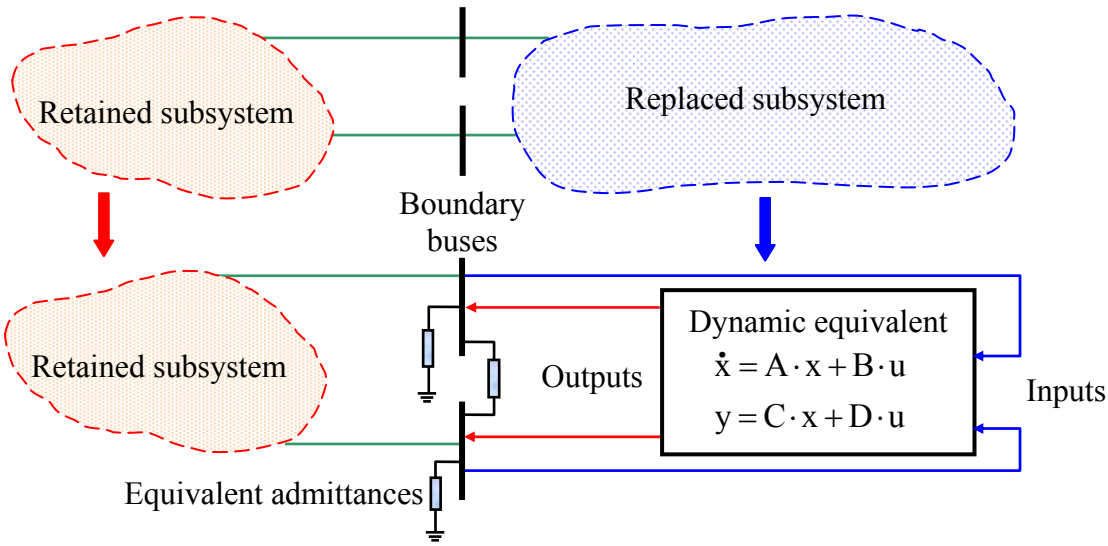

Fig 5-1 Representing the replaced subsystem using reduced linear model

The inputs and outputs of the linearized model vary from one approach to the other but the most practical one is that depends on the Norton model [61]. In this case, boundary bus voltages are used as the inputs to the linear model, while the outputs are the injected currents. With the new software and simulation packages, the reduction of power systems using linear-based approaches represents a simple task and can be accomplished in one step, despite the long processing time required when dealing with large interconnected power systems. However, the linear-based approaches have the following drawbacks [61, 62]:

- The results are accurate only around the operating point at which the reduction has been developed and will not adequately represent the system when the operating point moves away from the base case.
- Some restrictions arise when applying this method to strongly nonlinear problems and also the system dimension can cause some limitations in the computational procedures.
- It is difficult to define the modes, which could be safely eliminated without affecting the results. The reduced order model will not be adequate to study some modes if their dynamics are cancelled during the reduction process.

5.2.2 Nonlinear-based approaches

Nonlinear approaches for dynamic equivalents are usually based on the coherency concept, where a group of coherent generators is aggregated into a single equivalent one [63, 64]. The equivalent generators are then used to constitute the coherent groups in the reduced-order model. To define the coherent groups and to perform the aggregation process, a complete knowledge of the behaviour of the replaced generators is required. This approach has the advantage of describing the equivalent generators by similar nonlinear models as the replaced machines and, hence, they are compatible with other components in the network. To apply the coherency-based approach, the following steps are followed [63, 64].

- The coherency has to be identified and, consequently, the coherent generators are grouped. This process depends on the swinging of the generators, which is defined by rotor angles or rotor angular speeds.
- Generators in each coherent group are aggregated and suitable models for the equivalent generators are developed as shown in Fig 5-2.
- Suitable equivalent regulators are developed for the equivalent generators.

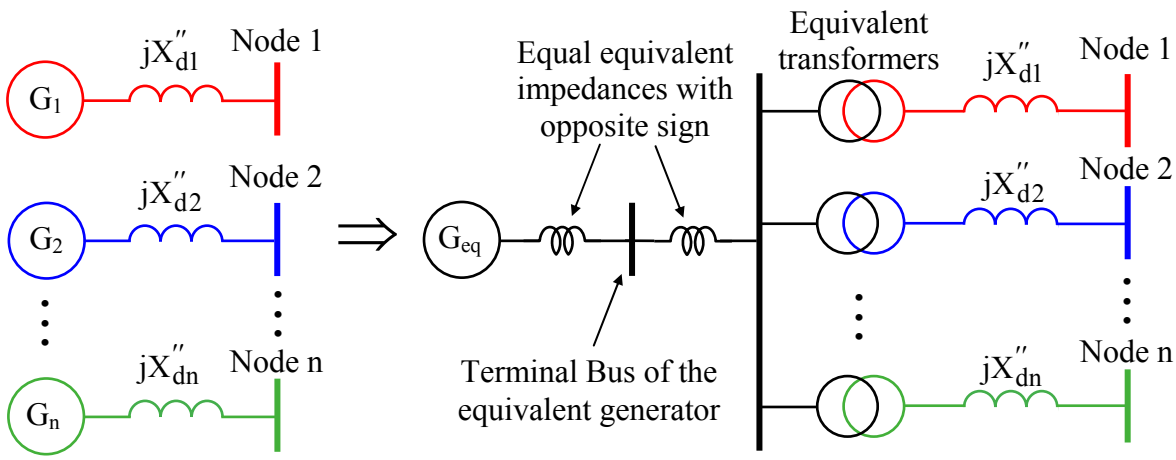

Fig 5-2 Representing coherent generators by a single equivalent one

The coherency-based approach has two main drawbacks:

- It requires the analysis of the electromechanical behaviour of all generators in the replaced subsystem to define the parameters of the dynamic equivalent
- In some cases, the available measurements may be insufficient to develop accurate and reliable equivalents [65]. This is true especially with the development of equivalent regulators, such as automatic voltage regulators and speed governors, for the equivalent generators [66, 67].

With the spread of active DG sources in power systems with effective dynamic impacts, some difficulties regarding classical equivalent approaches will arise. The coherency-equivalent techniques, which depend on analyzing the electromechanical behaviour of generators through angular speeds or rotor angles, will not be suitable for many DG units, which are linked to the network through inverter interfaces. In additions, several DG units, like FCs and photovoltaic, are not characterised by angles or speeds. Therefore, new general equivalent approaches have to be developed to take into account the nature of the new types of sources.

5.3 Proposed technique

The idea behind the proposed technique is to substitute all active components in the distribution system by a recurrent ANN, which is connected to the retained subsystem through the same boundary buses. The recurrent structure of the ANN is required to capture the dynamic behaviour of the replaced network and to enable the online interaction with the retained network. In addition, passive loads can be represented as lumped equivalent elements at the boundary nodes using the conventional practice. In the current investigated case, constant-impedance equivalent elements are used to represent the passive loads. Voltage-and frequency-dependency of the loads can also be modelled using the general exponential relations. The separation between active and passive elements extends the validity of the equivalent model to simulate changes in the generating and loading conditions inside the replaced system itself. In this case, changes in the loading conditions are simulated by adjusting the equivalent lumped elements at the boundary buses. On the other hand, slight modifications in the initial conditions can account for varying the generation status of the DG units. The entire distribution system can also be replaced by the recurrent ANN if there is a difficulty in representing the passive loads separately. However, the separation between active and passive elements gives more flexibility in the analysis. The principles of the proposed dynamic equivalent approach are explained in Fig 5-3 for only one boundary bus between the retained and the replaced subsystems.

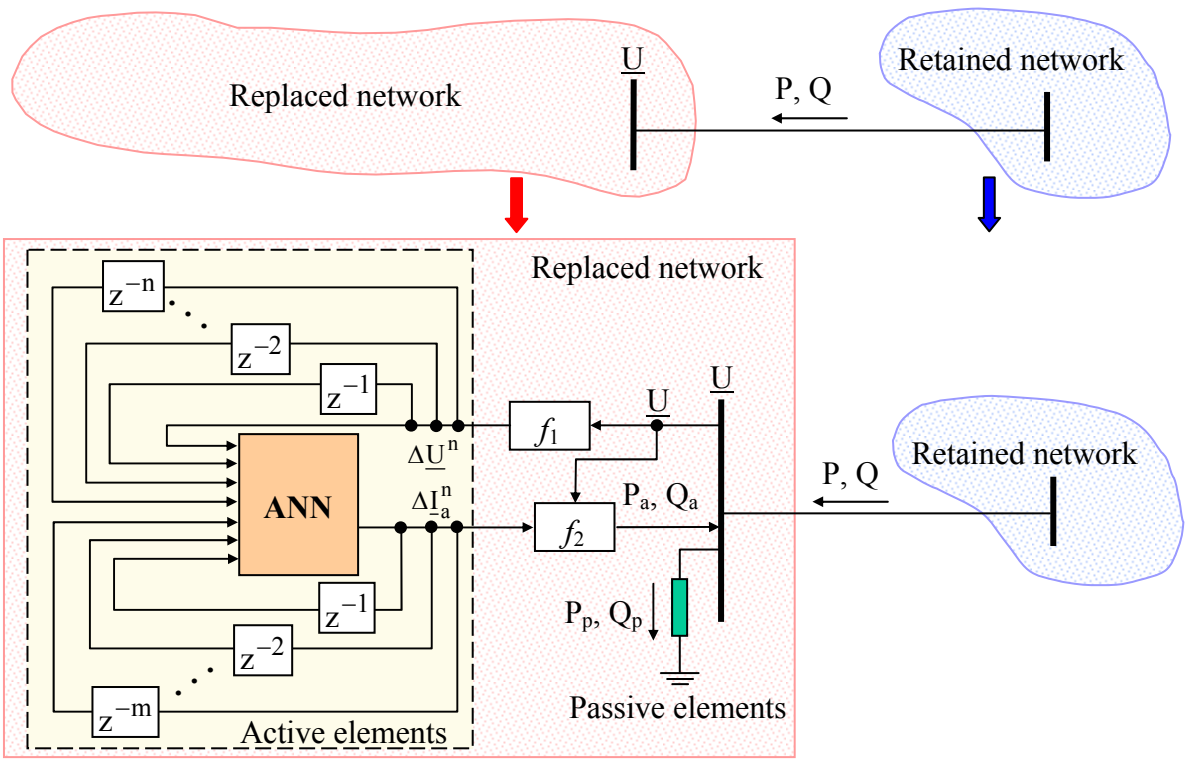

Fig 5-3 Principles of the proposed dynamic equivalent approach

In addition to the ANN itself, the model requires two supplementary functions: a mapping function to prepare the ANN inputs and demapping function to process the outputs from the ANN to calculate complex power. These two functions represent the interface between the ANN and the retained network. The equivalent model interacts with the retained system through the boundary buses. It is perturbed by the voltages at these buses and reacts by supplying the corresponding complex power at each time interval. The ANN itself acts as a Norton model, where the normalized deviations of voltages are used as main inputs and the normalized deviations of currents represent the outputs. In addition to the input voltages, past values of currents and voltages are also introduced at the input layer to achieve the recurrent structure. Thus, the ANN is able to capture the dynamic nature of the original system and to maintain the continuous-time operation of the entire network.

The current rather than power is used as output from the ANN as it represents independent variable, whereas power depends on the voltage, which is an input to the ANN. Therefore the use of current gives better convergence in the training process compared to the complex power due to the complete decoupling between outputs and inputs of the ANN. The use of normalized deviations as inputs and outputs in the ANN allows the use of the equivalent model under new initial power-flow condition. The ANN in this case represents a normalized model

scaled on initial conditions at the boundary buses. Augmenting this feature with the independent representation of active and passive elements results in a universal model, which is capable of simulating the original system under different operating conditions.

At each time interval, the dynamic equivalent recognizes the operating status of the retained network through the instantaneous values of boundary-bus voltages ($\underline{U}$). The normalized voltage-deviations ($\Delta\underline{U}^n$) are then computed through the mapping function (f_1). The ANN is used to define the corresponding normalized deviations of currents for the active components ($\Delta\underline{I}_a^n$). The complex power (P, Q) is calculated using the demapping function (f_2) and supplied to the retained network. The normalized deviations of currents and voltages are computed based on their initial conditions as follows:

$$\Delta\underline{I}_{a,i}^n = \frac{\underline{I}_{a,i} - \underline{I}_{a,i}^0}{\underline{I}_{a,i}^0} \qquad i=1,2\ldots j \tag{5-1}$$

$$\Delta\underline{U}_i^n = \frac{\underline{U}_i - \underline{U}_i^0}{\underline{U}_i^0} \qquad i=1,2\ldots j \tag{5-2}$$

where:

$\Delta\underline{I}_{a,i}^n$: normalized current-deviation of active components at boundary bus i

$\underline{I}_{a,i}$, $\underline{I}_{a,i}^0$: current of active sources at boundary bus i and its initial value

$\Delta\underline{U}_i^n$: normalized voltage-deviation at boundary bus i

$\underline{U}_i$, $\underline{U}_i^0$: voltage at boundary bus i and its initial value

j : number of boundary buses

Real and imaginary parts of $\Delta\underline{U}_i^n$ are used as separate inputs to the ANN, while real and imaginary components of $\Delta\underline{I}_{a,i}^n$ are obtained separately at the output layer. The actual values of complex currents are calculated inside the function (f_2) and used to calculate the active and reactive power at each boundary bus.

5.4 Application with the PST16 network

In the PST16 network, the 110kV system with the underlying 10 and 0.4kV parts is assumed as the replaced subsystem. This system, which contains 56 FCs and 56 MTs with different capacities, is to be replaced by the recurrent ANN and

the equivalent lumped loads. The retained subsystem is the rest of the high-voltage network including area "A", area "B" and the 220 and 380kV parts of area "C". The interface between the retained high-voltage system and the replaced system is through two buses, i.e. B_1 and B_2 in area C (see Fig 4-2). If the focus of the study is not directed to the distribution system itself, replacing this network with all active sources by a suitable dynamic equivalent will achieve a great simplification in the simulation. Table 5-1 summarizes the number of electric components in both the retained high-voltage network and the replaced distribution system.

Table 5-1 Summary of components in the retained and replaced subsystems

	Retained subsystem	Replaced subsystem
Buses	60	238
Branches	45	178
Transformers	26	64
Generators	16	0
Micro-turbines (MTs)	0	56
Fuel cells (FCs)	0	56

The large number of components in the distribution system complicates the dynamic simulation considerably. In real interconnected systems, where the number of elements in distribution systems reaches up to thousands of units, the detailed simulation of all elements will be unfeasible. Conventionally, lumped-load representation with suitable voltage-and frequency-dependant elements is used to represent distribution networks. With large power from active DG units, their impact on the high-voltage networks has to be considered. Neglecting this dynamic contribution will cause an unacceptable error in the analysis.

To assess this error in more detail, the performance of the entire network is investigated in three cases. In the first case, the distribution system is modelled in detail with all DG units. In the second case, the conventional lumped representation is considered, where the equivalent load at each boundary bus depends on the voltage at this bus with general exponential relation. In the third case, the power of the equivalent loads is related to the voltages at all boundary buses with general exponential relations as follows:

$$P_i = P_i^0 \left(\left| \frac{U_1}{U_1^0} \right|^{p1,i} \cdot \left| \frac{U_2}{U_2^0} \right|^{p2,i} \right) \qquad i=1,2 \qquad (5\text{-}3)$$

$$Q_i = Q_i^0 \left(\left| \frac{U_1}{U_1^0} \right|^{q_{1,i}} \cdot \left| \frac{U_2}{U_2^0} \right|^{q_{2,i}} \right) \qquad i=1,2 \qquad (5\text{-}4)$$

where:

P_i and P_i^0 : the active power at bus i and its initial value

Q_i and Q_i^0 : the reactive power at bus i and its initial value

$P_{1,i}, P_{2,i}, q_{1,i}, q_{2,i}$: coefficients

An optimization process is carried out with the second and third cases to define the best values of the unknown coefficients by minimizing the error between the actual and the calculated supplied power. The minimization in both cases is carried out without restricting the coefficients to the known typical limits and therefore, the obtained coefficients have values in the range of ±20. This is intended to get the best possible performance using the lumped representation. A comparison between the powers transferred to the 110kV area following a three-phase short circuit in the retained subsystem in the three cases is given in Fig 5-4. It is obvious from the large difference shown in the figure that this approximation cannot be used to represent distribution systems including active sources. When the coefficients are restricted to the typical limits, worse results are obtained, which emphasizes the unfeasibility of using this approximation.

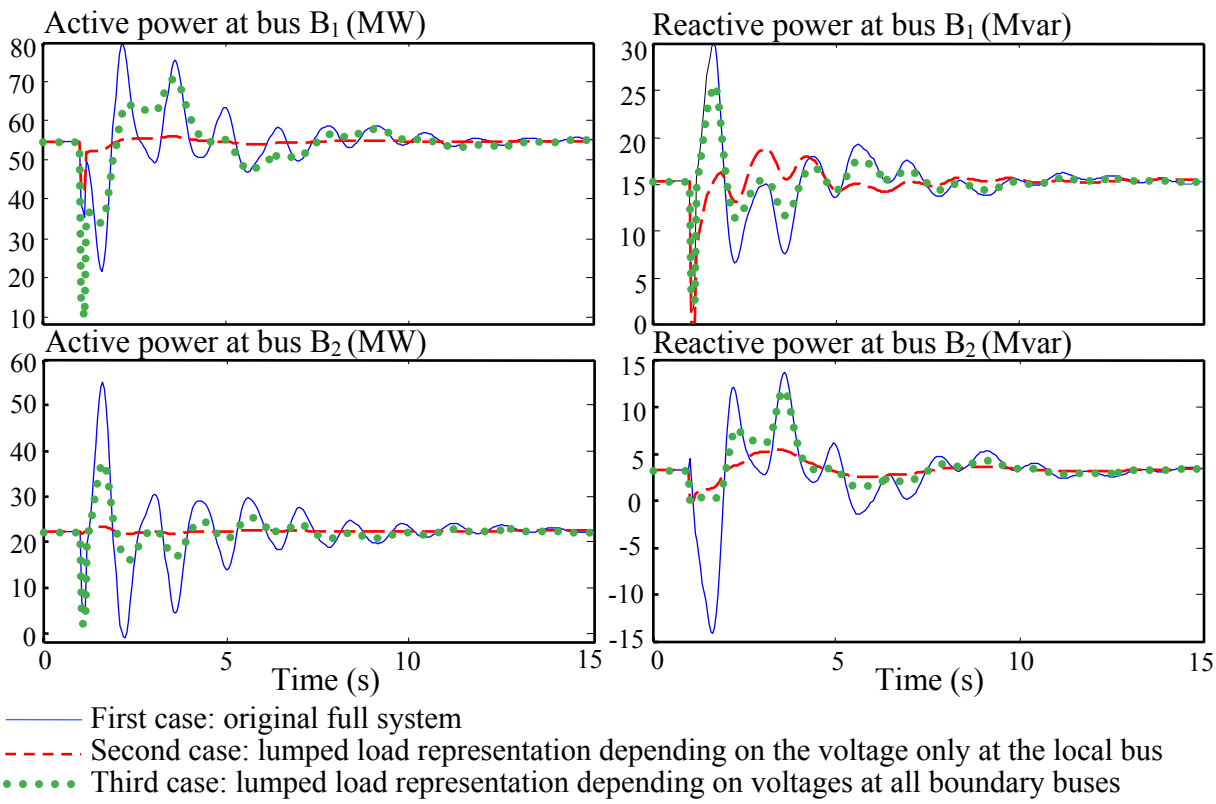

Fig 5-4 Comparison between the performance of the original full-system and the two-lumped load-modelling approximations

5.5 Recurrent ANNs for dynamic equivalents

ANNs have high capability to deal with complicated nonlinear problems in a general frame, which enables them to be successfully applied to new situations that are not used in the training phase [65]. Therefore, good-trained recurrent ANNs can replace complex distribution systems and are expected to properly interact with the retained network at a wide range of operating conditions. With the use of ANNs for dynamic modelling purposes, no information about the system structure is required and the use of complex mathematical analysis is avoided. This represents a significant advantage especially when there is a limited understanding of the relations between system variables.

5.5.1 Data preparation

Several three-phase short circuits are simulated at different locations in the retained network. The simulation of each fault is carried out for 10s, which is enough to restore the steady state conditions after the fault clearance. A 10ms integration time step is used in the simulation, which results in 1000 pattern with each fault. Complex voltages and injected currents at the boundary-buses are stored during the fault simulation and subsequently used to prepare suitable patterns for training the ANN.

5.5.2 ANN structure

Since the ANN is required to capture the dynamics of the replaced network, which is distinct by currents, recursive loops are used to feedback normalized current deviations to the input layer with time delays. In addition, the ANN interacts with the retained network and recognizes its dynamic behaviour through the voltages. Therefore, past values of normalized voltage deviations are also used at the input layer. With two boundary buses, the ANN has 4 main inputs representing the real and imaginary components of normalized voltage-deviations. Furthermore, normalized deviations of these voltages at four previous time intervals are received at the input neurons. On the other hand, four outputs representing the real and imaginary components of normalized deviations of currents are obtained from the ANN. Four recursive loops with delay actions from each output are fed back to the input layer of the ANN. This results in a total number of 20 inputs in addition to 16 recurrent loops.

The ANN contains two hidden layers with 10 and 5 neurons respectively. All hidden layers comprise neurons with nonlinear-sigmoid activation functions,

while neurons in the output layer have linear functions. The structure of the ANN is shown in Fig 5-5.

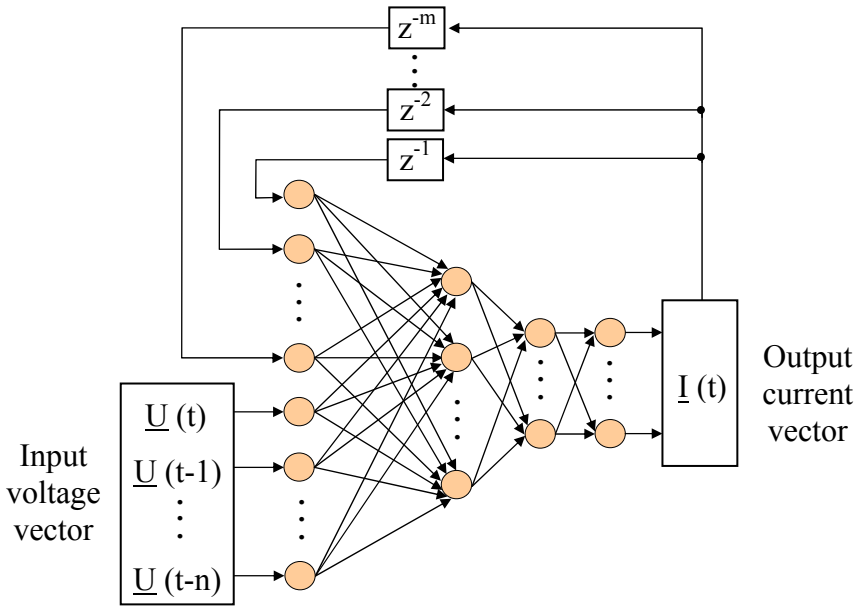

Fig 5-5 Structure of the ANN

5.5.3 Training process

Patterns corresponding to eight different three-phase short circuits are used in the training process. Time-histories of voltage variables are involved in the input features to the network, while real recurrent loops from output current variables are considered. A special program is developed to train the ANN with actual recurrent loops. With 1000 pattern belonging to each waveform, 8000 patterns are used in the training process, which is accomplished offline without actual interaction with the retained network. However, the test and validation of the developed dynamic model are based on real-online interactions. The results from the training process (i.e. biases and weights) are saved to be used in the implementation procedures.

5.6 Implementation of the ANN-based equivalent

Since the equivalent model is intended for online applications, it has to be implemented in such a way that it interacts with the retained subsystem at each time step to give similar behaviour like that of the original network. As mentioned in section 4.3, unconventional energy sources are simulated in the PSD package in a so-called “regulator files”. In these files, a complete description of the dynamic behaviour of the element can be stored and integrated into the network through one or more buses. The processing within the regulator files is accomplished using pre-constructed blocks to describe the dynamic behaviour of the element. The

ANN-based dynamic equivalent is implemented in the PSD simulation package as an unconventional power source to interact with the retained network in the online mode.

At each time step, state variables, boundary-bus voltages in this case, are captured and processed to get a complete input set to the ANN using the function (f_1). A block simulating the behaviour of the ANN is used to process the inputs with the help of the information about the ANN structure (such as biases, weights and types of activation functions) to get the corresponding output currents. The information describing the ANN structure is saved in a supplementary text file to be used through the simulation process. The outputs from the ANN are then used to calculate the active and reactive power using the function (f_2). The complex power is supplied to the retained network to contribute in defining the behaviour of the entire network. Fig 5-6 gives an idea about the implementation and the interaction of the ANN-based dynamic equivalent with the retained network.

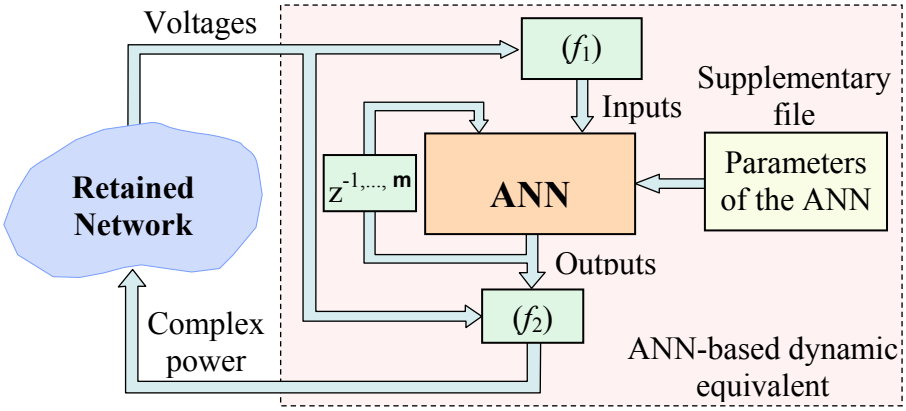

Fig 5-6 Implementation and interaction of the ANN-based dynamic equivalent with the retained network

5.7 Simulation results and discussion

After replacing the 110kV network and the underlying distribution systems by the ANN-based dynamic model, the performance is investigated online and compared to that of the full system. Fig 5-7 shows a comparison between the equivalent complex power supplied to all active units in the distribution system through each boundary bus after simulating a three-phase short circuit in the retained network in area B at a 220kV bus. This fault is one of the eight disturbances used to extract training patterns. The negative sign of "steady-state" values indicates that the power is flowing *out* of the sources (consumer oriented sign convention).

The coincidence between the performance of the original full system and that of the ANN-based model indicates that the ANN succeeded to learn the nonlinear

behaviour of the replaced subsystem. However, it is necessary to test the model under new disturbances, which are not used in the training mode to examine the generalization capability of the ANN.

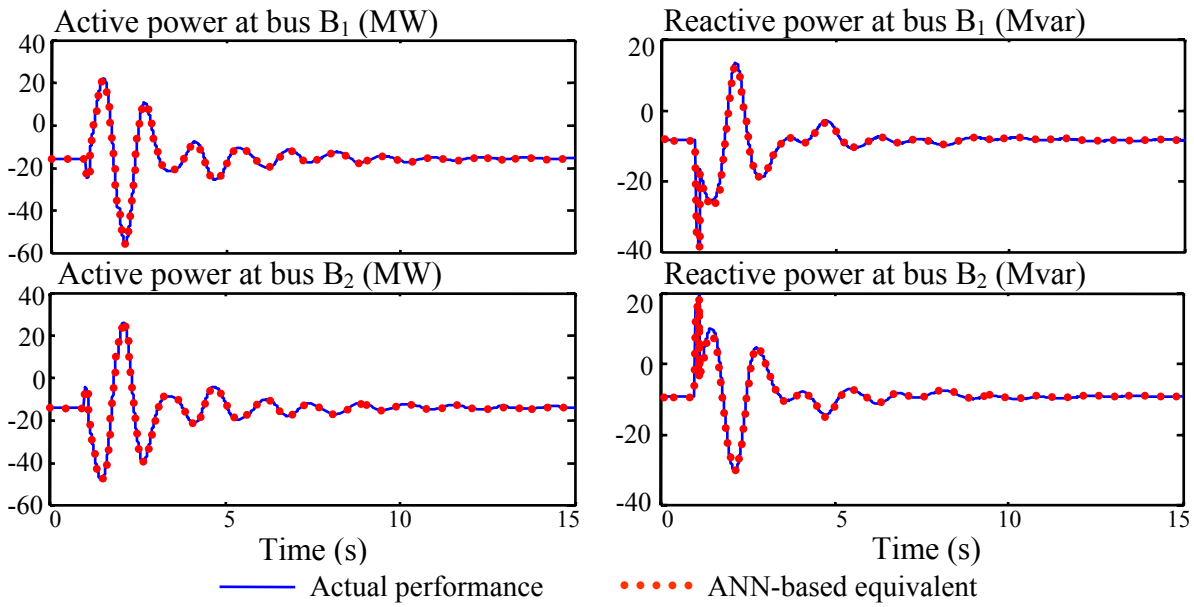

Fig 5-7 Comparing the equivalent power of active sources at boundary buses under a disturbance, which is used in the training process

Fig 5-8 shows a new comparison between the original and the equivalent models under a three-phase short circuit in area C at a 380kV bus. It is important to notice that this fault is not used in preparing the patterns for training the ANN.

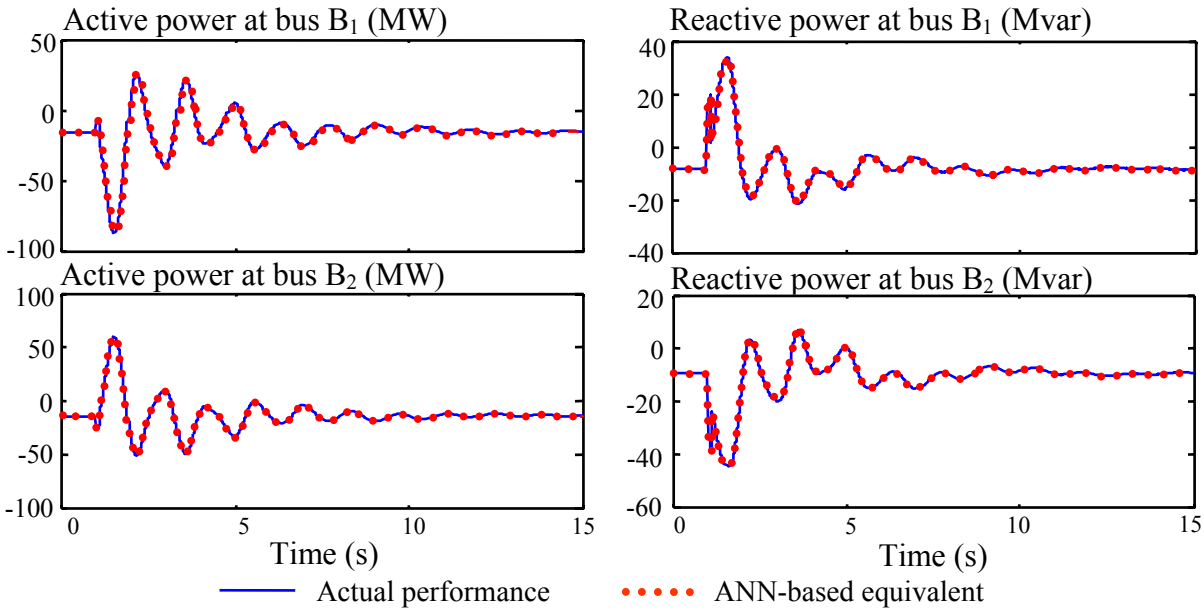

Fig 5-8 Comparing the equivalent power of active sources at boundary buses under a disturbance, which is not used in the training process

The similarity between the obtained responses is obvious, which means that the recurrent ANN is robustly successful in capturing the target waveforms. Several

comparisons are carried out under other new disturbances, where the performance is always similar to that of the original full model. This ensures that the ANN-based model effectively reproduces the behaviour of the replaced subsystem in a general form. Therefore, different studies of the entire network including the proposed equivalent model are possible with high accuracy.

To demonstrate the capability of the proposed equivalent model to cover new operating conditions, the behaviour of the same model is studied under new power-flow conditions by varying the loading status in the retained network. The generated power and load demand in the replaced subsystem are maintained constant. Thus, the total power transferred to the low-voltage network is not changed. However, the voltages and the partition of the power at the boundary buses are changed as shown in Table 5-2. The total power transferred is slightly increased to account for the increase in the power loss due to the voltage reduction.

Table 5-2 Voltages and powers at boundary buses for the base and the new power-flow cases

	U_1 (kV)	U_2 (kV)	S_1 (MVA)	S_2 (MVA)
Base case	381.150	222.530	54.823+j15.307	22.332+j3.262
New case	378.340	221.420	61.428+j13.431	15.844+j5.945

A new three-phase short circuit is simulated in area C at a 220kV bus under the new power-flow conditions with both the full network and that comprising the ANN-based equivalent model. Fig 5-9 compares between the powers supplied by active units through the two boundary buses using the full-model and the ANN-based model.

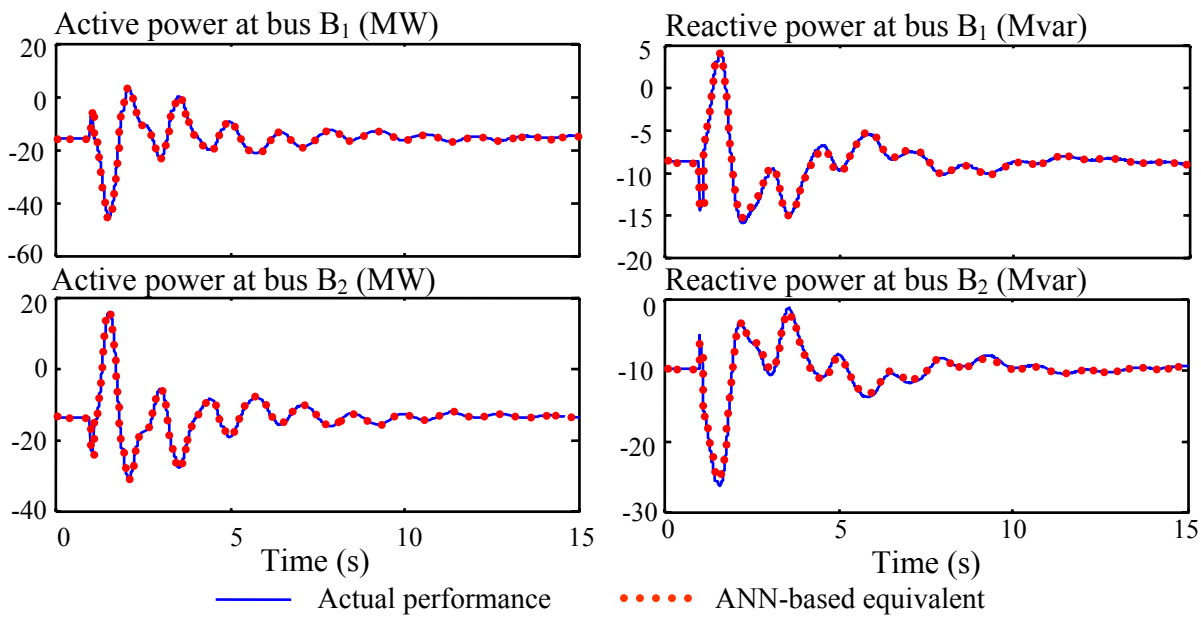

Fig 5-9 Comparing the performance of the original and the equivalent systems starting from a new power-flow initial condition

The results show that the performance of the equivalent model is still in a good agreement with the performance of original system. The use of normalized deviations rather than the variables themselves extends the validity of the dynamic equivalent to cover new initial conditions with high accuracy.

Most of the conventional dynamic equivalents fail to simulate the performance of the entire network if any change occurs inside the replaced system. The simulation of the new condition requires the development of a new dynamic model. This is not the case with the proposed dynamic equivalent due to the modelling of active components separately from passive loads in addition to normalizing the decision variables.

To examine the validity of the equivalent model under new generating conditions in the replaced network, the power from the active sources in the low-voltage area is decreased to about 50% of its original value. This is accomplished in the full-system model by switching off some of these units. In the equivalent model, the change of the power is carried out by modifying the initial values of currents and voltages in the functions (f_1) and (f_2). Table 5-3 gives the new contributions of active sources at each boundary bus under the new generating conditions in the distribution system. The loading conditions in the retained network as well as in the distribution system are held constant in the new case.

Table 5-3 The new loading conditions of the active units in the replaced network

	Power from active sources at the two boundary buses (MAV)	
	through bus B_1	through bus B_2
Base case	15.862 + j 8.284	13.851 + j 9.285
New case	8.301 + j 4.242	7.569 + j 4.958

After changing the power contribution of the DG units in the distribution system, a power flow analysis is carried out and a three-phase short circuit is simulated in area A at a 380kV bus. Fig 5-10 illustrates a comparison between the total power of active units using the full model and the equivalent model following this fault. The comparison shows a reasonable accuracy even with the large change in the generated power from these sources (50%). This confirms the universality of the proposed approach since no modifications in the structure or the parameters of the ANN-based model are necessary. This advantage is very important due to the regular variation in the switching status of the DG units. Therefore any equivalent model for distribution systems has to be flexible enough to consider the potential variations in the power supplied by the DG sources.

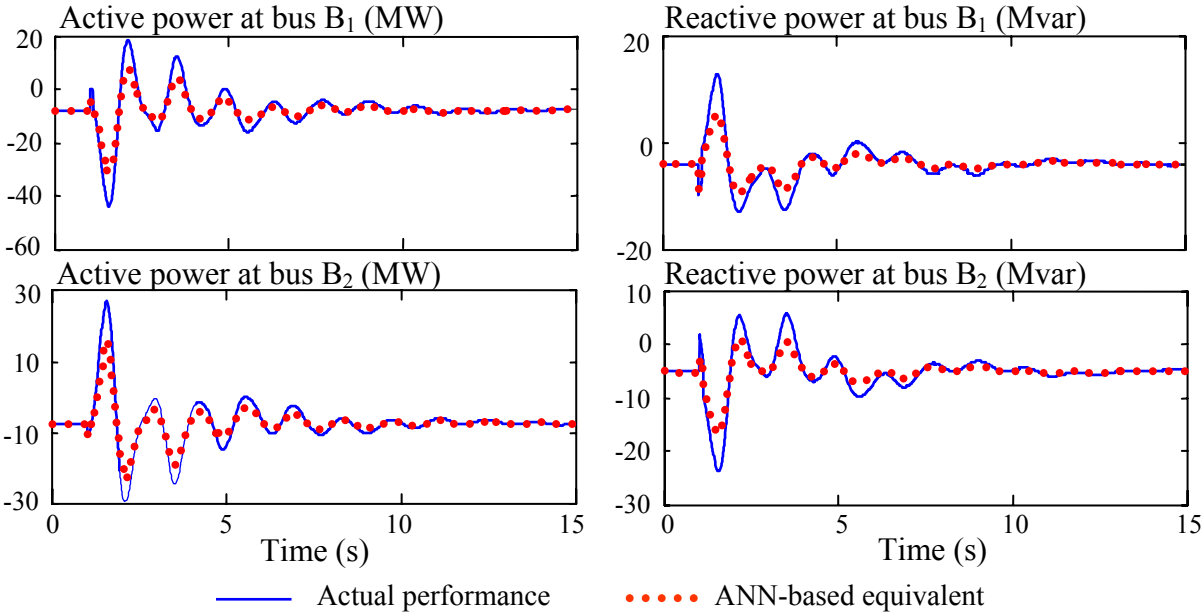

Fig 5-10 Comparing the full-model and the equivalent system after reducing the power of the DG sources to about 50% of the initial value

The integration time step used in the simulation after training the ANN and implementing the dynamic equivalent in the simulation package represents another important issue about the proposed technique. Since the ANN is trained by data prepared using a certain integration time step, results at other simulation time steps have to be verified to evaluate the effect of varying the integration time step on the results. Fig 5-11 shows a comparison between the power from active units using the ANN-based equivalent using three different integration time steps after a three-phase short circuit at a 380kV bus in area C. The three integration time steps are 1ms, 10ms in addition to the 5ms which is used in the training process.

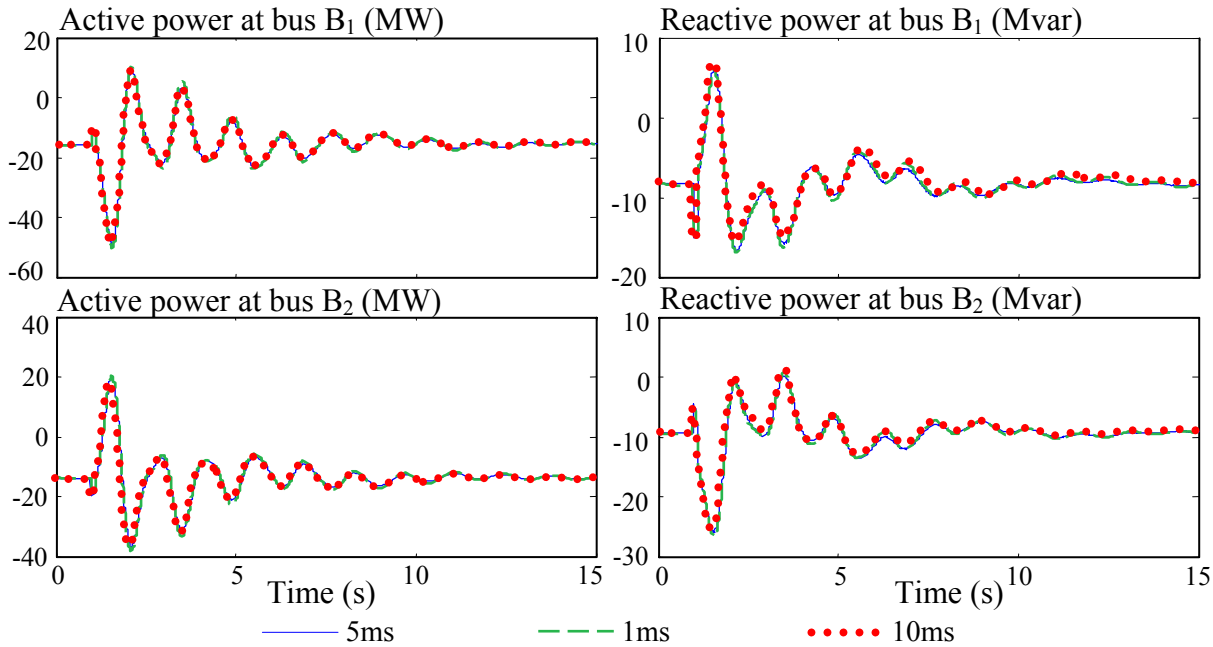

Fig 5-11 Comparison between the performance at three different integration time steps

Fig 5-12 illustrates another comparison with the same fault but when new regulators are used with the synchronous generators in the retained network. The integration time step is also changed to be 10ms. Even with the new regulators and the change of the integration time step, the performance is still in agreement with the original case. Depending on the results, it is possible to simulate the network including the ANN-based model with different integration time steps with acceptable accuracy. However, using an integration time-step which is equal or close to that used in the training process will ensure higher accuracy.

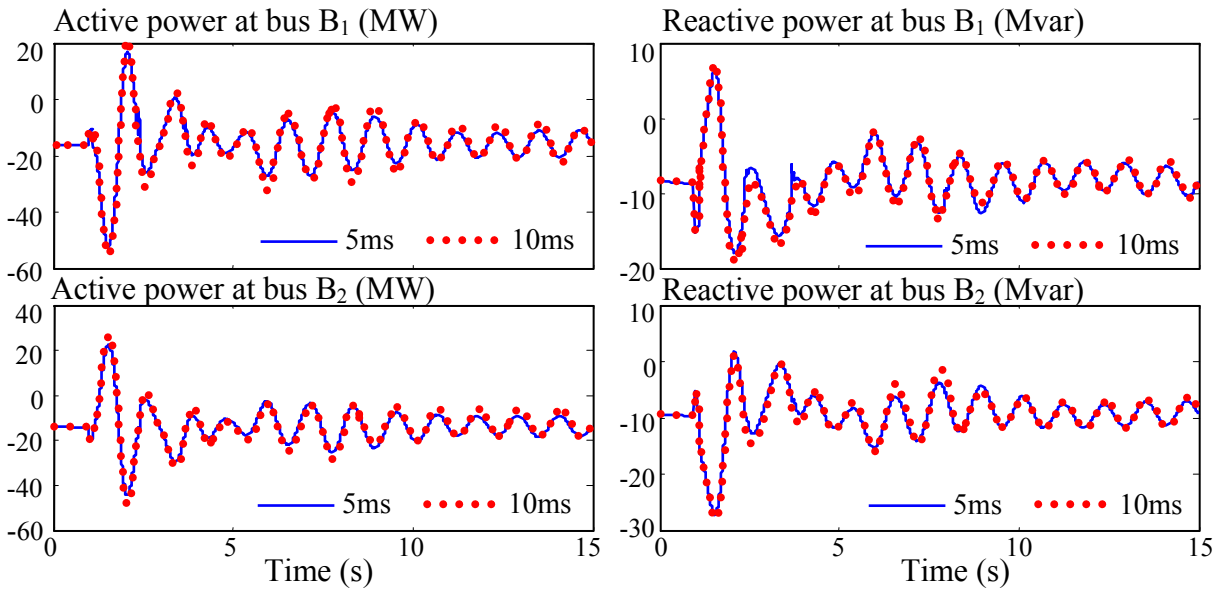

Fig 5-12 Comparison with a new integration time step and new regulators for generators

5.8 Conclusion

This chapter presents a new approach for dynamic equivalents of distribution networks with dispersed generation based on recurrent ANN. Since DG units are expected to feature prominently in distribution networks in the near future, any realistic dynamic model of a distribution system under these circumstances needs to take into account the effect of these units on the dynamics of the high voltage network. The proposed technique requires simulation results or measurements only at the boundary buses and is independent of the size and complexity of the electric network. The equivalent dynamic model thus obtained was implemented on a power system simulation package to investigate whether the model is capable of reproducing the dynamic behaviour of the replaced network in full. The results demonstrate the capability of the equivalent model to capture the dynamic behaviour of the replaced network in its entirety. The model provided outstanding conformity with the results obtained using the full dynamic model of the network even under new generation and loading conditions. The approach promises a significant simplification of the dynamic analysis of large interconnected networks.

Chapter 6

Impact of Distributed Generation on the Stability of Electrical Power Systems

6.1 Introduction

The special characteristics of DG units and their low inertia can cause many technical and operating challenges regarding the stability of power systems [24, 68]. Generally, few numbers of quite small-size DG units, compared to the large centralized power stations, will not influence the operation of the power network and, hence, their impact can be neglected. However, when networks begin to comprise large numbers of DG units with higher capacities, the overall dynamics and the stability of power systems are significantly impacted [24]. Therefore, power system analysis becomes more emerging problem especially with the wide range of technologies associated with the DG units and the configuration uniqueness of each distribution network [6].

Among numerous investigation issues related to power systems containing DG units, stability analysis becomes more critical, and adequate damping of the oscillatory behaviour is of major interest [6, 24, 68]. The conventional approach, which depends on representing DG units together with passive loads in an aggregated form or omitting their effect when analyzing power system stability, is about to be changed [68, 69]. Modern power systems are mostly operating close to their stability limits for economical reasons. This situation demands accurate modelling of power systems taking into consideration the different penetration levels of DG units to adequately evaluate their impacts on the stability of power systems.

This chapter aims at analysing the potential impacts that DG might have on the stability of electrical power networks. In particular, the performance of a power system with different penetrations of DG units is described to assess different types of stability of the bulk networks. For this purpose, a hypothetical network is simulated with two main centralized power plants and several DG units connected onto the electric distribution system. The investigation is carried out at constant load demands but with different contributions from FCs and MTs. Certain numbers of DG units are switched on to supply the required power in the range from 0.0% up to 28.3% of the total load demand in the distribution net-

work. Thus, the rated and supplied powers of the conventional synchronous generators are adjusted to achieve the power balance in the network. With each penetration level, the performance of the network is studied and different stability classes are demonstrated. The results are compared to the performance of the network without any DG units, as a reference case, to highlight the influence of penetration levels of such units on the stability of the entire network.

6.2 Power system description

The electrical network under consideration comprises a high-voltage area with two voltage levels, namely 380kV and 110kV. As centralized power plants, two synchronous generators are simulated and connected to the 380kV nodes via step-up transformers. The 110kV area and the underlying medium and low-voltage networks have the same structure like that simulated in the PST16 network (see section 4.2.1). However, the capacity of FCs and MTs as well as the load demands are changed. In addition, reactive power controller rather than voltage controllers are employed as more practical trend in power systems. The total active load demand in the network is about 250MW. Table 6-1 summarizes the number of components in the investigated network.

Table 6-1 The number of components in the investigated network

Synchronous generators	Buses	Branches	Transformers	Fuel cells	Micro-turbines
2	245	180	66	56	56

Fig 6-1 illustrates the one line diagram of the network showing only one distribution system with the DG units integrated near the load centres. The other five distribution networks have similar configurations like that shown in the figure. The contribution level of the DG units is defined by switching on a number of them at different feeders to give the required power. In all simulated cases, both active and reactive load demands are kept constant. Thus, the power required from the two synchronous generators decreases with the increase of the penetration level of the DG units in the network.

Typical parameters of thermal units are used to simulate the two synchronous generators using fifth-order models. IEEE standard regulators are used for simulating the speed governors and the excitation systems. Since the required power from the generators varies with the variation of the DG power, the rated MVA of the two generators is also changed in each case starting from 110MVA with the 28.3% penetration level up to 150MVA without DG units. The reserve power of each generator is assumed to be always 10% of the rated value and, hence, it is in

proportional with the nominal power. Consequently, the two generators will provide higher reserve power when they are used to fully supply the load due to their higher rating. In each investigated case, the reactive power of each generator is adjusted to obtain the same power factor like that without DG units.

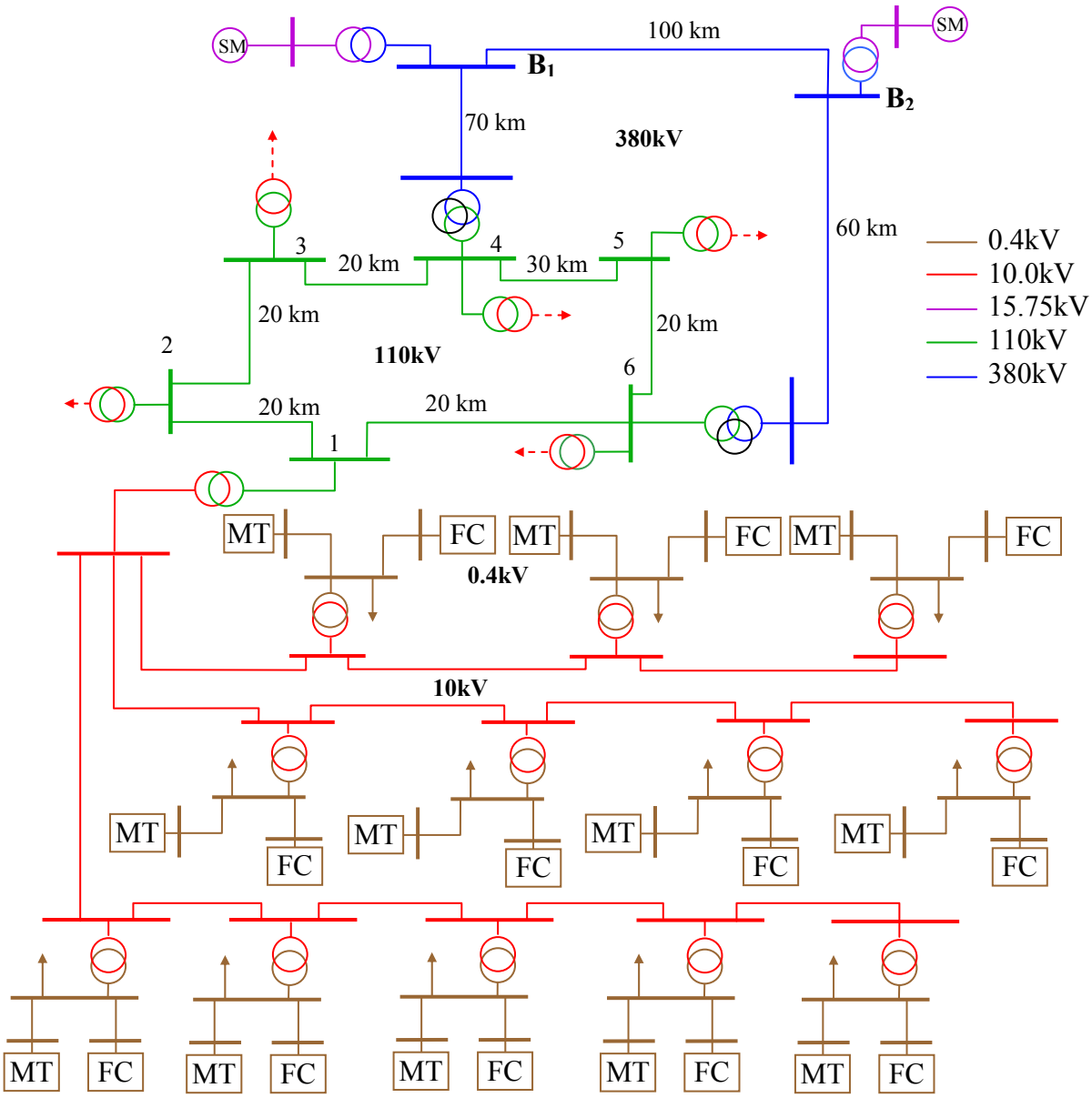

Fig 6-1 The one line diagram of the electrical network showing the integration of FCs and MTs near the end user terminals

The modelling of the MT units is explained in section 4.2.2. The ratings of the MT units in this case vary between 0.3MW and 0.8MW. At the same time, Different types of FCs are considered including PEMFC, AFC and SOFC. Also, various capacities are simulated in the range of 0.5MW up to 1.0MW. The details about the modelling of FC units are introduced in section 3.2. For more realistic simulation, reactive-power controllers instead of voltage controllers are designed to regulate the performance of the DG units.

Since most of the DG units are not utility owned, the power supplied from these units will be defined according to economic consideration. Therefore, it is assumed in the simulation that the power from the DG units will not be adjusted to follow up the load demand. Rather, the owner of the DG unit will supply a specific value of the power to achieve the maximum profit regardless of load changes. For secure operation, the DG units are assumed to be disconnected from the network if the voltages at their terminals decrease lower than 80% of their rated values. This is important to protect the power electronic converter with these units. A delay time of 100ms (five cycles) is assumed for measurements and disconnection of any DG unit after reaching the critical limit. The disconnection of some of the DG units during the simulation represents an additional disturbance to the network. Once any unit is switched off, it is not connected again since the simulation time is smaller than the time required for accomplishing the conventional procedures of the reconnection.

Before investigating the impact of DG units on the stability of the power system, it is appropriate to study their impacts on the power losses and the voltage profiles of the distribution network.

6.3 Impact on the power losses

Generally, the onsite power generation near the load centres causes reduction in the network power losses as a result of the reduction occurring in the transmitted and distributed power. Even if the power loss is increased in some parts in the distribution feeders, the overall losses within distribution systems, and hence in the entire network, will be reduced. In the investigated network, the power generated by any DG unit is lower than the local load demand and, as a result, the power losses will always be lower compared to the disconnection of all DG units. In spite of the relation between the power-loss reduction in the entire network and that in the distribution network, it is more realistic to observe the former for a comprehensive perspective. For different power levels from the DG units, power flow analyses are carried out and the total power losses in the entire network are computed. Fig 6-2 illustrates the percentage of the total power losses in the network versus the power contribution of the DG units. The power of the DG units is increased in steps from 0% up to 28.3%. As shown in the figure, the total power losses in the network decrease with the increase of the power generated in the DG units. However, the magnitude of this reduction depends not only on the power contribution of the DG units but also on their location within the distribution network.

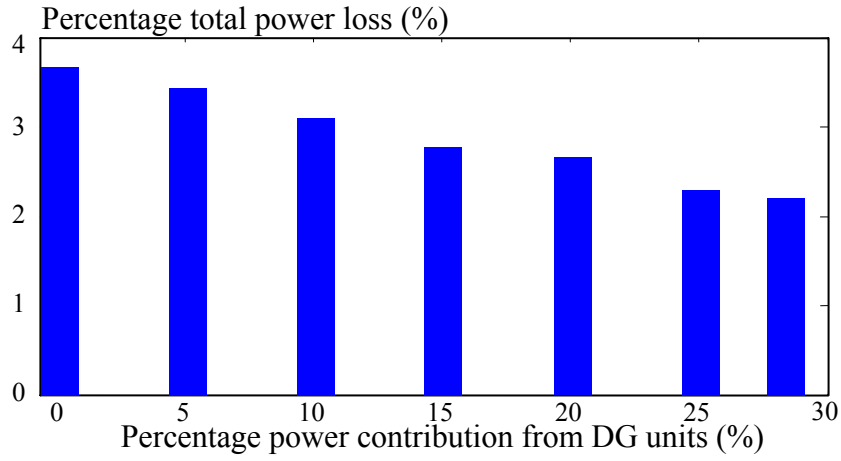

Fig 6-2 Total power loss with different power contributions from DG units

6.4 Impact on the voltage profiles

Keeping the voltage within typical limits along all feeders in the distribution network is necessary to avoid improper operation of power system and customer equipments. Common practice in regulating the voltages depends on tap-changing transformers to control the source voltages at substations [2]. In addition, switched capacitors, synchronous condensers, or static var compensators can also be used on feeders for controlling the reactive power [21]. Providing a portion of energy onsite using DG units can effectively improve and support feeder voltages if these units are properly integrated with the existing network. With the latest-type static converters, the utilization of the DG units could achieve the required voltage support in the distribution network. This can be accomplished by regulating the reactive power through the power factor of converters based on voltage levels on local nodes [2]. On the other hand, tap-changing transformers will not be suitable for the effective regulation of the voltages at all feeder nodes as they assume decreasing voltages along radial feeders [2, 21]. Furthermore, the voltage regulators will not correctly measure feeder demands, rather, the observed loads will be lower than actual values due to the onsite generated power.

To highlight the effect of DG on the voltage profiles, the voltages at different locations are observed considering different DG powers. Fig 6-3 shows the voltages at five nodes of one feeder with different contributions from DG units. The insertion of DG reduces the difference between maximum and minimum voltages of loads supplied from the same feeder. Without DG units, the voltage decreases with the distance of the bus from the power source. Adding DG units causes variations in the voltage levels depending on the location of the added units. With large contributions from DG units, the voltage can be maintained almost constant at different load nodes as in the last two cases with 25% and 28.3% contributions.

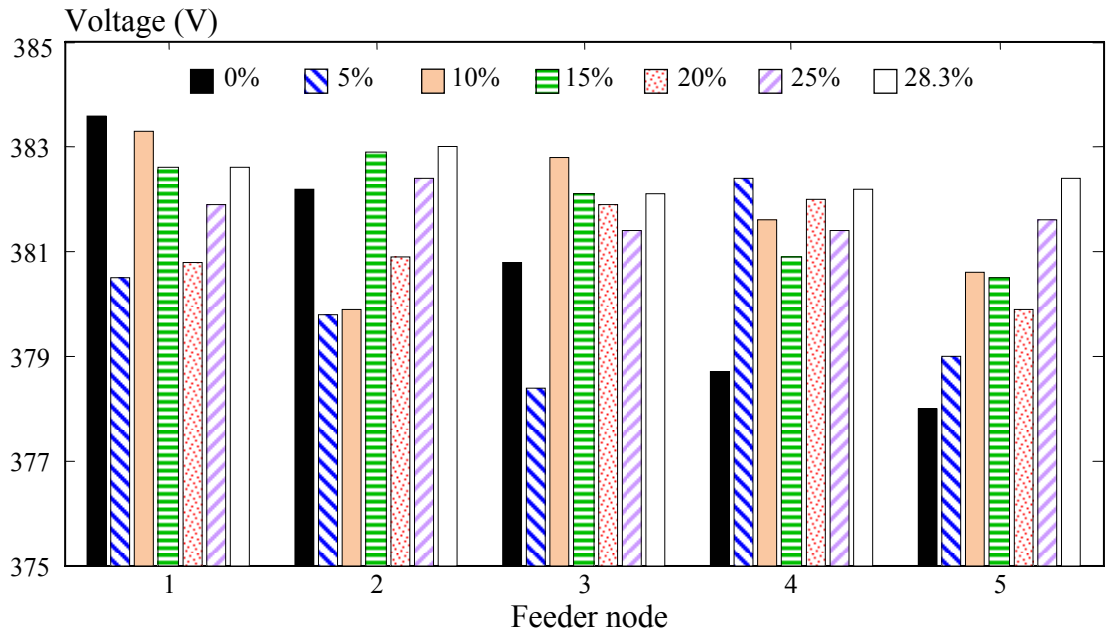

Fig 6-3 Voltage levels at 5 feeder nodes with different contributions from DG units

6.5 Angle stability analysis

6.5.1 Oscillatory stability

The interconnected power systems are continually subjected to small disturbances such as changes in loading conditions. The oscillatory behaviour of the network following such disturbances depends on the operating condition, controller settings and the structure of the network [6]. Due to economic considerations, the electrical power networks are commonly operating near their stability limits. Therefore, oscillatory stability is gaining more interest and its analysis is essential for power system security. The small-disturbance angle instability occurs usually due to the insufficient damping of the electromechanical oscillations. To assess the oscillatory stability of electrical power networks, the modal analysis is employed since it represents the most common approach in this field [6].

With each of the seven penetration levels of the DG units, a power flow computation is carried out to define the operating condition of the network. Modal analysis is then performed in each case and the results are illustrated in the “s” plane in Fig 6-4. A special interest is directed to critical modes, which have low damping ratios. Fig 6-5 illustrates the critical eigenvalues with different power contributions from DG units and Table 6-2 gives more information about them.

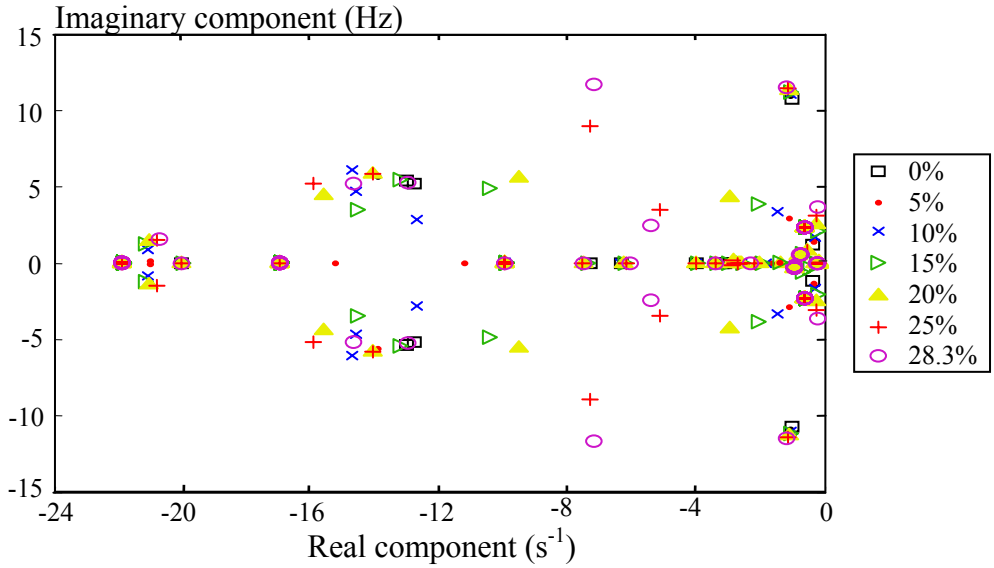

Fig 6-4 Eigenvalues with different power contributions from DG units

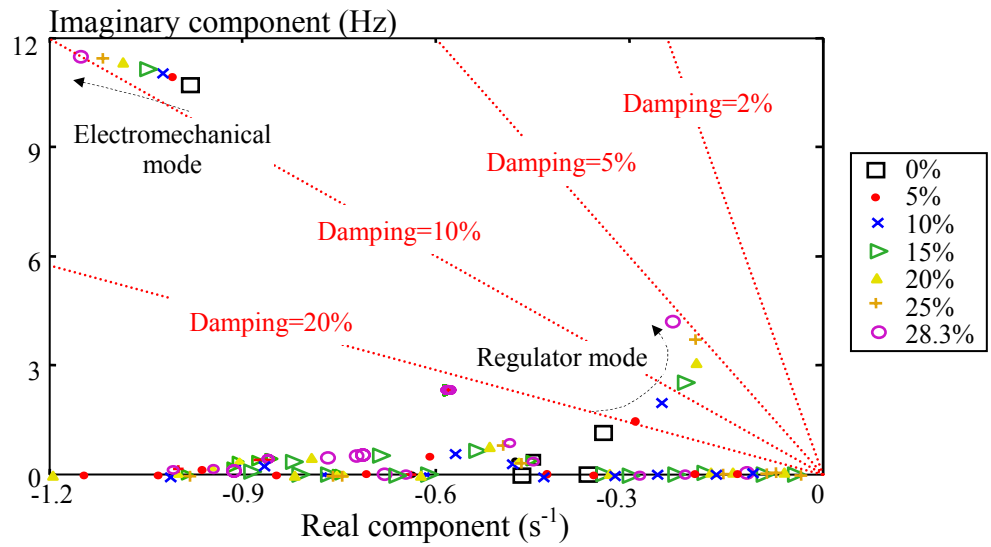

Fig 6-5 Critical eigenvalues with different power from DG units

Table 6-2 Critical modes with different power contributions from DG units

Penetration level	Electromechanical mode		Regulator mode	
	Eigenvalue	Damping factor	Eigenvalue	Damping factor
0.0%	-0.984±j10.774	9.095%	-0.340±j1.579	28.179%
5.0%	-1.009±10.933	9.188%	-0.294±1.397	20.607%
10.0%	-1.028±11.081	9.239%	-0.272±1.702	15.785%
15.0%	-1.052±11.204	9.347%	-0.240±2.092	11.377%
20.0%	-1.086±11.341	9.530%	-0.221±2.602	8.465%
25.0%	-1.118±11.471	9.702%	-0.222±3.122	7.086%
28.3%	-1.153±11.524	9.959%	-0.242±3.685	6.546%

From the modal analysis, two critical modes can be recognized. The first one represents the electromechanical mode. With the insertion of more DG units, the damping of this mode is slightly improved and the corresponding frequency is

increased. On the other hand, the second mode is more affected by the utilization of power from DG units. This mode belongs to the regulators of the synchronous generators. The utilization of the DG units causes lower damping and higher frequency for this mode. However, it seems that further utilization of DG units can then improve the damping factor of this mode. This would be caused by the interaction between the controllers of the synchronous generators and those of the DG units. With small numbers of DG units near some of the load nodes, the DG controllers have only local action and the global damping of the controller mode is worsened. The use of a large number of DG units, which are uniformly dispersed in the low voltage area, extends the controller action to cover most of the load nodes. Hence, the performance of this mode is slightly improved with the high penetration levels of the DG units.

6.5.2 Transient stability

Transient stability issues, also referred to as the first swing stability, are among the most important practical concerns in power system operation and planning studies. The assessment of transient stability, where the angle stability under large disturbances is investigated, is becoming an essential requirement for the security of electrical power systems. It is defined as the ability of the power system to maintain synchronism when subjected to severe disturbances such as short circuits or loss of large loads or generations. Transient stability depends on the initial operating conditions of the system as well as the type, severity and location of the disturbance [70].

The common methods for transient stability assessment are based on the time-domain simulations and the analysis of the transient energy function, which corresponds with the extended equal area criterion under some assumptions [71]. In this research, time-domain simulation technique is employed to assess the impact of DG penetration level on the transient stability of the power system. Here, the power angle between the two synchronous generators has been chosen as an indicator to assess the transient stability.

To investigate the transient stability of the test system, two 150ms self-clearing three-phase through impedance short circuits are simulated. The first one is at bus "B_1", while the second one is at bus "B_2" (see Fig 6-1). It is assumed that no parts of the network are disconnected due to the applied faults. As a result of the first fault, the voltage levels at the terminals of all DG units did not reach the 80%

limit and, hence, no DG unit is disconnected. Fig 6-6 shows the responses of the power angle between the two generators to this disturbance.

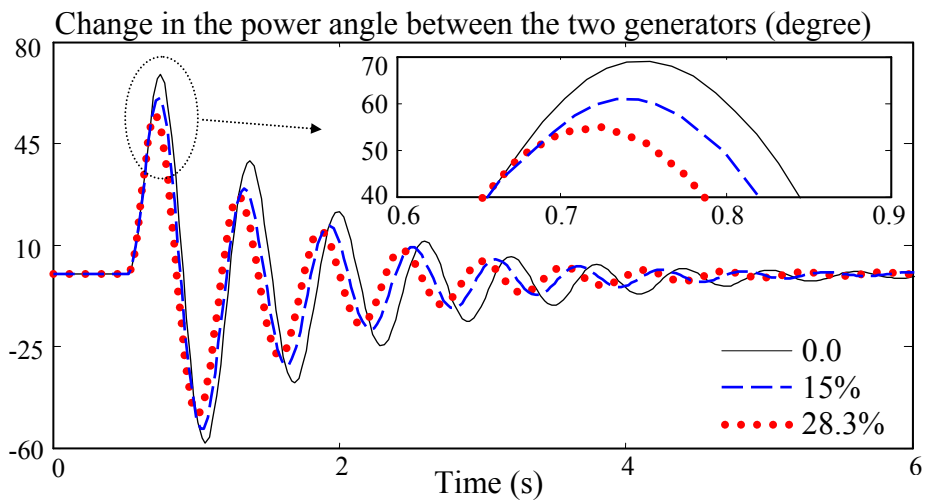

Fig 6-6 Change of the power angle due to a fault in the high-voltage network: case 1, no DG unit is switched off

On the other hand, some DG units are switched off as a consequence of the second fault due to the reduction of the voltage lower that the 80% limit. The disconnection of these units causes a loss of generating sources, which forces the network to operate at a new operating point. Fig 6-7 illustrates the change of the power angle with different penetration levels of the DG units.

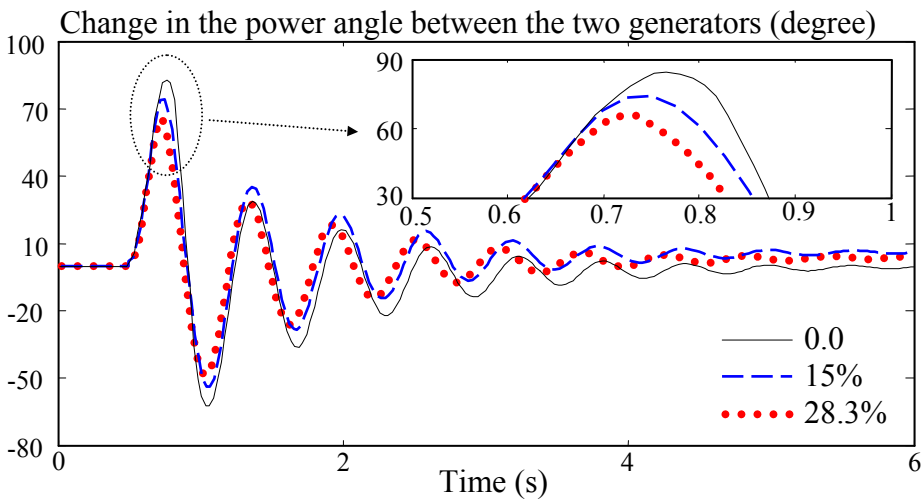

Fig 6-7 Change of the power angle due to a fault in the high-voltage network: case 2, some DG units are switched off

From the observation of the first swing, it is evident how the utilization of DG units reduces the magnitude of the maximum power-angle deviation. This indicates that the existence of the DG units improves significantly the transient stability of the system. This also means that the increase of the penetration level of DG units within power systems provides the opportunity to handle larger disturbances. In some critical cases and with more severe faults, the use of DG units

can maintain synchronism because of the reduction of the maximum power-angle deviation between generators. Due to the loss of some DG units in the second case shown in Fig 6-7, the power angle between the two generators reaches a new steady-state value after the fault clearance depending on the contribution of each generator to compensate the loss of power when disconnecting some DG units.

As expected from the modal analysis, the response shows higher frequency and somewhat more damping when more power from DG units is used. This more damping achieved when utilizing the DG units reflects the improvements in the post-fault performance of the network.

6.6 Frequency stability analysis

Following large disturbances in power systems, significant imbalance takes place between generated power and load demands. Furthermore, imbalances occur between the electromagnetic and the mechanical torques of the generators. The consequential accelerations or decelerations of generators due to this imbalance result in changes in the frequency of the network, which can impact the stability of the system. Frequency stability refers to the ability of electrical power systems to maintain fixed frequency after being subjected to a severe disturbance [70]. The frequency will not cause a stability problem if the equilibrium between generation and load is restored. This requires sufficient generation reserve and adequate response from the control and protection devices. If the disturbance results in sustained frequency oscillations, generating units will be sequentially tripped out of the network and the stability will be lost.

To examine the frequency response of the network after severe disturbances, 5MW and 10MW loads (~3 and 6% of the total power generation respectively) are switched on in the high-voltage network and the frequency response of the network is observed in each case. The loads are switching on at bus B_2 (see Fig 6-1). Fig 6-8 and Fig 6-9 show the frequency response with the two disturbances. Comparisons between the network performance without DG units and with 15% and 28.3% contributions are given in each case.

In all cases, the network succeeded to maintain new steady frequencies after load switching. In the case of supplying the load fully from the synchronous generators, the generators provide more absolute reserve power to the network (notice that the percentage reserve power is always constant as 10% of the rated power). This explains the increase of the maximum frequency deviation when

more power form DG units are utilized, which means lower rating and consequently lower absolute reserve power from the synchronous generators. It is therefore suggested to increase the percentage reserve power of the synchronous generators when DG units are utilized to maintain the total absolute reserve power of the network at acceptable levels. On the other hand, the inertia constant is lower with the increase of DG units due to the decrease of the rated power of the rotating synchronous generators. Thus, faster frequency response can be obtained in the transient period when DG units are used. Therefore, the minimum frequency level is reached faster than the case without DG units.

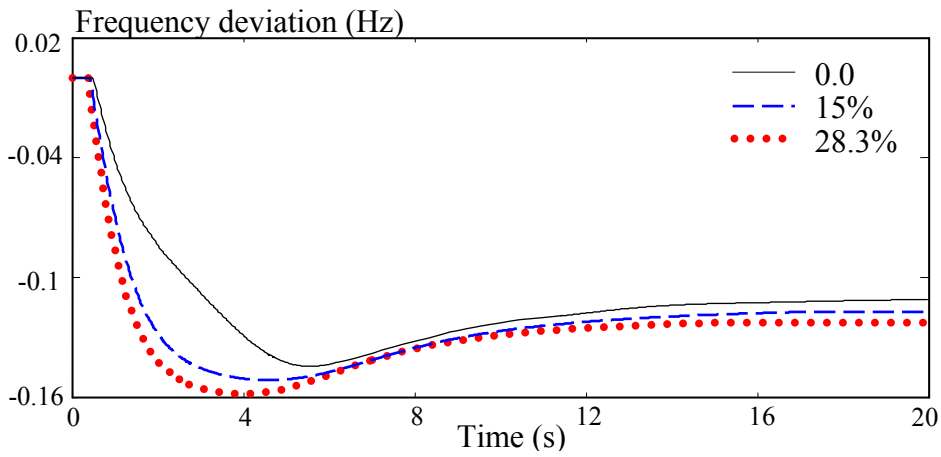

Fig 6-8 Frequency response as a result of a 5MW load switching in the high-voltage network (~3% of the total power generation)

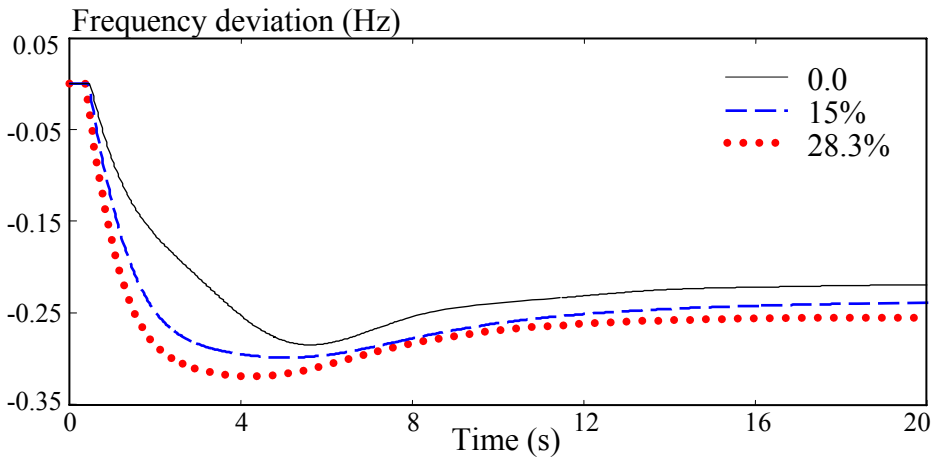

Fig 6-9 Frequency response as a result of a 10MW load switching in the high-voltage network (~3% of the total power generation)

6.7 Voltage stability analysis

Voltage stability is defined as the ability of a power system to maintain the voltages at all nodes within acceptable limits after being subjected to a disturbance [70]. Voltage instability results from the progressive collapse or rise of voltages of network nodes, which may cause the loss of some loads or transmission lines. The tendency of dynamic loads to restore their power after distur-

bances by adjusting their operating slips would increase the reactive power consumption causing further voltage reduction. If the reactive power consumption by loads is beyond the capability of the generators or transmission systems, a run-down situation causing voltage instability takes place.

The voltage stability of the investigated network is tested by applying some disturbances in both the high and the low-voltage networks. Fig 6-10 shows the voltage response to the abovementioned 150ms fault at bus (B_2). All DG units contain suitable reactive power controllers to regulate their performance. Since these units are located near the load centres, some improvements in the performance are achieved especially for the load during the short circuit.

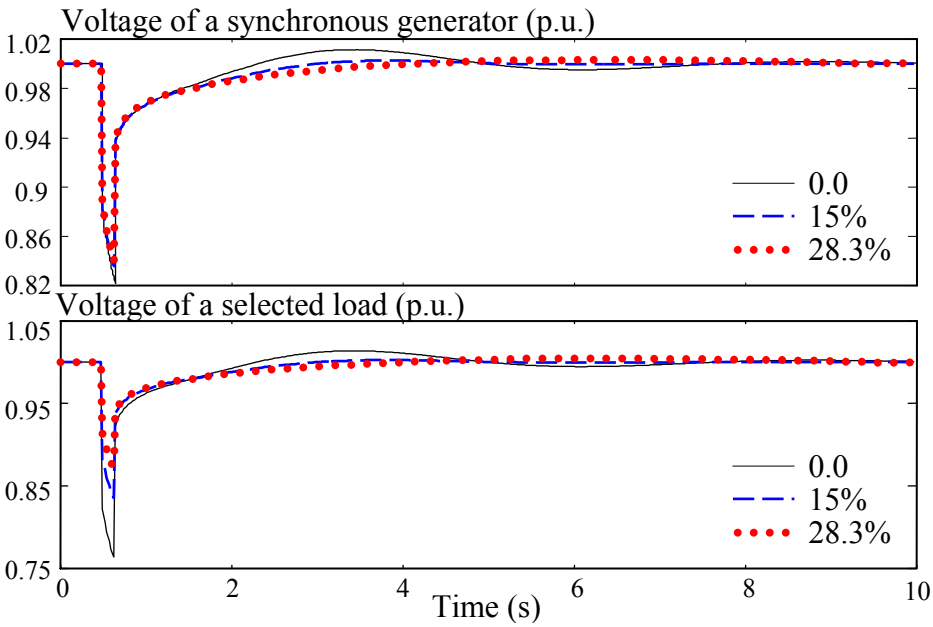

Fig 6-10 Voltage deviation of a synchronous generator and a selected load as a result of a three-phase fault in the high-voltage network

Fig 6-11 illustrates the voltage response to a 10Mvar load switching at bus (B_1) in the high-voltage network. The increase of the penetration level of the DG units causes more damping to the voltages in both the low-and the high-voltage parts. In addition, lower steady-state voltage deviations are achieved at load terminals when the DG sources are used near of them. However, the steady-state voltage deviations at the generator terminals are lower when no DG units are used. Due to the higher capacity of synchronous generators without DG units, they can achieve better local voltage support at their terminals. Therefore, the generators compensate the reactive-load switching with lower terminal-voltage deviations.

Fig 6-12 shows the voltage deviation at two load nodes when a load of 1Mvar is switched on at the terminals of the first one of them. The second load node is

about 2km away from the switching point. A large voltage decrease occurs at the switching point when the DG units are not utilized. This voltage decrease is significantly reduced when the 28.3% penetration level is considered. The other load terminals in the distribution system incorporate also some improvements in the voltage profiles when DG units are used. The voltage decrease and the relative improvements in the voltage profiles at these terminals vary depending on their relative locations with respect to the switching point.

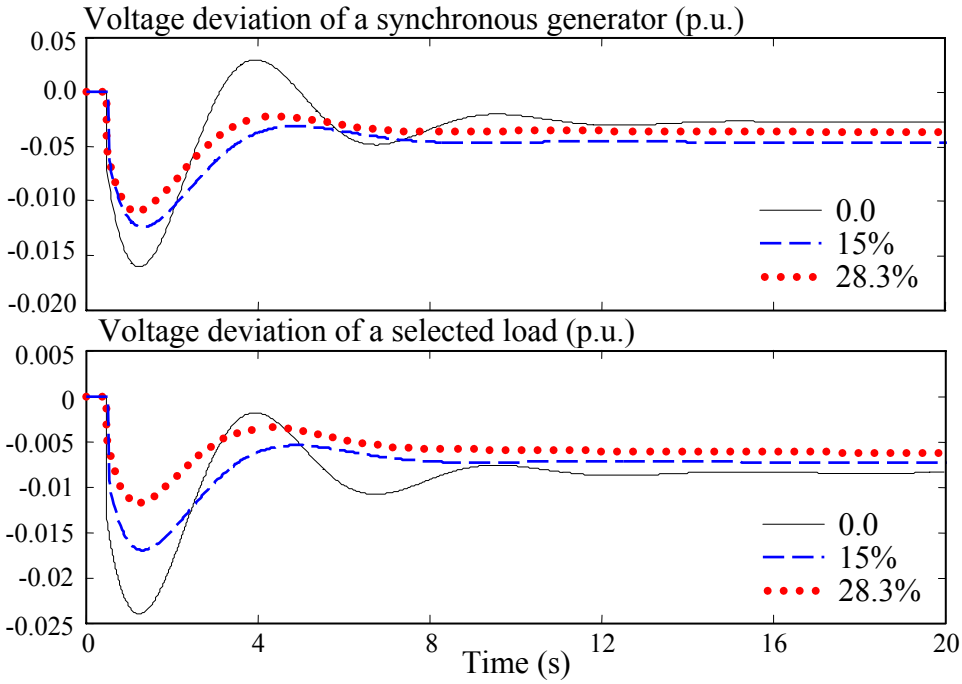

Fig 6-11 Voltage deviation of a synchronous generator and a selected load as a result of switching a load of 10Mvar in the high-voltage network

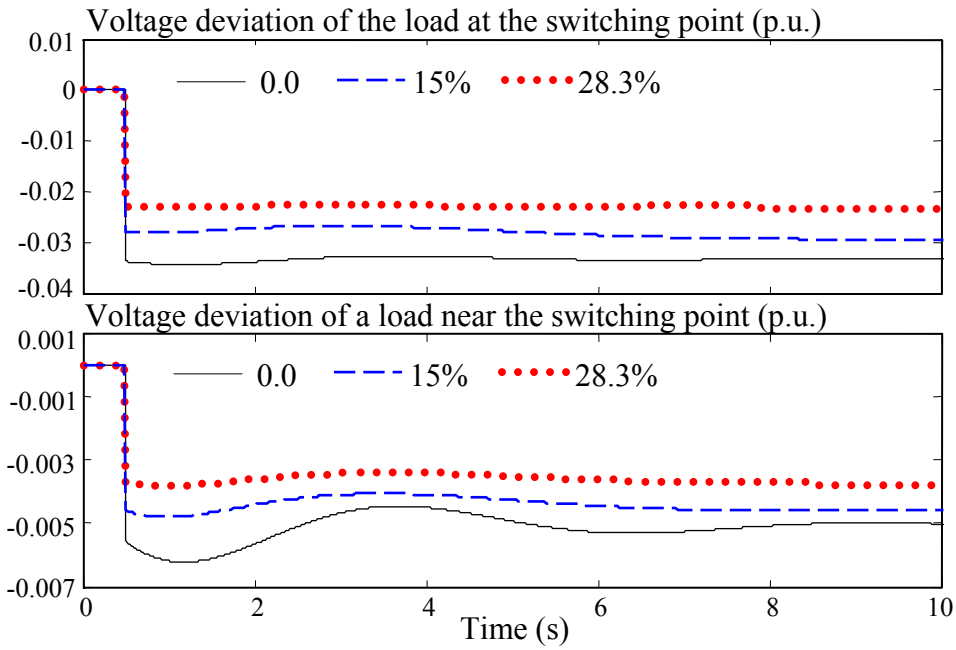

Fig 6-12 Voltage deviation at two load terminals as a result of switching a load of 1Mvar in the low-voltage network

Generally, the analysis of the voltage performance shows that DG can support and improve the voltage profiles at load terminals. This can extend the stability margin of dynamic loads, i.e. induction motors, which can loss their stability with large voltage dips.

6.8 Conclusion

This chapter addresses the impact of DG with different penetration levels on the stability of power systems. A hypothetical network with two conventional power plants and many DG units is simulated. Based on the results and discussion, it can be concluded that DG can improve the stability of power systems if suitable types and appropriate locations are selected. Regarding the oscillatory stability, the utilization of DG improves the damping of the electromechanical modes and slightly increases their frequency. This fact is confirmed through the time-domain simulation of some disturbances. The transient stability analysis shows that the maximum power-angle deviations between the generators are decreased with the increase of the penetration level of the DG units. However, the disconnection of some DG units when the voltage decreases lower than 80% of the nominal value represents an additional disturbance to the network. With more power from the DG units, the absolute reserve power from synchronous generators and the network inertia constant are smaller due to the lower rated power of the rotating synchronous generators. As a result, the frequency response shows faster behaviour with higher maximum-frequency deviations when more DG units are employed. The voltage profiles at load terminals are also improved due to the use of active DG sources near end-user terminals. The controllers designed to regulate the performance of the DG units participate also in improving the voltage stability of the network. To maximize the benefits behind utilizing DG units, the stability of the individual DG units themselves has to be improved to ensure their continuous and reliable operation to provide effective support to the stability of the entire network.

Chapter 7

Online Management of DG Units for Residential Applications

7.1 Introduction

One of the important applications of DG units, where FCs and MTs are particularly suitable, is the utilization of small-modular commercial or residential units for onsite service. In this case, the capacity of the DG unit can be chosen to cover most of the load demand most of the time, where the surplus/shortage is exported to/imported from the main grid system. Thus, the reduction of energy price is becoming increasingly important in order to bring DG units to competition with the main-grid system [30]. To decrease the generation cost, both the capital and the operating costs should be reduced. Therefore, the operation of the DG units has to be properly managed to reduce the operating cost to the minimum level. This reduction in the operating cost can significantly contribute in decreasing the total energy price and, as a result, improving the economic feasibility of these units. Among the different types of FCs, the PEMFCs have approved good features especially for low-capacity applications [72]. PEMFCs are candidates to be used in many fields because of their quick start-up characteristics and high power densities, which reduced the required accommodation place.

The management of DG units requires an accurate economic model to describe the operating cost of the unit taking into account both electrical and thermal relations. Such a model is discontinuous and nonlinear in nature and, hence, necessitates the utilization of a robust optimization tool. The GA has proven high capabilities for handling such optimization problems because of its flexibility and robustness [73]. Obviously, the optimized settings will be valid only for certain operating conditions and have to be recomputed after each variation. However, the optimization process, which can be carried out only in the offline mode, is a complicated and a time-consuming task and, therefore, requires high computational capabilities. It is important to standardize a simple management method, which is probably adapted by the manufacturer and has to be online and locally updated by the operator. Therefore, a generalization framework has to be applied to extend the optimization results in a generic form. The ANN can be used for

this task due to its capabilities of learning and generalizing large scales of nonlinearities by extracting system features using training data [48, 49]. Also, the Decision Tree "DT" methodology can be employed as a nonparametric learning technique, which is capable of deducing solutions for new unobserved cases [74, 75].

This chapter demonstrates a new-two-stage intelligent technique to manage the operation of DG units for residential utilization. In the first stage, a GA is used to define the optimal settings of DG units depending on detailed economic models. This process is applied for three alternative scenarios: utilizing a single PEMFC, using three identical PEMFCs in parallel and utilizing a MT. For online applications and to avoid the repetitive time-consuming optimization process, the procedure is generalized in the second stage using ANNs and DTs as two alternatives. The objective is to develop an intelligent management tool, which can be used in the online mode and depends only on the structure and parameters obtained from the second stage. The generalization process is applied only with the single PEMFC as it shows the most economic operation among the three alternatives.

7.2 Structure of the residential system

The electrical and thermal load demands are supplied mainly by the DG. However, the shortage in electricity can be covered from the main grid system and the surplus of electricity can be sold back to the grid at different tariffs. The tariffs of sold and purchased electricity vary from one market to the other and from one season to the other. Two energy meters can separately measure the purchased and the sold electricity from/to the grid system. The thermal energy produced in the DG unit(s) is utilized for water and space heating of the domestic building. The load is provided also by a natural-gas supply to compensate for expectable deficiencies in thermal production in the DG unit(s). Most natural gas suppliers offer several tariffs depending on the field of application (e.g. residential, commercial, industrial, electric generation... etc). The consumptions of natural gas by the DG unit and the thermal load are measured independently to calculate the cost of each part depending on its own tariff.

Fig 7-1 shows the structure of the residential system supplied by a single FC. For simplicity, the auxiliary devices (e.g. dump-electric-and-thermal loads, pumps, fans... etc) are not illustrated in the figure. No electrical or thermal storage devices are assumed in the study as they may increase the capital cost of the system. At the same time, the maintenance and technical considerations of these devices may cause many difficulties to the operator.

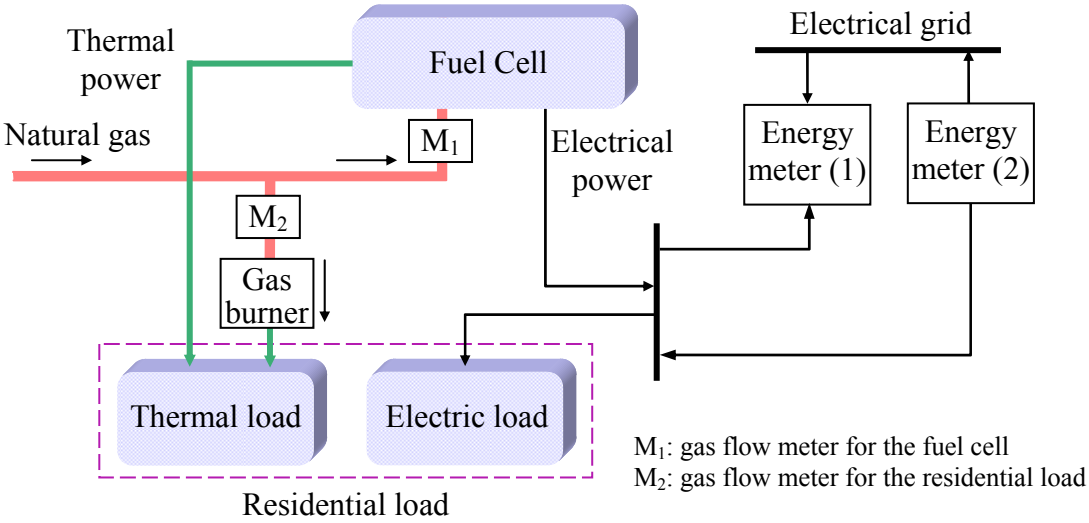

Fig 7-1 Structure of the residential system supplied by a fuel cell

7.3 PEM fuel cell economic model

The management process aims at minimizing the daily operating cost of the PEMFC under the following assumptions:

- the FC will supply both electrical and thermal power to the load (CHP)
- there is a possibility to sell back the excess of electricity to the main grid at different tariffs, which are always lower than the purchased electricity tariffs
- the surplus thermal power in the FC will be absorbed through a dump thermal load
- a part of the generated power is utilized for auxiliary devices provided with the unit (e.g. pumps, fans... etc)
- the prices of the natural gas for the FC are lower than or equal to those for the residential thermal load

7.3.1 Objective function

While the capital cost of the FC is defined by the type, design and technology, the operating cost varies depending on the setting point. The objective function is developed according to the mentioned assumptions to minimize the total daily operating cost of the PEMFC in the following form:

$$DOC=DFC+DCPF+DCPE-DISE+O\&M+STC \tag{7-1}$$

Where:

DOC : daily total operating cost to be minimized ($)

DFC : daily fuel cost of the FC ($)

DCPF : daily cost of purchased fuel for residential load if the produced thermal power in the FC is not enough to meet the thermal load demand ($)

DCPE: daily cost of purchased electricity if the demand exceeds the produced electrical power in the FC ($)
DISE : daily income for sold electricity if the output electrical power from the unit exceeds the electrical load demand ($)
O&M : daily operating and maintenance cost ($)
STC : daily start up cost ($)

The daily cost of the natural gas consumed by the FC depends on the supplied electrical power, the operating efficiency and the tariff of the natural gas:

$$DFC = C_{n\text{-}FC}\, T \sum_{J} \frac{P_J + P_a}{\eta_J} \tag{7-2}$$

where:
$C_{n\text{-}FC}$: natural gas price for supplying the FC ($/kWh)
T : time duration between two successive settings of the FC (h)
P_J : net electrical power produced in the FC unit at interval "J" (kW)
P_a : power required for auxiliary devices (kW)
η_J : the efficiency of the FC at interval "J"

The power required for auxiliary devices is almost constant regardless of the supplied power. Therefore it is assumed as 5% of the unit maximum capacity in all cases. On the other hand, the efficiency of the FC depends on the operating point. This efficiency refers to the ratio of the stack output power to the input energy content in the natural gas. It is normally calculated as the ratio of the actual operating voltage of a single cell to the reversible potential (1.482V) [72]. The overall unit efficiency is the efficiency of the entire system including auxiliary devices. Fig 7-2 shows typical efficiency curves of the PEMFC including the cell and the overall efficiencies [72]. A typical efficiency curve is used to develop the cell efficiency as a function of the electrical power and used in equation (7-2).

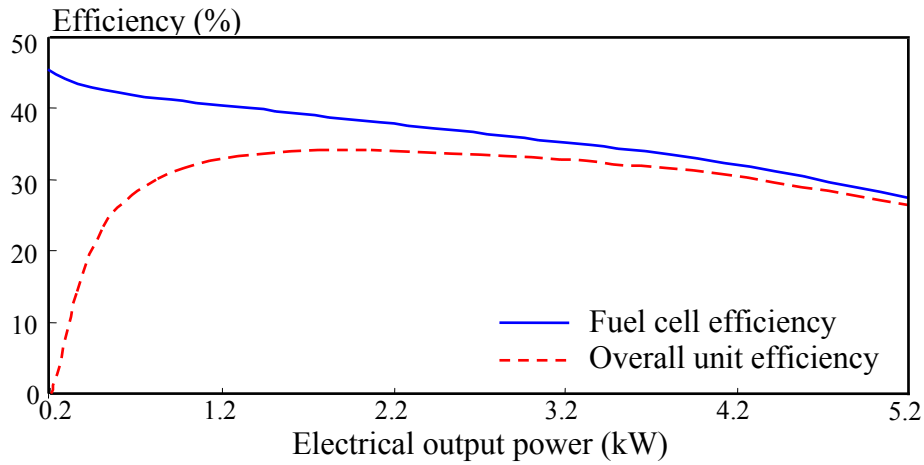

Fig 7-2 Typical efficiency curves of PEM fuel cell

As shown in Fig 7-1, the main grid system balances the difference between the electrical load demand and the net electrical output power from the FC. A daily cost has to be paid for the purchased electricity to cover the load demand when the electrical load requirements exceed the produced electrical power. On the other hand, there can be a daily income because of the sold electricity when the generated electrical power in the FC exceeds the electrical load demand. It is common to cell-back the excess of electricity at lower tariffs than those of the purchased prices. In some other cases it will not be possible to cell this electricity at all. Therefore, two different tariffs are considered in the model for the purchased and the sold electricity. This gives more flexibility to consider most of the possible real situations. The following equations define the daily cost of the purchased electricity and the daily income due to the sold electricity:

$$DCPE = C_{el\text{-}p}\, T \sum_{J} \max\left(L_{el,J} - P_J, 0\right) \tag{7-3}$$

$$DISE = C_{el\text{-}s}\, T \sum_{J} \max\left(P_J - L_{el,J}, 0\right) \tag{7-4}$$

where:

$C_{el\text{-}p}$, $C_{el\text{-}s}$: tariffs of purchased and sold electricity respectively ($/kWh)

$L_{el,J}$: electrical load demand at interval "J" (kW)

The thermal output power from the FC depends on the electrical power. The relation is almost linear at the lower values, while the ratio of the thermal power is relatively higher at the upper operating power limits [76]. For low-temperature FCs, the electrical efficiency is relatively lower and more thermal power is produced. The situation is reversed with the high-temperature FCs, where the thermal power is lower than the generated electrical power. For PEMFCs, the ratio of the thermal power is about 120% to 150% of the electrical power depending on the operating point [72, 76]. A nonlinear equation is developed using curve-fitting technique to give the value of the output thermal power from the unit depending on the generated electrical power as shown in Fig 7-3. Depending on this relation, it will be possible to calculate the produced thermal power according to the generated electrical power at each time interval. The thermal power is used to calculate the daily cost of purchased fuel for residential load as in equation (7-5).

$$DCPF = C_{n\text{-}RL}\, T \sum_{J} \max\left(L_{th,J} - P_{th,J}, 0\right) \tag{7-5}$$

where:

$C_{n\text{-}RL}$: natural gas price for supplying the residential load ($/kWh)

$L_{th,J}$: thermal load demand at interval "J" (kW)

$P_{th,J}$: thermal power produced in the FC at interval "J" (kW)

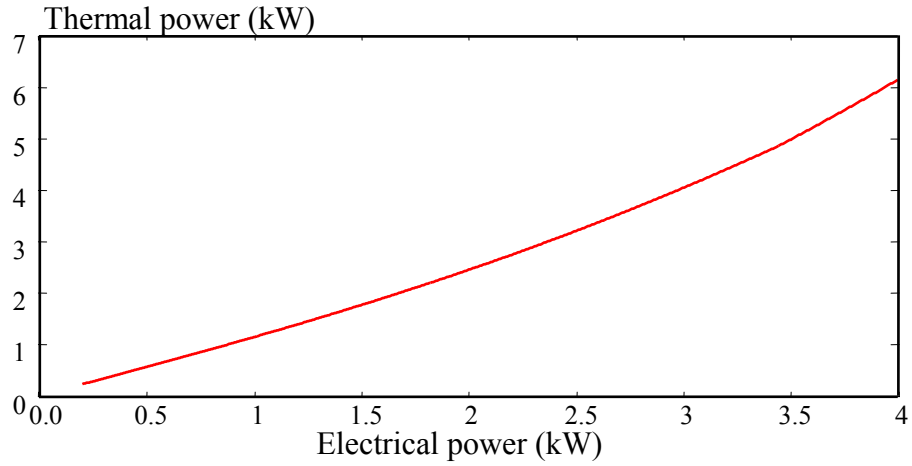

Fig 7-3 Relation between the thermal and the electrical power in the FC

The operating and maintenance cost (O&M) is assumed to be in proportional with the produced energy, where the proportional constant is ($K_{O\&M}$).

$$O\&M = K_{O\&M}\, T \sum_{J} P_J \tag{7-6}$$

The start-up cost depends on the temperature of the unit and consequently on the time terminated where the unit was in the off mode before starting it up once again [77].

$$STC = \alpha_h + \beta \cdot \left(1 - e^{\frac{-T^{off}}{\tau}} \right) \tag{7-7}$$

where:

α_h : hot start up cost

$\alpha_h+\beta$: cold start up cost

T^{off} : the time terminated where the unit was in the off mode (h)

τ : the FC cooling time constant (h)

The fuel and electricity tariffs (i.e. $C_{n\text{-}FC}$, $C_{n\text{-}RL}$, $C_{el\text{-}p}$ and $C_{el\text{-}s}$) in the presented model represent the four decision variables, which affect the optimal settings of the FC.

7.3.2 Constraints

The operation of the FC to supply the residential load is restricted by many limitations. Mathematically, the minimization of the objective function (7-1) is limited by the following operational and technical constraints:

Upper and lower capacity constraints: $P_{min} \leq P_J \leq P_{max}$ (7-8)

Constraints of upper ramp rate: $P_{J,t}-P_{J,t-1} \leq \Delta P_U$ (7-9)

Constraints of lower ramp rate: $P_{J,t-1}-P_{J,t} \leq \Delta P_D$ (7-10)

where:

P_{min}, P_{max} : the minimum and maximum limits of the generated power respect.

ΔP_U, ΔP_D : the upper and lower limits of the ramp rate respectively

$P_{J,t-1}$: the power generated at interval "t-1"

Once the FC unit is switched on, it has to operate continuously at least for a certain minimum time before switching it off again. On the other hand, a certain stop time has to be terminated before starting the unit. The violation of such constraints can cause shortness in the life time of the unit. These constraints are formulated as continuous running/stop time constraint as follows:

$$\left(T_{t-1}^{on} - MRT\right)\cdot\left(U_{s,t-1} - U_{s,t}\right) \geq 0 \quad (7\text{-}11)$$

$$\left(T_{t-1}^{off} - MST\right)\cdot\left(U_{s,t} - U_{s,t-1}\right) \geq 0 \quad (7\text{-}12)$$

where:

T_{t-1}^{on}, T_{t-1}^{off} : the FC running and stop periods at time interval "t-1" respect. (h)

MRT, MST : the minimum running and stop periods of the FC respectively (h)

U_s : the unit on/off status: U_s=1 for running mode and 0 for stop mode

Finally, the number of starts and stops per day ($n_{start\text{-}stop}$) should not exceed a certain maximum number (N_{max}).

$$n_{start\text{-}stop} \leq N_{max} \quad (7\text{-}13)$$

The parameters used in the FC economic model are given in appendix E.

7.4 Multi-population real-coded genetic algorithm

The model of the FC presented in the previous section requires a special optimization tool to handle the discontinuity and nonlinearity of such highly-constrained model. Most of the deterministic optimization methods are not suitable to simulate and solve the presented optimization problem due to many simulation difficulties. The GA is a probabilistic intelligent search algorithm, which searches a population of points in parallel [48, 78]. Basically, GA differs from other traditional optimization methods in three significant points. It searches a

population of points in parallel, it uses probabilistic rules rather than deterministic ones, and it can process an encoding set of parameters. The real coding is used in this research since it provides better performance and faster conversion compared to other coding methods [73]. With other coding, it is required to alternate to the real coding in the phase of calculating the total daily cost, which results in additional processing time.

7.4.1 Constraints representation

To employ GA with a tightly-constrained problem, such as the economic model of the FC, it is possible to generate only feasible solutions by avoiding individuals which violate the given constraints. Since the infeasible solutions mostly cover the search space at the initial generation, the complete avoidance of the infeasible solutions gives a high possibility for missing the area of global minimum [73]. Another approach is to move the infeasible individuals to the nearest feasible area. For the highly-constrained problem, this would be too complex and a very time consuming process. The penalty function approach is another alternative that converts the constrained problem to an unconstrained one by augmenting additional cost terms with the main objective function. The additional terms assign nonlinear costs for solutions that violate the constraints depending on their relative locations with respect to the feasibility boundaries [73].

The adequate choice of the penalty functions and their parameters is an essential requirement to achieve rapid rejection of the infeasible solutions. It is necessary for this approach to differentiate in performance between the infeasible individuals themselves, which will help in the evolution process. To ensure fast rejection of the solutions that violate the constraints, a higher cost value has to be assigned to any infeasible solution than the feasible members. In this research, exponential penalty factors are used for ramp rate violation, while quadratic ones are applied when violating the constraints of minimum running/stop periods and maximum number of starts and stops per day.

7.4.2 Evolution process

The GA searches for the global optimum value of the objective function through a search space, which is called **population**. The population is constituted from a number of possible solutions known as **individuals**. Each individual, which is also called **chromosome,** represents a definite scenario of the output electrical power from the FC through one day. It is assumed that the setting of the FC is updated each 15 minutes and, thus, 96 unknown variables are associated

with each individual. The main implementation steps of the GA-based optimization are summarized in the flowchart shown in Fig 7-4.

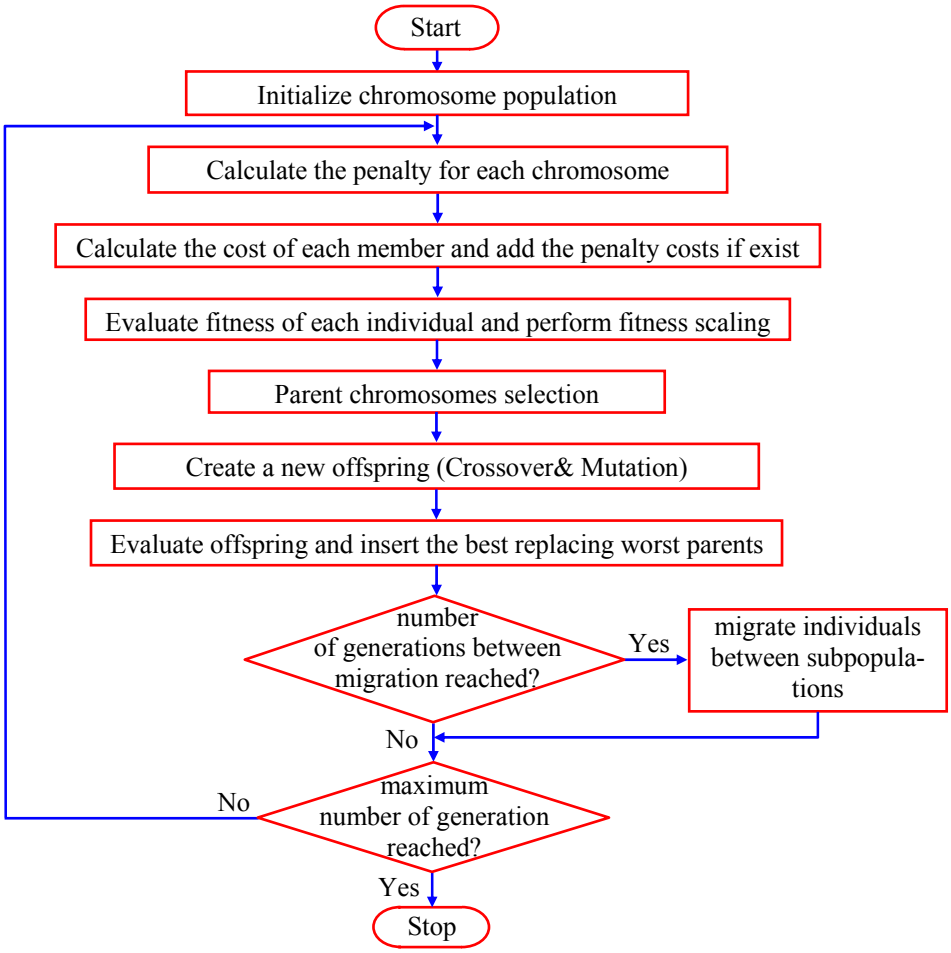

Fig 7-4 Flowchart of the GA evolution process

To initiate the population, a number of individuals are randomly formulated in the range between 0 and 4kW which satisfies the first constraint given by equation (7-8). Each individual in the randomly-created population is tested for violating the constraints. If the solution is infeasible, a suitable additional penalty cost is assigned to the individual. The performance of each individual is evaluated by calculating the total cost according to equation (7-1) and adding the corresponding penalty term if exists. The individuals are then ranked depending on their corresponding costs and a suitable fitness value is assigned to each one. The fitness values are calculated depending on the position of the individuals within the population rather than their distinct performance. Fitness values between maximum and minimum limits are calculated with fixed incremental steps and assigned to the ranked individuals as follows:

$$f(x_i) = 2 - f_{max} + 2 \cdot (f_{max} - 1) \frac{x_i - 1}{N_{ind} - 1} \tag{7-14}$$

where:
$f(x_i)$: the fitness value of the individual with a position (x_i) in the population
f_{max} : maximum fitness value (typically has a value between 1.1 and 2.0)
N_{ind} : number of the individuals within the population

The fitness scaling represents a basic step to select parents to create new offsprings. Strings with higher fitness are selected using the roulette wheel technique and used in the recombination process [48]. With "N" required selections, "N" equally spaced pointers can be used instead of a single selection pointer, which is conventionally employed in the classical roulette wheel method. This idea is shown in Fig 7-5 with 9 individuals and 8 pointers.

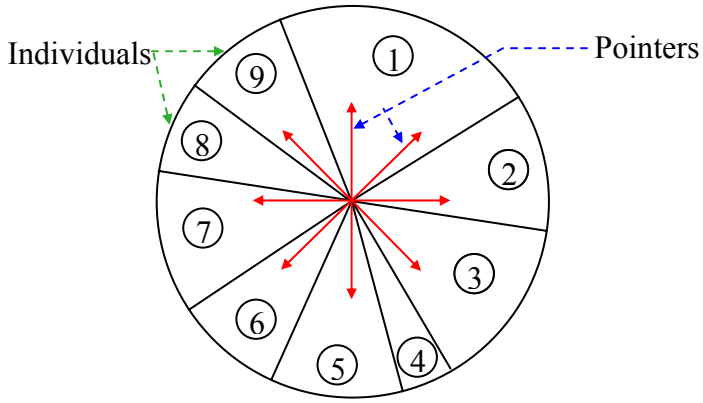

Fig 7-5 Roulette wheel selection

The new generation is produced by means of two main processes: crossover and mutation. Crossover is a genetic process by which information can be exchanged between the members of the population, possibly creating more highly fit members. For the real-valued encoding, the max-min arithmetical crossover operator is used as follows [73]:

$$G_1 = \alpha_s \cdot P_1 + (1 - \alpha_s) \cdot P_2 \tag{7-15}$$

$$G_2 = (1 - \alpha_s) \cdot P_1 + \alpha_s \cdot P_2 \tag{7-16}$$

where:
G_1, G_2 : the new generation "strings" of individuals
P_1, P_2 : the parents selected using the roulette wheel technique
α_s : a scaling factor

Mutation is the second process in the recombination, which is used to escape from possible local minima. The mutation in the real-coded representations is accomplished by disturbing the gene values with low probability [73].

Care has to be taken to ensure that the best solutions are not lost in moving from one generation to the next. According to this strategy, which is known as 'Elitism' some of the fittest members of each generation are saved and copied into the next generation. With this process, it is expected that the average fitness of the new generation is improved. Furthermore, the multi-population structure is found to improve the quality of the obtained results and, therefore, it is employed in this study. As shown in Fig 7-4, the individuals migrate periodically between subpopulation to exchange information between them.

7.4.3 GA parameters

Table 7-1 summarizes the parameters of the GA-based optimization process.

Table 7-1 Parameters used in the GA-based optimization process

Number of subpopulations	10
Number of individuals per subpopulation	20
Total population size	200
Generation gap	0.8
Insertion rate	0.9
Probability of crossover	0.9
Probability of mutation	0.01
Maximum generations	1000
Migration rate between subpopulations	0.2
Number of generations between migration	20

7.4.4 Results of the optimization process

The GA-based optimization process is carried out using 10 typical load curves of a family house under different electricity and fuel prices. A special attention is directed to carry out the optimization with load curves at different seasons and weekdays. Table 7-2 lists the load curves used in the study [79].

Table 7-2 A list of load curves used in the study

Load curve	Date	Weekday	Season
1	9/5/2002	Thursday	Spring
2	10/7/2002	Wednesday	Summer
3	14/7/2002	Saturday	Summer
4	31/8/2002	Sunday	Summer
5	13/12/2002	Friday	Autumn
6	26/1/2003	Sunday	Winter
7	8/2/2003	Saturday	Winter
8	25/2/2003	Tuesday	Winter
9	18/3/2003	Tuesday	Winter
10	12/4/2003	Saturday	Spring

Fig 7-6 and Fig 7-7 show two examples for the optimal settings of the FC with the load curve number (8). In the first case, no electricity is sold back to the main grid. In this case, the output power covers the electrical demand and a part of the thermal demand. In the second case, the excess of electricity is sold back for 0.07$/kWh. This gives the possibility to produce more electrical power and to cover the thermal load demand. In both cases, the other three tariffs are kept constant as shown in the following table:

$C_{n\text{-}FC}$	$C_{n\text{-}RL}$	$C_{el\text{-}p}$
0.03$/kWh	0.05$/kWh	0.12$/kWh

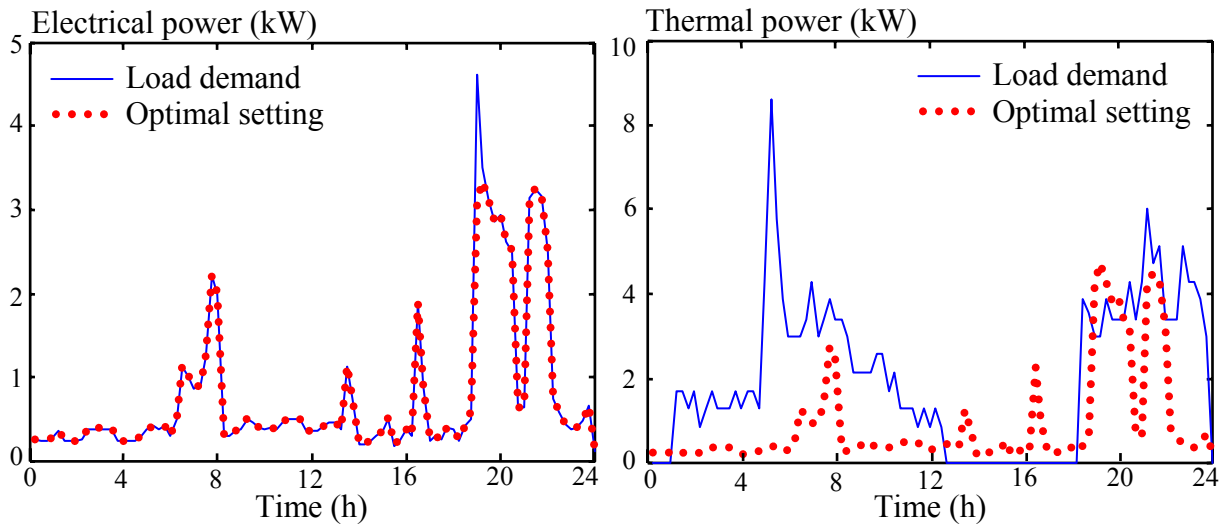

Fig 7-6 Unit optimal output power without selling electricity

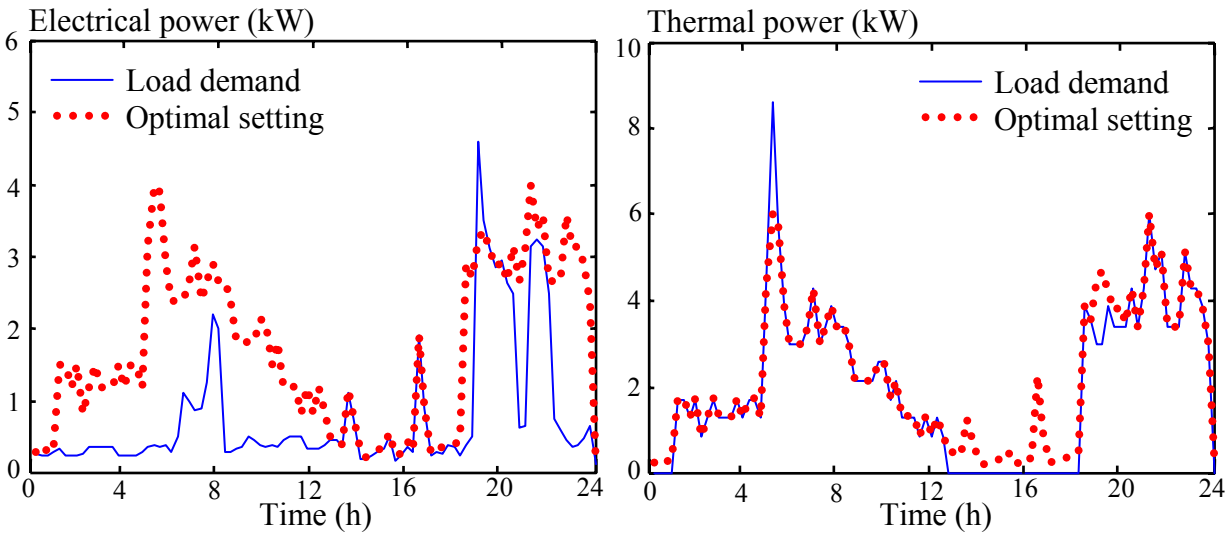

Fig 7-7 Unit optimal output power when selling electricity for 0.07$/kWh

To evaluate the effect of varying the four tariffs on the optimal settings, some comparisons are given in Fig 7-8 through Fig 7-11 for load curve (1). One tariff is changed each time, while the others are held constant. Fig 7-8 shows the effect of varying the sold-electricity tariff with the other tariffs kept constant as follows:

$C_{n\text{-}FC}$	$C_{n\text{-}RL}$	$C_{el\text{-}p}$
0.03$/kWh	0.05$/kWh	0.12$/kWh

With lower values of the sold-electricity tariff, the FC follows up the electrical load demand, while thermal load demand impacts the optimal settings more than the electrical demand with intermediate values (i.e. 0.07$/kWh). At higher values of the sold electricity tariff, the optimal scenario is to produce electrical power that exceeds the 2.35kW level over the whole day.

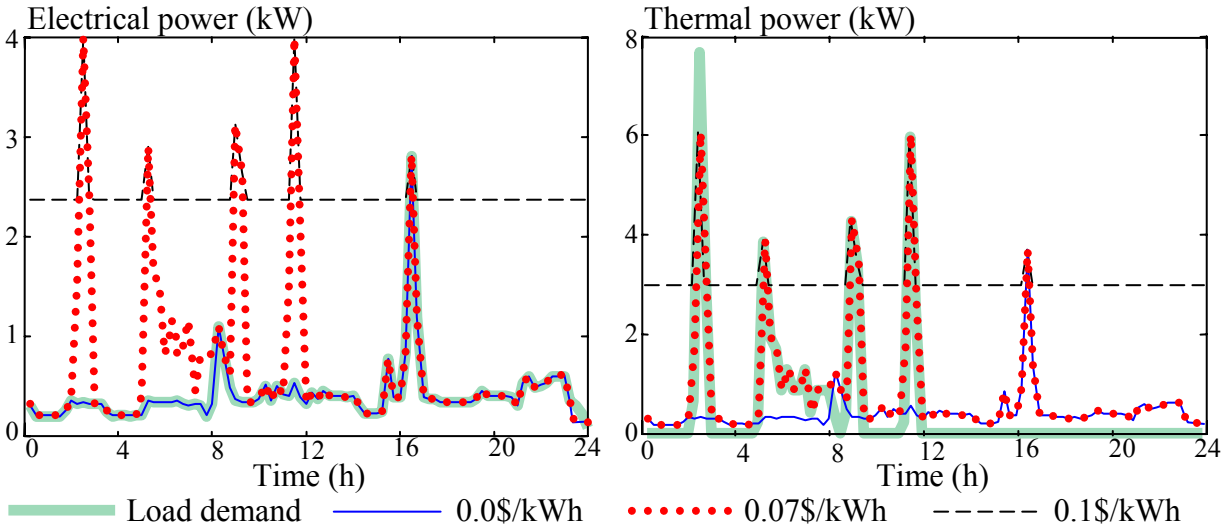

Fig 7-8 Effect of varying the sold electricity tariff

Fig 7-9 depicts the effect of varying the purchased-electricity tariff for the same load curve, while the other tariffs are given as follows:

$C_{n\text{-}FC}$	$C_{n\text{-}RL}$	$C_{el\text{-}s}$
0.05$kWh	0.09$/kWh	0.1$/kWh

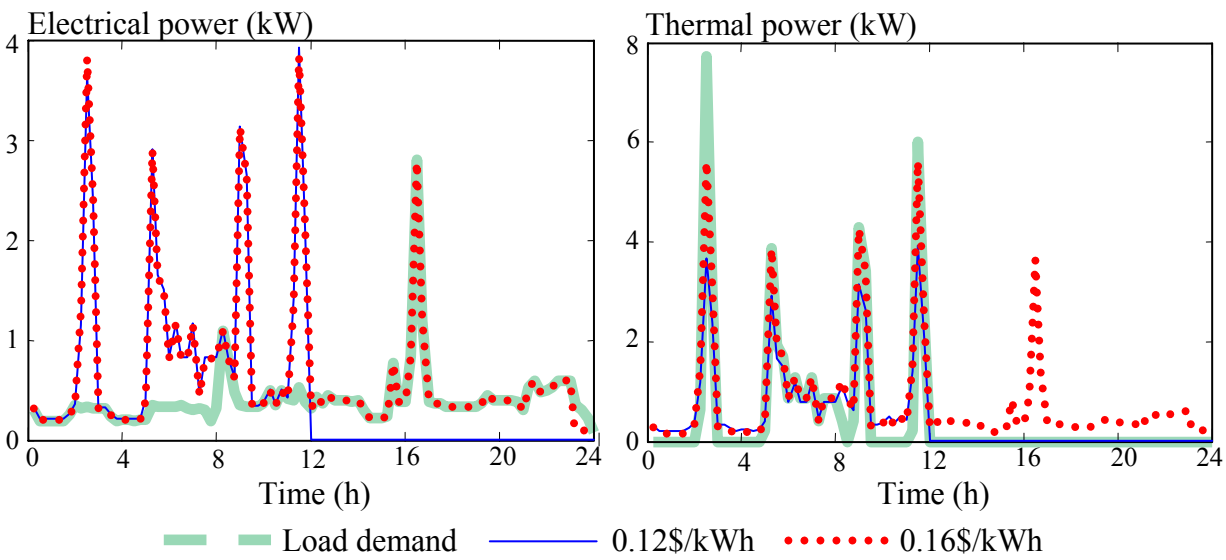

Fig 7-9 Effect of varying the purchase electricity tariff

It is noticable from the figure with the 0.12$/kWh tariff that the optimal setting is to use the unit only for 12 hours since there is no thermal load demand after this period. Therefore, it will be more economic to disconnect the unit and purchase the required electrical power from the main grid system. However, the higher price of the purchased electricity in the second case (0.16$/day) gives the favorability to generate the required electrical power in the FC itself. Therefore, the FC continued supplying power for the whole day.

The effect of varying the natural-gas tariff for supplying the FC is shown in Fig 7-10 with the other three tariffs held constant as follows:

$C_{n\text{-}RL}$	$C_{el\text{-}p}$	$C_{el\text{-}s}$
0.05$/kWh	0.12$/kWh	0.1$/kWh

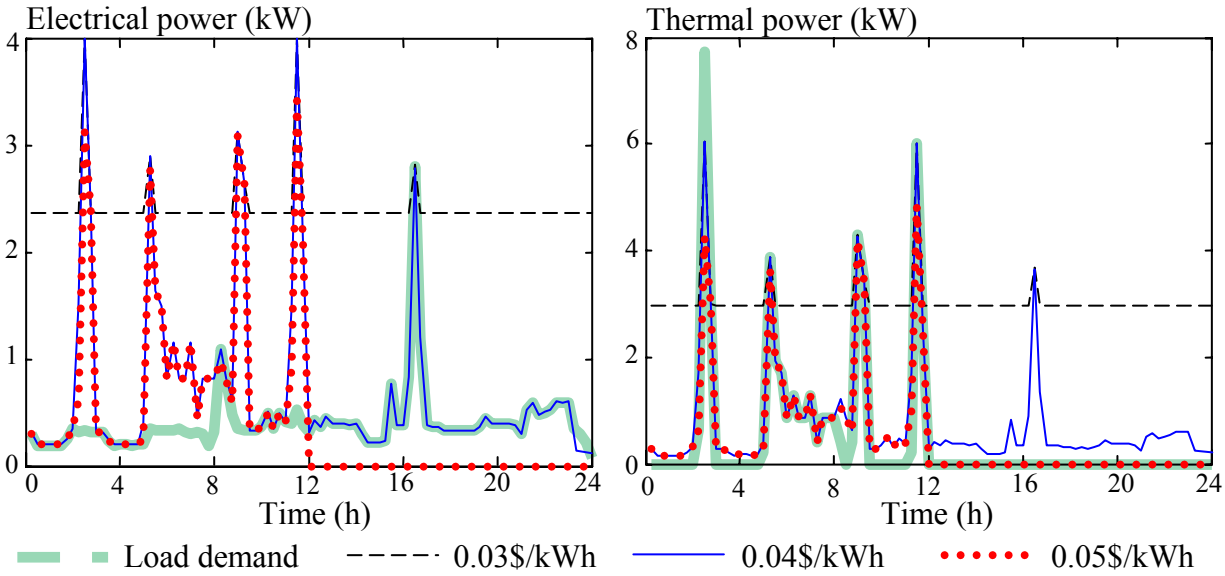

Fig 7-10 Effect of varying the natural gas tariff for supplying the fuel cell

Varying the fuel tariff for supplying the thermal load has the effect illustrated in Fig 7-11 with the other three tariffs are always constant as follows:

$C_{n\text{-}FC}$	$C_{el\text{-}p}$	$C_{el\text{-}s}$
0.03$/kWh	0.12$/kWh	0.0$/kWh

The repetitive start/stop cycles of the unit causes higher daily operating cost due to the associated start-up cost “STC” and, as a result, individuals that lead to this situation are avoided during the evolution process. The priority is given always for the continuous running or, in few cases, for the complete shut down of the unit. In some other cases, the optimal scenario is to run the unit continuously for a certain time and then to switch it off for the rest of the day as the situations shown in Fig 7-9 (with 0.12$/kWh) and Fig 7-10 (with 0.05$/kWh). Therefore,

the constraint, which limits the start/stop cycles below a certain number (see equation 7-13), is always inactive since this situation is completely avoided.

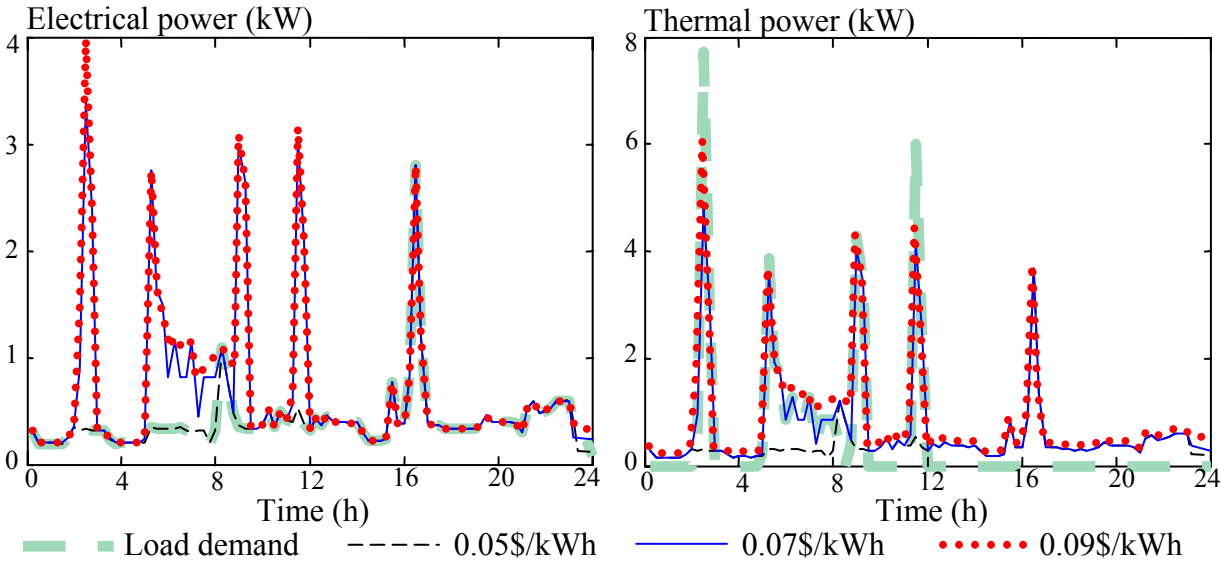

Fig 7-11 Effect of varying the natural gas tariff to supply the residential load

It is noticeable from the results that the FC supplies low power for prolonged periods within the day. It supplies the rated or near rated power only for short time. Therefore, it is adequate to investigate whether the utilization of smaller identical units with total equivalent capacity would be more economic regarding the operating cost. In this case, one unit is used when low power is to be supplied and the other units are added when required.

7.5 Management of three identical units simultaneously

The structure of the residential system when three identical units are used in parallel is shown in Fig 7-12.

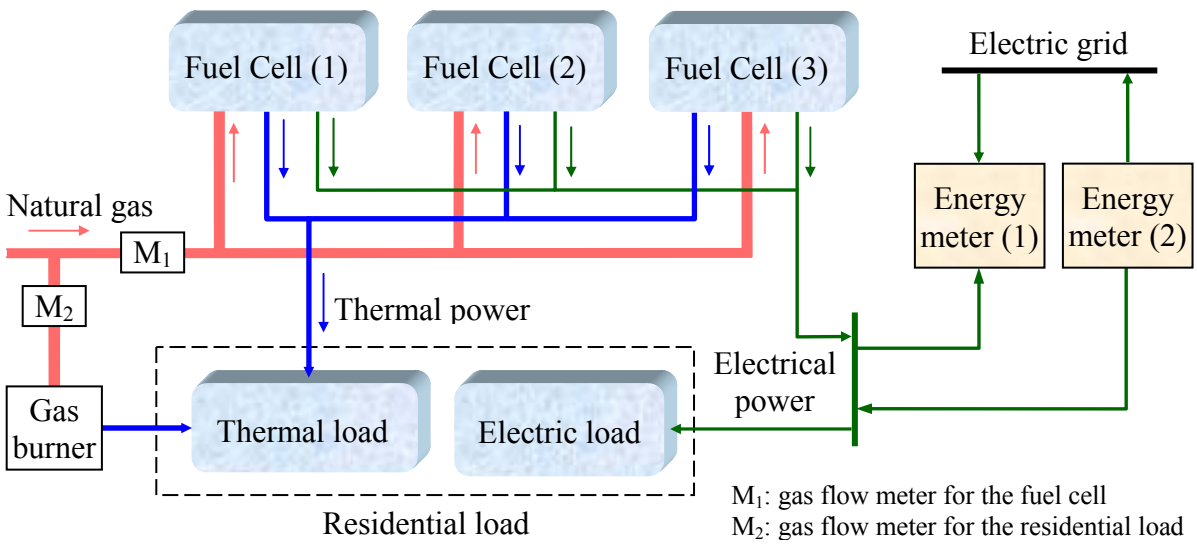

Fig 7-12 Structure of the residential system supplied by three FCs in parallel

Some modifications are introduced to the GA-optimization program to carry out the management of three units simultaneously. Now, each individual comprises 288 unknown, with 96 unknown belonging to each unit. Two times during the evolution process, the individuals are divided into three sub-individuals and the calculations are carried out regarding each sub-individual separately. The first time is when calculating the daily fuel cost of each unit and its additional penalty costs. The total daily cost is then calculated depending on the sum of the generated electrical and thermal power in the three units. The second time is when creating the new offsprings since the crossover and the mutation processes have to be applied to the chromosomes belonging to each individual unit. The economic-model parameters of the three FCs operating in parallel are given in appendix F.

The optimization process is carried out using the same load curves and operating tariffs as in the case of a single FC. Fig 7-13 through Fig 7-15 show the optimal output electrical power from the three FCs in addition to the total electrical and thermal power to supply load curve number (5) in three different cases. The optimal electrical and thermal power from one FC to supply the same load under the same conditions is also illustrated in the figures. Table 7-3 summarizes the used tariffs in the three cases and gives the corresponding total operating cost when supplying the load by one and three FC units.

Table 7-3 Different tariffs and the corresponding operating cost when optimizing the operation of one and three fuel cell units to supply a residential load

	$C_{n\text{-}FC}$ (\$/kWh)	$C_{n\text{-}RL}$ (\$/kWh)	$C_{el\text{-}p}$ (\$/kWh)	$C_{el\text{-}s}$ (\$/kWh)	Total operating cost (\$/day)	
					One unit	Three units
case (1)	0.03	0.07	0.16	0.1	1.603	1.915
case (2)	0.03	0.09	0.16	0.0	3.656	4.591
case (3)	0.03	0.05	0.12	0.0	3.473	3.637

The total electrical and thermal output power from the three units together is similar to that obtained from a single FC. However, the contributions from individual units vary depending on the load curves and the operating tariffs. In some cases, one or two units are not used for the whole day. In other cases, one or two units are used only for short periods, particularly at peak-load time, as shown in Fig 7-14 and Fig 7-15. Generally, the total daily operating cost using three units in parallel is higher than utilizing a single unit. Switching on one or two units increases the total operating cost as a result of the start-up costs. In addition, the utilization of three units in parallel results in operating the units at lower efficiencies compared to a single unit since they generate higher percentage power based on their ratings. As shown in Fig 7-2, the FC exhibit lower efficiency when generating higher percentage power.

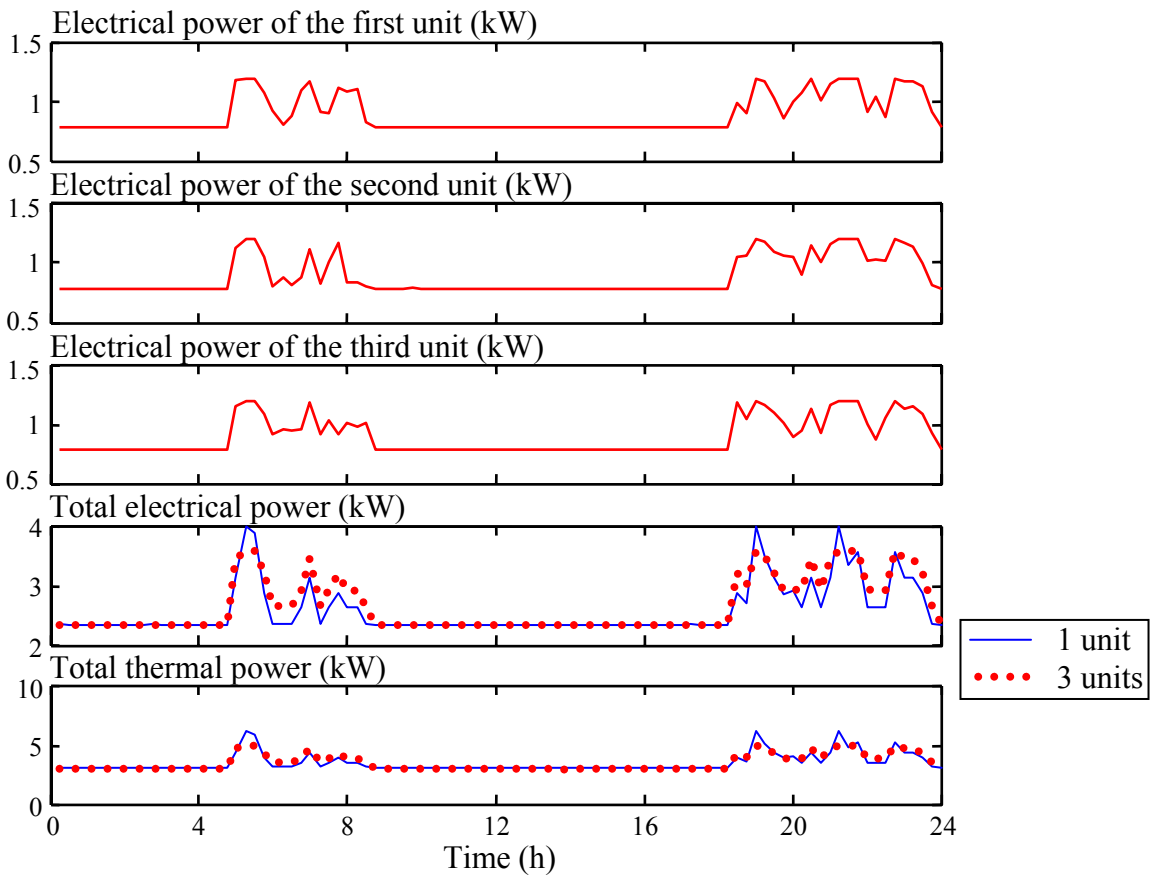

Fig 7-13 Comparing the performance of one and three fuel cells: case (1)

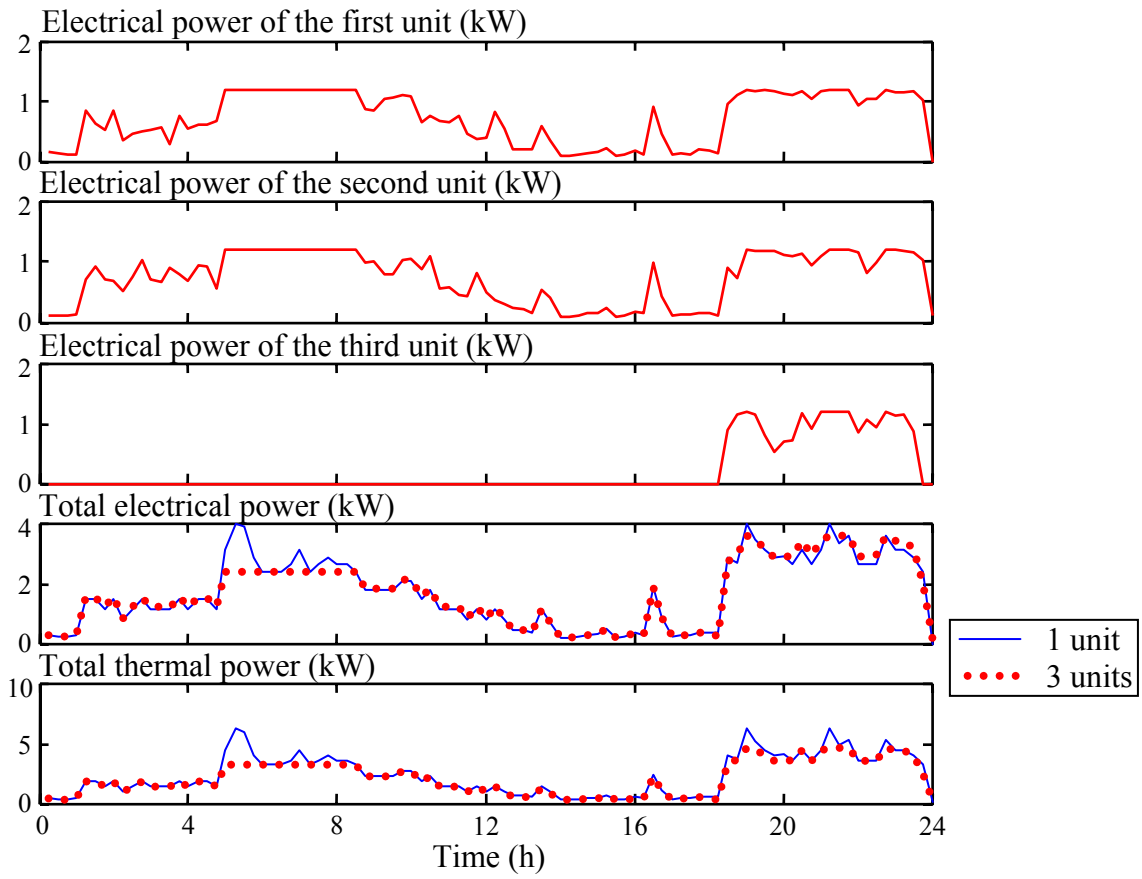

Fig 7-14 Comparing the performance of one and three fuel cells: case (2)

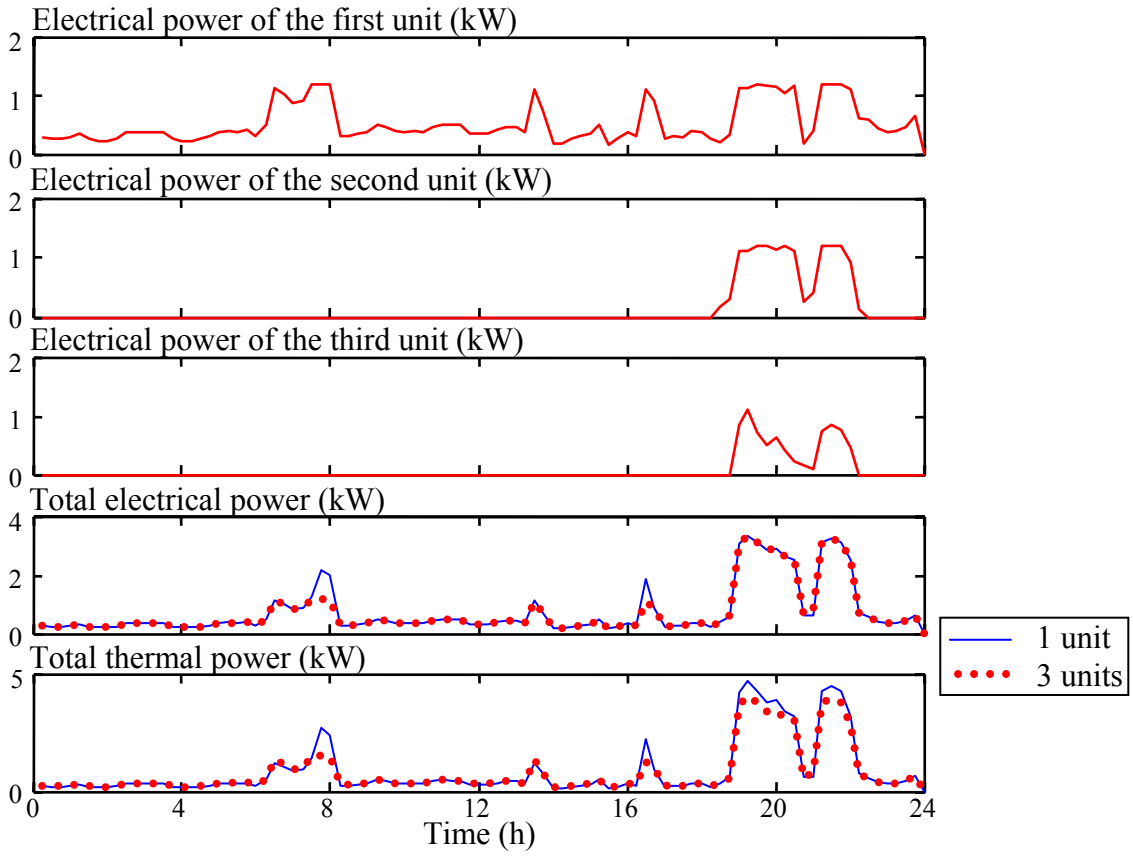

Fig 7-15 Comparing the performance of one and three fuel cells: case (3)

7.6 Management of a micro-turbine unit

The structure of the residential system supplied by a MT is similar to that with the FC as shown in Fig 7-1 and, as a result, the economic models are similar to each other. However, the parameters and curves are modified to properly describe the performance of the MT unit. Unlike the FC, the efficiency of the MT increases with the increase of the supplied power. Fig 7-16 shows typical electrical and thermal efficiency curves of a 25kW Capstone-C30 MT [80].

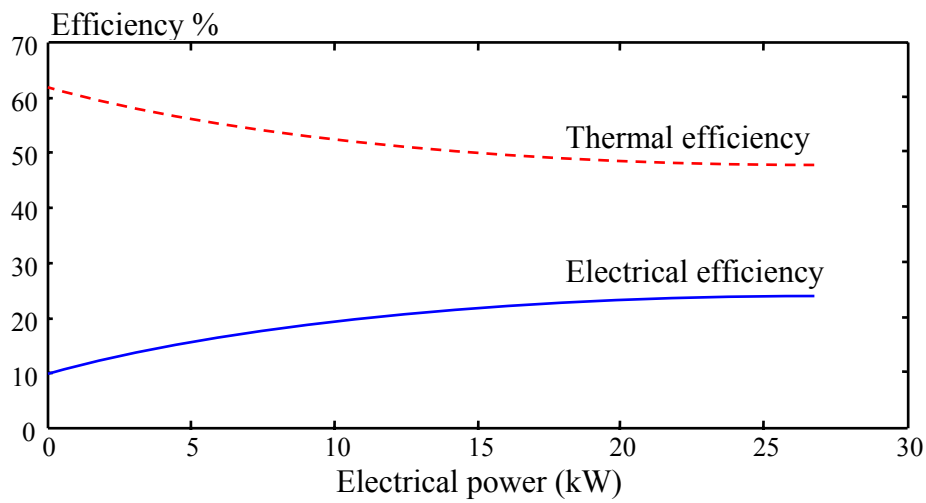

Fig 7-16 Electrical and thermal efficiency curves of the MT

Since the typical power required by a conventional residential load is much lower than this level and due to lack of information, the curves of this MT are rescaled to be suitable for a unit with a 4kW rating. Fig 7-17 shows the rescaled electrical efficiency and the thermal power as functions of the generated electrical power. These curves are used to derive the electrical efficiency and the thermal power as functions of the electrical power to be used in the economic model of the MT. The parameters of the MT economic model are given in appendix G.

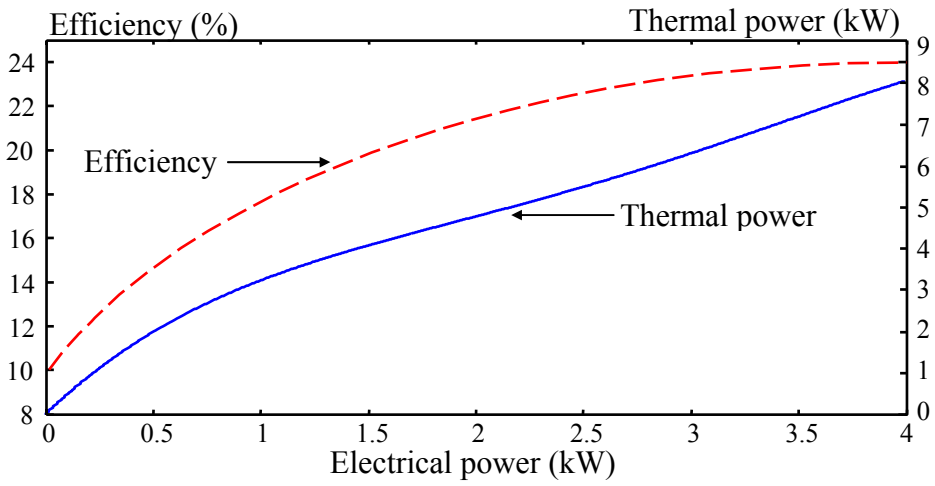

Fig 7-17 The electrical efficiency and the thermal power of the MT

The same load curves and operating tariffs used with the FC are used with the MT after modifying the economic model. The dissimilarity between the parameters and the characteristics of the two units result in significant changes in the optimal operation in the two cases. To compare the performance of the MT to that of the FC, three examples from the optimization process are given. The load curves and the operating tariffs used in the three selected cases are summarized in Table 7-4. In addition, the total daily operating costs are listed in the same table.

Table 7-4 Load curves, operating tariffs and the corresponding operating costs when optimizing the operation of a FC and a MT to supply a residential load

	Load curve	$C_{n\text{-}FC}$ (\$/kWh)	$C_{n\text{-}RL}$ (\$/kWh)	$C_{el\text{-}p}$ (\$/kWh)	$C_{el\text{-}s}$ (\$/kWh)	Total operating cost (\$/day)	
						FC unit	MT unit
Case(1)	6	0.03	0.07	0.14	0.1	1.2412	2.8997
Case(2)	6	0.04	0.05	0.12	0.07	3.6942	4.3213
Case(3)	8	0.03	0.05	0.16	0.07	2.4463	3.5845

Fig 7-18 through Fig 7-20 illustrate the optimized electrical and thermal power in the MT and the FC with the corresponding load demands in the three cases. In most investigated cases, the settings of the MT are mainly affected by the thermal demand. In Fig 7-18 for example, the FC produces a high value of electrical

power due to the high tariff of sold-electricity (0.1$/kWh) and the low tariff of purchased fuel (0.03$/kWh). On the other hand, the output from the MT is close to the thermal load demand. The reason can be explained regarding the efficiency and the thermal-power curves shown in Fig 7-16. It is clear from the figure that the MT generates higher thermal power than the electrical power, which gives the priority to supply thermal power. Following the electrical load demand will result in an excess of thermal energy, which will be wasted.

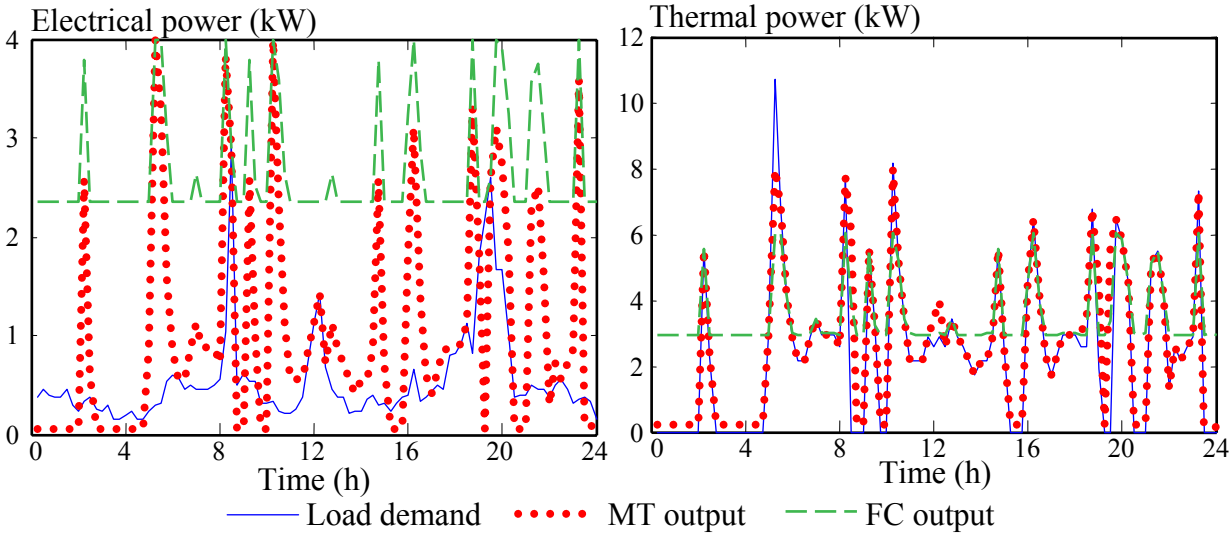

Fig 7-18 A comparison between using a MT and a FC: case (1)

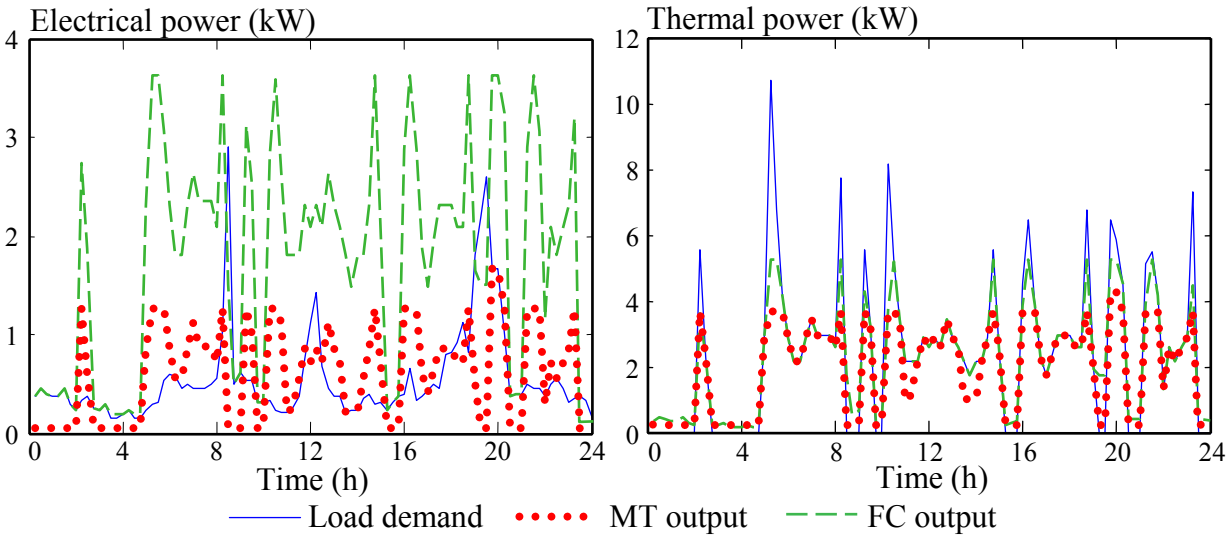

Fig 7-19 A comparison between using a MT and a FC: case (2)

The comparisons between the FC and the MT under different tariffs and load curves ensure that the FC results in lower operating costs. In spite of the higher thermal efficiency of the MT, the higher electrical efficiency of the FC causes lower operating cost in most investigated cases. This is owing to the high price of electrical energy compared to that of the thermal energy. Generally, the MT will be more economic under certain circumferences, but the average daily cost will

be always lower with the FC. For special loads, which have high thermal and low electrical demands, MT units may be favourable in terms of operating costs.

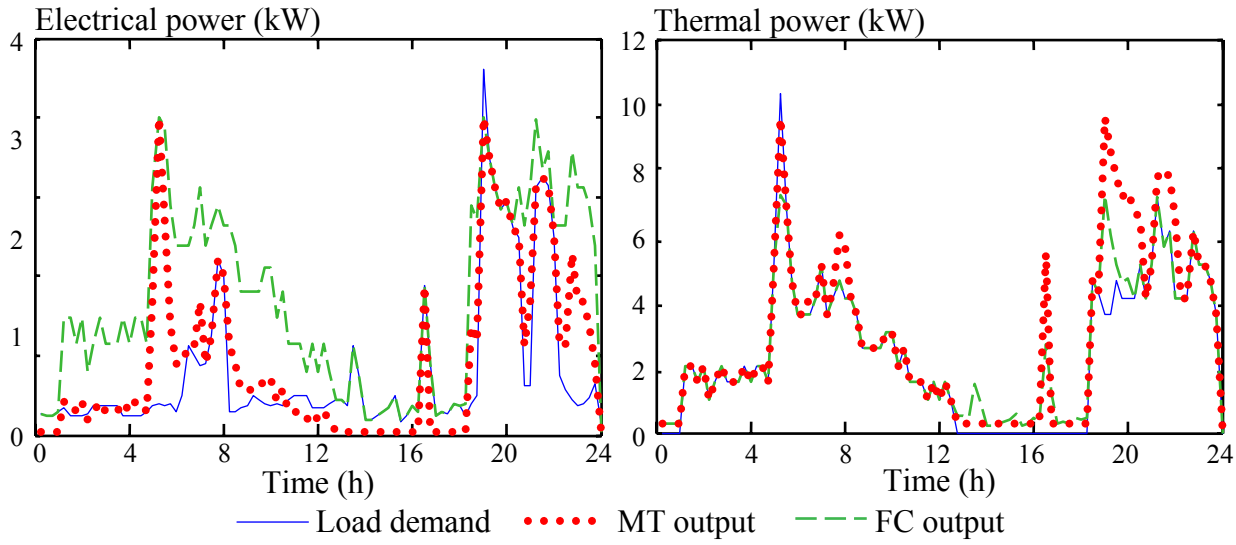

Fig 7-20 A comparison between using a MT and a FC: case (3)

To evaluate the potential reduction in the total daily operating cost when the optimization process is applied, the results of optimizing a single FC, as the most economic choice among the three alternatives, are compared with three conventional settings. The first one is to operate the unit always at its rated power. The second and third cases are to follow up the electrical or thermal load demands respectively. Table 7-5 gives the average cost as well as the average difference of the three conventional settings with respect to the GA-based optimal case for one load curve under 81 different operating conditions.

Table 7-5 Average daily cost and average difference with respect to optimal case

	Average cost ($/day)	Average difference with respect to optimal case	
		Average difference ($/day)	Average percentage difference
Optimal settings (from GA)	3.722	0.0	0.0
Settings=rating	8.582	4.860	130.575 %
Settings=electrical demand	4.855	1.133	30.441 %
Settings=thermal demand	4.637	0.915	24.584 %

The high operating cost of the first conventional case indicates that this scenario is not relevant. The high electrical power results in surplus thermal power, which is wasted since no thermal storage is assumed. The unit in the second and third scenarios will cover either the electrical or the thermal load demands and, therefore, the cost is relatively decreased. Following the optimal scenario can achieve a reduction of 0.915$/day (334$/year) compared to the best conventional settings. This represents a significant reduction not only in the operating cost of the FC but also in the total energy price. However, evaluating the optimization

process depending on the best conventional settings alone is not fair and misleading. The type and natural of load demands affect the results considerably. For other loads, following the thermal demand can be more expensive than other conventional choices. Therefore, various conventional settings have to be considered when evaluating the reduction achieved using the optimization process.

7.7 Generalizing the optimization for online employment

Regardless the significant reduction in the daily operating cost, it is obvious that the optimal output varies within the same day depending on the operating tariffs and the electrical and thermal demands. Therefore, it is obligatory to repeat the management process everyday and also with each variation in the operating tariffs. This restricts the online application of the optimization process, especially in liberal markets with the frequently variations of the operating tariffs. The objective behind extending the management process through a generalization stage is to overcome the time-consuming problem characterizing the GA-based optimization and to enable the online application of the approach. The generalization is carried out only for the single FC as the most economic alternative as discussed in the previous section. Two techniques are employed to accomplish the generalization process: ANNs and DTs.

7.7.1 ANN-based generalization

An ANN is used to generalize the results obtained in the first stage due to its high capability of generalizing such nonlinear complicated problems [48, 49]. After training and testing the ANN, it will be prepared for the onsite application to define the settings of the FC in the online mode. A simple hardware can be developed based on the structure and parameters of the ANN to define the optimal or quasi-optimal settings of the unit.

7.7.1.1 Neural network structure

Beside the input and output layers, the ANN comprises also three hidden layers, which gives the best results among the other structures experimented in this research. The number of neurons in the first, second, and third hidden layers are 40, 30, and 20 neurons respectively. Tanh-sigmoid transfer functions are used as activation functions for all neurons in the hidden layers, while a log-sigmoid transfer function is used for the output neuron. The nodes in the input layer receive 54 inputs, while a single output is obtained at the output layer. The inputs to the network include two different natural gas tariffs for supplying the FC and the

thermal loads and two different tariffs for purchased and sold electricity. Also, information about the present electrical and thermal demands is used as inputs to the network.

Except for the last constraint given by equation (7-13), information for only three previous and three following hours are required to define the present setting of the FC. Since this constraint is always inactive as mentioned earlier, historical and prospective data for only three hours are enough to get satisfactory results. Hence, 12 previous values and 12 prognoses of both the electrical and thermal load demands are introduced at the input layer representing the last three hours prior to, and the next three hours following the present time interval. The single output from the network represents the desired optimal electrical-power setting of the FC in the next time interval. The configuration of the proposed ANN is illustrated in Fig 7-21. This structure enables the simulation of changes in the natural gas and electricity prices even within the same day. Since the prognosis at the input layer are required only for a short period, the error in forecasting the load demand will be small and accurate results are expected to be obtained.

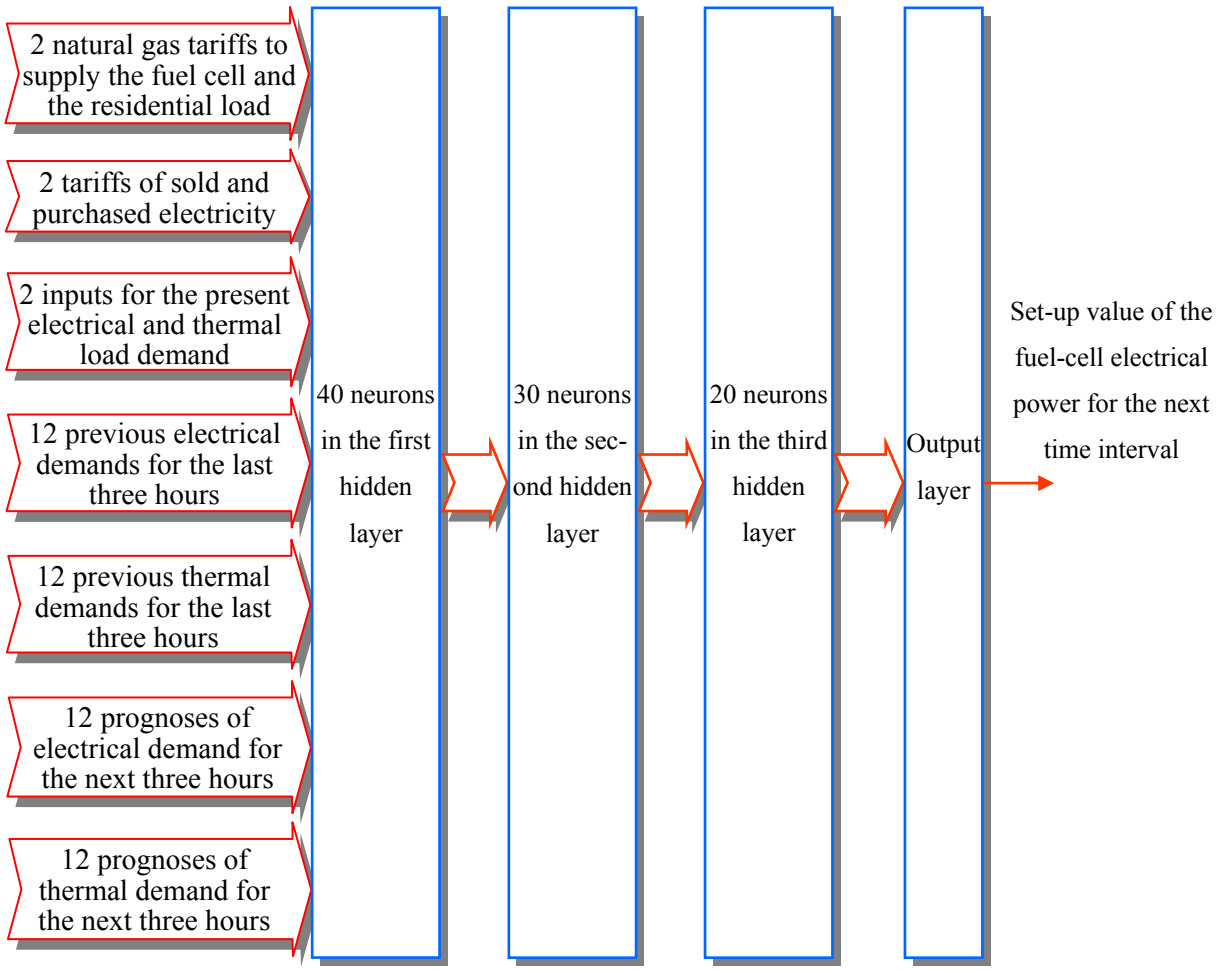

Fig 7-21 Neural Network structure

7.7.1.2 Training process

The results obtained from the optimization process are managed and suitable patterns are extracted. Results corresponding to eight load curves are used in the training process, while results regarding another load curve are kept for testing the trained network. For each one of the four operating tariffs, between three and four different values are used with each load curve, resulting in more than 56000 patterns. The online back propagation approach is followed in the training process, where the weights are updated after the representation of each pattern. The training is carried out for more than 1000 epochs to ensure high accuracy in the training process.

To evaluate the effectiveness of the training process, Fig 7-22 through Fig 7-24 illustrate three comparisons between the optimal targets as obtained from the GA-based optimization and the output from the ANN. The three cases correspond to different load curves and operating tariffs as listed in the following table.

	Load curve	$C_{n\text{-}FC}$ (\$/kWh)	$C_{n\text{-}RL}$ (\$/kWh)	$C_{el\text{-}p}$ (\$/kWh)	$C_{el\text{-}s}$ (\$/kWh)	Total operating cost (\$/day)	
						GA-based settings	ANN settings
Case 1	2	0.05	0.07	0.12	0.1	2.413	2.481
Case 2	3	0.04	0.09	0.14	0.04	2.233	2.303
Case 3	4	0.03	0.05	0.16	0.0	2.041	2.088

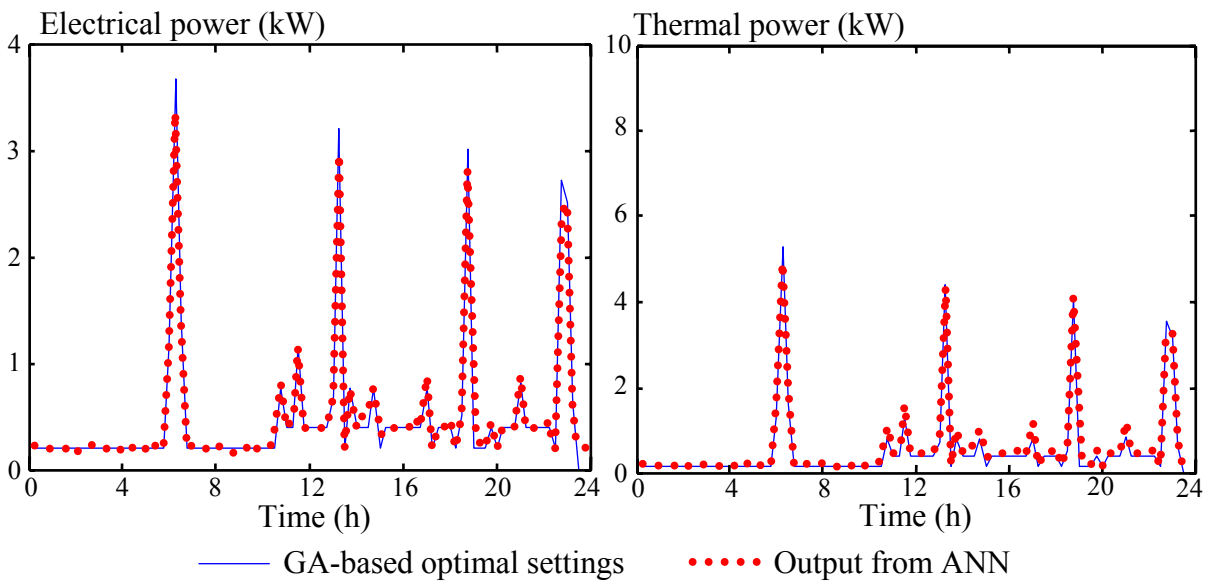

Fig 7-22 Comparing the ANN output with the optimal target: case (1)

The agreement between the ANN-based settings and the GA-based optimal target reflects the high accuracy of the training process, ensuring the high capability of the ANN to extract the features of the optimal performance.

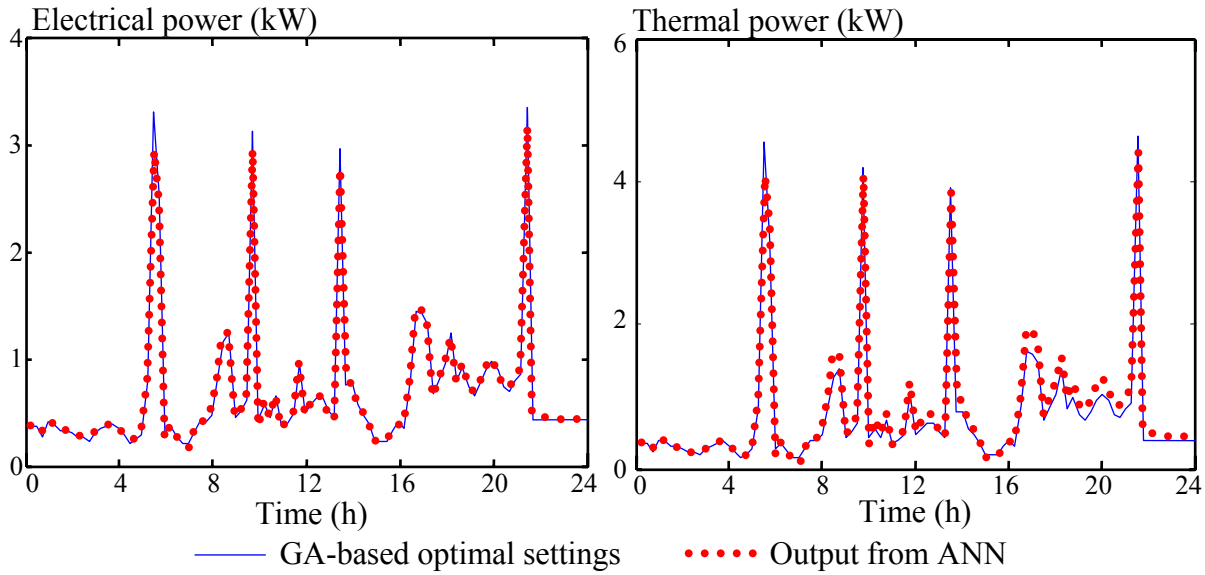

Fig 7-23 Comparing the ANN output with the optimal target: case (2)

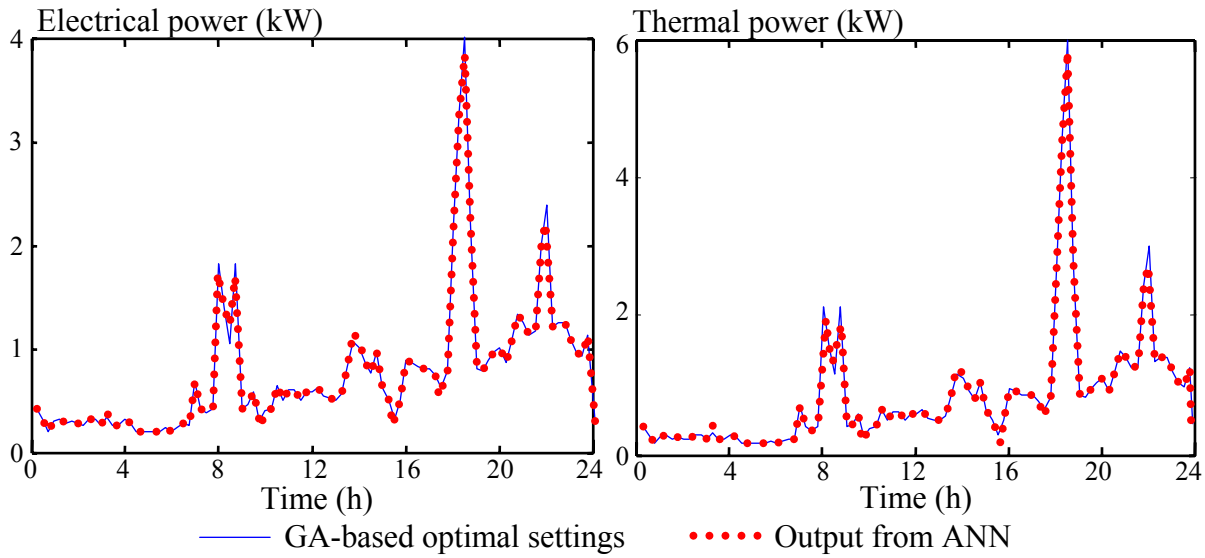

Fig 7-24 Comparing the ANN output with the optimal target: case (3)

7.7.1.3 Testing the trained neural network

In the testing phase, the trained ANN is activated by new testing data to verify the generalization capability of the network. Load curve number (8), which is not used in the training process, is used to test the trained network at different fuel and electricity tariffs. This includes 81 different investigated cases with a total number of 7776 patterns. Fig 7-25 through Fig 7-27 illustrate three selected comparisons between the optimal target and the ANN-based settings as obtained from the test results. The different tariffs and the corresponding daily operating cost in each case are given in the following table.

	$C_{n\text{-}FC}$ ($/kWh)	$C_{n\text{-}RL}$ ($/kWh)	$C_{el\text{-}p}$ ($/kWh)	$C_{el\text{-}s}$ ($/kWh)	Total operating cost ($/day)	
					GA-based settings	ANN settings
Case 1	0.03	0.05	0.12	0.0	3.473	3.605
Case 2	0.04	0.09	0.16	0.1	3.047	3.169
Case 3	0.05	0.05	0.12	0.1	4.182	4.354

The ANN outputs show good agreements with the target, which demonstrates the capability of the ANN and the effectiveness of the presented approach. It is expected that defining the settings depending on ANN decisions will not lead to a significant increase in the operating cost compared to the optimal cases.

The average optimal daily operating cost is about 3.732$/day depending on analyzing the 81 cases in the test phase. This value increases to 3.904$/day if the settings are defined bases on the outputs from the ANN. Compared to the reduction achieved using the proposed technique, this difference represents a minor increase in the daily operating cost.

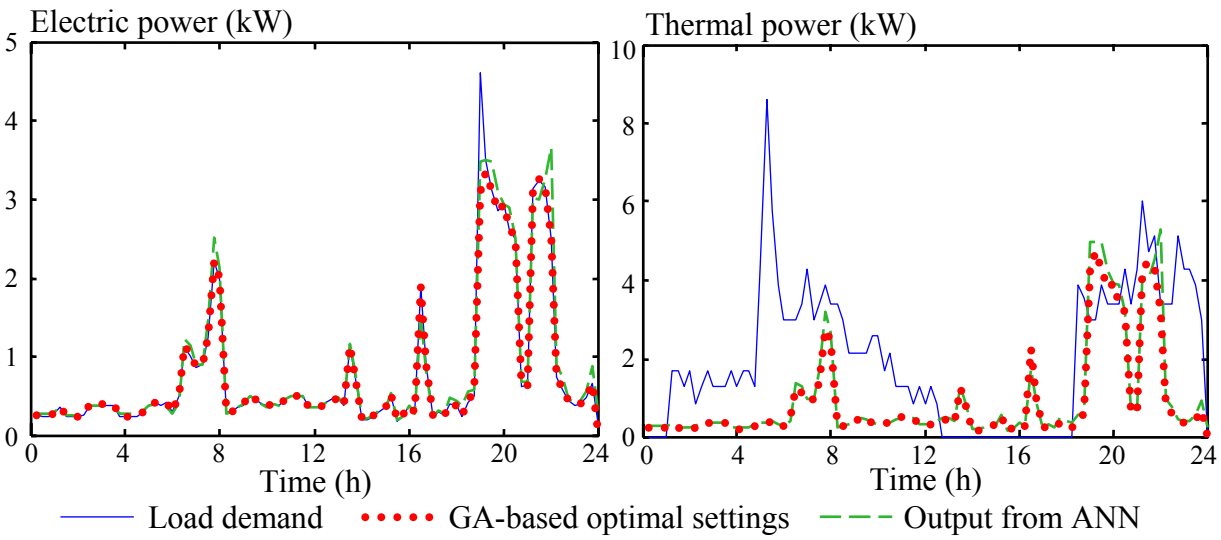

Fig 7-25 Comparing the ANN output with the optimal test target: case (1)

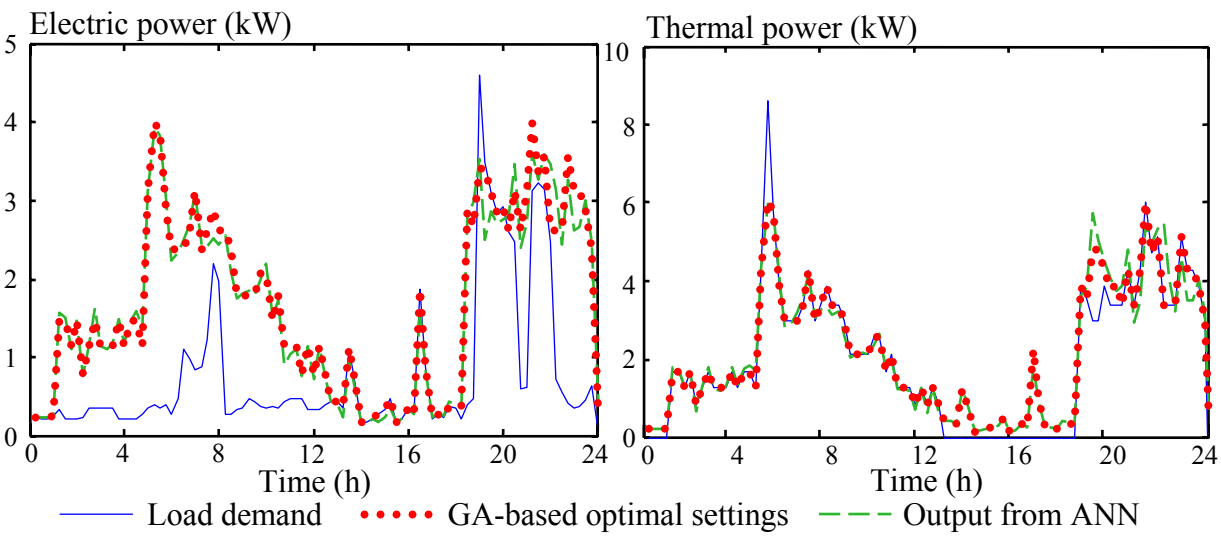

Fig 7-26 Comparing the ANN output with the optimal test target: case (2)

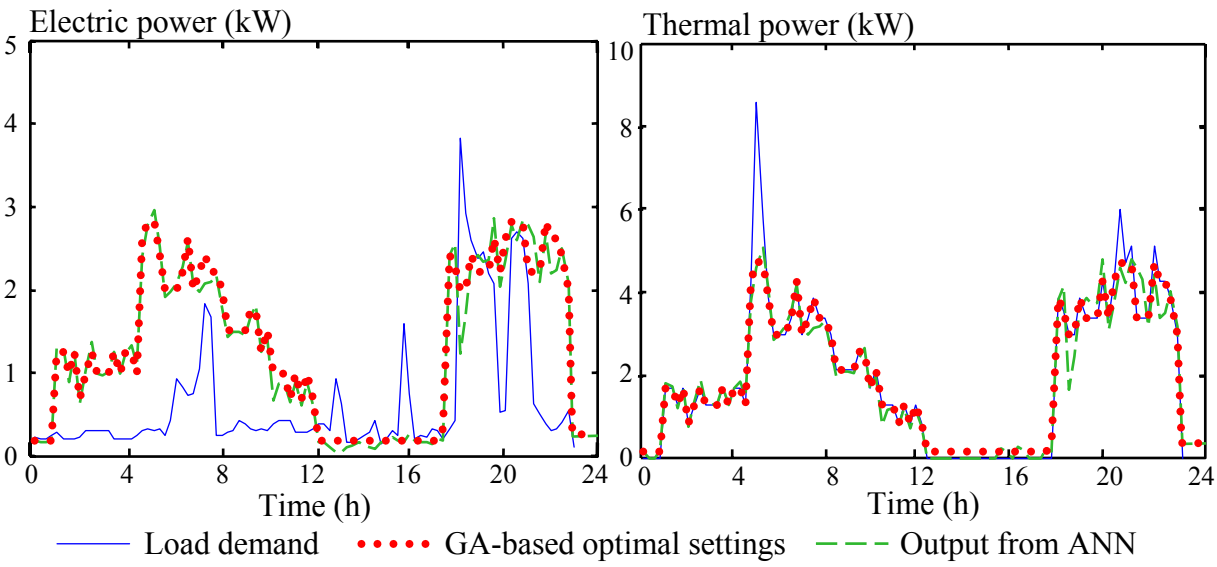

Fig 7-27 Comparing the ANN output with the optimal test target: case (3)

These results reflect the success of the ANN to capture the optimal behaviour of the unit with high accuracy even with new unobserved cases.

Fig 7-28 compares the total daily operating costs when the ANN is used to define the settings of the FC with the costs considering the optimal settings for the 81 investigated cases.

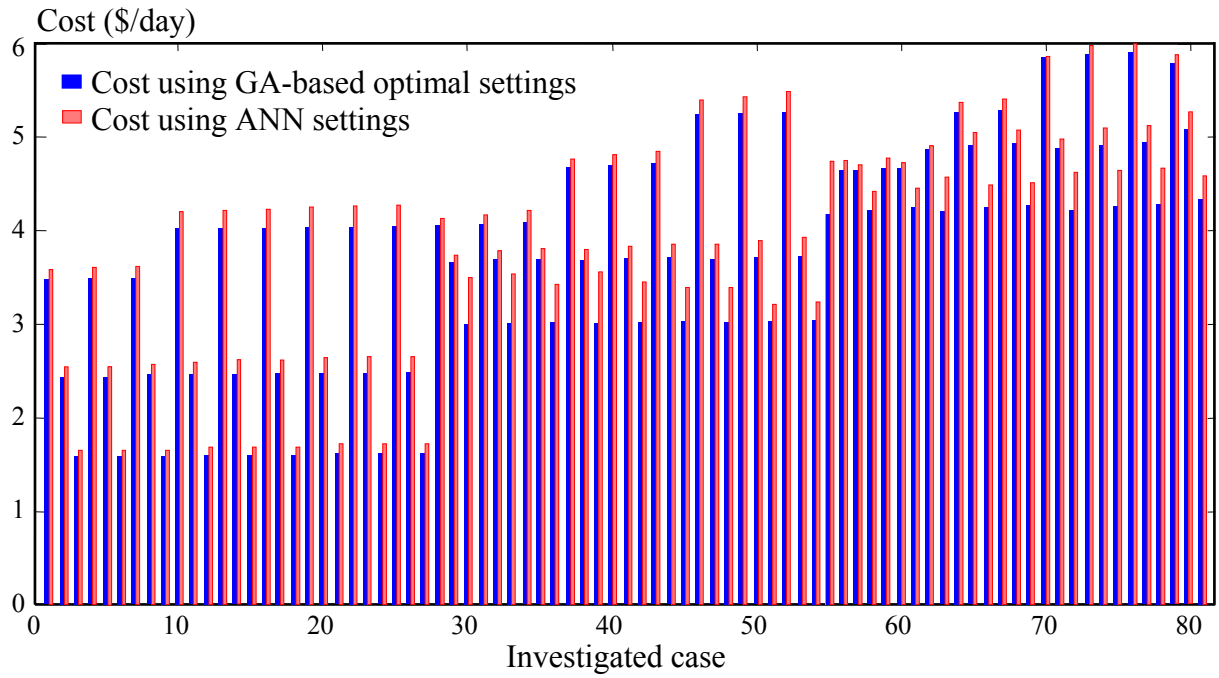

Fig 7-28 Daily operating cost using optimal settings and applying ANN

In addition, Fig 7-29 illustrates the percentage difference between the operating cost using ANN settings and the optimal settings for the 81 investigated cases.

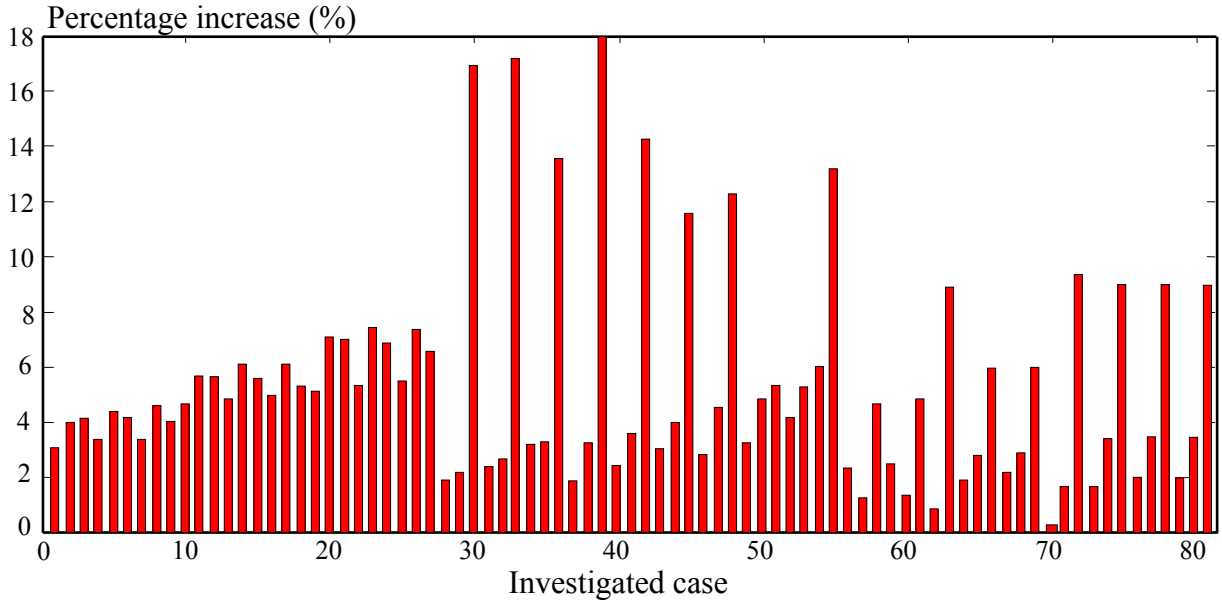

Fig 7-29 Percentage increase in the operating costs as a result of using the ANN settings

7.7.2 Decision tree-based generalization

The DT classifier is an intelligent approach for multistage decision making, which is widely used in many applications [74, 75]. It is one of the simplest representations of complicated functions that can be successfully used to classify new unobserved data and thus, has a talented generalization feature. The main advantage of DTs is their capability to break up a complex decision into a set of simpler decisions, predominantly providing correct solutions similar to the desired targets [74]. Other benefits of DTs for classification problems include their robustness, nonparametric nature and their high computational efficiency [75]. The employment of DTs as an alternative to the ANN is therefore proposed in this section to extend the optimization approach in a generalized frame.

7.7.2.1 Overview

DTs are widely-used supervised learning techniques for approximating discrete functions [74]. They represent a nonparametric approach that can provide classifications for complex problems to deduce suitable decisions for new unobserved cases [75]. DTs depend in their work on dividing complex problems into simpler sub-problems and solving each sub-problem separately [75]. They are constructed using a data base extracted from all possible states of the investigated problem and are proposed for deriving a model describing the behaviour of the original system. The configuration of DTs consists of nodes, branches and leaves. Every node in the DT stands for a specific decision rule. This rule is examined and a corresponding decision is taken. Excluding the root one, each node in the DT has only one incoming edge, while two branches start from all nodes to repre-

sent the two possible decisions. Every final leaf characterizes the corresponding output value, which satisfies all the given conditions [75].

The variables in the input vector to the DT are called predictors and the final decision value is called the target. Constructing the DT from training data is thus the process of finding a correlation between predictors and targets depending on a certain set of data. Any DT can be converted into a number of rules where the different paths are followed to reach a final leaf starting from the root. When new predictors are applied to the DT, the roles will be tested at each node to select the suitable branch until the final leaf is reached and thus the target value. Normally, the database is formulated to represent all the possible operating cases and, as a result, extremely large DT is often produced. However, it is more practical to create the smallest possible tree, which still accurately classifies the training data [81]. This is aimed not only to simplify the resulting set of rules but also to diminish the possibility of overfitting [81]. For this reason, the DT is commonly prunes by removing some branches from the structure and converting the corresponding nodes to leaves [81].

7.7.2.2 Constructing the decision tree

The DT is created using the same database applied with the ANN. Also, it has the same inputs and output described in section 7.7.1.1. Constructing the DT is accomplished with the help of the MATLAB toolbox. Due to the large size of the database, the DT involves a total number of 2454 terminal nodes. The quality of the classification rules is evaluated by applying some sets of the same predictors, which are used in the creation process, and comparing the outputs with the optimal targets. Fig 7-30 shows a comparison with load curve number (2).

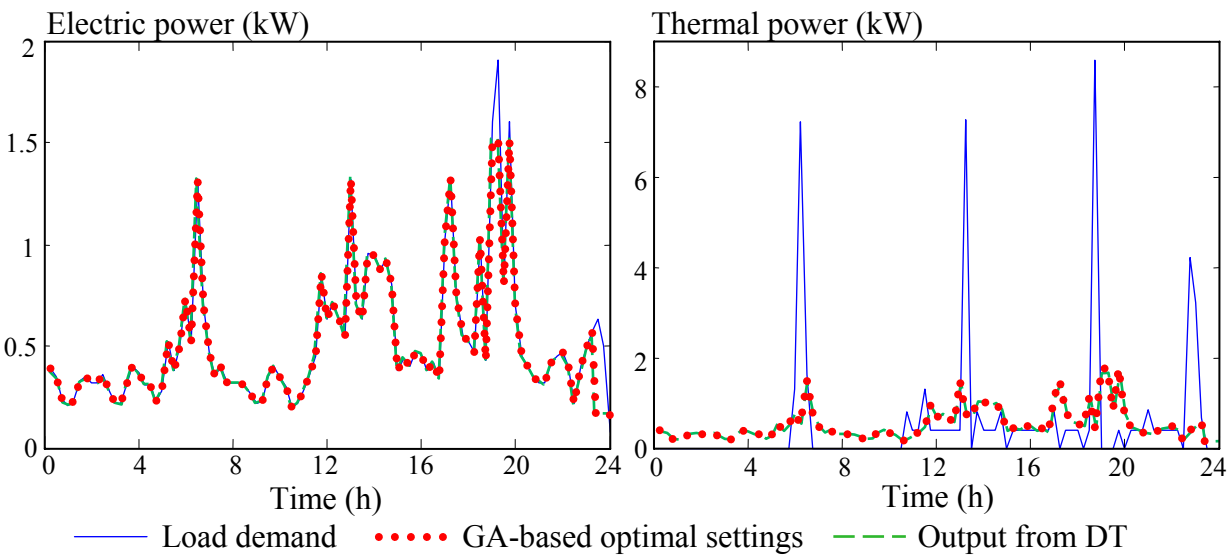

Fig 7-30 Comparing the DT outputs with the GA-based optimal target

The different tariffs and the daily operating cost are given as follows:

$C_{n\text{-}FC}$ ($/kWh)	$C_{n\text{-}RL}$ ($/kWh)	$C_{el\text{-}p}$ ($/kWh)	$C_{el\text{-}s}$ ($/kWh)	Total operating cost ($/day)	
				GA-based settings	DT-based settings
0.04	0.05	0.12	0.04	2.090	2.125

The DT succeeded to provide high accuracy in defining the correct settings of the FC through one day under certain circumstances. Despite this high accuracy, the large size of the tree gives the opportunity for overfitting. Pruning the tree simplifies the rule base and improves the generalization performance

7.7.2.3 Pruning the decision tree

A DT constructed from a large training set usually fits these data until all leaves contain information for a single class [75]. In this case, many branches in the DT are specified only for this particular data and can not provide general underlying relationships. Such branching is not likely to take place under new situations, which results in poor performance with new unobserved cases. Removing these unreliable branches via the pruning process can achieve better classification over the expected operating space [75]. Thus, the pruning process is required for reliable and robust operation of the DT. It is convenient to consider the full tree as a reference measure when evaluating the accuracy of the pruned tree.

The best pruned tree is selected based on evaluating the average daily cost regarding 81 new cases. The average percentage increase in the daily operating cost is illustrated in Fig 7-31 for different pruning levels considering the full tree as a reference measure. From this figure, the best pruning level can be defined as 1149 which represents about 47% reduction in the tree size without significant change in the accuracy (about 0.0156% increase in the average daily cost).

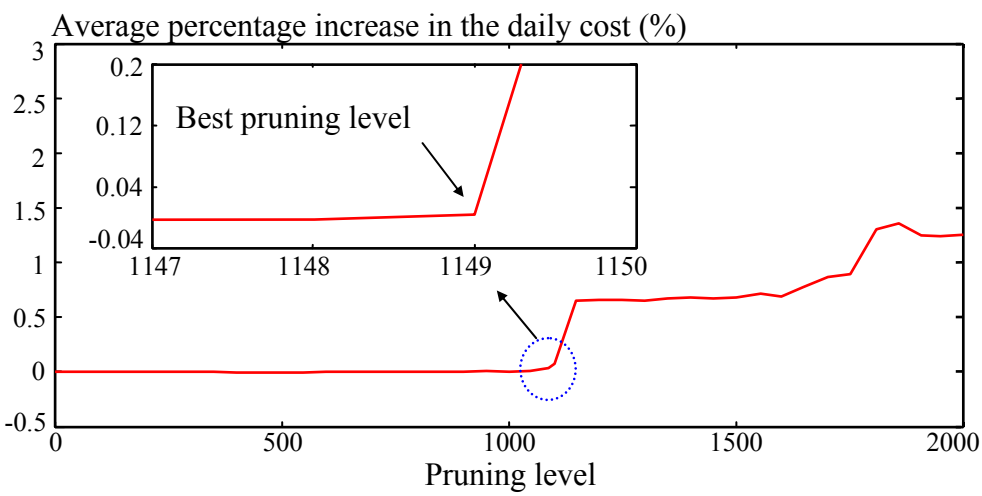

Fig 7-31 Average percentage increase in the daily cost for the different pruning levels considering the full tree as a reference measure

The performance of the pruned tree is evaluated using the two new load curves that are not used to create the DT under different operating tariffs. Fig 7-32 through Fig 7-34 show comparisons between the GA-based optimal targets and the outputs from the DT for three selected cases out of 162 investigated cases. The first two cases belong to load curve (8) under different operating tariffs, while the third case belongs to load curve (10). The different tariffs and the corresponding daily operating costs are given in the following table:

	Load curve	$C_{n\text{-}FC}$ (\$/kWh)	$C_{n\text{-}RL}$ (\$/kWh)	$C_{el\text{-}p}$ (\$/kWh)	$C_{el\text{-}s}$ (\$/kWh)	Total operating cost (\$/day)	
						GA-based settings	DT-based settings
Case 1	8	0.03	0.05	0.12	0.0	3.473	3.521
Case 2	8	0.05	0.09	0.16	0.07	4.276	4.347
Case 3	10	0.04	0.07	0.14	0.1	2.156	2.229

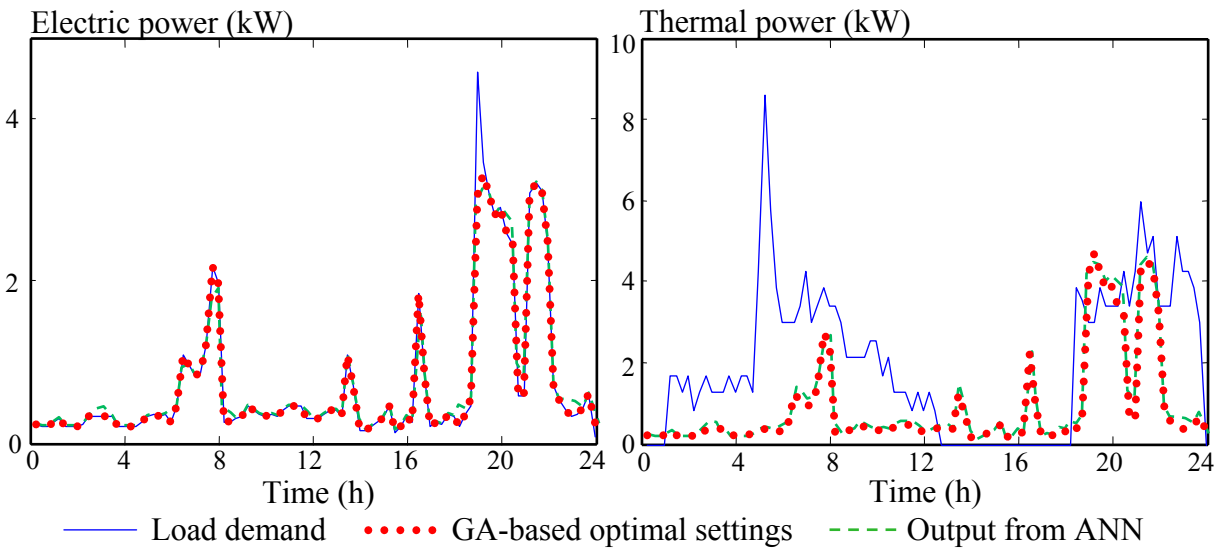

Fig 7-32 Comparing the DT output with the optimal target: case (1)

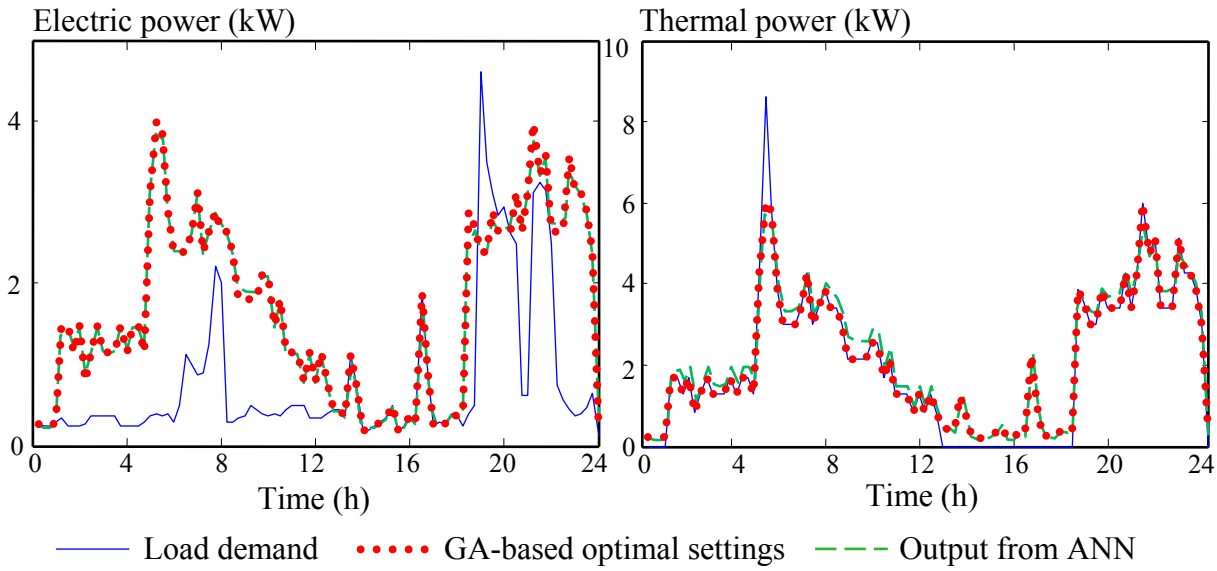

Fig 7-33 Comparing the DT output with the optimal target: case (2)

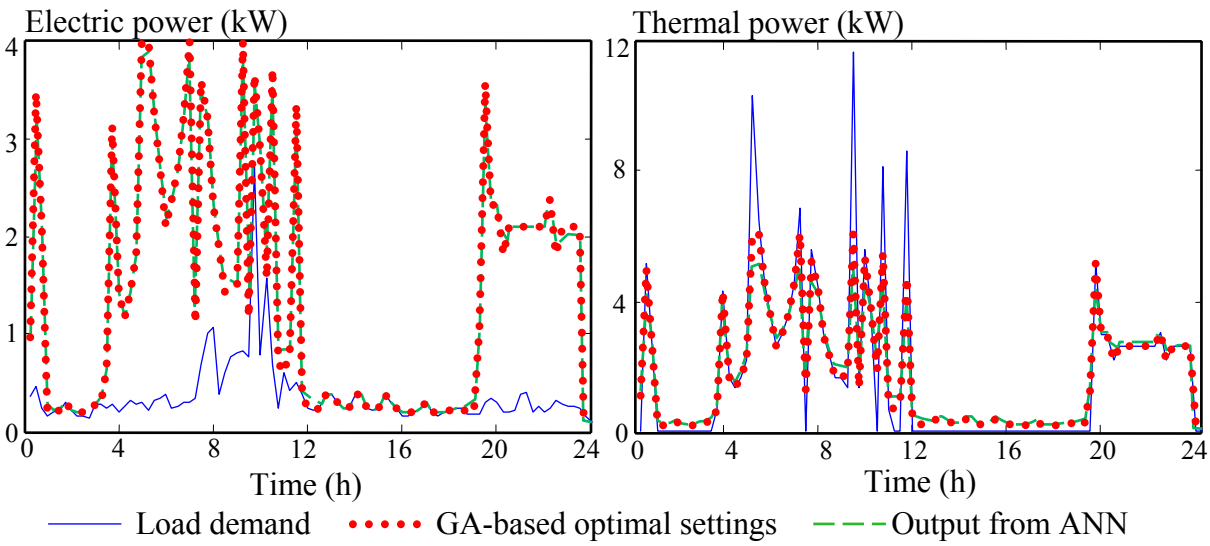

Fig 7-34 Comparing the DT output with the optimal target: case (3)

The coincidence between the DT-based settings and the optimal ones confirms the robustness of the proposed approach. In all cases, the DT classifier shows a high capability of identifying settings for the FC very close to the optimal ones.

7.7.3 Decision trees versus ANN

Both the ANN and the DT can provide the required general frame to implement the proposed approach in the online mode. Their high accuracy and generalization capability have been proven through the results introduced in sections 7.7.1 and 7.7.2. Compared with the ANN, DTs learning time is much smaller and, hence, they are more suitable for frequently-requisite training [82]. At the time where the DTs are sequential in nature, the ANNs depend on parallel processing in the training [75]. ANN continually tests the whole training data for updating its weights [48, 49]. Conversely, the DT learning is accomplished by dividing the training data into smaller subsets and testing the subsets separately [75]. So far, there is no definitive evidence to prefer one of the two approaches on the other. However, ANNs are generally more likely to give better results for highly nonlinear problems since DTs approximate the nonlinear behaviour with a set of linear relations. On the other hand, the nature of the DTs makes them much more practical for data interpretation than ANN [75].

A comparison between the performance of the ANN and the DT to handle the current problem is carried out based on the average daily cost of the 162 new cases. These cases are related to the two new load curves at different operating tariffs. The results of this comparison are shown in Fig 7-35 for the GA-based optimal settings, the ANN-based settings, the full DT-based settings and the

Pruned DT-based settings (PDT). The comparison indicates that the DT can be better than the ANN if the pruning level is lower than 1790. The best pruning level is 1149, which confirms the previous results shown in Fig 7-31.

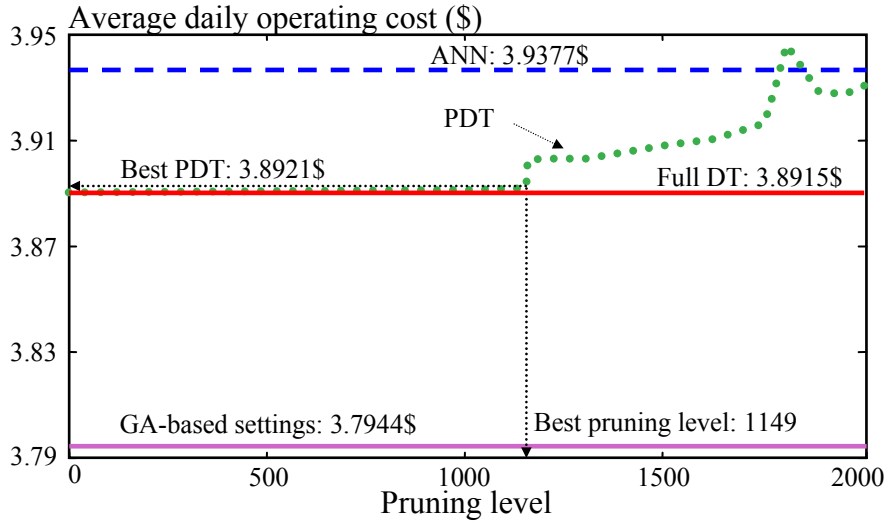

Fig 7-35 Average daily operating cost with the GA-based settings, ANN-based settings and DT-based settings at different pruning levels

Table 7-6 gives the average cost in $/day and the average difference of the quasi-optimal settings with respect to the GA-based optimal values. The average daily costs with the three conventional settings are also given in the table for comparison reasons. From these results, it is obvious that following the settings from the ANN or the DT will not cause a significant increase compared to the GA optimal ones. It is also clear that the DT is slightly better than the ANN but the latter still gives good results close to the optimal values.

Table 7-6 Average cost and the average difference of the quasi-optimal settings with respect to the GA-based optimal values

		Average cost ($/day)	Average difference with respect to the optimal case	
			Average difference ($/day)	Average percentage difference
Conventional settings	Settings=rating	8.7466	4.9522	130.513%
	Settings=electrical demand	5.3981	1.6037	42.265%
	Settings=thermal demand	4.9822	1.1878	31.304%
Optimal and quasi-optimal settings	GA-based optimal settings	3.7944	0	0%
	ANN-based settings	3.9377	0.1433	3.7766%
	DT-based settings	3.8915	0.0971	2.5590%
	PDT-based settings	3.8921	0.0977	2.5748%

Generally, the proposed approach can be applied to provide a simple and effective optimization technique for FCs and also other DG sources in the online mode with a high accuracy.

7.8 Conclusion

This chapter presents a new approach for optimizing the performance of PEMFCs and MTs for residential applications. A real-coded multi-population GA is used offline to carry out the optimization process under different operating tariffs and load curves. The performances of a single FC, three FCs operating in parallel and a single MT, as three alternatives, are optimized based on detailed economic models. The GA has proven good capability to handle the operation management problem of the selected DG units when supplying a residential load. Analyzing the obtained results demonstrates a significant reduction in the daily operating costs using the management process, which contributes in improving the economic feasibility of the DG units. Supplying the residential load using a single FC shows lower daily operating cost compared to the other two alternatives. The high electrical efficiency of the FC results in lower operating cost compared to the use of a MT. Also, the nature of the FC efficiency curve, which decreases with the increase of the supplied power, shifts the optimum allocation in favour of using a single unit rather than using smaller identical units in parallel.

It is also proposed to formulate the management process in a general frame using ANNs and DTs as two alternatives to avoid the need for repetitive optimization after changes in operating conditions take place. Both the ANN and the DT are trained and tested using a database extracted from the GA-based optimization for different load curves and operating tariffs. The inputs, which represent the load demand and the operating tariffs, can be updated online to simulate the variations in the operating conditions. The generalization stage is applied only with the single FC as the most-economic alternative. The effectiveness of the suggested approach is confirmed through the agreement between the optimized settings and the outputs from the ANN and the DT. The results show that the DT can be better than the ANN for this application if a suitable pruning level is selected. However, the ANN will give better results if the DT is pruned beyond this level. The online adjustment of the settings in a fast and simple manner demonstrates the viability of this approach for optimum deployment of different DG units for residential applications.

Chapter 8

Conclusion and Future Directions

8.1 Conclusion

The defined scope of the thesis is on some topics related to the utilization of DG units within electrical power networks. The growing importance of such units and their expected impact on the dynamics of power networks encourage the investigation of these subjects to overcome the potential challenges of increasing their penetration levels. In particular, the following issues are addressed in this dissertation to highlight a vital area related to future power systems.

8.1.1 Dynamic modelling of fuel cells

A third order equivalent circuit is proposed to simulate the dynamics of different types of FCs for stability analysis and control design purposes. The model can be extended to involve the effect of varying the cell temperature and pressure using empirical formulas. The use of an ANN to develop a detailed model directly from measured input/output data is also discussed. The structure of the ANN can be modified to include as many variables as required and to change the order of the model to ensure high performance accuracy. In view of the fact that no experimental data was available, the ANN is trained using patterns extracted from the proposed equivalent circuit. This can be accepted since the main objective is not to develop a specific dynamic model but to introduce the approach itself. The comparisons between the output from the ANN and the target behaviour confirm the capability of the ANN to capture the dynamic performance of the FC and encourage the use of this technique to obtain suitable models for different types of FCs directly from the input/output measurements.

8.1.2 Simulation of a large number of DG units incorporated into a multi-machine network

A hypothetical multi-machine network is simulated and a total number of 112 FCs and MTs are connected in the low-voltage area of the network. This required the development of suitable dynamic models for MTs and different types of FCs with various capacities. The total power from the DG units covers up to 30% of the total load demand in the 0.4kV system. The performance of the entire net-

work is investigated under different disturbances in both the low and high-voltage parts. At the time where the DG units succeeded to absorb large disturbances within the network, they did not respond to interarea oscillations as a result of the local task of their controllers. The dynamic performance of the low-voltage area is somewhat improved due to the existence of active sources near the load centres and the decrease of the voltage drop over transformers and transmission lines.

8.1.3 Dynamic simulation of hybrid fuel cell/micro-turbine units

The construction and the dynamic performance of hybrid FC/MT units are studied and the two integration approaches of the augmented configuration are discussed. A suitable dynamic model is developed and used to investigate the performance of such units in a multi-machine network. The performance of the hybrid units is compared to the performance of separate units operating in parallel under the same conditions. The idea is to identify the effect of augmenting the two units on their dynamic performance. The active power of the hybrid unit is significantly affected by the new structure due to the impact of the FC dynamics on the turbine power. As a result, the angular speed of the PMSG is also strongly affected. A similar behaviour of the reactive power is obtained from the hybrid units compared to separate sources due to its dependency on the terminal voltage, which is defined by the network rather than the individual units.

8.1.4 Dynamic equivalents of distribution power networks

A new approach is developed and applied to identify generic dynamic equivalents for distribution systems containing large numbers of active DG units based on recurrent ANNs. The model, which has a nonparametric nature, requires simulation results or measurements only at the boundary buses. The proposed technique is not based on electromechanical analyses and, therefore, it will not conflict with the characteristics of DG units, which are mostly connected to the network through inverters and in some cases are not distinct by angles or speeds. In addition, the proposed approach would be favourable when there is limited understanding of the relations between system variables. It is also advantageous regarding the complicated mathematical models required to precisely reflect the performance of the replaced network under various operating conditions.

A training program for the ANN with actual recurrent loops is developed and used to obtain the parameters of the dynamic model. The equivalent dynamic model thus obtained was implemented on a power system simulation package to verify its capability of reproducing the dynamic behaviour of the replaced net-

work in full. The results demonstrate the capability of the equivalent model to capture the dynamic behaviour of the replaced networks in its entirety. The model provided outstanding conformity with the results obtained using the full dynamic model of the network even under new generation and loading conditions. The approach promises a significant simplification of the dynamic analysis of large interconnected networks without significant loss of accuracy.

8.1.5 Impact of distributed generation on power systems stability

The impact of DG units with different penetration levels on the stability of power systems is addressed. The results showed the possibility of improving the power system stability when DG units are utilized. Regarding the oscillatory stability, the damping of the electromechanical mode is somewhat improved and the corresponding frequency is slightly increased. The maximum power-angle deviations between the generators are also decreased with the increase of the penetration level of the DG units, which reflects the enhancement in the transient stability of the overall power system. In addition, the network requires smaller time to reach the minimum frequency level when more DG units are employed. Furthermore, the voltage profiles at load terminals are improved due to the use of active DG sources near end-user terminals. The controllers designed to regulate the performance of the DG units participate also in improving the voltage stability of the network.

8.1.6 Online management of fuel cells and micro-turbines

A novel intelligent approach for optimizing the performance of DG units for residential applications is presented. The investigation involves the management of a single FC, three FCs operating in parallel and a single MT as three alternatives. In the first stage of the proposed approach, a real-coded multi-population GA is used offline to carry out the optimization process for different operating conditions and load curves. This stage showed a significant reduction in the daily operating costs with large influence from the fuel and electricity tariffs on the optimal settings of the DG units. The comparisons demonstrated that the single FC is the favourite alternative regarding the operating cost due to the level and nature of its electrical efficiency.

Repetitive optimization processes are obligatory with the variation of the operating circumstances, which requires long time and complex computations in addition to advanced experience from the operator. Therefore, ANNs and DTs are used in the second stage as two alternatives to facilitate the online employment of

the optimization procedures. The second stage is employed only with the single FC as the most economic choice regarding the operating costs. Both the ANN and the DT are trained and tested using the same knowledgebase with all decision variables included in the input vector. To simulate the variations in the operating conditions, it will be enough to update these inputs online without any modifications in the structure of the developed model. The results confirmed the high accuracy of the proposed approach to define online settings for DG units that are very close to the optimal ones in a fast and simple manner. This encourages the utilization of this methodology for optimum deployment of different DG units for residential applications. A comparison between the ANN and DT showed that the DT can outperform the ANN for this application under certain conditions. However, the latter gives also a high accuracy with respect to the optimal values.

8.2 Future directions

It is not sought to provide solutions to specific problems related to DG in power systems. Rather, the research represents a beginning attempt in addressing areas of concern and opportunities for utilizing DG units in the future networks. Moving forward, some possible future directions can be identified as follows:

- using ANNs to develop specific dynamic models for FCs regarding the comprehensive performance using real input/output measurements
- designing centralized robust controllers to achieve more damping in interconnected power systems including large numbers of DG units over a wide range of operating points
- developing more accurate mathematical models for the CFCMT units including topping and bottoming modes with more sophisticated controllers
- applying the proposed ANN-based equivalent approach for identifying suitable equivalents for some subsystems in high-voltage networks including the conventional generators with their regulators
- investigating the impact of using distinct types of DG units with different characteristics on the stability of large interconnected power systems
- online operation management of DG units supplying residential loads considering storage devices with identifying the optimal storage capacity
- applying stochastic optimization methods to consider uncertainties in the online operation management of DG units supplying residential loads

References

[1] T. E. Hoff, H. J. Wenger and B. K. Farmer, "Distributed generation: an alternative to electric utility investments in system capacity" Energy policy, Vol. 24, No. 2, pp. 137-147, 1996

[2] T. Ackermann and V. Knyazkin, "Interaction between distributed generation and the distribution network: operation aspect" IEEE/PES Transmission and Distribution Conf. and Exhibition 2002: Asia Pacific, Vol. 2, 6-10 Oct. 2002, pp. 1357-1362, Yokohama, Japan

[3] M. T. Doyle, "Reviewing the impacts of distributed generation on distribution system protection" Power Engineering Society Summer Meeting, 2002 IEEE, Chicago, USA, Vol. 1, 21-25 July 2002, pp. 103-105

[4] P. P. Barker and B. K. Johnson, "Power system modeling requirements for rotating machine interfaced distributed resources" Power Engineering Society Summer Meeting, 2002 IEEE, Chicago, USA, Vol. 1, 21-25 July 2002, pp. 161-166

[5] P. P. Barker and R. W de Mello, "Determining the impact of distributed generation on power systems: Part I. Radial distribution systems" Power Engineering Society Summer Meeting, Seattle, Washington, USA, 2000 IEEE, Vol. 3, 16-20 July 2000, pp. 1645-1656

[6] F. V. Edwards, G. J. W. Dudgeon, J. R. McDonald and W. E. Leithead, "Dynamics of distribution networks with distributed generation" Power Engineering Society Summer Meeting, Seattle, Washington, USA, 2000 IEEE, Vol. 2, 16-20 July 2000, pp. 1032-1037

[7] In-Su Bae, Jin-O Kim, Jae-Chul Kim and C. Singh, "Optimal operating strategy for distributed generation considering hourly reliability worth" Power Systems, IEEE Transactions on, Vol. 19, No. 1, February 2004

[8] A. G. Amendola and M. C. Rocha, "Fuel cell plant-a proposed analysis for economical feasibility of implantation" Electricity Distribution, 16th Int. Conference and Exhibition on, Amsterdam, the Netherlands, 18-21 June 2001, Part 1, (IEE Conf. Publ. No. 482), Vol. 4

[9] C. Haynes and W.J. Wepfer, "'Design for power' of a commercial grade tubular solid oxide fuel cell" Energy Conversion & management, Vol. 41, Issue 11, July 2000, pp. 1123-1139

[10] D. J. Hall and R. G. Colclaser, "Transient modelling and simulation of a tubular solid oxide fuel cell" Energy Conversion, IEEE transactions on, Vol. 14, No. 3, September 1999

[11] D. Singh, D. M. Lu and N. Djilali, "A two-dimensional analysis of mass transport in proton exchange membrane fuel cell" International Journal of Engineering science, Vol. 37, Issue 4, March 1999, pp. 431-452

[12] Bagnasco, B. Delfino, G.B. Denegri and S. Massucco, "Management and dynamic performances of combined cycle power plants during parallel and islanding operation" Energy Conversion, IEEE Transactions on, Vol. 13, No. 2, June 1998

[13] Borghetti, G. Migliavacca, C. A. Nucci and S. Spelta, "Black-startup simulation of a re-powered thermoelectric unit" IFAC Symposium on power plants & Power Systems Control, 26-29 April, 2000, Brussels, Belgium, pp. 119-126

[14] Amer Al-Hinai and Ali Feliachi, "Dynamic model of a microturbine used as a distributed generator" System Theory 2002, Proceedings of the 34th Southeastern Symposium on, Huntsville, Alabama, 18-19 March 2002, pp. 209-213

[15] W. G. Scott, "Micro-Turbine Generators for Distribution Systems," IEEE Applications Magazine, Vol. 4, Issue 4, pp. 57-62, May/June, 1998.

[16] K. Tomsovic and T. Hiyama, "Intelligent control methods for systems with dispersed generation" Power Engineering Society Winter Meeting, 2001 IEEE, Columbus, Ohio, USA, Vol. 2, 28 Jan.-1 Feb., 2001, pp. 913-917

[17] J. A. Smith, M. H. Nehrir, V. Gerez and S. R. Shaw, "A broad look at the workings, types, and applications of fuel cells" Power Engineering Society Summer Meeting, 2002 IEEE, Chicago, USA, Vol. 1, 21-25 July 2002, pp. 70-75

[18] Shinji Kimijima and Nobuhuíde Kasagi, "Performance evaluation of gas turbine-fuel cell hybrid micro generation system" Proceedings of ASME TURBO EXPO 2002, June 3-6, 2002, Amsterdam, the Netherlands

[19] F. Jurado and J. Saenz, "Adaptive control of a fuel cell-microturbine hybrid power plant" Power Engineering Society Summer Meeting, 2002 IEEE, Chicago USA, Vol. 1, pp. 76-81

[20] Peter A. Daly and Jay Morrison, "Understanding the potential benefits of distributed generation on power delivery systems" Rural Electric Power Conference, 29 April-1 May 2001, pp. A2-1–A2-13, Little Rock, Arkansas, USA

[21] A. Agustoni, M. Brenna, R. Faranda, E. Tironi, C. Pincella and G. Simioli, "Constraints for the interconnection of distributed generation in radial distribution systems" Harmonics and Quality of Power, 10th International Conference on, Vol. 1, 6-9 Oct. 2002, pp. 310-315, Rio de Janeiro, Brazil

[22] M. Begovic, A. Pregelj, A. Rohatgi and D. Novosel, "Impact of renewable distributed generation on power systems" System Sciences, 2001, Proceedings of the 34th Annual Hawaii International Conference on, Jan. 3-6, 2001, pp. 654- 663, Maui, Hawaii

[23] Bruno Delfino, "Modelling of the integration of distributed generation into the electrical system" Power Engineering Society Summer Meeting, 2002 IEEE, Chicago USA, Vol. 1, 21-25 July 2002, pp. 170-175

[24] J. G. Slootweg and W. L. Kling, "Impacts of distributed generation on power system transient stability" Power Engineering Society Summer Meeting, 2002 IEEE, Chicago USA, Vol. 2, 21-25 July 2002, pp. 862-867

[25] A. Girgis and S. Brahma, "Effect of distributed generation on protective device coordination in distribution system" Power Engineering, 2001, LESCOPE '01, Large Engineering Systems Conference on, 11-13 July 2001, pp. 115-119, Halifax, Nova Scotia, Canada

[26] Kauhaniemi, K., Kumpulainen, L.: Impact of distributed generation on the protection of distribution networks. Developments in Power System Protection, IEE International Conference, 5-8 April 2004, Amsterdam, pp. 315-318

[27] Stan Blazwicz and David Kleinschmidt, "Distributed Generation: System Interfaces" White paper prepared by Arthur D. Little, Cambridge, MA. 1999, http://www.encorp.com/dwnld/pdf/whitepaper/wp_ADL_2.pdf

[28] S. J. C. Cleghorn, X. Ren, T. E. Springer, M. S. Wilson, C. Zawodzinski, T. A. Zawodzinski and S. Gottesfeld, "PEM fuel cells for transportation and stationary power generation applications" Int. Journal of Hydrogen Energy, Vol. 22, No. 12, 1997, pp. 1137-1144

[29] W. Morgantown, "Fuel Cell Handbook" 6th Edition, EG&G Technical Services, Virginia, November 2002, http://www.rwth-aachen.de/lbz/FCHandbook6.pdf

[30] M. W. Ellis, M. R. Von Spakovsky and D. J. Nelson, "Fuel cell systems: efficient, flexible energy conversion for the 21st century" Proceedings of the IEEE , Vol. 89, Issue: 12, Dec. 2001, pp. 1808-1818

[31] Kyoungsoo Ro and Saifur Rahman, "Two-loop Controller for Maximizing Performance of a Grid-Connected Photovoltaic-Fuel Cell Hybrid Power Plant" Energy Conversion, IEEE transactions on, Vol. 13, No. 3, September 1998

[32] P.A. Lehman, C.E. Chamberlin, J.I. Zoellick and R. Engel, "A photovoltaic/fuel cell power system for a remote telecommunications station" Photovoltaic Specialists Conference, 2000, Conference Record of the 28th IEEE, 15-22 Sept. 2000, pp. 1552-1555, Alaska, USA

[33] Valery Knyazkin, Lennart Söder and Claudio Canizares, "Control challenges of fuel cell-driven distributed generation" the 2003 IEEE Bologna Power Tech Conference, June 23rd-26th, Bologna, Italy

[34] K. Sedghisigarchi and A. Feliachi, "Control of grid-connected fuel cell power plant for transient stability enhancement" Power Engineering Society Winter Meeting, 2002 IEEE, New York, USA, 27-31 Jan. 2002, Vol. 1, pp. 383-388

[35] Saifur Rahman and Kwa-sur Tam, "A feasibility study of photovoltaic-fuel cell hybrid system" Energy Conversion, IEEE Transactions on, Vol. 3, No. 1, March 1988

[36] F. Ordubadi, "PEM fuel cells and future opportunities" Power Engineering Society Summer Meeting, 2001. IEEE, Vancouver, Canada, Vol. 1, 15-19 July 2001, pp. 710-716

[37] R.Anahara, S.Yokokawa and M.Sakurai, "Present status and future prospects for fuel cell power systems" Proceedings of the IEEE, Vol. 81, Issue: 3, March 1993, pp. 399-408

[38] J. T. Brown, "Solid oxide fuel cell technology" Energy Conversion, IEEE Transactions on, Vol. 3, No. 2, June 1988

[39] Michael D. Lukas, Kwang Y. Lee and Hossein Ghezel-Ayagh, "Development of a stack simulation model for control study on direct reforming molten carbonate fuel cell power plant" Energy Conversion, IEEE Transactions on, Vol. 14, No. 4, December 1999

[40] S. Matsumoto, A. Sasaki, H. Urushibata and T. Tanaka, "performance model of molten carbonate fuel cell" Energy Conversion, IEEE Transactions on, Vol. 5, No. 2, June 1990

[41] K. Y. Ho and K. S. Sun, "An electrical modelling and fuzzy logic control of a fuel cell generation system" Energy Conversion, IEEE Transactions on, Vol. 14, No. 2, June 1999

[42] W. Shepherd, L. N. Hulley and D. T. W. Liang, "Power electronics and motor control" 2nd edition, Cambridge University Press, New York, NY, USA, 1995

[43] M. H. R. Fazlur Rahman and R. Devanathan, "Feedback linearisation of a heat exchanger" systems & Control Letters, Vol. 26, Issue 3, 20 October 1995, pp. 203-209

[44] Jörg M. Baur, Sanford A. Klein and William A. Beckman, "Simulation of water tanks with mantle heat exchangers" Proceedings of Solar '93, the 1993 American Solar Energy Society Annual Conference, Washington DC, April 22-28, 1993

[45] I. Varga, K. M. Hangos and F. Szigeti, "Controllability and observability of heat exchanger networks in the time-varying parameter case" Control Engineering Practice, Vol. 3, Issue. 10, October, 1995, pp. 1409-1419

[46] A. M. Shaw, F. J. Doyle III and J. S. Schwaber, "A Dynamic Neural Network Approach to Nonlinear Process Modeling" Computer and Chemical Engineering, Vol. 21, Issue 4, p. 371-385, 1997

[47] T. Fukukda and T. Shibata, "Theory and applications of neural network for industrial control systems" Industrial Electronics, IEEE Transactions on, Vol. 39, No. 6, 1992, pp. 472-489

[48] T. T. Chow, Z. Lin, C.L. Song and G.Q. Zhang, "Applying neural network and genetic algorithm in Chiller system optimization" 7th International IBPSA Conference, Rio de Janeiro, Brazil, August 13-15, 2001

[49] W. Charytoniuk and Mo-Shing Chen, "Very short-term load forecasting using artificial neural network" Power Systems, IEEE transactions on, Vol. 15, No. 1, February 2000

[50] R. J. Galarza, J. H. Chow, W. W. Price, A. W. Hargrave and P. M. Hirsch, "Aggregation of exciter models for constructing power system dynamic equivalents" Power Systems, IEEE Transactions on , Vol. 13, Issue: 3, Aug. 1998, pp. 782-788

[51] Test network, PST16, www.uni-duisburg.de/FB9/EAN/doku/teeuwsen/PST16.html

[52] C. Sharma, "Modeling of an Island Grid" Power Systems, IEEE Transactions on, Vol. 13, Issue. 3, August 1998, pp. 971-978

[53] M. H. Rashid, "Power electronics- circuits, devices and applications" 2nd Edition, Prentice-Hall, New Jersey, 1993

[54] E. Han, I Eroglu and L. Türker, "Performance of an alkaline fuel cell with single or double layer electrodes" Int. Journal of Hydrogen Energy, Vol. 25, Issue 2, Feb. 2000, pp. 157-165

[55] M. Wöhr, K. Bolwin, W.Schnurnberger, M. Fischer, W. Neubrand and G. Eigenberger, "Dynamic modelling and simulation of a polymer membrane fuel cell including mass transport limitation" International Journal of Hydrogen Energy Vol. 23, Issue 3, March 1998, pp. 213-218

[56] István Erlich, "Analysis and simulation of dynamic behaviour of power system", Postdoctoral lecture qualification, Dept. of elect. engineering , Dresden University, Germany, 1995

[57] Scott Samuelsen, "Fuel cell/gas turbine hybrid systems" © 2004 ASME Int. Gas Turbine Institute, http://www.asme.org/igti/resources/articles/turbo-fuel-cell_report_feb04.pdf

[58] O. Lamquet, R. Massa, F. Parodi, W. Prandoni and S. Spelta, "Dynamic model of an hybrid plant based on MCFC fuel cells and microturbine for process analysis and control" the 2003 IEEE Bologna Power Tech Conf., June 23th-26th, Bologna, Italy

[59] L. Wang, M. Klein, S. Yirga and P. Kundur, "Dynamic reduction of large power systems for stability studies" Power Systems, IEEE Transactions on, Vol. 12, Issue: 2, May 1997, pp. 889-895

[60] P. Ju and X. Y. Zhou, "Dynamic equivalents of distribution systems for voltage stability studies" Generation, Transmission and Distribution, IEE Proceedings, Vol. 148, Issue: 1, Jan. 2001, pp. 49-53

[61] Sven Demmig, Habil Hans Pundt and István Erlich, "Identification of external system equivalents for power system stability studies using the software package MATLAB" 12th power systems computation conference, Dresden, Germany, August 19-23, 1996

[62] K. Nojiri, S. Suzaki, K. Takenaka and M. Goto, "Modal reduced dynamic equivalent model for analog type power system simulator" Power Systems, IEEE Transactions on, Vol. 12, Issue: 4, Nov. 1997, pp. 1518-1523

[63] S. K. Joo, C. C. Liu and J. W. Choe, "Enhancement of coherency identification techniques for power system dynamic equivalents" Power Engineering Society Summer Meeting 2001, IEEE, Vancouver, Canada, Vol. 3 ,15-19 July 2001, pp. 1811-1816

[64] Mang-Hui Wang and Hong-Chan Chang, "Novel clustering method for coherency identification using an artificial neural network" Power Systems, IEEE Transactions on, Vol. 9, Issue: 4, Nov. 1994, pp. 2056-2062

[65] Aleksander M. Stankovic, Andrija T. Saric and Mirjana Milosevic, "Identification of nonparametric dynamic power system equivalents with artificial neural network" Power Systems, IEEE Transactions on, Vol. 18, Issue: 4, Nov. 2003, pp. 1478-1486

[66] M. Miah, "Simple dynamic equivalent for fast online transient stability assessment" Generation, Transmission and Distribution, IEE Proceedings, Vol. 145, Issue: 1, January 1998, pp. 49-55

[67] S. K. Joo, C. C. Liu, L. Jones and J. W. Choe, "Coherency techniques for dynamic equivalents incorporating rotor and voltage dynamics" Bulk Power Systems Dynamics and Control–V, Security and Reliability in a Changing Environment, Aug. 2001, Hiroshima, Japan

[68] M. K. Donnelly, J. E. Dagle, D. J. Trudnowski and G. J. Rogers, "Impacts of the distributed utility on transmission system stability" Power Systems, IEEE Transactions on, Vol. 11, Issue: 2, May 1996, pp. 741-746

[69] N. W. Miller, R. A. Walling and A. S. Achilles, "Impact of distributed resources on system dynamic performance" Transmission and Distribution Conference and Exposition, 2001 IEEE/PES, Vol. 2, 28 Oct.-2 Nov, 2001, pp. 951- 952, Atlanta, USA

[70] P. Kundur, J. Paserba, V. Ajjarapu, G. Andersson, A. Bose, C. Canizares, N. Hatziargyriou, D. Hill, A. Stankovic, C. Taylor, T. Van Cutsem and V. Vittal, "Definition and classification of power system stability" IEEE/CIGRE joint task force on stability terms and definitions, Power Systems, IEEE Transactions on, Vol. 19, Issue 3, pp. 1387-1401, Aug. 2004

[71] Y. H. Song, L. Z. Yao, Y. X. Ni and P. L. Mao, "Integrated direct methods for transient stability analysis" Electric Machines and Power Systems, 1 February 1999, Vol. 27, issue 2, pp. 139-155

[72] Barbir and T. Gomez, "Efficiency and Economics of Proton Exchange Membrane (PEM) Fuel Cell" Int. Journal of Hydrogen Energy, Vol. 21, Issue 10, pp 891-901, October 1996

[73] Ioannis G. Damousis, Anastasios G. Bakirtzis, and Petros S. Dokopoulos, "Network-Constrained Economic Dispatch Using Real-Coded Genetic Algorithm" Power Systems, IEEE Transactions on, Vol. 18, No. 1, February 2003

[74] K. Mei and S. M. Rovnyak, "Response-based decision trees to trigger one-shot stabilizing control" Power Systems, IEEE Transactions on, Vol. 19, Issue: 1, Feb. 2004, pp. 531-537

[75] S. R. Safavian and D. Landgrebe, "A survey of decision tree classifier methodology" Systems, Man and Cybernetics, IEEE Transactions on, Vol. 21, issue 3 , May-June 1991, pp. 660-674

[76] Ian Beausoleil-Morrison, Dave Cuthbert, Gord Deuchars and Gordon McAlary, "The simulation of fuel cell cogeneration systems within residential buildings" The bi-annual conference of International Building Performance Simulation Association IBPSA-Canada, September 11th-13th, 2002, Montréal, Canada

[77] S. O. Orero and M. R. Irving, "Large scale unit commitment using a hybrid genetic algorithm" International Journal of Electrical Power & Energy systems, Vol. 19, No. 1, pp. 45-55, 1997, (UK)

[78] C. R. Houck, J.A. Joines and M. G. Kay, "A genetic algorithm for function optimization: A Matlab implementation" NCSU-IE technical report 95-09. North Carolina State University, 1995, http://www.fmmcenter.ncsu.edu/fac_staff/joines/papers

[79] Solarsiedlung Gelsenkirchen Bramkampstrasse, http://www.50solarsiedlungen.de

[80] R. J. Yinger, "Behaviour of capstone and Honeywell microturbine generators during load changes" Lawrence Berkeley National Laboratory (LBNL-49095) for CERTS, July 2001, http://certs.lbl.gov/pdf/LBNL_49095.pdf

[81] Almuallim Hussein, "An efficient algorithm for optimal pruning of decision trees" Artificial Intelligence, Vol. 83, Issue: 2, June, 1996, pp. 347-362

[82] L. Atlas, R. Cole, Y. Muthusamy, A. Lippman, J. Connor, D. Park, M. El-sharkawi and R. J. Marks, "A performance comparison of trained multilayer perceptrons and trained classification trees" Proceedings of the IEEE, Vol. 78, Issue. 10, pp. 1614-1619, October 1990

Appendices

Appendix A

Parameters of the fuel cell equivalent circuit

	Value	Unit
τ_R	0.5	s
τ_S	0.15	s
inductance	150	mH

Base Values: Voltage: 60 V

Impedance: 0.73 Ω

The curve describing the resistance as a function of the supplied current is given by the following relation:

$$R_{loss}\,(\Omega) = K_1 + K_2 \cdot I + K_3 \cdot I^2 + K_4 \cdot I^3$$

$K_1 = 0.808$

$K_2 = -0.0325$

$K_3 = 0.000452$

$K_4 = -0.00000195$

Appendix B

Parameters of the heat recovery system

	Value	Unit
A_t	22400.0	cm^2
a_1	60.0	cm^2
a_2	2.0	cm^2
C_P^S	0.05	cal/gm · K
C_P^W	1.0	cal/gm · K
C_P^1	0.5	cal/gm · K
C_P^2	1.0	cal/gm · K
d	2.0	cm
L	90.0	cm
$\dot{M}_L$	18.0	gm/s
M_t	500000	gm
$\dot{M}_1$	26.0	gm/s
$\dot{M}_2$	18.0	gm/s
T_a	283	K
U	0.05	cal/s . cm^2K
U_t	0.0008	cal/s . cm^2K
V_S	3000	cm^3
ρ_1	0.0426	gm/cm^3
ρ_2	1.0	gm/cm^3
ρ_S	2.0	gm/cm^3

Appendix C

Parameters of the micro-turbine model

	Value	Unit
f_{ref}	1.0	p.u.
H	5.0	s
K_g	25	-
K_{gen}	1.0	-
P_{ref}	1.0	p.u.
V_{ref}	1.0	p.u.
W_{min}	0.23	p.u.
ω_{ref}	1.0	p.u.
τ_{cd}	0.15	s
τ_f	0.3	s
τ_g	0.05	s
τ_{gen}	1.5	s
τ_{vp}	0.05	s

Appendix D

Parameters of the fuel cell units integrated into PST16 network

	τ_R (s)	τ_S (s)	Inductance (mH)
PEMFC (250kW)	0.8	0.08	110
PEMFC (350kW)	1.0	0.12	120
AFC (400kW)	1.3	0.15	130
SOFC (450kW)	1.5	0.18	140
SOFC (500kW)	1.7	0.20	150

The loss resistance as a function of the supplied current is given as:

Supplied current (p.u.) / Loss resistance (p.u.)	0.25	0.5	0.75	1.0	1.25	1.5	1.75	2.0
PEMFC (250kW)	0.759	0.41	0.35	0.34	0.34	0.345	0.36	0.393
PEMFC (350kW)	0.759	0.41	0.35	0.34	0.34	0.345	0.36	0.393
AFC (400kW)	0.821	0.482	0.367	0.333	0.333	0.334	0.337	0.413
SOFC (450kW)	0.516	0.417	0.380	0.379	0.379	0.382	0.400	0.425
SOFC (500kW)	0.516	0.417	0.380	0.379	0.379	0.382	0.400	0.425

Appendix E

Parameters of the economic model of the fuel cell

	Value	Unit
$K_{O\&M}$	0.005	\$/kWh
MST	2.0	h
MRT	2.0	h
N_{max}	5.0	-
P_a	0.2	kW
P_{max}	4.0	kW
P_{min}	0.2 or 0.0	kW
α_h	0.05	\$
β	0.15	\$
ΔP_U	10.0	kW/h
ΔP_D	12.0	kW/h
τ	0.75	h

The relation between cell efficiency and supplied electrical power is given as follows:

$$\eta_J = 0.4484 - 0.05359\ P_J + 0.01267\ P_J^2 - 0.00182\ P_J^3$$

The relation between thermal power and supplied electrical power is given as follows:

$$P_{th,J} = -\ 0.0715 + 1.15\ P_J - 0.0236\ P_J^2 + 0.0442\ P_J^3 - 0.0037\ P_J^4$$

Appendix F

Parameters of the economic model of 3 FCs operating in parallel

The parameters of the identical fuel cell units are:

	Value	Unit
$K_{O\&M}$	0.005	\$/kWh
MDT	2.0	h
MUT	2.0	h
N_{max}	5.0	-
P_a	0.08	kW
P_{max}	1.3	kW
P_{min}	0.1 or 0.0	kW
α_h	0.02	\$
β	0.06	\$
ΔP_U	3.2	kW/h
ΔP_D	4.0	kW/h
τ	0.5	h

The relation between cell efficiency and supplied electrical power is given as follows:

$$\eta_J = 0.4484 - 0.16076 \cdot P_J + 0.11399 \cdot P_J^2 - 0.049072 \cdot P_J^3$$

The relation between thermal power and supplied electrical power is given as follows:

$$P_{th,J} = - 0.020723 + 1.0 \cdot P_J - 0.061653 \cdot P_J^2 + 0.34064 \cdot P_J^3 - 0.08752 \cdot P_J^4$$

Appendix G

Parameters of the economic model of the micro-turbine

	Value	Unit
$K_{O\&M}$	0.007	\$/kWh
MDT	2.0	h
MUT	2.0	h
N_{max}	5.0	-
P_a	0.0	kW
P_{max}	4.0	kW
P_{min}	0.05 or 0.0	kW
α_h	0.005	\$
β	0.005	\$
ΔP_U	16.0	kW/h
ΔP_D	16.0	kW/h
τ	0.15	h

The relation between cell efficiency and supplied electrical power is given as follows:

$$\eta_J = 0.1 + 0.0888 \cdot P_J - 0.0187 \cdot P_J^2 + 0.00131 \cdot P_J^3$$

The relation between thermal power and supplied electrical power is given as follows:

$$P_{th,J} = 4.9351 \cdot P_J - 2.29033 \cdot P_J^2 + 0.6194 \cdot P_J^3 - 0.05757 \cdot P_J^4$$

Curriculum Vitae

Personal data

Name:	Ahmed Mohamed Refaat Azmy
Gender:	Male
Date, place of birth:	August 17, 1968, Quesna, Menoufiya, Egypt
Nationality:	Egyptian
Marital status:	Married

School education

1974 ~ 1980	Attended the primary school, Quesna City, Menoufya, Egypt
1980 ~ 1983	Attended the Middle school, Quesna City, Menoufya, Egypt
1983 ~ 1986	Attended the High School, Quesna City, Menoufya, Egypt

Study

1986 ~ 1991	Undergraduate student, Department of Electrical Engineering, Faculty of Engineering, Menoufya University, Egypt
1993 ~ 1996	Graduate student, Department of Electrical Engineering, Faculty of Engineering, Menoufya University, Egypt

Work experience

1992 ~ 1996	Instructor, Department of Power Engineering and Electrical Machines, Faculty of Engineering, Tanta University, Egypt
1996 ~ 2001	Assistant lecture, Department of Power Engineering and Electrical Machines, Faculty of Engineering, Tanta University, Egypt
2001 ~ Present	Research assistant, Department of Electrical Engineering, University Duisburg-Essen, Germany

Published Papers

Journal Paper

1- Ahmed M. Azmy, I. Erlich and P. Sowa, "Artificial neural network-based dynamic equivalents for distribution systems containing active sources" Generation Transmission and Distribution, IEE Proceedings, Vol. 151, Issue: 6, pp. 681–688, ISSN: 1350-2360, Nov. 2004

2- Ahmed M. Azmy and I. Erlich, "Online optimal management of PEM fuel cells using neural networks" accepted for publication in the Power Delivery, IEEE Transactions on

Conference Proceedings

1- Ahmed M. Azmy and I. Erlich, "Dynamic simulation of fuel cells and micro-turbines integrated with a multi-machine network" Power Tech Conference Proceedings, 2003 IEEE Bologna, Italy, Vol. 2, June 23-26, 2003, pp. 550-555

2- Ahmed M. Azmy and I. Erlich, "Dynamic simulation of hybrid fuel cell/micro-turbine units integrated into large power systems" The Ninth International Middle-East Power Systems Conference (MEPCON), Egypt, December, 16-18, 2003

3- Ahmed M. Azmy, B. P. Wachholz and I. Erlich, "Management of PEM fuel cells for residential applications using genetic algorithms" The Ninth International Middle-East Power Systems Conference (MEPCON), Egypt, December, 16-18, 2003

4- Ahmed M. Azmy and I. Erlich "Intelligent operation management of fuel cells and micro-turbines using genetic algorithms and neural networks" International Conference on new and renewable energy technologies for sustainable development, 28 June-1 July 2004, Évora, Portugal

5- Ahmed M. Azmy, I. Erlich and P. Sowa, "Dynamic equivalents for calculation of power system restoration" the 8th international scientific conference in current electrical energy problems (APE'04), 7-9 June, Wisla, Poland, pp. 104-108

6- Ahmed M. Azmy and I. Erlich, "Identification of dynamic equivalents for distribution power networks using recurrent ANNs" IEEE 2004 Power Systems Conference and Exposition, October 10-13, 2004, New York City

7- Ahmed M. Azmy and I. Erlich, "Impact of Distributed Generation on the Stability of Electrical Power Systems" accepted for publication in the 2005 IEEE PES General Meeting, San Francisco, California, 12-16 June 2005

Papers under publications

1- Ahmed M. Azmy and I. Erlich, "Decision Trees-Based Online Management of PEM Fuel Cells for Residential Applications"